



<https://theses.gla.ac.uk/>

Theses Digitisation:

<https://www.gla.ac.uk/myglasgow/research/enlighten/theses/digitisation/>

This is a digitised version of the original print thesis.

Copyright and moral rights for this work are retained by the author

A copy can be downloaded for personal non-commercial research or study,
without prior permission or charge

This work cannot be reproduced or quoted extensively from without first
obtaining permission in writing from the author

The content must not be changed in any way or sold commercially in any
format or medium without the formal permission of the author

When referring to this work, full bibliographic details including the author,
title, awarding institution and date of the thesis must be given

Enlighten: Theses

<https://theses.gla.ac.uk/>
research-enlighten@glasgow.ac.uk

CHEMISTRY OF SOLVATED CATIONS
IN ACETONITRILE

THESIS SUBMITTED TO THE UNIVERSITY OF GLASGOW
FOR THE DEGREE OF Ph.D.

BY

RANA MUHAMMAD SIDDIQUE

FACULTY OF SCIENCE
DEPARTMENT OF CHEMISTRY
FEBRUARY, 1988.

ProQuest Number: 10997905

All rights reserved

INFORMATION TO ALL USERS

The quality of this reproduction is dependent upon the quality of the copy submitted.

In the unlikely event that the author did not send a complete manuscript and there are missing pages, these will be noted. Also, if material had to be removed, a note will indicate the deletion.



ProQuest 10997905

Published by ProQuest LLC (2018). Copyright of the Dissertation is held by the Author.

All rights reserved.

This work is protected against unauthorized copying under Title 17, United States Code
Microform Edition © ProQuest LLC.

ProQuest LLC.
789 East Eisenhower Parkway
P.O. Box 1346
Ann Arbor, MI 48106 – 1346

Dedication

To my Late mother(13-11-1986)

ACKNOWLEDGEMENTS.

I wish to express my sincere thanks to my supervisor, Dr. J.M. Winfield for extending his valuable advice, guidance and tolerance during the course of this work. I owe a special debt of gratitude to Professor D.W.A. Sharp for his continuous encouragement.

I am also grateful to Messrs. J. Gall, J. McIver, W. McCormack, R. Wilson, G. McCulloch and Mrs. F. Lawrie for their cooperation. Many thanks are due to all my research colleagues in the Fluorine Chemistry Group for providing a very conducive and working atmosphere; particularly to Mr. L. McGhee for his help and assistance.

A great deal of the credit for successful completion of this work must go to my father who gave me an immense amount of encouragement and inspiration, in spite of the shock which he received from the tragic death of my mother in my absence. I would like to thank Liz for typing my thesis.

Finally I gratefully acknowledge the financial support provided to me by the Ministry of Education Islamabad, Government of Pakistan in the form of Central Overseas Training Scheme Award.

Rana Muhammad Siddique.

C O N T E N T S

	page
Summary	(i)
CHAPTER ONE	
Introduction	1
1:1 Cations in Solution	3
1:2 Acetonitrile - an Aprotic Solvent	5
1:3 Generation of Solvated Cations	7
1:3:1 Oxidation of Metals by NO^+	7
1:3:2 Oxidation of Metals and Non-metals by Covalent High Oxidation State Fluorides	8
1:3:3 Lewis Acid - Lewis Base Reactions	14
1:4 [^{205}Tl]-Thallium N.M.R. Spectroscopy	15
1:5 Redox and Substitution Reactions	16
1:5:1 Redox Reactions	17
1:5:2 Substitution Reactions	18
1:6 Aim of the Present Work	21
CHAPTER TWO	
[^{205}Tl]-Thallium N.M.R. Study of Tl^{I} and Tl^{III} Salts of Complex Fluoroanions in Acetonitrile.	24
2:1 Introduction	24
2:1:1 Evidence for Coordination of Complex Fluoroanions in the Solid State.	24
2:1:2 Properties of Solvated Cation, Fluoroanion Salts in Solution.	28
2:1:3 [^{205}Tl]-Thallium N.M.R. Spectroscopy	30
2:2 Results	31
2:2:1 Study of Thallium (I) Salts.	31
2:2:2 Study of Thallium (III) Salts with Paramagnetic Fluoroanions	36
2:2:3 Study of Mixtures Containing Tl^{I} and Tl^{III}	37
2:3 Discussion	41

2:4 Conclusions	45
2:5 Experimental	45

CHAPTER THREE

Substitution Reactions of the Solvated Fe^{II} Cation in Acetonitrile.	51
3:1 Introduction	51
3:1:1 Iron(II) Salts with Nitrogen Donor Ligands	51
3:1:2 Iron(II) Salts with Phosphorus Donor Ligands	53
3:2 Results	57
3:2:1 Preparation and Characterization of Iron(II) Cations with Nitrogen or Sulphur Donor Ligands	57
3:2:2 Replacement of Nitrogen Donor Ligands at Iron(II) by Trimethylphosphite	60
3:2:3 Replacement of Nitrogen Donor Ligands at Iron(II) by Trimethyl Phosphine	67
3:3 Discussion	69
3:4 Conclusions	78
3:5 Experimental	79

CHAPTER FOUR

Redox and Substitution Reactions of Solvated Cu^{II} and Cu^{I} , and Solvated Tl^{III} and Tl^{I} Cations in Acetonitrile.	91
4:1 Introduction	91
4:1:1 Redox Chemistry of Copper	91
4:1:2 Redox Chemistry of Thallium	96
4:2 Results	97
4:2:1 Reactions of Dimethylsulphide with Solvated Cu^{I} and Cu^{II} Cations in MeCN.	97
4:2:2 Reactions of Dimethylsulphide with Solvated Tl^{I} and Tl^{III} Cations in MeCN	100
4:2:3 Reactions of Trimethylamine with Solvated Cu^{I} and Cu^{II} Cations in MeCN.	102

4:2:4 Reactions of Trimethylamine with Solvated Tl ^I and Tl ^{III} Cations in MeCN	104
4:2:5 Reactions of Trimethylphosphine with Solvated Cu ^I and Cu ^{II} Cations in MeCN.	106
4:2:6 Reactions of Trimethylphosphine with Solvated Tl ^I and Tl ^{III} Cations in MeCN	108
4:2:7 Reactions of Tetramethylthiourea with Solvated Cu ^I and Cu ^{II} Cations in MeCN	109
4:3 Discussion	111
4:4 Conclusions	121
4:5 Experimental	122
 CHAPTER FIVE	
Redox and Substitution Reactions of the Solvated Iodine(+1) Cation in Acetonitrile.	131
5:1 Introduction	131
5:1:1 Historical Background	131
5:1:2 Charge Transfer Complexes of Iodine	133
5:1:3 Solid Complexes of the I ⁺ Cation	134
5:1:4 Reactions of the I ⁺ Complexes	136
5:2 Results	138
5:2:1 Reactions of the Solvated I ⁺ Cation	138
5:2:2 Reactions of the Solvated Fe ²⁺ Cation with [14]-aneN ₄ and [15]-aneN ₄	142
5:3 Discussion	144
5:4 Conclusions	150
5:5 Experimental	151
 CHAPTER SIX	
Experimental Techniques.	158
6:1 Vacuum Line and Dry Box Techniques.	158
6:2 Vibrational Spectroscopy.	158

6:3 Electronic Spectroscopy	161
6:4 Stopped-Flow Spectroscopy	164
6:5 Cyclic Voltammetry.	167
6:6 Purification of Acetonitrile	172
6:7 Nuclear Magnetic Resonance Spectroscopy.	172
6:8 Magnetic Susceptibility.	174

CHAPTER SEVEN

Conclusions.	176
--------------	-----

SUMMARY

The solution chemistry of solvated cations, $[\text{Fe}(\text{NCMe})_6]^{2+}$, $[\text{Cu}(\text{NCMe})_4]^+$, $[\text{Cu}(\text{NCMe})_6]^{2+}$, $[\text{Tl}(\text{NCMe})_6]^{3+}$ and $[\text{I}(\text{NCMe})_2]^+$, in acetonitrile is described in this thesis. The ligands used in this study are the simple N,P and S-donor species such as NH_3 , NMe_3 , pyridine(py), PMe_3 , $\text{P}(\text{OMe})_3$, Me_2S and tetramethylthiourea(tmtu). Macrocyclic N-donor ligands such as 1,4,8,11-tetraazacyclotetradecane ($[\text{14}]\text{-aneN}_4$) and 1,4,8,12-tetraazacyclopentadecane ($[\text{15}]\text{-aneN}_4$), are also used in some cases.

A ^{205}Tl n.m.r. study of the Tl^{I} salts having diamagnetic complex fluoroanions, PF_6^- and WF_7^- , in MeCN solution indicates a high field shift of the ^{205}Tl n.m.r. resonances with an increase in salt concentration. The increase in the concentration of the Tl^{I} salts with paramagnetic anions, MoF_6^- and UF_6^- , on the other hand, results in a low field shift. The concentration dependent behaviour observed for ^{205}Tl n.m.r. resonances in the Tl^{I} salts, in MeCN indicates that some degree of ion-pairing is present in these solutions. The effect of paramagnetic anions on the ^{205}Tl resonances in the Tl^{I} salts is far greater but their effect on Tl^{III} is very small. It is suggested that Tl^{3+} is more effectively solvated by MeCN as compared with Tl^+ hence direct ion-pairing is less important. The ^{205}Tl shielding of Tl^{I} and Tl^{III} is decreased respectively in the presence of Tl^{III} and Tl^{I} .

Coordinated acetonitrile in the cation $[\text{Fe}(\text{NCMe})_6]^{2+}$, is replaced readily by NH_3 and pyridine (L) at room temperature to form $[\text{FeL}_6]^{2+}$. Only one Me_3N ligand is coordinated to Fe^{II} under normal conditions to form $[\text{Fe}(\text{NMe}_3)(\text{NCMe})_5]^{2+}$. The reaction of $[\text{Fe}(\text{NCMe})_6]^{2+}$ with tmtu in MeCN presumably results in the formation of $[\text{Fe}(\text{tmtu})_6]^{2+}$ whereas no reaction is observed when Me_2S is reacted with $[\text{Fe}(\text{NCMe})_6]^{2+}$.

The cation, $[\text{Fe}(\text{NMe}_3)(\text{NCMe})_5]^{2+}$, reacts with $\text{P}(\text{OMe})_3$ in MeCN solution forming $[\text{Fe}\{\text{P}(\text{OMe})_3\}_5(\text{NMe}_3)]^{2+}$ as the final product. The reaction involves a stepwise substitution of $\text{P}(\text{OMe})_3$ for coordinated MeCN and is followed by $^{31}\text{P}\{-^1\text{H}\}$ n.m.r. spectroscopy. The formation of the first low spin species, cis and trans- $[\text{Fe}\{\text{P}(\text{OMe})_3\}_2(\text{NMe}_3)(\text{NCMe})_3]^{2+}$ is followed by stopped-flow spectrophotometry and confirmed by $^{31}\text{P}\{-^1\text{H}\}$ n.m.r. spectroscopy. The species, $[\text{Fe}\{\text{P}(\text{OMe})_3\}_2(\text{NMe}_3)(\text{NCMe})_3]^{2+}$, on further substitution forms fac- $[\text{Fe}\{\text{P}(\text{OMe})_3\}_3(\text{NMe}_3)(\text{NCMe})_2]^{2+}$. The formation of the final product, $[\text{Fe}\{\text{P}(\text{OMe})_3\}_5(\text{NMe}_3)]^{2+}$, from fac- $[\text{Fe}\{\text{P}(\text{OMe})_3\}_3(\text{NMe}_3)(\text{NCMe})_2]^{2+}$ occurs via the route in which the cation, trans- $[\text{Fe}\{\text{P}(\text{OMe})_3\}_4(\text{NMe}_3)(\text{NCMe})]^{2+}$ is dominant whereas in the $[\text{FeL}_6]^{2+}$ (L = NCMe or py) and $\text{P}(\text{OMe})_3$ systems, the route involving the cation, cis- $[\text{Fe}\{\text{P}(\text{OMe})_3\}_4\text{L}_2]^{2+}$ is important.

The cations, $[\text{FeL}_6]^{2+}$, L = NCMe, py or NH_3 , and $[\text{Fe}(\text{NMe}_3)(\text{NCMe})_5]^{2+}$ react with PMe_3 in MeCN at room temperature forming low spin iron(II) cations with three ligated PMe_3 molecules. The dominant cations are the fac- $[\text{Fe}(\text{PMe}_3)_3\text{L}_3]^{2+}$ or fac- $[\text{Fe}(\text{PMe}_3)_3(\text{NMe}_3)(\text{NCMe})_2]^{2+}$. The complexes having four ligated PMe_3 molecules, cis- $[\text{Fe}(\text{PMe}_3)_4\text{L}_2]^{2+}$ or cis- $[\text{Fe}(\text{PMe}_3)_4(\text{NMe}_3)(\text{NCMe})]^{2+}$ are present only in trace quantities. The replacement of nitrogen donor ligands by PMe_3 at iron(II) in MeCN is very fast as compared with $\text{P}(\text{OMe})_3$. The reactions are complete within the time of mixing the reactants.

The reaction of $[\text{Cu}(\text{NCMe})_4]^+$ with Me_2S or Me_3N in MeCN does not result in the coordination of the ligand whereas the cations, $[\text{CuL}_4]^+$ L = PMe_3 or tmtu, are formed when $[\text{Cu}(\text{NCMe})_4]^+$ is reacted with PMe_3 or tmtu. $\text{Tl}^{\text{I}}\text{UF}_6$ reacts with Me_3N or $\text{Me}_3\text{P}(\text{L})$ in MeCN solution forming insoluble Tl^{I} salts, $[\text{TlL}_2][\text{UF}_6]$. Dimethyl sulphide on the other hand does not react with Tl^{I} in MeCN solution.

The cations, $[\text{Cu}(\text{NCMe})_6]^{2+}$ and $[\text{Tl}(\text{NCMe})_6]^{3+}$, react with Me_2S , Me_3N , Me_3P and tmtu , in MeCN solution undergoing redox reactions. Solvated Cu^{2+} and solvated Tl^{3+} cations in these redox reactions are reduced to the +1 oxidation state whereas the ligands are oxidised to the corresponding monomeric radical cations. The radical cations, $\text{Me}_2\text{S}^{+\cdot}$ or $\text{Me}_3\text{N}^{+\cdot}$ formed in the redox reactions involving Me_2S or Me_3N , combine with free ligands forming the dimeric radical cations, $[\text{Me}_2\text{S-SMe}_2]^{+\cdot}$ or $[\text{Me}_3\text{N-NMe}_3]^{+\cdot}$. The dimeric radical cations then lose methyl radicals, Me^\cdot , forming the cations $[\text{Me}_2\text{S-SMe}]^+$ or $[\text{Me}_3\text{N-NMe}_2]^+$. The methyl radicals dimerize forming ethane. In the redox reactions involving PMe_3 or tmtu , the radical cations, $\text{PMe}_3^{+\cdot}$ or $(\text{Me}_2\text{N})_2\text{CS}^{+\cdot}$ react with other radical cations forming dimeric dication, $[\text{Me}_3\text{P-PMe}_3]^{2+}$ or $[(\text{Me}_2\text{N})_2\text{CS-SC}(\text{NMe}_2)_2]^{2+}$. The reactions of $[\text{Cu}(\text{NCMe})_6]^{2+}$ with Me_2S , Me_3N and tmtu (L) in MeCN are followed by conventional electronic spectroscopy. The electronic spectra consist of two bands, the low energy band is assigned to the species, $[\text{CuL}_x(\text{NCMe})_{6-x}]^{2+}$, ($x = 0-2$) in which MeCN is the predominant ligand and the high energy band is assigned to the more highly substituted species, $[\text{CuL}_x(\text{NCMe})_{6-x}]^{2+}$ ($x = 3-5$). These highly substituted species are assumed to be redox active.

The cation, $[\text{I}(\text{NCMe})_2]^{2+}$, reacts with Me_2S , tmtu , 2,2'-bipyridyl, [14]-ane N_4 and [15]-ane N_4 (L), in MeCN solution, undergoing substitution reaction to form the cations, $[\text{IL}_n]^+$, $n = 2$ for Me_2S , tmtu and 2,2'-bipyridyl, and $n = 1$ for [14]-ane N_4 and [15]-ane N_4 . The reaction of $[\text{I}(\text{NCMe})_2]^+$ with PMe_3 is complicated. The cation $[\text{I}(\text{NCMe})_2]^+$, in MeCN solution acts as an oxidising agent but it is stabilized by the substitution of MeCN with the above mentioned ligands.

The iodine (+1) complexes prepared in this work are investigated by cyclic voltammetry. The stabilizing ability of the ligands

is evident from the size of the respective I^+ / I^- couples of the complexes.

The cation, $[\text{Fe}(\text{NCMe})_6]^{2+}$ reacts with [14]-aneN₄ or [15]-aneN₄ (L) in MeCN solution forming $[\text{FeL}(\text{NCMe})_2]^{2+}$. Iron (II) in the cations, $[\text{FeL}(\text{NCMe})_2]^{2+}$, is oxidised to Fe^{III} using NO⁺ as an oxidising agent. The oxidation $\text{Fe}^{\text{II}} \longrightarrow \text{Fe}^{\text{III}}$ in these complexes is possible because of the high stabilizing ability of the ligands.

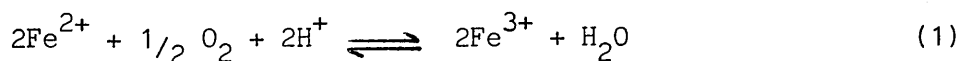
CHAPTER ONE

INTRODUCTION

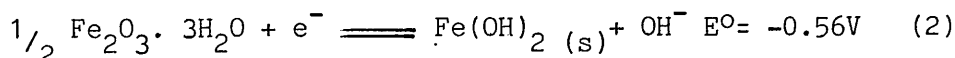
CHAPTER ONE

INTRODUCTION

A considerable amount of work in inorganic chemistry is carried out in solution, for this reason alone solution chemistry is a worthwhile area for study. The majority of inorganic reactions have naturally been carried out in aqueous medium and the behaviour of a large number of cations, having different oxidation states, is well established. However, some cations have oxidation states which are unstable with respect to hydrolysis or oxidation, or can not be prepared at all in aqueous solution. For example aqueous solutions of iron(II), in the absence of complexing agents, contain the pale blue green hexa-aquo ion, $[\text{Fe}(\text{H}_2\text{O})_6]^{2+}$, which is unstable with respect to oxidation by molecular oxygen.¹ The oxidation of iron(II) to iron(III) by molecular oxygen, in acid solution is represented by equation (1).

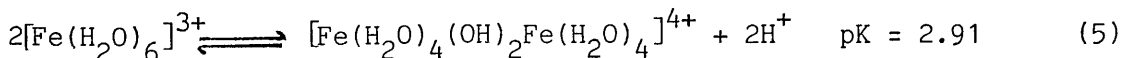
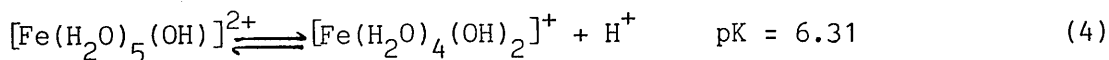
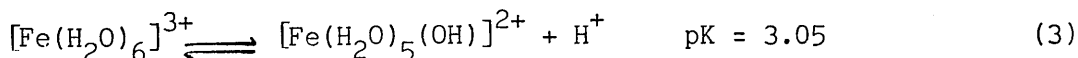


The oxidation process, in basic solution is represented by equation (2).

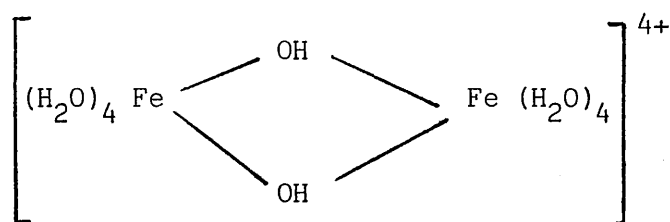


In neutral solution, the oxidation of Fe(II) to Fe(III) by molecular oxygen, may involve a reaction between FeOH^+ and O_2OH^- .

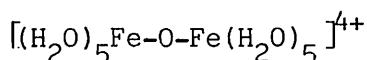
Iron(III), in aqueous solution, is unstable with respect to hydrolysis, unless the pH of the solution is around zero. The hydrolysis, in the initial stages, is governed by the following equilibrium constants.²



The dimer, in equation (5), has been formulated as:³



The formulation with a linear Fe-O-Fe bridge has also been proposed as an alternative.⁴



In aqueous solution, the Cu(I) ion is very unstable with respect to disproportionation to Cu(II) and copper metal, (equation 6)



because of the high heat of hydration of the divalent ion.⁵ However, Cu(I), in aqueous medium can be stabilized by complexing with suitable ligands. The usual stereo-chemistry is tetrahedral as in complexes, $[\text{Cu}(\text{CN})_4]^{3-}$ ⁶ and $[\text{Cu}(\text{py})_4]^+$ ⁵ but lower coordination numbers are also known such as $[\text{CuCl}_2]^-$,⁷ $[\text{Cu}(\text{NH}_3)_2]^+$,⁸ $[\text{CuCl}_3]^{2-}$,⁷ $[\text{Cu}(\text{NH}_3)_3]^+$ ⁸ and $[\text{Cu}(\text{CN})_3]^{2-}$.⁹

Thallium(III), in aqueous solution is extensively hydrolysed to $[\text{Tl}(\text{OH})_2]^+$ and the colloidal oxide even at pH 1 to 2.5. The presence of Cl^- ions, in aqueous solution, stabilizes Tl^{3+} forming the very stable TlCl_2^+ (aq) species.¹⁰

Oxidation states of the cations, in solution, can be stabilized, not only, by the addition of suitable ligands but also by using a suitable solvent. The cations, classified as hard acids, prefer to form stable oxidation states in solvents grouped as hard bases whereas those termed as soft acids prefer to form stable oxidation states in solvents grouped as soft bases. Thus the cations having oxidation states, unstable in water,

can be stabilized by using a suitable non-aqueous solvent. The use of non-aqueous solvents also enhances the field of redox reactions as water is attacked readily by oxidising agents with standard potentials greater than about 1.70 V and by reducing agents with oxidation potentials below about -0.40 V.¹¹

1:1 Cations in Solution.

The behaviour of a cation in solution can be interpreted in terms of ion-solvent interactions which mostly involve the Lewis acidity and Lewis basicity of the ion and the solvent respectively.¹² There are, however, some special cases such as hydrogen bonding interactions involving donor properties of the solvent and the acceptor properties of the anion, and dispersion force interactions. Some of these interactions are inter-related, for example hydrogen bonding properties of the solvents influence their structure. It is, however, convenient to explain solvation phenomena by singling out a particular interaction when it is clearly dominant. Examples are, the hydrogen bonding interaction between chloride ion and water; the dispersion force interaction between tri-iodide ion and dimethyl sulphoxide (DMSO), and the covalent bond formation between acetonitrile ligands and Cu^+ or Ag^+ .

The molecular environment in the solution of a particular cation, (a) in water and (b) in an aprotic solvent, is illustrated in Figure 1.¹²

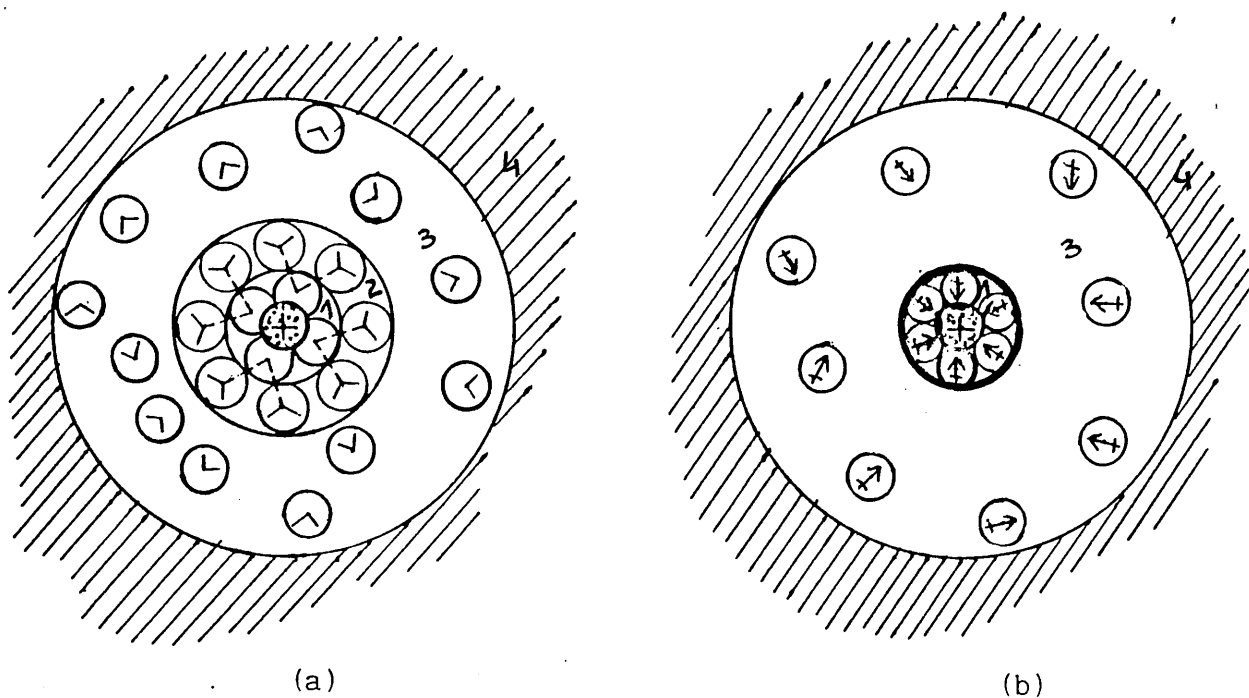


Figure 1. Schematic diagram to indicate the molecular environment in the solvation of a particular cation (a) in water and (b) in an aprotic solvent.

Region 1 is the primary solvation shell of the cation. Often it is the formal co-ordination shell of ligands having a co-ordination number of 4 or 6. This is the ordered region and its formation produces a loss of entropy relative to that of the pure solvent if the new order is more developed than that of the pure solvent. The extent of this entropy loss depends on the difference in entropy between solvent molecules in regions 1 and 4. Solvents like water and formamide have an extensively ordered bulk structure whereas acetonitrile and dimethylformamide have much less ordered bulk structures as indicated by their lower Trouton constants.¹³ Thus simple cations experience less entropy loss in water as compared with acetonitrile and dimethylformamide.

Region 2 is the secondary solvation shell. In water, the electron withdrawing effect of the cation on the primary waters of hydration, encourages them to hydrogen bond to secondary waters of hydration (Figure 1(a)). The volume of this secondary shell varies greatly with the nature of the cation, being large for small ions of high charge and small or negligible for large monovalent cations. In non-aqueous solvents much less structured than water, for example, acetonitrile, region 2 is absent (Figure 1(b)).

The region 3 is the disordered zone separating the ordered region 1 from the differently ordered region 4 which corresponds to the bulk solvent.

The model of a cation in solution, represented in Figure 1, is dynamic not static.¹⁴ Solvent molecules move between the various regions at rates characteristic of the cation, the solvent and the conditions such as temperature. This model is based on the experimental evidence derived mainly from thermodynamic parameters such as free energies, enthalpies and entropies of single ions in solution.

1:2 Acetonitrile - an Aprotic Solvent.

A number of protonic and aprotic solvents are available for studying the non-aqueous chemistry of cations. Protonic solvents such as liquid ammonia, are mostly self-ionizing with the ionization taking place through the transfer of a proton from one molecule of the solvent to another. This results in the formation of a solvated proton and a deprotonated anion. The solvents which do not involve the transfer of a proton are called aprotic solvents and may conveniently be divided into three groups.¹⁵ Solvents such as benzene and cyclohexane, form the first group, are non-polar, do not undergo self-ionization and thus behave as non-solvating agents. The second group

consists of solvents that are polar yet do not ionize to an appreciable extent. Examples of this type are, acetonitrile (MeCN), dimethylacetamide (DMA), dimethylsulphoxide (DMSO) and sulphur dioxide. They are good co-ordinating solvents because of their polarity which ranges from low (SO_2) to extremely high (DMSO). Most of the solvents belonging to this group are Lewis bases. The third group consists of those solvents that are highly polar and auto-ionizing. An example of such a solvent is bromine trifluoride.

Acetonitrile is a dipolar, aprotic solvent and has been proved to be a good solvent for studying the non-aqueous chemistry of cations.¹⁶ Its physical properties, m.pt. = 228 K, b.pt. = 354 K, make it an ideal solvent for vacuum line work at ambient temperatures, and it can be handled easily in greaseless, Pyrex apparatus. It has a relatively high dielectric constant, 37.5 at 293 K, for an organic liquid and is thus a suitable solvent for many ionic compounds. Acetonitrile is relatively simple to purify and has a large working potential range of 5.7 V. It is a strong enough Lewis base to solvate effectively a large number of cations, particularly those of 3d and post transition elements; it can be readily displaced by stronger bases, for example ammonia. Acetonitrile has a simple vibrational spectrum and is transparent in the visible and u.v. regions down to a wavelength of 175 nm. These properties, with the availability of CD_3CN , make it an ideal solvent for spectroscopic work.

The role of acetonitrile as a donor solvent and the nature of its co-ordination to the metal centre has been extensively reviewed.¹⁷ The most common way of co-ordination is through the lone pair of electrons on nitrogen. This causes an increase in the vibrational stretching frequencies of the $\text{C}\equiv\text{N}$ and $\text{C}-\text{C}$ bonds over those of the free molecule.¹⁸ This is mainly attributed to the enhancement of the $\text{C}\equiv\text{N}$ stretching force constant of the sigma bond system that results from a

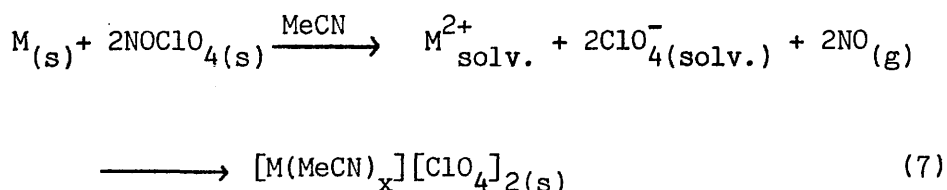
shortening of the C≡N bond.¹⁹ The increase in the infra-red stretching frequency of the C≡N bond is a very useful method of establishing the presence of co-ordinated acetonitrile.

1:3 Generation of Solvated Cations.

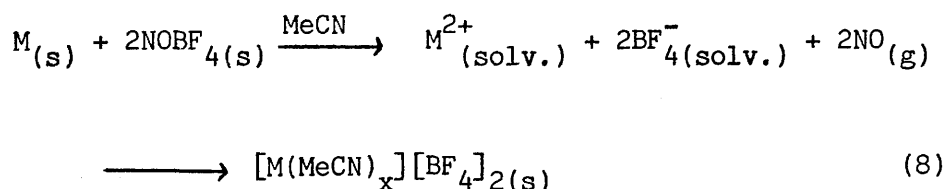
Three main routes have been used to generate solvated cations, that is cations having only solvent molecules in the primary co-ordination sphere, in acetonitrile.

1:3:1 Oxidation of Metals by NO⁺

A number of solvated cations of the first row transition metals have been prepared by the oxidation of metals with NOClO₄²⁰ or NOBF₄²¹ as oxidising agents. The metals react with suspensions of nitrosyl perchlorate or nitrosyl tetrafluoroborate in acetonitrile, according to the equations 7 and 8.



M = Co, Mn, Cu and Zn, x = 4 for Mn, Cu and Zn, and 6 for Co.



M = Fe, Co, Mn, Ni, Cu and Zn, x = 4 for Mn, Cu, and Zn, and 6 for Fe, Co and Ni.

All the above solvated metal cations are obtained in the +2 oxidation states except copper, where a mixture of Cu(II) and Cu(I) species is formed.

1:3:2 Oxidation of Metals and Non-metals by Covalent High Oxidation State Fluorides.

The use of covalent high oxidation state fluorides as oxidising agents for metals and non-metals provides a useful route to the generation of solvated cations. The main advantage of the route is that these fluorides can be obtained in rigorously anhydrous condition. The use of very strong oxidising agents is not feasible in MeCN solution, as these agents interact with the solvent causing its polymerization, however, oxidising agents with milder ability, have been used with great effect. The relative oxidising abilities of the second and third row transition metal fluorides, have been discussed in a semi-qualitative manner.²²

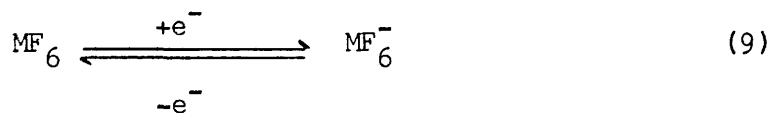
The most commonly studied hexafluorides, in MeCN, are those of molybdenum, tungsten and uranium. These fluorides are monomeric having an octahedral arrangement of six fluorine atoms around the central metal atom. The hexafluorides of molybdenum, tungsten and uranium possess orthorhombic symmetry in their solid lattices. Neutron powder diffraction²³ studies of MoF₆ and WF₆ have been carried out and comparison of results with similar work on UF₆ indicates that MoF₆ and WF₆ exist as more compact and spherically shaped molecules than UF₆ in the solid state.

The electron affinities of the hexafluorides of molybdenum, tungsten and uranium, have been determined by various methods, for example, ion cyclotron resonance spectroscopy,^{24,25} molecular beam reactions with alkali metals,^{26,27} thermochemistry of hexafluoro-metallate(V) salts,^{28,29} effusion mass spectrometry^{30,31} and hexafluoride oxidation of graphite.^{32,33} Although there is some disagreement as to their precise values, particularly for MoF₆, most data indicate that the order of electron affinities is UF₆ > MoF₆ > WF₆. This order is also indicated by the electronic spectra of the

hexafluorides charge transfer complexes³⁴⁻³⁶ and is consistent with their gas phase redox chemistry.^{37,38}

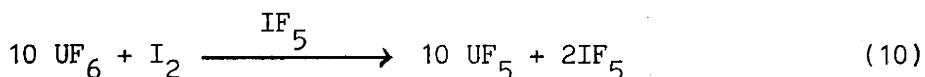
The oxidising abilities of MoF₆, WF₆ and UF₆, have been demonstrated by a number of redox reactions both in the gas phase and the solution state. Nitric oxide is found to react with MF₆, (M = Mo or U), when the two gases are condensed into an evacuated nickel reactor³⁷ or in a Kel-F tube³⁹ and the mixture allowed to warm up to room temperature. Salts of the general formula, NO⁺MF₆⁻, are formed, thus the central atom of the hexafluorides is reduced to a pentavalent state. No reaction is observed with WF₆ even at 373 K. O'Donnell and Stewart investigated³⁸ the reduction of molybdenum, tungsten and uranium hexafluorides using trifluorides of phosphorus, arsenic, antimony and bismuth. Uranium hexafluoride was found to react readily with PF₃, molybdenum hexafluoride was reduced partially as the PF₅ formed during the reaction was capable of oxidising MoF₅, whereas reduction of tungsten hexafluoride was very slow and occurred only to a limited extent. In all these systems, addition of anhydrous hydrogen fluoride appeared to be necessary to catalyse the redox reactions. All these gas phase reactions indicate that MoF₆ and UF₆ have comparable oxidising ability whereas WF₆ is found to be the weakest among the three agents.

The reactivity of MoF₆, WF₆ and UF₆, in solution, has been demonstrated in a number of ways. The redox couples, MF₆/MF₆⁻ (M = Mo, W), in anhydrous hydrogen fluoride have been investigated by A.M. Bond *et al.*⁴⁰ using the technique of cyclic voltammetry at platinum and glassy carbon electrodes. The process involves a simple one electron reversible reaction, as shown in equation 9.

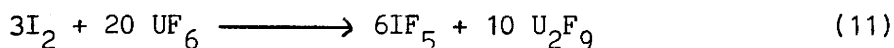


The electro-chemical potential value of the couples, (MF₆/MF₆⁻), were

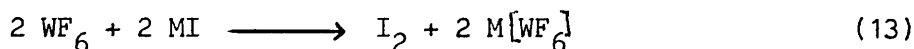
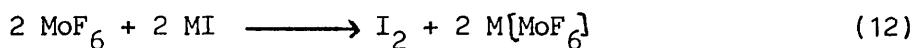
determined by measuring the half wave potentials with an $E_{\frac{1}{2}}$ (WF_6/WF_6^-) = -0.11V and $E_{\frac{1}{2}}$ (MoF_6/MoF_6^-) = +0.91V versus CuF_2/Cu . The observed values for $E_{\frac{1}{2}}$ are direct measures of the reduction potentials, E^0 , for the WF_6/WF_6^- and MoF_6/MoF_6^- couples. A comparison of the two couples shows WF_6 to be a mild oxidising agent since it is reduced at a negative potential (-0.11V) with respect to CuF_2/Cu reference electrode and MoF_6 , a stronger oxidising agent as it is reduced at a much more positive potential. No electrochemical data for UF_6 , in anhydrous hydrogen fluoride, are available. The oxidising abilities of MoF_6 , WF_6 and UF_6 towards I_2 in iodine pentafluoride have been investigated by Berry et al.⁴¹ The hexafluorides of molybdenum and tungsten are found to be inert towards I_2 in IF_5 whereas UF_6 oxidised I_2 to I_2^+ . The product, $I_2^+UF_6^-$, undergoes decomposition to UF_5 and IF_5 , in iodine pentafluoride whatever mole ratio of the reactants is used. However, this decomposition is complete when the mole ratio, $UF_6:I_2$, is greater than 10:1 and is represented by equation 10.



This behaviour of MoF_6 , WF_6 and UF_6 towards I_2 in iodine pentafluoride, is consistent with similar work involving the reaction of I_2 with the hexafluorides at high temperature.⁴² Molybdenum and tungsten hexafluorides do not react with iodine whereas uranium hexafluoride undergoes the reaction according to equation 11.



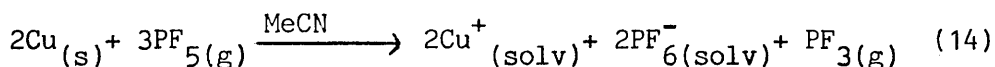
The non-volatile uranium fluoride, U_2F_9 , presumably arises from the disproportionation of UF_5 . Reactions of molybdenum and tungsten hexafluorides, with alkali metal iodides have been studied in liquid sulphur dioxide.⁴³ The alkali metal iodides are found to be oxidised to iodine whereas the hexafluorides are reduced to hexafluoro-metallates(V).



M = alkali metals except lithium.

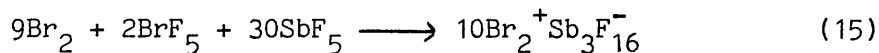
Molybdenum, tungsten and uranium hexafluorides, in acetonitrile, are capable of oxidising a number of transition and post-transition metals to give solvated metal cation salts of the appropriate MF_6^- anion.^{44,45} For example copper and cadmium react with the hexafluorides, in MeCN, forming the products, $[\text{A}(\text{NCMe})_5]_2[\text{MF}_6]_2$, (A = Cu and Cd, and M = Mo, W and U). In some cases, the oxidation state of the metal cation obtained, depends on the hexafluoride used, thus thallium metal is oxidised to Tl(III) by MoF_6 or UF_6 but to Tl(I) by WF_6 . The redox couples, $\text{MF}_6/\text{MF}_6^-$, (M = Mo, W or U) have been identified in MeCN, with half-wave potentials, $E_{1/2}(\text{UF}_6/\text{UF}_6^-) = 2.33\text{V}$, $E_{1/2}(\text{MoF}_6/\text{MoF}_6^-) = 1.60\text{V}$ and $E_{1/2}(\text{WF}_6/\text{WF}_6^-) = 0.51\text{V}$ versus Ag^+/Ag . The difference between $E_{1/2}(\text{MoF}_6/\text{MoF}_6^-)$ and $E_{1/2}(\text{WF}_6/\text{WF}_6^-)$ in HF and MeCN, is almost identical. The order of oxidising ability, in MeCN, determined from a combination of cyclic voltammetry and redox chemistry is shown to be $\text{UF}_6 > \text{MoF}_6 > \text{WF}_6$.⁴⁶ The redox reactions alone do not differentiate between UF_6 and MoF_6 but the chemical behaviour of WF_6 is clearly differentiated both by its weaker oxidising power and by its ability to participate in F^- ion transfer equilibria.^{46,47} Molecular iodine is oxidised by MoF_6 or UF_6 but not by WF_6 , in acetonitrile, to give isolable salts, $[\text{I}(\text{NCMe})_2][\text{MF}_6]$, (M = Mo or U).⁴⁸ This behaviour is in contrast to that observed in IF_5 solution⁴¹ where I_2 is oxidised to I_2^+ by UF_6 but not by MoF_6 . This difference in the behaviour is discussed in a later part of this chapter.

Of the group V A pentafluorides, PF_5 is found to oxidise slowly Cu metal to Cu(I) with the formation of phosphorus trifluoride.⁴⁹



On the other hand AsF_5 , in MeCN, has no oxidising ability towards Cu or Ag metals. This is ascribed to the formation of the adduct, $\text{AsF}_5 \cdot \text{NCMe}$, which is kinetically stable to reduction. In SO_2 solution, AsF_5 has been used as an oxidising agent to form salts such as CuAsF_6 or $\text{Ni}(\text{AsF}_6)_2 \cdot 2\text{SO}_2$.⁵⁰ In the latter complex, it has been suggested that four oxygens from two SO_2 molecules are co-ordinated to Ni(II) in a bidentate arrangement. Pentafluorides of group V A have also been used for the generation of a number of homopolyatomic cations especially those of group VI and VII elements. Kemmitt *et al.*⁵¹ isolated blue solids from mixtures of I_2 , IF_5 and SbF_5 or TaF_5 , which they formulated as $\text{I}_2^+ \text{Sb}_2\text{F}_{11}^-$ and $\text{I}_2^+ \text{Ta}_2\text{F}_{11}^-$. Gillespie and co-workers⁵² obtained dark blue crystals of $\text{I}_2^+ \text{Sb}_2\text{F}_{11}^-$ by treating I_2 in liquid SO_2 with an approximate three fold excess of SbF_5 . The pentafluoride acted as an oxidant and as a Lewis acid producing the very weakly basic anion $\text{Sb}_2\text{F}_{11}^-$. Neither the reduction product, SbF_3 nor the solvent SO_2 , is sufficiently basic to cause the disproportionation of the cation I_2^+ . Subsequently, Passmore and co-workers⁵³ isolated and structurally characterized compounds containing the I_3^+ and I_5^+ cations under non-basic conditions. They reacted I_2 and AsF_5 in SO_2 solution to form crystalline $\text{I}_3^+ \text{AsF}_6^-$. Similarly $\text{I}_5^+ \text{SbF}_6^-$ was isolated from a stoichiometric mixture of I_2 and SbF_5 in liquid AsF_3 .⁵⁴

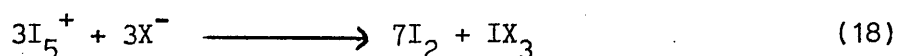
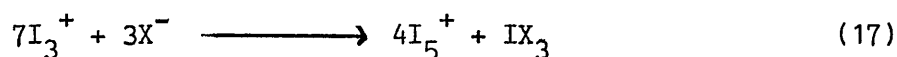
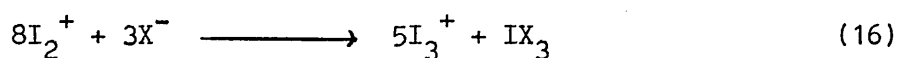
The polyatomic cation of bromine, $\text{Br}_2^+ \text{Sb}_3\text{F}_{16}^-$, has been generated by reacting Br_2 and SbF_5 in the oxidising solvent, BrF_5 , under weakly basic conditions.⁵⁵



The polyatomic cations of sulphur have been obtained by reacting

stoichiometric amounts of sulphur and either SbF_5 or AsF_5 in HF .⁵⁶ From the reacting proportions, 2:3, products of the general formula, $\text{S}_{16}(\text{MF}_6)_2$, (M = As or Sb), are isolated. The reaction of sulphur with excess SbF_5 directly or in liquid SO_2 , produces the cation, S_4^{2+} , thus showing the greater oxidising ability of SbF_5 over AsF_5 .⁵⁷

From the above survey, it can be concluded that the homopolyatomic cations of non-metals, are stabilized as the acidity of the medium increases. Increasing acidity of the medium implies decreasing availability of the base of the solvent systems, which otherwise has resulted in the disproportionation of the cationic species. For all of the above homopolyatomic cations, progressive addition of the base leads ultimately to disproportionation of the cations to the elements itself and to a non-ionic compound between the base and the particular element in an oxidation state higher than that in the cation which disproportionated. Typical generalized equations representing the disproportionation reactions of polyatomic iodine cations are represented in the equations:⁵⁸



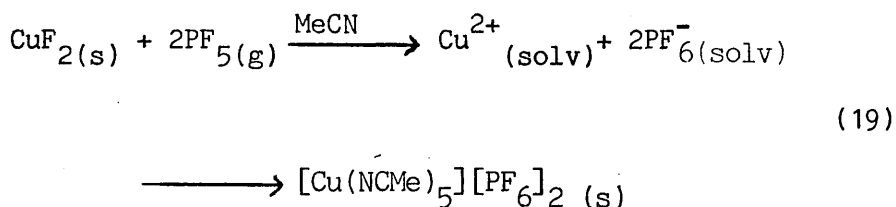
$\text{X} = \text{HSO}_4^-$, SO_3F^- or F^-

Polynuclear cations, for example, I_2^+ , I_3^+ and I_5^+ which are characteristically formed when iodine is oxidised in strongly acidic solvents such as IF_5 or SO_2 ,⁵⁸ are apparently not formed in the basic solvent, MeCN. The acidic solvents, that is IF_5 or SO_2 are poor solvating agents whereas acetonitrile has a good solvating ability hence favours the formation of mono-nuclear cations e.g. I^+ .

1:3:3 Lewis Acid - Lewis Base Reactions.

A number of complexes with the general formula, $[M(\text{CH}_3\text{CN})_n]_2[\text{SbCl}_6]_2$, ($M = \text{Fe, Co, Mn, Ni, Cu, Zn}$ and $n = 4$ or 6) have been synthesized by the reaction of SbCl_5 with metal chlorides in acetonitrile.⁵⁹ In these reactions, metal chlorides act as Lewis bases and SbCl_5 as a Lewis acid. Recently, salts of the type, $[\text{MCl}_x(\text{MeCN})_{6-x}][\text{SbCl}_6]$, have been isolated from reactions of transition metal halides, MCl_n , ($M = \text{Ti, } n = 4$; $M = \text{V or Fe, } n = 3$; $M = \text{Fe, } n = 2$) with SbCl_5 in acetonitrile.⁶⁰ Similar reactions involving metal chlorides as Lewis bases and SnCl_4 as a Lewis acid, in acetonitrile, result in the formation of complexes, $[\text{M}(\text{MeCN})_n][\text{SnCl}_6]_2$.⁶¹

Heterogeneous Lewis acid-base reactions involving covalent high oxidation state fluorides as Lewis acids and metal binary fluorides as Lewis bases, have been used to generate solvated metal cations in acetonitrile. For example anhydrous CuF_2 or TlF react with WF_6 in acetonitrile forming the soluble $\text{Cu}(\text{II})$ or $\text{Tl}(\text{I})$ heptafluorotungstates.⁶² The solid salts isolated are $[\text{Cu}(\text{NCMe})_5][\text{WF}_7]_2$ and TlWF_7 respectively. The pentafluorides of phosphorus, arsenic and tantalum react with CuF_2 , in the same way, forming the corresponding solvated $\text{Cu}(\text{II})$ hexafluoro-anion salts.⁴⁹



Copper(II) fluoride, in the same way, reacts with UF_5 in acetonitrile at room temperature to give the solvated copper(II) hexafluorouranate(V) salt.⁶³

The complex fluoro-anions formed in the above reactions, generally show little or no tendency to co-ordinate to the cation. This is not

the case for the chloro-anion species formed in other similar reactions. The greater co-ordinating ability of chloro-anions as compared with fluoro-anions, is explained on the basis of lower electronegativity of chlorine than that of fluorine thus making it easier to form chlorine bridges. This property of little or no co-ordination of fluoro-anions is very important as the metal cation being studied, has only the solvent in its co-ordination sphere and thus free from the effect of anion. The assumption of little or no co-ordination of fluoro-anions to the cation, is based largely on indirect methods such as infra-red and Raman spectroscopy. ^{205}Tl n.m.r. spectroscopy provides a direct spectroscopic method for probing cation-anion interactions and is of considerable importance because of the exceptional sensitivity of the thallium nucleus to its environment. It has been used in the present work as a probe for cation-anion interaction.

1:4 [^{205}Tl]-Thallium N.M.R. Spectroscopy.

The advent of Pulsed Fourier Transform nuclear magnetic resonance spectroscopy has attracted many investigators to explore the n.m.r. properties of the elements of the periodic table. Thallium is one of the elements studied during the early period in the history of n.m.r. spectroscopy. The outer electronic configuration of thallium, $6s^2 6p^1$, suggests that +1 and +3 are the two possible oxidation states. The Tl^+ ion is a good replacement for the Na^+ and K^+ ion in many biological systems,^{64,65} thus providing a convenient spectroscopic alternative for the study of such phenomena as, ion transport across the membranes, activation and regulation of enzymes etc. Kayne determined the number of monovalent binding sites in rabbit muscle pyruvate kinase through substitution of Tl^+ for K^+ and also found Tl^+ to activate yeast pyruvate kinase and AMP amino-hydrolyse.⁶⁶ Williams et al. found that Tl^+

activated 1,2-propanediol dehydrase.⁶⁴ Krasne and Elsenman have used Tl^+ to investigate the type of ligand groups responsible for binding ions in biological ion carriers.⁶⁷

The spectral parameters of the ^{205}Tl nucleus are exceptionally sensitive to its chemical environment. This exceptional sensitivity arises from the paramagnetic term of the nuclear shielding tensor.⁶⁸ For thallium, the diamagnetic contribution per valence electron is of the order of 100-250 p.p.m. This is small compared to the observed chemical shift range of about 7000 p.p.m. This means that the paramagnetic term must be responsible for about 95% of the variation observed in thallium chemical shifts.

Thallium(I) salts in general, show low solubility in most solvents even water. However, liquid ammonia is an excellent solvent for $TlNO_3$ and $TlClO_4$. The $Tl(I)$ resonance frequency, for liquid NH_3 solutions of $TlNO_3$ and $TlClO_4$, has been determined as a function of salt concentration.⁶⁹ The dependence of the resonance frequency on concentration suggests the presence of free, fully solvated thallium ions, ion-pairs and higher order aggregates as the concentration is varied.

^{205}Tl n.m.r. spectroscopy, in the present study, has been used to investigate the effect of complex fluoroanions on $^{205}Tl^{3+}$ and $^{205}Tl^+$ chemical shifts, in MeCN solution, in order to probe cation-anion interactions. The second aspect of this work that requires ^{205}Tl n.m.r. is concerned with the redox behaviour of the solvated Tl^{3+} cation in MeCN since oxidation states of thallium, that is Tl^{3+} and Tl^+ , are readily differentiated from their chemical shifts.⁴⁸

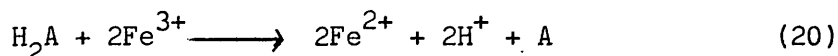
1:5 Redox and Substitution Reactions.

A number of redox and substitution reactions involving solvated cations and simple N, P and S-donor ligands, have been studied during the course of the present work. Although the mechanisms of such

reactions have not been investigated here, it is appropriate to describe briefly the mechanisms involved in such reactions.

1:5:1 Redox Reactions.

Redox reactions involve a change in the oxidation state of at least two reactants. Such reactions usually lead to a marked change in the species as indicated in equation (20).⁷⁰

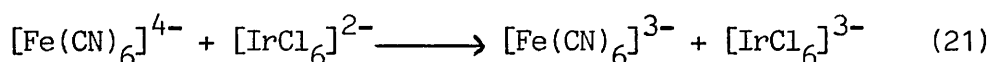


H_2A = ascorbic acid

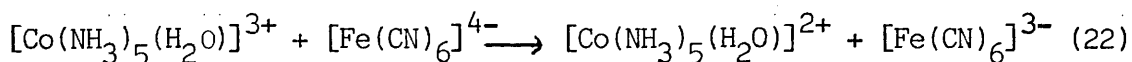
The first step in the overall process appears to be complex formation between the metal and the substrate species often behaving as ligands. This is followed by the redox reaction involving a direct intramolecular electron transfer within the adduct. Two distinct mechanisms for redox reactions of complexes are recognised. These are the inner-sphere and outer-sphere mechanisms.

(i) The Outer Sphere Mechanism.

In this mechanism, the redox step simply involves electron transfer from reductant to oxidant, with the co-ordination spheres of each staying intact. One reactant becomes involved in the secondary co-ordination sphere of the other reactant and an electron flows from reductant to oxidant.⁷¹ For example, equation (21)

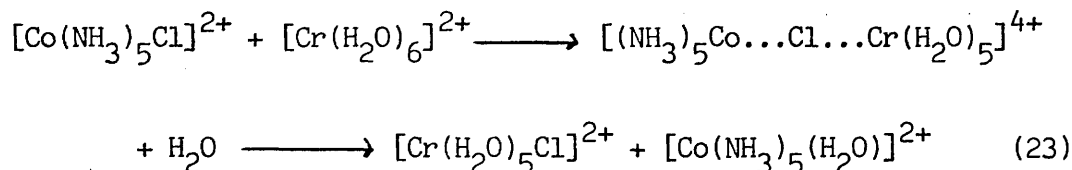


Such a mechanism is established when rapid electron transfer occurs between two substitution inert complexes as in the reaction,⁷² equation (22)



(ii) The Inner Sphere Mechanism.

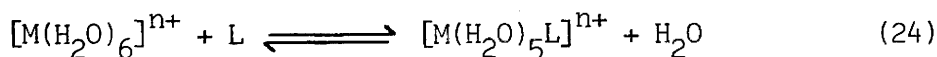
The essential feature of this mechanism is that the reductant and oxidant share a ligand in their primary co-ordination spheres, the electron being transferred across a bridging group as in the reaction,⁷³ equation (23)



The lability of the cobalt(II) species, thus generated is such that it will instantly form, $[\text{Co}(\text{H}_2\text{O})_6]^{2+}$ and ammonium ions in acidic aqueous solution.⁷⁴ For an inner sphere mechanism, there are two prerequisites, the first requirement is that one reactant (usually the oxidant) possesses at least one ligand capable of binding simultaneously to two metal ions, however transiently. Although this bridging ligand is frequently transferred from oxidant to reductant, ligand transfer is not a requirement for an inner sphere mechanism. The second requirement is that one ligand of one reactant, usually the reductant, be substitutionally labile, that is one ligand must be capable of being replaced by a bridging ligand in a facile substitution process.

1:5:2 Substitution Reactions

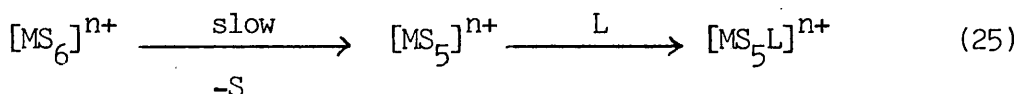
Solvent molecules in the solvated cations can be replaced by other ligands. For example, in the simplest case, the replacement of water in an hexa-aquo ion, $[\text{M}(\text{H}_2\text{O})_6]^{n+}$, by a neutral unidentate ligand, L, is represented by equation (24).⁷⁵



and ultimately results in the formation of $[ML_6]^{n+}$. Metal complexes that react within a time of few seconds or less are termed labile whereas those taking minutes or longer for completion of the substitution reactions are considered inert.⁷⁶ The mechanisms of ligand substitution reactions, for an octahedral complex, are generally divided into four groups.⁷⁷

(i) Dissociative (D)

This mechanism involves the removal of a ligand from the complex cation, forming a five co-ordinate intermediate, which then picks up the incoming ligand.

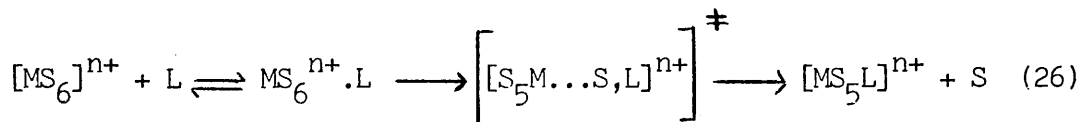


S = the solvent molecule and L = incoming ligand.

The rate of this reaction is governed by the first dissociative step which is far slower than the subsequent uptake of the incoming ligand, L, hence dissociative reactions are also termed as limiting S_N1 reactions.

(ii) I_d Mechanism

This is the dissociative interchange mechanism. In this mechanism the transition state formation involves a considerable extension of the metal to leaving group bond but very little interaction between the cation and the incoming group. However, this mechanism does involve outer sphere association between the starting complex and the incoming ligand.



The outer sphere associated species, $MS_6^{n+} \cdot L$, is simply an ion pair if the complex and the incoming group have opposite charges. However,

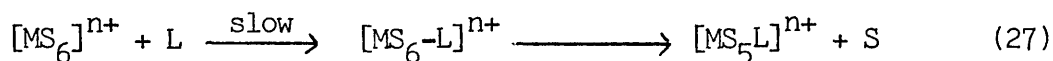
it is not necessary for the incoming group to be charged for this mechanism to operate.

(iii) I_a Mechanism

This is the associative interchange mechanism. This mechanism involves an interchange of ligands between the primary and secondary co-ordination regions and the interaction between the cation and the incoming group is much more significant as compared to I_d mechanism.

(iv) Associative (A)

This mechanism involves the association of the incoming ligand to the original complex cation, forming a seven co-ordinated intermediate which subsequently loses one of the original ligands.



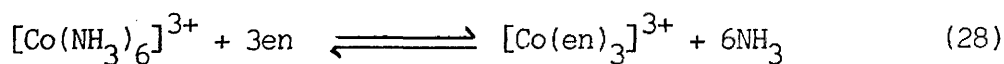
The associative step involving the formation of the seven co-ordinated species, MS_6L^{n+} , is slow and is the rate determining step hence associative reactions are also called limiting S_N2 reactions.

The correlation of a reaction with a particular mechanism may be achieved by a number of ways.⁷⁸ These include, rate law determination, comparing the rate of a reaction of a metal ion with different ligands, especially for solvent exchange, and evaluating the activation parameters of the reaction. For the bivalent 1st row transition metal ions, $[\text{M}(\text{Solvent})_6]^{2+}$, (M = Mn, Fe, Co, Ni and Cu) in a number of solvents e.g. CH₃OH, CH₃CN, Me₂SO, DMF, NH₃ and CH₃COOH, it has been found by using high pressure n.m.r. spectroscopy that activation parameters, for solvent exchange reaction, display a gradual mechanistic change, associative to dissociative, on going from left to right across the periodic table.⁷⁹

1:6 Aim of the Present Work.

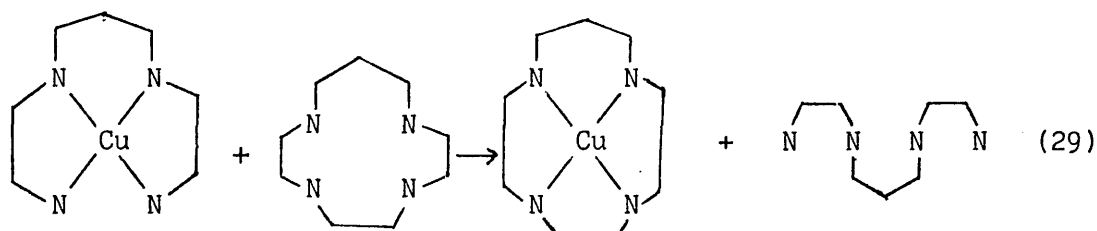
The aim of the work described in this thesis, is to study the co-ordination chemistry of selected solvated metal and non-metal cations, in acetonitrile, under conditions in which oxygen and moisture are excluded. The syntheses of the solvated cations, in acetonitrile, have been carried out by (i) the oxidation of metals and non-metals using transition metal hexafluorides or NO^+ as oxidising agents and (ii) Lewis acid-Lewis base reactions between covalent high oxidation state fluorides and metal binary fluorides. Where possible, the complexes are obtained as PF_6^- salts because this anion is very stable with respect to hydrolysis in MeCN solution.

The ligands used in the present study are the simple N,P and S-donor species such as NH_3 , NMe_3 , pyridine, PMe_3 , P(OMe)_3 , Me_2S and tetramethylthiourea. These species are regarded as weak ligands compared with chelating and macrocyclic ligands which possess greater stabilizing ability. The extra stability of complexes containing chelate or macrocyclic ligands, is mostly due to the thermodynamic factors. For example in the reaction represented by equation (28),⁸⁰



the bonding of ammonia and ethylenediamine (en) to metal centre is very similar, hence the enthalpy change for this reaction is near to zero. The change in entropy for the reaction is proportional to the difference in the number of unco-ordinated species present in the system. The reaction proceeds to the right with an increase in the number of unco-ordinated species and hence the entropy factor favours the formation of the chelate system instead of the hexa-ammine. Macrocyclic ligands give even more stable complexes than the most similar n-dentate open chain ligands. For example, in the reaction

represented by equation (29)



the entropy always favours the macrocycle with a value of ca. $70 \text{ J mol}^{-1} \text{ deg}^{-1}$.⁸¹

The main objective of selecting the simple N,P and S- donor species as ligands, in the present study, is to investigate how far these ligands are able to stabilize metal and non-metal cations, in acetonitrile. The simple, N,P and S- donor ligands are quite susceptible to hydrolysis in aqueous solution and some of them are very good proton acceptors hence are not able to retain their identity in aqueous acidic medium. The ligands are volatile and, therefore, require vacuum technique where it is also easy to maintain rigorous anhydrous conditions. The N-donor species such as NH_3 and pyridine are comparatively weak ligands hence easily replaced by other potential ligands thus provide a base for studying the substitution reactions of the cations.

The elements selected for this project are the transition metals, iron and copper, the post transition metal, thallium and the non-metal, iodine. Iron(II) forms stable, low spin octahedral or distorted octahedral complexes with ligands such as phenanthroline, dipyrindyl and others supplying imine nitrogen donor atoms,⁸² whereas in the present work, iron(II) has been found to form high spin complexes with N-donor ligands such as NH_3 , NMe_3 and pyridine. The behaviour of these high spin iron(II) cations, in substitution reactions with simple P-donor ligands, for example P(OMe)_3 and PMe_3 , has been investigated.

Unlike the situation in water, the dominant species in acetonitrile is iron(II) and no iron(III) species with simple N-donor ligands have been formed in the present study. Copper(II) and Copper(I) species are well known in acetonitrile. Previous work has shown very interesting behaviour for copper(II), in MeCN, in reactions with tetramethylthiourea,⁸³ and P(OMe)₃.⁸⁴ The metal ion is reduced to copper(I) with concomitant oxidation of the ligand. This work has been extended and similar reactions with other ligands such as NMe₃, PMe₃ and Me₂S, were attempted. Of the post transition elements, thallium has been selected for a number of reasons. In aqueous solution, Tl(I) is distinctly more stable than Tl(III), (Tl³⁺-Tl⁺ couple, E⁰ = 1.25V relative to N.H.E.). Solutions of [Tl(H₂O)₆]³⁺ are subjective to extensive hydrolysis forming [Tl(H₂O)₅(OH)]²⁺ and H⁺. The value of K_a is 7 x 10⁻².⁸⁵ In the present study, complex fluoroanion salts of Tl(I) and Tl(III) have been investigated with a view to probe cation-anion interactions, in MeCN. Among the non-metals, iodine is one of the widely studied elements and has been found to form a number of charge transfer complexes with the donor solvents.⁸⁶ In acetonitrile, oxidation of iodine by UF₆ or MoF₆, results in the formation of the mononuclear cation, [I(MeCN)₂]⁺, rather than polynuclear cations, because of its good solvating ability. In the present work, substitution reactions of solvated I⁺ cation with simple N,P and S-donor ligands, and macrocyclic nitrogen donor ligands, for example, 1,4,8,11-tetraazacyclotetradecane (cyclam) and 1,4,8,12-tetraazacyclopentadecane, ([15]ane-N₄), have been investigated. The electrochemistry of the resulting I⁺ complexes as MoF₆⁻ salts, in acetonitrile, has also been studied using the technique of cyclic voltammetry.

CHAPTER TWO

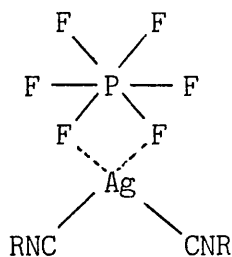
^{205}Tl -Thallium N.M.R. Study of Tl^{I}
and Tl^{III} Salts of Complex
Fluoroanions in Acetonitrile

2:1 Introduction.

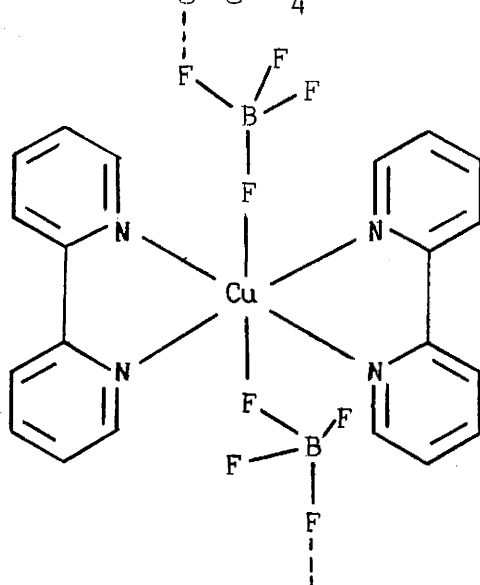
Complex fluoroanions are regarded as very weak bases and the fluoroanions such as BF_4^- , PF_6^- , AsF_6^- and SbF_6^- are generally non-coordinating with both hard and soft cations.⁸⁷⁻⁹⁰ A survey of the Cambridge Crystallographic Data Base reveals that out of over 500 crystal structures containing the BF_4^- anion, only 1% shows the anion to be semicoordinated.⁹¹ Semicoordination is the term used to represent the coordination in which bond distance is greater than the normal covalent bond but nonetheless smaller than the sum of Van der Waal's radii of the two species involved.

2:1:1 Evidence for Coordination of Complex Fluoroanions in the Solid State.

The semicoordination of complex fluoroanions has been reported in a number of salts and the definite way to establish it is by x-ray crystallography. The x-ray crystal structure of the complex, $\text{NiL}_4(\text{PF}_6)_2$, (L = 4-methyl pyridine), has been determined by Morrison et al. and consists of a square planar array of 4-methyl pyridine ligands about nickel with hexafluorophosphate groups above and below the plane.⁹² The Ni-F distance of 3.031 Å is only marginally less than the estimated sum of the Van der Waal's radii, 3.1 to 3.2 Å, therefore, the anions are not fully coordinated to nickel but are nonetheless held in axial positions by weak, essentially ionic interactions. An x-ray crystallographic analysis of the compound, $\text{Ag}(\text{RNC})_2(\text{PF}_6)$, (R=2,4,6-t. $\text{Bu}_3\text{C}_6\text{H}_2$) has been carried out by Yamamoto et al.⁹³ and the complex has been shown to have a distorted tetrahedral configuration, in which the PF_6 group behaves as a bidentate ligand.



A different type of coordination has been observed in the x-ray crystallographic study of the complexes, $(\text{CO})_5\text{Re}(\text{FAsF}_5)^{94}$ and $(\text{CO})_5\text{Re}(\text{FBF}_3)^{95}$, where the anions are behaving as monodentate ligands. The crystal structure of the complex $[\text{Cu}(\text{BF}_4)(\text{bipy})_2][\text{BF}_4]$, (bipy = bipyridyl) has recently been determined by the x-ray diffraction technique.⁹⁶ The crystal structure is composed of BF_4^- anions and polymeric chains of cations, $[\text{Cu}(\text{BF}_4)(\text{bipy})_2]^+$, in which each BF_4^- group bridges two adjacent copper centres through its two fluorine atoms. The coordination polyhedron around the copper is a tetragonally distorted octahedron; the four nitrogen atoms of bipyridine molecules are arranged in a flattened tetrahedral manner above and below the equatorial plane, and the axial positions are occupied by fluorine atoms of the bridging BF_4^- ions.

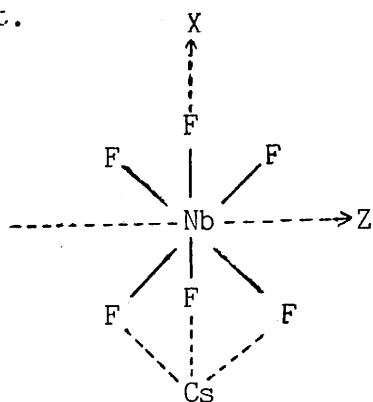


Crystallographic and infrared evidence for the unidentate coordination of BF_4^- anion has been observed in the complexes, $[\text{Ni}(\text{en})_2(\text{OH}_2)(\text{FBF}_3)][\text{BF}_4]$,⁹⁷ $[\text{Cu}(\text{FBF}_3)(\text{PPh}_3)_3]$,⁹⁸ and

$[\text{CuL}_2(\text{OH}_2)(\text{FBF}_3)_2]$,⁹⁹ (L = nicotinamide). The infrared spectrum of the nickel complex shows significant splitting of the $\nu_3(\text{BF}_4^-)$ mode into three peaks and ν_1 appears with medium intensity, consistent with the short Ni-F bond distance. The copper(I) complex shows no infrared evidence for semicoordination of the BF_4^- anion despite the relatively short Cu-F distance. For the copper(II) nicotinamide complex, the infrared spectrum is not reported. Semicoordination of the BF_4^- anion has been observed in the complex, $[\text{CuL}_2(\text{FBF}_3)_2]$,¹⁰⁰ (L = 2,5-dithiohexane) by means of crystallographic study but no infrared spectrum is reported.

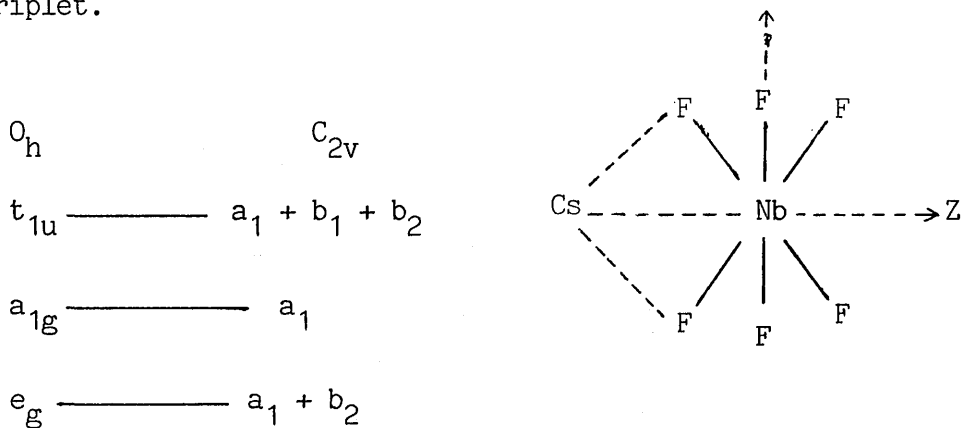
I.R. Beattie and K.R. Millington have recently demonstrated that heavier alkali metal salts of a number of hexafluoroanions, can be vaporized as molecular species.¹⁰¹ From the matrix isolated infrared spectrum of CsNbF_6 , it is found that for matrices where the host-guest interaction is expected to be weak (Ne,Ar), a characteristic doubling of the ν_3 mode of the NbF_6^- anion is observed and interpreted as being due to the presence of a tridentate (facial) interaction between the Cs^+ and the NbF_6^- ions. This facial interaction results in the lowering of the NbF_6^- anion symmetry from O_h to C_{3v} which leads to the splitting of the $\nu_3(t_{1u})$ mode into a doublet.

O_h	C_{3v}
t_{1u} —————	$a_1 + e$
a_{1g} —————	a_1
e_g —————	e



For matrices where the host-guest interaction is expected to be strong (CO, N_2), a characteristic triplet, due to a bidentate (edge) interaction between the Cs^+ and NbF_6^- ions, is observed. This bidentate

interaction leads to C_{2v} symmetry in which the $\nu_3(t_{1u})$ mode splits into a triplet.



From a combination of electronic, e.p.r. and infrared spectroscopy, semicoordination of PF_6^- anion has been suggested to be present in the complex $Cu(py)_4(PF_6)_2$.¹⁰² Similarly the electronic and vibrational spectra and magnetic susceptibility data of the complex, $Ni(py)_4(AsF_6)_2$, suggest that the compound has a structure similar to that of $NiL_4(PF_6)_2$, (L = 4-methyl pyridine), with the anions only weakly interacting with the cation at high temperature and fully coordinated at low temperature.⁹² The semicoordination of the fluoroanion has been observed in the copper(II) complexes $CuL_4(EF_6)_2$, (L = pyridine or 4-methyl pyridine, and E = P or As), from a combination of electronic, e.p.r. and infrared spectral studies.¹⁰³ A comparison of the infrared spectra of the copper(II) complexes with those of the analogous, $CoL_4(EF_6)_2$,^{104,105} and $NiL_4(EF_6)_2$ complexes,⁹² provides evidence for semicoordination of the fluoroanion. In the infrared spectrum the $\nu_1(a_{1g})$ and $\nu_2(e_g)$ vibrational modes, which are formally forbidden in O_h symmetry but become allowed when the symmetry of the fluoroanion is reduced to C_{4v} due to its coordination to the metal, are observed. These bands are weak or not observed in the cobalt(II) complexes where the anions are non-coordinated. In the nickel(II) complexes where the fluoroanions are weakly coordinated, these bands appear with medium intensity whereas in the copper(II),

complexes where even stronger coordination is evident, the bands are generally more intense, ν_2 being split into strong a_1 and weak b_1 components (the latter forbidden in infrared) in the AsF_6^- complexes. The electronic spectra of the copper(II) complexes, consist of a single broad asymmetric band in the visible region with band maxima around 18000 to 19000 cm^{-1} , and are consistent with either a square coplanar CuN_4 chromophore or with an elongated tetragonal-octahedral ligand field as would be obtained in a structure involving four neutral ligands forming a square plane about copper with fluoroanions coordinated in axial positions.¹⁰⁶ The e.p.r. data provide clear support for the second type of structure. The infrared evidence for the semicoordination of BF_4^- anion, as a unidentate species,²¹ is observed in the complexes, $\text{Mn}(\text{MeCN})_4(\text{FBF}_3)_2$ and $\text{Zn}(\text{MeCN})_4(\text{FBF}_3)_2$, and as a bidentate group, in the complex, $\text{SnMe}_3(\text{F}_2\text{BF}_2)$.¹⁰⁷ The coordination of BF_4^- anion has also been observed in the complex, $\text{CoL}_4(\text{BF}_4)_2 \cdot \text{H}_2\text{O}$, (L = 2,6-dimethyl pyridine N-oxide) by infrared spectroscopy when each of the ν_3 and $\nu_4(\text{BF}_4^-)$ modes are triply split while ν_1 and $\nu_2(\text{BF}_4^-)$ modes become infrared active.¹⁰⁸ The monodentate coordination of the BF_4^- and the AsF_6^- anions, has been observed by infrared spectroscopy in the complexes $[\text{Re}(\text{CO})_3(\text{L})(\text{FBF}_3)](\text{H}_2\text{O})$, (L = N,N,N',N'-tetramethylethane-1,2-diamine) and $[\text{Re}(\text{CO})_3(\text{bipy})(\text{FAsF}_5)](\text{H}_2\text{O})$.¹⁰⁹

2:1:2 Properties of Solvated Cation, Fluoroanion Salts in Solution.

A number of metal and non-metal complex fluoroanion salts have been prepared using acetonitrile as solvent in this Department over the past few years. The salts are soluble in acetonitrile and have been characterized by a number of techniques. In these salts, no definite spectroscopic evidence is observed for interaction between the cations and the anions either in the solid state or in solution. For example the

^{31}P n.m.r. spectrum in CD_3CN , of the complex $[\text{Cu}(\text{NCMe})_5][\text{PF}_6]_2$, having the paramagnetic cation, Cu^{2+} , and the diamagnetic anion, PF_6^- consists of a 1:6:15:20:15:6:1 septet due to the coupling with six equivalent fluorine nuclei and is characteristic of the free PF_6^- anion. The solid state infrared spectrum of the complex, however, shows a splitting of the ν_3 mode of the PF_6^- anion into two components.⁴⁹ This phenomenon is observed in some of the other PF_6^- salts and by itself does not constitute a proof of cation-anion interaction.

Another example is the complex $[\text{Ag}(\text{py})_4(\text{NCMe})][\text{MoF}_6]_3$, in which the Ag^{III} cation is diamagnetic and the MoF_6^- anion is paramagnetic.¹¹⁰ The ^{13}C - ^1H n.m.r. spectrum of the complex, in EtCN , consists of three sharp singlets assigned to coordinated pyridine and a relatively broad peak due to the cyano- ^{13}C nuclei of MeCN and EtCN . These observations are consistent with a square planar, $[\text{Ag}(\text{py})_4]^{3+}$, cation having weakly coordinated MeCN . The paramagnetic anion, MoF_6^- does not seem to have any noticeable effect on the n.m.r. resonances of the complex cation. It has also been observed that the symmetry of the MoF_6^- anion is not apparently affected by the counter cation. For example there is no spectroscopic evidence for interaction between $[\text{Ag}(\text{py})_4]^+$ ¹¹⁰ or $[\text{I}(\text{NCMe})_2]^+$ ⁴⁸ and the MoF_6^- anion, either in the solid state or in acetonitrile solution. Both solid and solution Raman spectra contain a strong band at 680 cm^{-1} assigned to the ν_1 mode of MoF_6^- anion. Bands in the infrared spectrum at 635 (solid) and 645 cm^{-1} (MeCN) are assigned to the ν_3 mode and a band at 252 cm^{-1} in the solid state infrared spectrum, to the ν_4 mode of the MoF_6^- anion. The molybdenum EXAFS spectra¹¹¹ of these complexes are consistent with the presence of a regular octahedral MoF_6^- anion, $\text{Mo}-\text{F} = 1.79 \pm 0.01\text{ \AA}$ compared with $1.74 \pm 0.03\text{ \AA}$ determined from an x-ray powder diffraction study of NaMoF_6 .¹¹²

The evidence obtained in all the above cases from spectroscopic studies (infrared, Raman, electronic and e.p.r.) about the cation-anion interactions may be regarded as indirect. The exceptional sensitivity of the ^{205}Tl nucleus to its environment and the accessibility to Tl^{3+} and Tl^+ oxidation states, in acetonitrile solution, makes ^{205}Tl n.m.r. spectroscopy an excellent probe for studying cation-anion interactions in solution and provides a direct method for observing the behaviour of complex fluoroanions towards the cations.

2:1:3 [^{205}Tl]-Thallium N.M.R. Spectroscopy.

Thallium has two isotopes, ^{203}Tl (29.5%, natural abundance) and ^{205}Tl (70.5% natural abundance), both of which have spin, $I = \frac{1}{2}$. The relative receptivity of ^{205}Tl nucleus is 0.1355 compared to 1 for the proton. The nuclear properties of ^{205}Tl nucleus make it easy to be observed in the n.m.r. experiments. The chemical shift range for thallium is extremely large, about 7000 ppm for Tl^{III} species and over 3400 ppm for Tl^{I} species.⁶⁸ The origin of this large chemical shift range lies with the paramagnetic term of the nuclear shielding tensor as has been discussed in chapter one.

The aim of the work described in this chapter is to investigate the effect of different complex fluoroanions, that is PF_6^- , WF_7^- , WF_6^- , MoF_6^- and UF_6^- on $^{205}\text{Tl}^+$ and $^{205}\text{Tl}^{3+}$ chemical shifts over a range of concentrations, with a view to probing cation-anion interactions in MeCN solution. The present work appears to be the first study in which both Tl^{I} and Tl^{III} have been examined under comparable conditions of solvent and counteranion. Previous work carried out in the Department has shown that solvated Tl^{3+} and Tl^+ cations in MeCN, are readily differentiated from their ^{205}Tl chemical shifts.⁴⁸ The present work involves a more detailed study of the concentration dependence of ^{205}Tl chemical shifts and includes experiments designed

to investigate possible interactions between Tl^I and Tl^{III} in mixed oxidation state compounds.

2:2 Results.

2:2:1 Study of Thallium(I) Salts.

The thallium(I) salts, $TlPF_6$, $TlMoF_6$ and $TlUF_6$ are soluble in acetonitrile up to a concentration of 0.34 mol dm^{-3} . Thallium(I) heptafluorotungstate(VI) was an exception. It was observed that all of the solid salt did not go into solution, presumably some thallium fluoride, formed from the decomposition of $TlWF_7$, was precipitated. This material was redissolved by the addition of a trace of WF_6 to the mixture.

The variation of ^{205}Tl chemical shift as a function of salt concentration, in acetonitrile solutions of thallium(I) salts with diamagnetic anions, PF_6^- and WF_7^- , is represented in Figure 1 and found to be non-linear. It was observed that an increase in salt concentration resulted in a small increase of about 3 to 5 ppm in ^{205}Tl shielding over a concentration range of 0.04 to 0.14 mol dm^{-3} . The $^{205}Tl^+$ chemical shifts observed for $TlPF_6$ were -232.3 and -236.98 ppm at 0.0405 and $0.134 \text{ mol dm}^{-3}$ concentrations, whereas for $TlWF_7$ these were -235.1 and -240 ppm at concentrations 0.0402 and $0.134 \text{ mol dm}^{-3}$ respectively. A high field shift in ^{205}Tl resonance was thus observed in acetonitrile solutions of $TlPF_6$ and $TlWF_7$ with an increase in salt concentration, the WF_7^- induced shift being larger than the PF_6^- induced shift. The peak widths at half heights of ^{205}Tl signals originating from $TlPF_6$ and $TlWF_7$ solutions were in the range 30-40Hz. The $^{205}Tl^+$ chemical shift data for $TlPF_6$ were obtained using eight different concentrations whereas only four different concentrations were studied for $TlWF_7$ because of the precipitation of TlF during the dissolution in MeCN.

Figure 1. Variation of ^{205}Tl Chemical Shift (w.r.t. $\text{Tl}^+\text{aq.}$) with Concentration in MeCN.

TlPF_6 , \circ ; TlWF_7 , \square

δ_f = 'Free ion' chemical shift of Tl^+ ion.

δ_{ip} = Chemical shift of the ion-pair

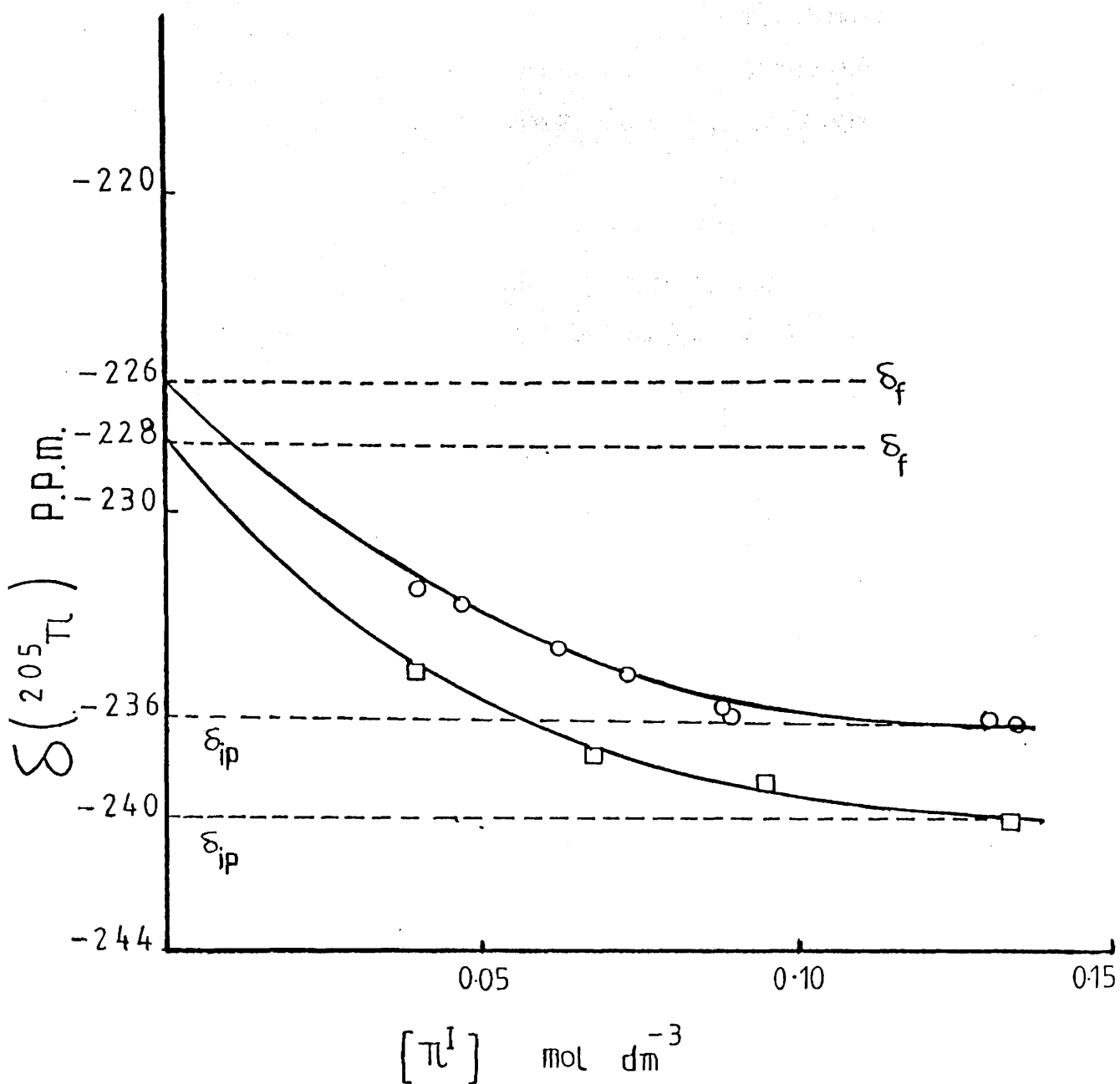


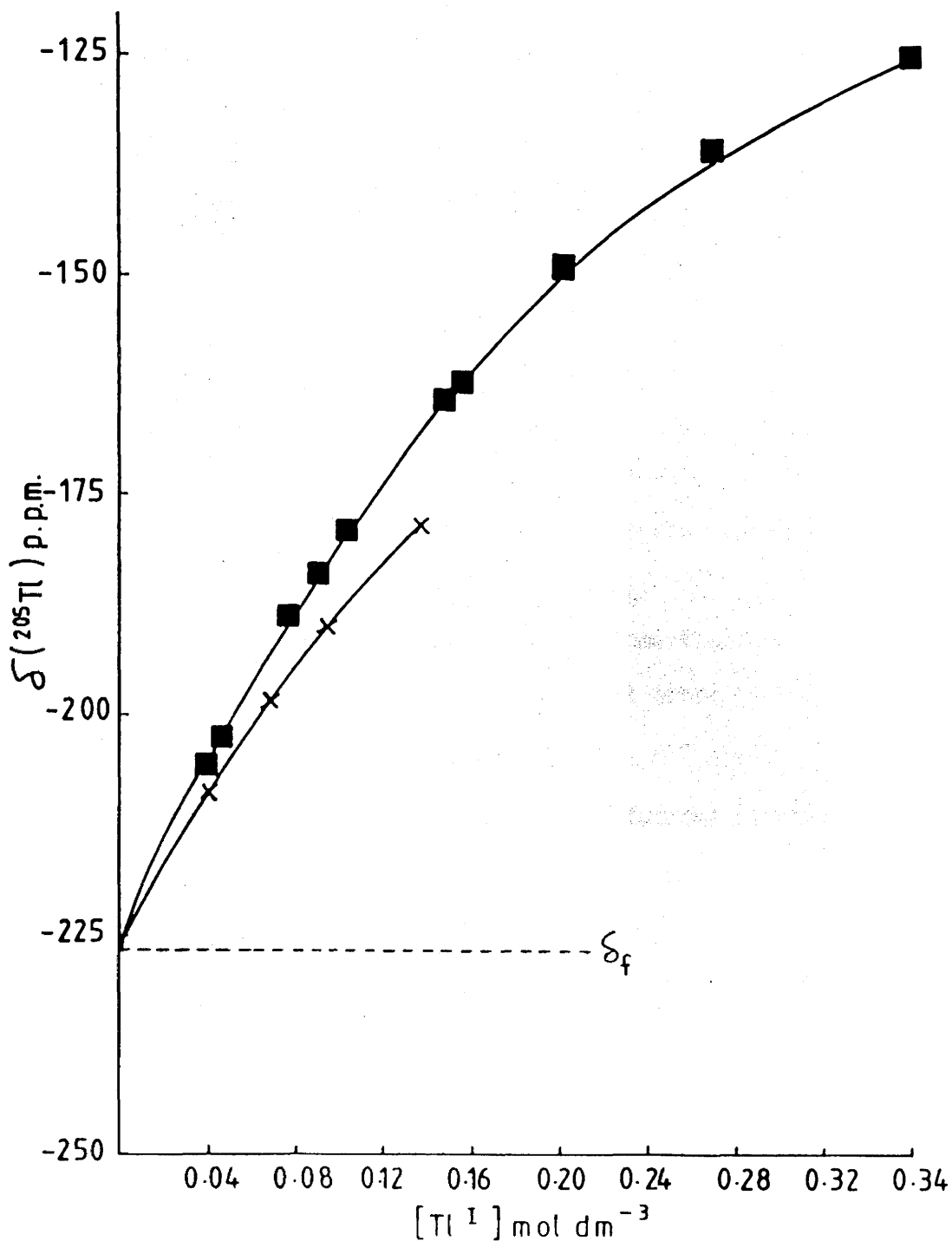
Figure 2 represents the variation of ^{205}Tl chemical shift with increasing salt concentration in acetonitrile solutions of thallium(I) salts with paramagnetic anions, MoF_6^- and UF_6^- . This relationship is non-linear and a low field shift of ^{205}Tl resonance was observed with an increase in salt concentration. The signals due to solvated Tl^+ are very sensitive to the presence of paramagnetic anions, MoF_6^- and UF_6^- , for example ^{205}Tl resonance from TlUF_6 solution occurs at 30 ppm to lower applied field than that from TlWF_7 solution at comparable concentrations, that is 0.04 mol dm^{-3} . The $^{205}\text{Tl}^+$ chemical shifts for TlUF_6 solutions at concentrations 0.044 and 0.34 mol dm^{-3} were -206.5 and -125 ppm whereas for TlMoF_6 solutions, these were -209 and -178 ppm at 0.042 and 0.14 mol dm^{-3} concentrations respectively. An increase in the concentration of thallium(I) salts having paramagnetic fluoroanion, MoF_6^- or UF_6^- , thus has a significant effect on ^{205}Tl deshielding, about 30 ppm for TlMoF_6 and 80 ppm for TlUF_6 over a concentration range of 0.04 - 0.14 and 0.04 - 0.34 mol dm^{-3} respectively. The line widths at half heights of ^{205}Tl signals originating from TlUF_6 solutions were in the range 180 - 620Hz corresponding to concentrations 0.04 - 0.34 mol dm^{-3} . The ^{205}Tl signals arising from TlMoF_6 solutions, showed an unusual behaviour of peak widths at half heights, that is the ^{205}Tl signals became broader with decreasing salt concentrations and were in the range 570 - 1900Hz . The origin of this unusual behaviour is not clear. The $^{205}\text{Tl}^+$ chemical shift data for TlUF_6 were obtained using solutions of ten different concentrations whereas for TlMoF_6 , solutions of only four different concentrations were used.

The 'infinite dilution' resonance frequency of an ion, that is the resonance frequency in the absence of any effect due to ion-pairing, relates the resonance frequency of the ion to some property of the solvent such as basicity, and reflects the strength of interaction between the ion and the solvent.⁶⁸ Hence the resonance frequency of

Figure 2. Variation of ^{205}Tl Chemical Shift (w.r.t. Tl^+aq) with Concentration in MeCN.

TlUF_6 , ■ TlMoF_6 , ×

δ_f = 'Free ion' chemical shift of Tl^+ ion



the nucleus as a function of decreasing salt concentration was obtained to define the resonance frequency - salt concentration curve well enough to extrapolate to the 'infinite dilution' resonance frequency. The extreme sensitivity of the thallium resonance frequency to its chemical environment, and the non-linear relationship between the resonance frequency and salt concentration makes this extrapolation dangerous. Therefore, four thallium(I) salts, having different anions, TlPF_6 , TlWF_7 , TlMoF_6 and TlUF_6 , were used to approach the 'infinite dilution' point. A computer analysis of the resonance frequency-concentration curve for each salt yielded the 'infinite dilution' resonance value for a particular solute-MeCN system. A least squares fit second degree analysis employing a curve fitting computer programme, was used to extrapolate the resonance frequency-concentration curve of each salt. This yielded the same 'infinite dilution' chemical shift value, -226 ppm, for acetonitrile solvent with an uncertainty of ± 1 ppm (Figure 3). The extrapolated infinite dilution chemical shift values for the particular thallium(I) salts were TlPF_6 , -226, TlUF_6 , -225.5, TlMoF_6 , -226.5 and TlWF_7 , -228 ppm. The 'infinite dilution' chemical shifts of some thallium(I) salts, in different solvents together with some solvent properties such as dielectric constant and Gutmann donor number, are given in Table 1.

A correlation between the 'infinite dilution' resonance frequency of the Tl(I) ion and the Gutmann donor number,¹¹³ has been made for a number of different solvents¹¹⁴⁻⁵ and is represented in Figure 4. The Gutmann donor number, a measure of the solvent basicity, is defined as the negative of the enthalpy of interaction of a base with SbCl_5 when the two are dissolved in equimolar amounts in the inert solvent, 1,2-dichloroethane. The 'infinite dilution' resonance frequency of the thallium(I) ion determined for acetonitrile in the present work when plotted against the Gutmann donor number for

Figure 3. Variation of ^{205}Tl Chemical Shift (w.r.t. Tl^+aq) with Concentration in MeCN.

TlPF_6 , ● ; TlWF_7 , ▲ ; TlUF_6 , ■ TlMoF_6 , ×

δ_f = 'Free ion' chemical shift of Tl^+ ion in MeCN.

δ_{ip} = chemical shift of the Tl^+PF_6^- ion pair

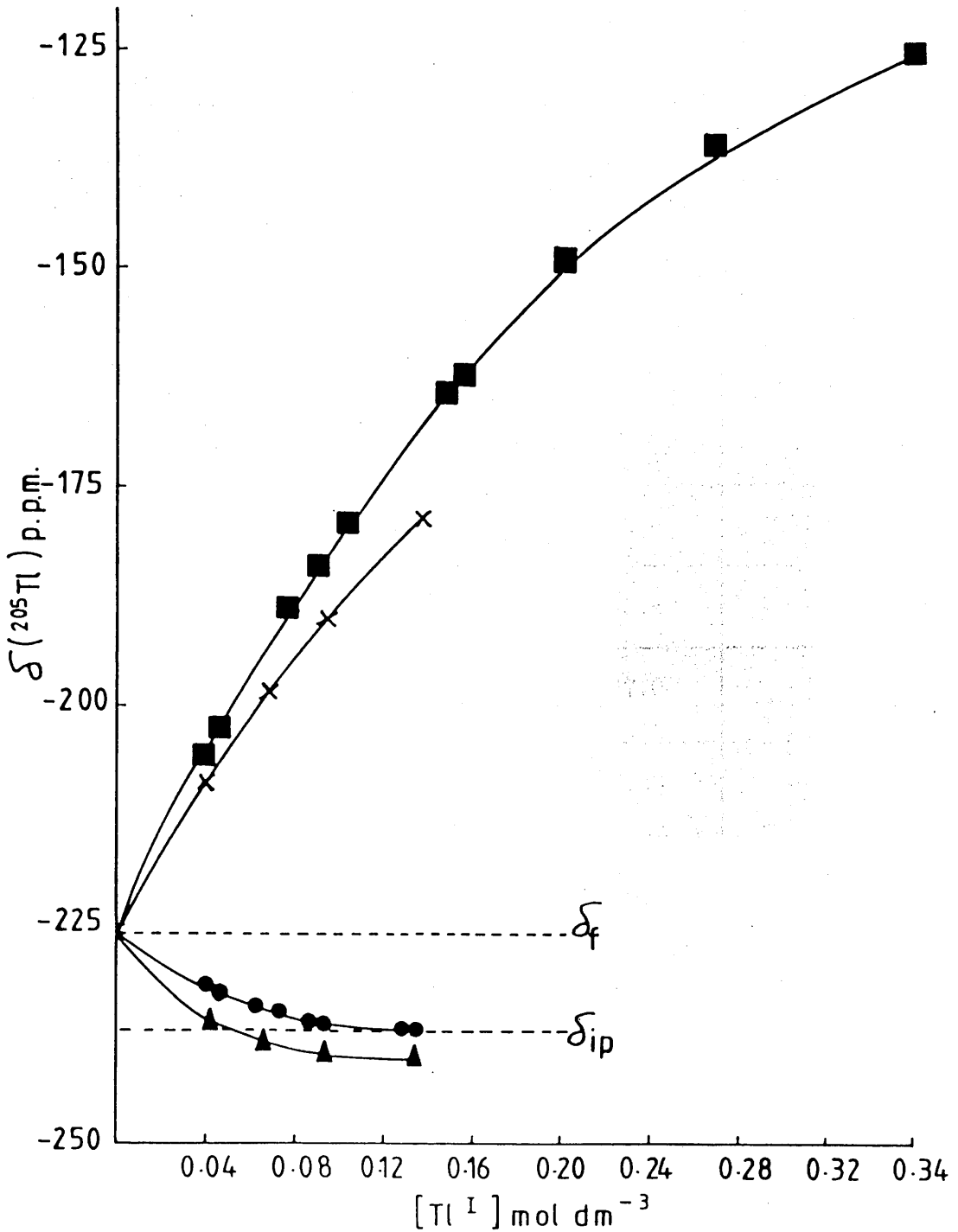


Table 1.

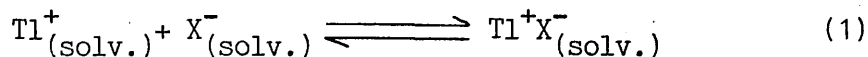
Infinite-Dilution $^{205}\text{Tl}^+$ Chemical Shifts and Some Selected Solvent Properties.

Salt	Solvent	Infinite dilution Chemical shift $^{205}\text{Tl}\delta_f, \text{ppm}^a$	Solvent Properties		Ref.
			Dielectric Constant	Gutmann Donor No.	
TlPF_6	MeCN	-226 ± 1	37.5	14.1	this work
TlWF_7	MeCN	-226 ± 1	37.5	14.1	this work
TlMoF_6	MeCN	-226 ± 1	37.5	14.1	this work
TlUF_6	MeCN	-226 ± 1	37.5	14.1	this work
TlNO_3	Pyridine	783.2 ± 5	12.4	33.1	114
TlClO_4	Pyridine	783.2 ± 5	12.4	33.1	114
TlNO_3	liquid NH_3	1819 ± 3	17.0	-	69
TlClO_4	liquid NH_3	1819 ± 3	17.0	-	69

^a. All the chemical shifts are referenced to aqueous TlNO_3 at infinite dilution.

acetonitrile, was found to fit well in the relationship and is represented by 'X' in Figure 4.

The formation of an ion-pair in a solvent is represented by means of the equilibrium shown in equation (1)



The ion-pair formation constant, K_{ip} , for this equilibrium can be defined by equation (2)⁶⁸

$$K_{ip} = \frac{[\text{Tl}^+\text{X}^-]}{\gamma_{\pm}^2 [\text{Tl}^+][\text{X}^-]} \quad (2)$$

where $[\text{Tl}^+\text{X}^-]$ = concentration of the ion pair, $[\text{Tl}^+]$ and $[\text{X}^-]$ are concentrations of Tl^+ ion (free or solvated) and anion respectively, and γ_{\pm} is the mean activity coefficient of the ions. The exchange of solvent molecules between the solvation sphere of a monovalent cation and the bulk solvent, is usually fast to ensure the observation of only one time averaged nmr signal from the cation species. Its chemical shift is given by equation (3)

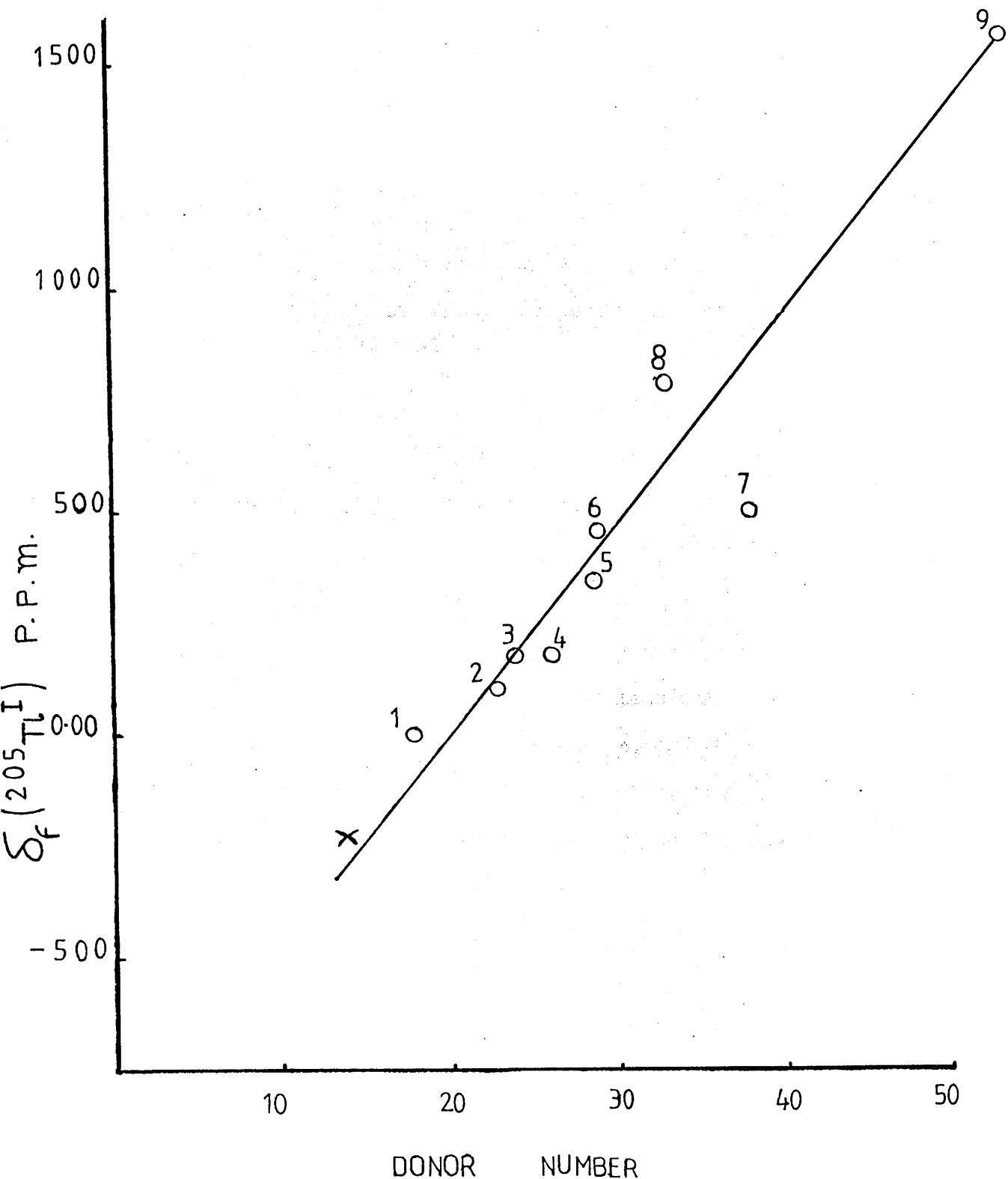
$$\delta_{\text{obs}} = X_f \delta_f + X_{ip} \delta_{ip} = \frac{C_f}{C_t} (\delta_f - \delta_{ip}) + \delta_{ip} \quad (3)$$

in which δ_f and δ_{ip} are the chemical shifts of the free (solvated) and ion-paired cations respectively, X_f and X_{ip} are the corresponding mole fractions, and C_f and C_t are the free and total cation concentrations. The free cation concentration, C_f is obtained from the following rearranged form of equation (3)

$$C_f = \frac{\delta_{\text{obs}} - \delta_{ip}}{\delta_f - \delta_{ip}} C_t \quad (4)$$

Figure 4. Correlation of the ^{205}Tl Chemical Shift and the Gutmann Donor Number for Solutions of Tl^{I} Salts.

Solvents: 1)water; 2)formamide; 3)N-methylformamide;
 4)N-N-dimethylformamide; 5)dimethyl sulphoxide;
 6)N,N-dimethylacetamide; 7)hexamethylphosphorotriamide;
 8)pyridine; 9)n-butylamine; X acetonitrile



From the experimentally determined values of δ_{obs} , the extrapolated values of δ_f and estimated values of δ_{ip} , the free cation concentration, C_f can be calculated by equation (4). This value of C_f is then used to calculate the mean activity coefficient, γ_{\pm} from the Debye Huckel equation.¹¹⁶

$$\log \gamma_{\pm} = AC^{\frac{1}{2}} \quad (5)$$

In the present work the value of constant 'A' for acetonitrile was assumed to be the same as that for water (0.5115 at 298 K) because of the non-availability of such data for MeCN in the literature. The values of K_{ip} for TlPF_6 and TlWF_7 , were estimated only for the lowest concentrations, 0.04 mol dm^{-3} , studied in the present work. The estimated values of δ_{ip} and K_{ip} for TlPF_6 and TlWF_7 in acetonitrile along with the values for thallium(I) salts in other solvents are given in Table 2. The K_{ip} values, given in Table 2, increase with decreasing dielectric constant of the medium as expected.

The K_{ip} values for thallium(I) salts having paramagnetic anions, MoF_6^- and UF_6^- , were not estimated since the literature method used for the calculation of K_{ip} ⁶⁸ has the limitation that it can only be used for salts where the difference between δ_f and δ_{ip} , is not large. The salt concentration, in the thallium(I) salts, TlMoF_6 and TlUF_6 has a significant effect on the ^{205}Tl chemical shifts, hence the estimation of δ_{ip} was not possible.

The ^{205}Tl chemical shift data for MeCN solutions of the solid obtained from the oxidation of Tl metal with WF_6 , which should result in the formation of TlWF_6 , are plotted as a function of salt concentration in Figure 5. Thallium hexafluorotungstate(V) has the paramagnetic anion WF_6^- , but the ^{205}Tl chemical shift data obtained were different from those of the other paramagnetic salts, TlMoF_6 and

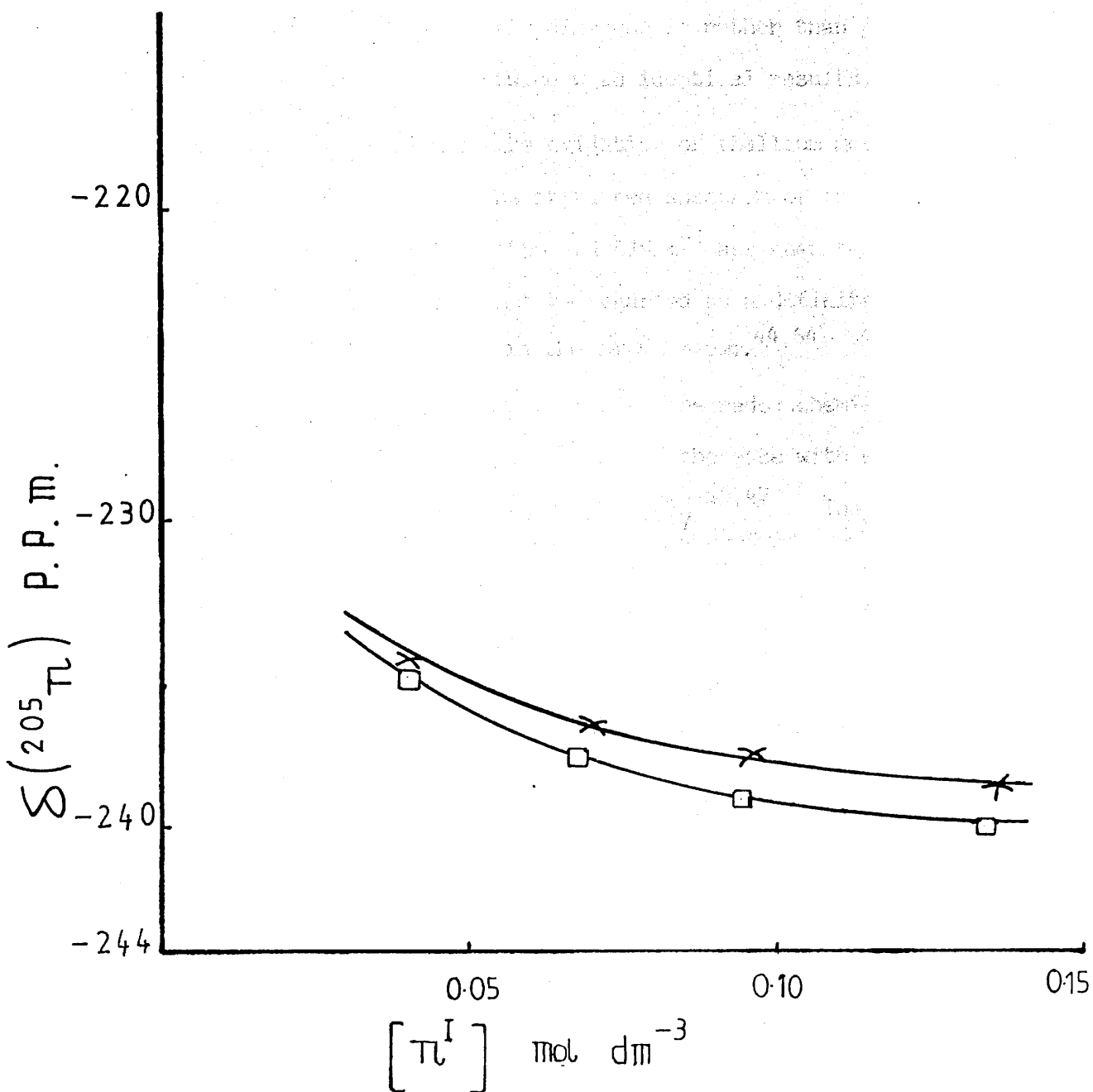
Table 2.

Ion-pair Formation Constants of Tl^+ Salts in Various Solvents.

Salt.	Solvent.	Infinite dilution chemical shift $^{205}Tl^+ \delta_f$, ppm	Estimated ion-pair chemical shift $^{205}Tl^+ \delta_{ip}$, ppm	Ion-pair formation constant K_{ip}	Dielectric Constant of the solvent	Reference
$TlNO_3$	Dimethyl Sulphoxide	359.7 ± 0.4	353.2 ± 1.5	75 ± 50	46.7	114
$TlPF_6$	MeCN	-226 ± 1	-236 ± 1	120 ± 20	37.5	this work
$TlWF_7$	MeCN	-226 ± 1	-240 ± 1	140 ± 20	37.5	this work
$TlNO_3$	Pyrrrole	-382.8 ± 1	-420.4 ± 1.5	208 ± 50	8.13	114
$TlClO_4$	Pyridine	783.2 ± 5	656.6 ± 0.5	1750 ± 200	12.4	114

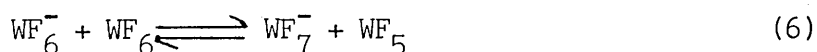
Figure 5. Variation of ^{205}Tl Chemical Shift (w.r.t. Tl^+aq) with Concentration in MeCN.

TlWF_7 , \square ; Product obtained from the oxidation of Tl metal with WF_6 , \times



TlUF₆. The behaviour observed was very similar to that of TlWF₇, a salt having a diamagnetic anion. The ²⁰⁵Tl chemical shifts observed were -236 and -238.6 ppm at concentrations 0.041 and 0.137 mol dm⁻³, respectively. Thus an increase of salt concentration resulted in a small increase, 2.6 ppm, in ²⁰⁵Tl shielding and the line widths at half heights were in the range 56-98Hz. The ²⁰⁵Tl chemical shift data, therefore, suggest that the counteranion, in the solid obtained from the oxidation of Tl metal with WF₆, is predominantly diamagnetic rather than paramagnetic. The experiment was repeated twice with identical results.

The solid isolated from the oxidation of thallium metal with WF₆, was thus a mixture. The infra-red spectrum of the solid product consisted of bands at 590 and 615cm⁻¹ assigned to WF₆⁻ and WF₇⁻ respectively but this cannot be regarded as a definite identification as the two bands occur in the same region.^{44,64} There are other reports in the literature where the redox chemistry of WF₆ was shown to be complicated because of the ease with which WF₆⁻ reacts with WF₆ in acetonitrile, to give WF₇⁻.^{46,47} The other product from these reactions was presumably solvated tungsten pentafluoride. Therefore, the fluoride ion transfer equilibrium in which all the species are solvated, is represented by equation (6).



2:2:2 Study of Thallium(III) Salts with Paramagnetic Fluoroanions.

Solvated thallium(III) is readily characterized from its ²⁰⁵Tl chemical shift, in acetonitrile solution.⁴⁸ Resonance from thallium(III) occurs at higher frequencies than that from thallium(I) and this situation is consistent with previous studies of compounds of Tl^{III} and Tl^I in various solvents.^{68,117} The concentration

dependence of the $^{205}\text{Tl}^{3+}$ chemical shift in the complex, $[\text{Tl}(\text{NCMe})_5]^-$ - $[\text{UF}_6]_3$, is represented in Fig.6. An increase in salt concentration resulted in decreased shielding of ^{205}Tl resonances but the effect is far smaller, ca.5 ppm, as compared with the behaviour of ^{205}Tl resonance frequencies from $\text{Tl}^{\text{I}}\text{UF}_6$ ca. 80 ppm, over a concentration range of 0.04-0.34 mol dm $^{-3}$. One possible explanation for this difference is that Tl^{3+} is more effectively solvated by MeCN as compared with Tl^+ , hence direct ion-pairing is less important. The ^{205}Tl chemical shifts for acetonitrile solutions of the compound, $\text{Tl}^{\text{III}}-(\text{UF}_6)_3 \cdot 5\text{MeCN}$, were 1992.2 and 1997.9 ppm at the salt concentrations, 0.045 and 0.34 mol dm $^{-3}$ respectively. The relationship between $^{205}\text{Tl}^{3+}$ chemical shift and the salt concentration is non-linear (Fig.6) and the 'infinite dilution' chemical shift for Tl^{3+} ion, in acetonitrile as determined by computer analysis, is 1991 ppm. This value of the 'infinite dilution' chemical shift is not as certain as in the Tl^{I} case because it has been determined only for one Tl^{III} salt. An attempt to make $\text{Tl}^{\text{III}}(\text{MoF}_6)_3 \cdot 5\text{MeCN}$, according to the literature method was unsuccessful as discussed in the next section. The ^{205}Tl chemical shifts for thallium(III) salts in the solid state, the melt form and in solution are given in Table 3. This table shows that the $^{205}\text{Tl}^{3+}$ chemical shifts determined in the present work, are in good agreement with the values obtained in other solvents or even in the solid state. The determination of an ion-pair formation constant, K_{ip} in the salt, $\text{Tl}^{\text{III}}(\text{UF}_6)_3 \cdot 5\text{MeCN}$, was not attempted because of the assumptions that would be required regarding the presence of thallium (III) ions, such as $[\text{Tl}(\text{NCMe})_x(\text{UF}_6)_2]^+$, $[\text{Tl}(\text{NCMe})_x(\text{UF}_6)]^{2+}$ and $[\text{Tl}(\text{NCMe})_x]^{3+}$, in MeCN solution.

2:2:3. Study of Mixtures Containing Tl^{I} and Tl^{III} .

Mixtures of Tl^{I} and Tl^{III} with UF_6^- as counteranion, were prepared by mixing standard solutions of $\text{Tl}^{\text{I}}\text{UF}_6$ and $\text{Tl}^{\text{III}}(\text{UF}_6)_3 \cdot 5\text{MeCN}$, in a 1:1 mole ratio. Solution concentrations were in the range 0.04 -

Figure 6. Variation of ^{205}Tl Chemical Shift with Concentration in Tl^{III} Hexafluorouranate(V) Solutions.

δ_f = 'Free ion' chemical shift of Tl^{3+} in MeCN.

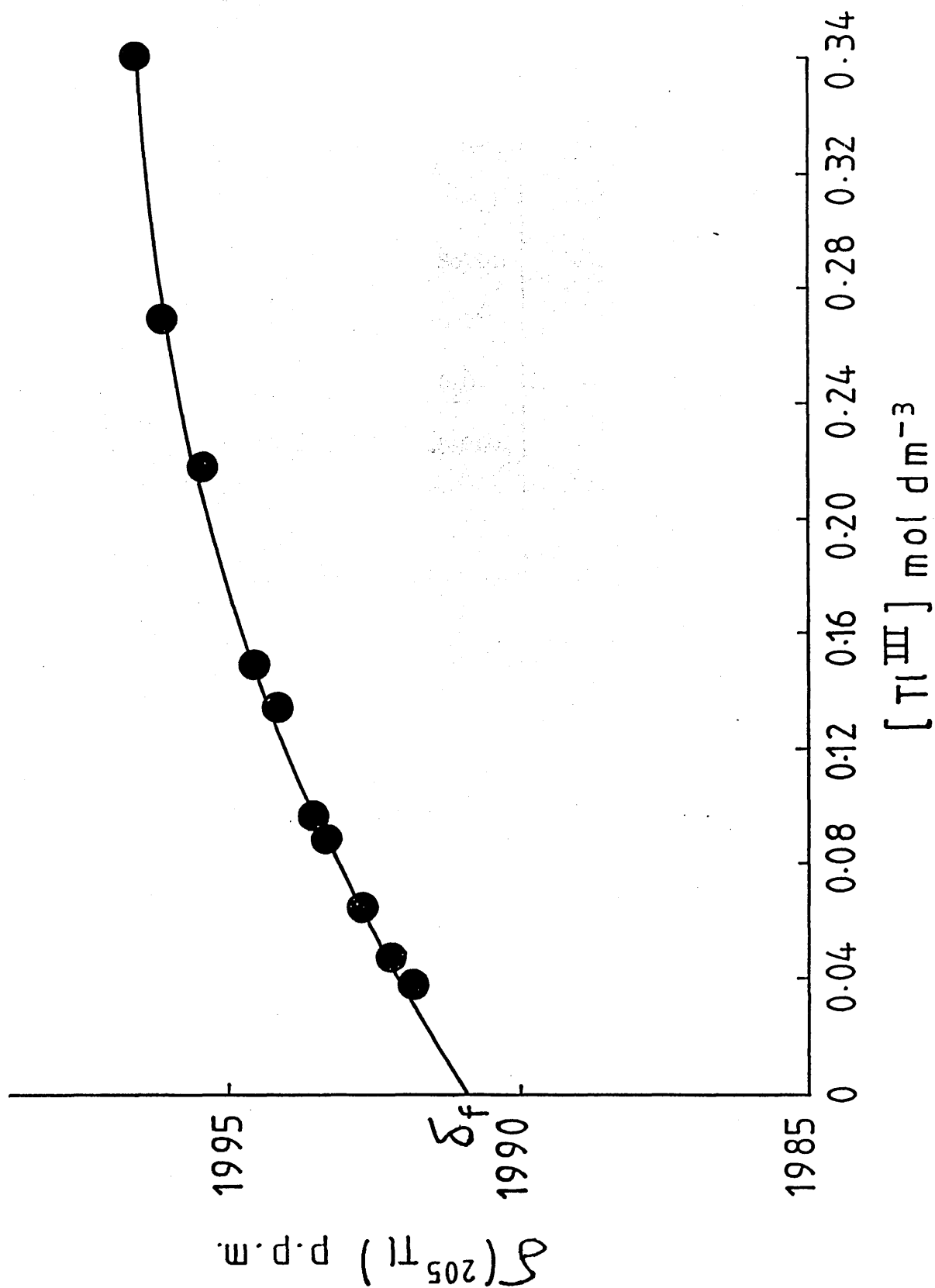


Table 3.

 $^{205}\text{Tl}^{3+}$ Chemical Shifts of Some Tl^{III} Salts.

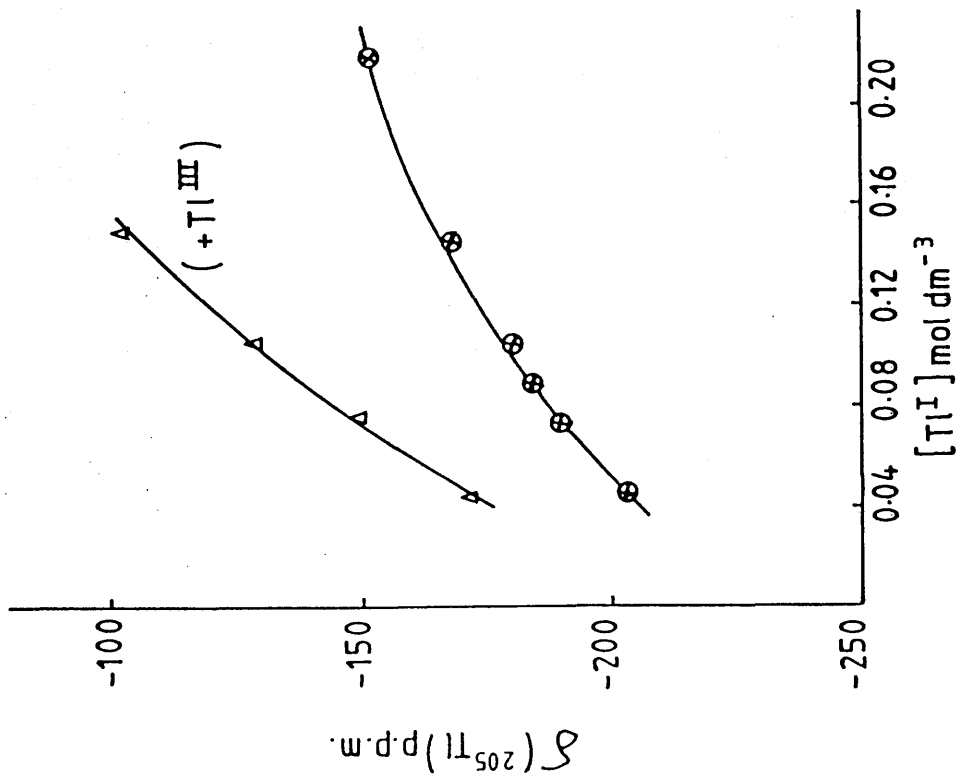
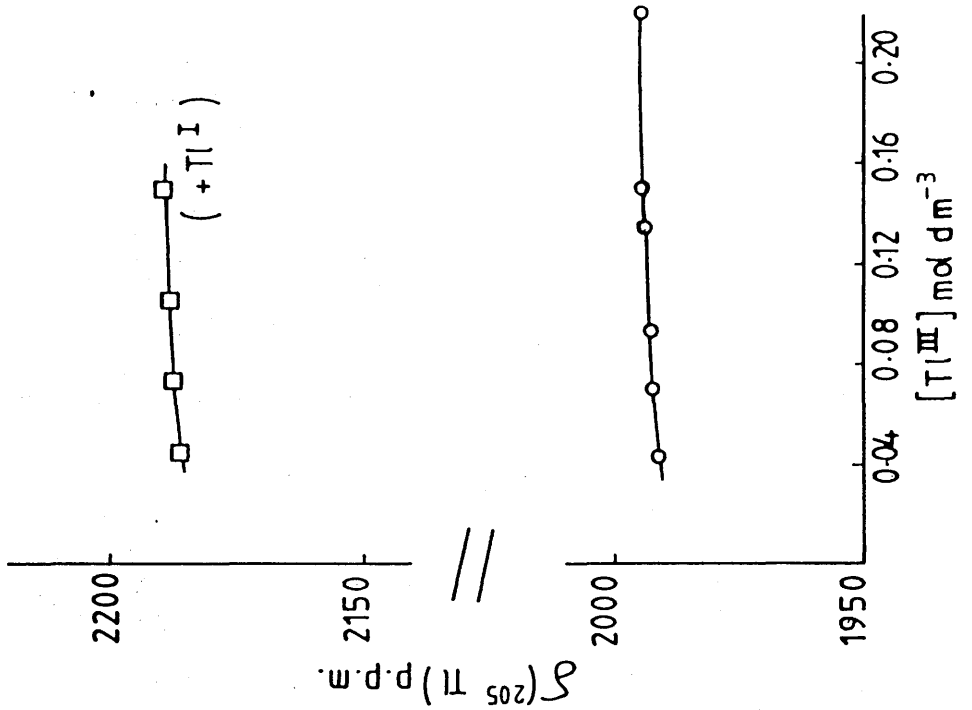
Salt	Concentration. (mol dm ⁻³)	Solvent	$^{205}\text{Tl}^{3+}$ Chemical shift (ppm)	Reference
$\text{Tl}(\text{UF}_6)_3 \cdot 5\text{MeCN}$	∞ -dilution	MeCN	+ 1991	this work
$\text{Tl}(\text{MoF}_6)_3 \cdot 5\text{MeCN}$	0.2	MeCN	+ 2067	48
$\text{Tl}(\text{ClO}_4)_3 \cdot 6\text{H}_2\text{O}$	-	Solid	+ 2175	118
$\text{Tl}(\text{ClO}_4)_3$	-	melt	+ 1885	119
$\text{Tl}(\text{NO}_3)_3$	1.5	H_2O	+ 1850	120
$\text{Tl}(\text{NO}_3)_3$	0.61	1.5M HNO_3	+ 1860	121
TlCl_3	∞ -dilution (0.1)	H_2O	+ 2307	121

0.15 mol dm⁻³ which enabled ²⁰⁵Tl resonances to be observed easily. The change in the ²⁰⁵Tl chemical shifts of Tl^I and Tl^{III} with increasing Tl^I and Tl^{III} concentration and keeping the mole ratio 1:1 in all the cases is represented in Figure 7. The chemical shifts of Tl^I and Tl^{III}, in the presence of one another, were both shifted to the lower applied field as compared with ²⁰⁵Tl chemical shifts of Tl^I and Tl^{III} in the individual salts. For example the ²⁰⁵Tl⁺ chemical shift in the mixture was -172 ppm at a concentration, 0.045 mol dm⁻³ compared with a value of -206.5 ppm for TlUF₆ at a concentration, 0.044 mol dm⁻³, thus a deshielding of ²⁰⁵Tl⁺ resonance of about 35 ppm was observed in the mixture. This deshielding of ²⁰⁵Tl resonance, in the mixture, became much more significant, ca. 70 ppm, at higher concentrations, for example the ²⁰⁵Tl⁺ chemical shift, in the mixture was -98.7 ppm at 0.15 mol dm⁻³ concentration compared with -164.5 ppm at 0.147 mol dm⁻³ concentration in the pure TlUF₆ solution. The deshielding of ²⁰⁵Tl³⁺ chemical shift in the mixture was almost the same with an increase in concentration but its magnitude was much higher than deshielding of ²⁰⁵Tl⁺ chemical shift. For example the ²⁰⁵Tl³⁺ chemical shifts, in the mixture were 2187.1 and 2189.6 ppm at the concentrations 0.045 and 0.15 mol dm⁻³ compared with 1992.2 and 1994.5 ppm at the same concentrations in pure Tl³⁺ solution, a deshielding of ²⁰⁵Tl³⁺ resonance to about 195 ppm was thus observed. The ²⁰⁵Tl⁺ signals in the mixture were much broader than the case where no Tl^{III} was present, for example the line width at half height, $\Delta V_{\frac{1}{2}}$, was 330Hz compared with 180Hz for TlUF₆, at concentration 0.045 mol dm⁻³. No significant change in peak widths at half heights were observed for ²⁰⁵Tl³⁺ signals in the mixture.

The shifting of ²⁰⁵Tl resonances due to Tl^I and Tl^{III} towards lower applied field in the mixture, can be explained as follows. The concentration of anion, in the mixture, is greater than in pure

Figure 7. Variation of ^{205}Tl Chemical Shifts with Concentration for Tl^{I} , Tl^{III} Hexafluorouranate(V) Mixtures in MeCN.

$[\text{Tl}^{\text{I}}]:[\text{Tl}^{\text{III}}] = 1:1$, Δ and \square
 Tl^{I} alone, \otimes ; Tl^{III} alone, \circ

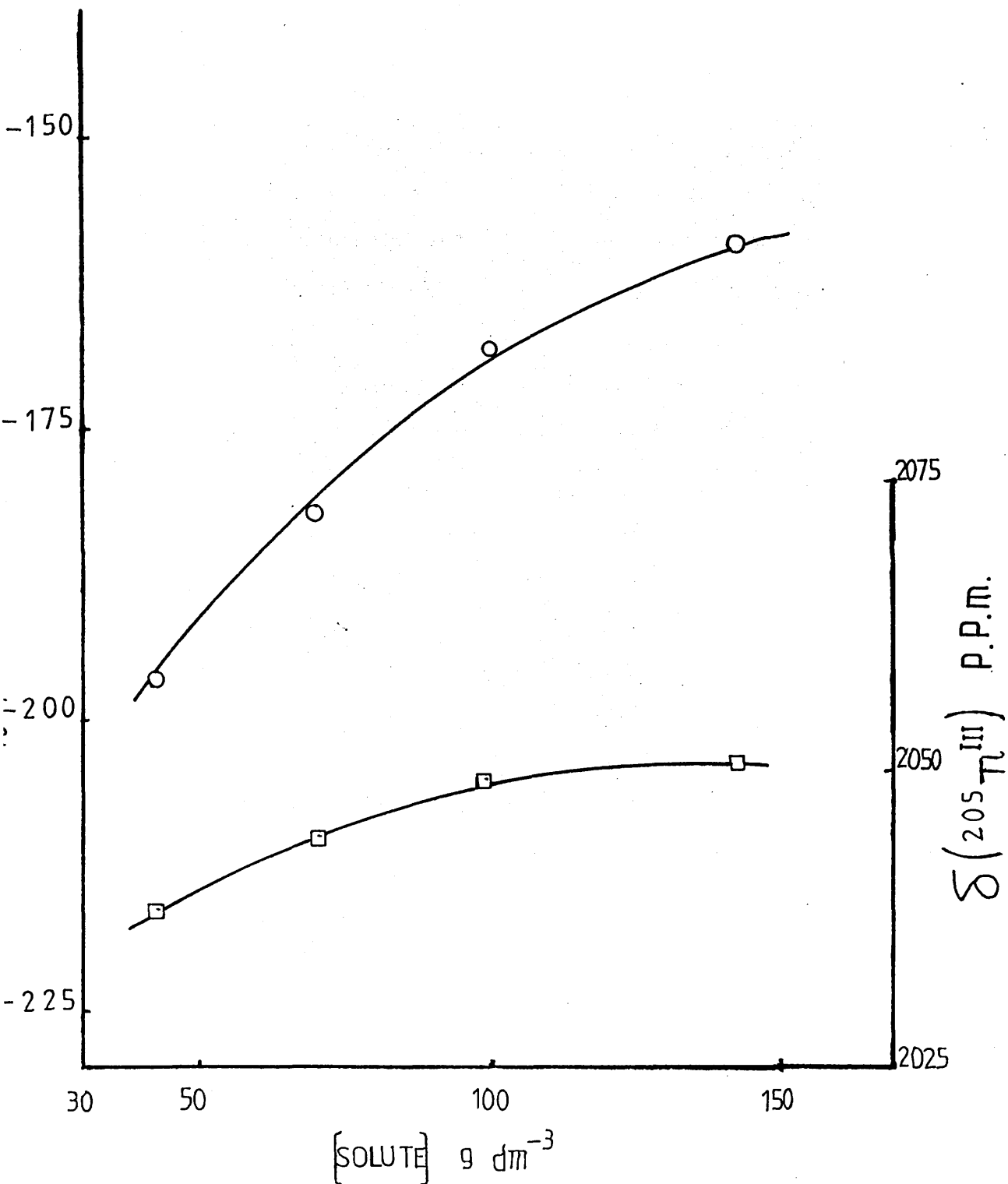


Tl^I or Tl^{III} salts of comparable concentration being $4/3$ times for thallium(III) and 4 times for thallium(I). It has been observed that the concentration has a very small effect on $^{205}Tl^{3+}$ chemical shifts, hence the shifting of $^{205}Tl^{3+}$ resonance to lower applied field, in the mixture, is attributed mainly to Tl^I and Tl^{III} interactions in solution. On the other hand, salt concentration has a significant effect on $^{205}Tl^+$ chemical shifts, hence shifting of $^{205}Tl^+$ resonances to lower applied field, in the mixture, may be related either to the increase in anion concentration or $Tl^{III}-Tl^I$ interaction or both. The broadness of $^{205}Tl^+$ signals, in the mixture, is due to an increase in anion concentration.

Oxidation of thallium metal using a large excess of MoF_6 in MeCN at 298 K resulted in the formation of a pale yellow solution from which an off-white solid was isolated after removal of volatile material. The infrared spectrum of the solid contained bands due to coordinated MeCN, 2320 (comb.) 2290 ν (CN) and 950 cm^{-1} ν (CC), and MoF_6^- , 640 (ν_3) and 250 cm^{-1} (ν_4). The procedure followed was that given in the literature⁴⁵, which should have resulted in the formation of a pure Tl^{III} salt, $Tl^{III} (MoF_6)_3 \cdot 5MeCN$. Accordingly standard solutions of the solid were made in MeCN but the ^{205}Tl chemical shift data showed the compound to be a mixture of Tl^I and Tl^{III} . The variation of ^{205}Tl chemical shift with an increase in concentration ($g\ dm^{-3}$) in this mixed oxidation state compound, is represented in Figure 8. The $^{205}Tl^+$ and $^{205}Tl^{3+}$ chemical shifts, in the mixed oxidation state compound, were shifted to lower applied field with an increase in concentration and this is consistent with the behaviour of a mixture of Tl^I and Tl^{III} salts, having UF_6^- as counter-anion, described above. The $^{205}Tl^+$ signals, in the mixed oxidation state compound, were broader than the situation in which no Tl^{III} was

Figure 8. Variation of ^{205}Tl Chemical Shifts with Concentration in the Mixed Oxidation State Compound $\text{Tl}^{\text{I}}\text{MoF}_6 \cdot \text{Tl}^{\text{III}}(\text{MoF}_6)_3 \cdot 5\text{MeCN}$.

Variation of Tl^{I} chemical shift in the mixture, \circ
 Variation of Tl^{III} chemical shift in the mixture, \square



present, thus behaving similar to a mixture of Tl^I and Tl^{III} with UF_6^- as counteranion and described above.

By assuming that the deshielding of $^{205}Tl^{3+}$ resonance, in the 1:1 mixture of the Tl^{III} and Tl^I salts, arises entirely from the interaction of Tl^I with Tl^{III} and is proportional to the $Tl^I:Tl^{III}$ mole ratio, the composition of the mixed oxidation state compound, Tl^I, Tl^{III} hexafluoromolybdate, having unknown mole ratio can be determined from the magnitude of the deshielding in the $^{205}Tl^{3+}$ resonance. In the 1:1 mole ratio, $Tl^I:Tl^{III}$ mixture with UF_6^- as counteranion, a deshielding of about 195 ppm was observed for $^{205}Tl^{3+}$ resonance (Figure 7) whereas the magnitude of deshielding observed for the $^{205}Tl^{3+}$ resonance in the mixed oxidation state compound, Tl^I, Tl^{III} hexafluoromolybdate was about 50 ppm (Figure 8). This suggested a far smaller interaction between Tl^I and Tl^{III} in the mixture of unknown mole ratio. From a comparison of the deshielding of the $^{205}Tl^{3+}$ resonances in the above two cases, the concentration ratio of Tl^I and Tl^{III} , in the mixture, Tl^I, Tl^{III} hexafluoromolybdate is estimated to be ca. 1:4.

2:3 Discussion

When the concentration of a Tl^{I} salt having a diamagnetic counteranion, PF_6^- or WF_7^- , is increased, a high field shift of the ^{205}Tl resonance is observed whereas increase in the concentration of a Tl^{I} salt with a paramagnetic anion, MoF_6^- or UF_6^- , results in a low field shift, the shift induced by UF_6^- is greater than the shift induced by MoF_6^- . The greater effect of salt concentration on ^{205}Tl chemical shifts in Tl^{I} salts with paramagnetic anions, is the result of the additional magnetic field contributed by the paramagnetic anions, MoF_6^- and UF_6^- . The 'infinite dilution' chemical shift of $^{205}\text{Tl}^+$ ion, in acetonitrile, is determined by the least squares fit second degree analysis of the $^{205}\text{Tl}^+$ chemical shift - concentration plots of thallium(I) salts, TlPF_6 , TlUF_6 , TlMoF_6 and TlWF_7 , using a curve fitting computer programme. The extrapolated value of 'infinite dilution' chemical shift, in all the Tl^{I} salts is found to be the same, -226 ppm, with an uncertainty of ± 1 ppm. This is the only ^{205}Tl 'infinite dilution' chemical shift value which has been determined by using Tl^{I} salts with four different anions.

The previously determined relationship between the infinite dilution resonance frequency of Tl^+ ions and the Gutmann donor numbers of the solvents is linear (Figure 4) and the infinite dilution chemical shift of Tl^+ ion in MeCN, fits well in this relationship. It is observed from this relationship that the more basic the solvent, the higher is the infinite dilution resonance frequency of the Tl^+ ion. The increase in resonance frequency with

increasing solvent basicity is thus a measure of the strength of interaction between the ion and the solvent molecules, with the solvent acting as a Lewis base and interacting electrostatically and covalently with the ion. Transient orbital mixing created by ion-solvation collision induced polarization of the ion electron cloud may also contribute to the observed resonance frequency changes.

The $^{205}\text{Tl}^+$ chemical shift data suggest that a definite cation-anion interaction is present in MeCN solutions of Tl^{I} salts. The formation of contact or direct ion pairs and solvent separated ion pairs, is, therefore, possible and from the experimental results it is difficult to make a distinction between them. The formation of solvent separated ion pairs in the Tl^{I} salts, TlPF_6 and TlWF_7 , is supported by the comparatively small difference between the free ion chemical shift, δ_f , and the ion-pair chemical shift, δ_{ip} , suggesting less perturbation of Tl^+ ion than might be anticipated from replacement of a primary solvent molecule by the PF_6^- or WF_7^- anion. A rather constant ^{205}Tl chemical shift in the above Tl^{I} salts, at higher concentration implies the presence of some degree of contact ion pairing. In the Tl^{I} salts having paramagnetic anion, TlMoF_6 and TlUF_6 , salt concentration has a significant effect on ^{205}Tl chemical shift, although most of it arises from the additional magnetic field of the paramagnetic anion, it does suggest the close proximity of the anion to the Tl^+ ion.

Considering the model of a cation in solution described in chapter one, Figure 1, it is, therefore, considered that the anions in the Tl^{I} salt solutions are present either in the secondary solvation sphere or in the primary solvation region. In any event there is a rapid exchange between the two situations. It is this possibility

which seems to be the most reasonable one taking into consideration the experimental evidence discussed above.

The formation of ion pairs in the Tl^I salts studied in the present work, is consistent with a recent solid state and solution study of the Tl^I compound $[Tl(mes)_2][B(OTeF_5)_4]$, ¹²² (mes = mesitylene). The structure of this compound has been determined by x-ray diffraction and consists of a chain of $[Tl(mes)_2]^+$ cations and $[B(OTeF_5)_4]^-$ anions connected by extremely weak $Tl...F$ interactions. The ¹⁹F n.m.r. spectra of the compounds, $[Tl(mes)_2]^+[B(OTeF_5)_4]^-$ and $[N(n-Bu)_4]^+[B(OTeF_5)_4]^-$ in dichloromethane solution at two different concentrations (0.76 and 0.38 mol dm⁻³) show a very little cation dependence of δ_A , the ¹⁹F chemical shift of the axial fluorine which is trans to oxygen, for the $[B(OTeF_5)_4]^-$ anion, and a smaller concentration dependence. The cation dependence of δ_A for the substitution of Tl^+ with tetra-n-butyl ammonium ion is 0.54 ppm and that for concentration it is 0.06 ppm. From the above data, the authors suggest the presence of some degree of ion-pairing in the Tl^I compound $[Tl(mes)_2][B(OTeF_5)_4]^-$ in dichloromethane solution. Although these findings are consistent with some degree of ion-pairing, they are not regarded as definitive.

Only a few ion-pair formation constants for Tl^I salts are available in the literature and the Tl^I salts, $TlPF_6$ and $TlWF_7$ have not been studied previously. A comparison of K_{ip} values determined for $TlPF_6$ and $TlWF_7$, in acetonitrile, with the K_{ip} values of other Tl^I salts reported in the literature in different solvents (Table 2) is in agreement with general expectation that ion pair formation is favoured by solvents which have low dielectric constants.

An increase in concentration of the Tl^{III} salt, $Tl(UF_6)_3 \cdot 5MeCN$, results in a low field shift of the ²⁰⁵Tl resonance but the effect is

far smaller as compared with the ^{205}Tl resonance from the Tl^{I} salt having the same counteranion, UF_6^- . The $^{205}\text{Tl}^{3+}$ chemical shift data suggest that Tl^{3+} is more effectively solvated by MeCN as compared with Tl^+ , hence direct ion-pairing is less important. The radius of Tl^{3+} ion (0.95 \AA) is far smaller than Tl^+ (1.40 \AA) and it might have been expected that ion-pairing should be more significant in the Tl^{III} salt. The observation of far smaller effect of the concentration of the paramagnetic anion, UF_6^- , on $^{205}\text{Tl}^{3+}$ chemical shift, however, does not support this view. The electronic configuration of the Tl^{3+} ion in the outermost shell is d^{10} and like other d^{10} ions such as Cu^+ which is strongly solvated in acetonitrile due to back bonding effect involving a $d_{\pi}-p_{\pi}$ interaction with the π^* orbitals of the nitrile group,¹²³ it is expected that Tl^{3+} ion should also be effectively solvated by MeCN. However the Tl^{3+} ion has a greater positive charge than Cu^+ , hence the degree of back bonding is expected to be much less than in Cu^+ , therefore the effective solvation of the Tl^{3+} ion in MeCN is not solely due to this reason.

Considering the model of cation in solution discussed in chapter one, it is assumed that Tl^{3+} ion has the solvent molecules in the primary and secondary solvation shells. The anions are expected to be present in the disordered zone. The greater positive charge on Tl^{3+} ion experiences some influence on the anions, thus causing them to move to the secondary shell. Therefore, a situation in which the anions exchange positions between the disordered and the secondary zone is more likely and the formation of solvent separated ion pair, $[\text{Tl}(\text{NCMe})_x(\text{UF}_6)]^{2+}$, is not ruled out.

The model of a cation in solution, described in chapter one, is based on the assumption that the anion is not interacting, in any way,

with the cation. The ^{205}Tl n.m.r. study of Tl^{I} and Tl^{III} salt solutions, in the present work, does suggest an interaction between the cation and anion. It can, therefore, be assumed in case of Fe^{2+} and Cu^{2+} cations whose substitution and redox reactions in acetonitrile will be described in the forthcoming chapters, that the cations are not entirely free from the effect of the counter anion.

2:4 Conclusions.

^{205}Tl n.m.r. spectroscopy is a powerful probe for cation-anion interactions in solution because of the sensitivity of the ^{205}Tl chemical shift to the nature of Tl^+ and Tl^{3+} environment in solution. The ^{205}Tl chemical shift data obtained for a number of Tl^{I} and Tl^{III} complex fluoroanion salts, suggest the presence of definite cation-anion interactions in Tl^{I} salts and that some degree of ion-pairing is present in these salts. Thallium(III) is found to be more effectively solvated, in acetonitrile solution as compared with thallium(I).

2:5 Experimental.

All the reactions, loading of chemicals in the reaction vessels, handling of products and the preparation of samples for spectroscopic analysis, described throughout this work, were carried out by using a conventional high vacuum system and a N_2 atmosphere glove box. The detail of all these manipulations, is described in chapter 6. The high oxidation state fluorides, that is PF_5 , WF_6 and MoF_6 (Fluorochem Ltd. or Ozark Mahoning), and UF_6 (British Nuclear Fuels plc), were purified by low temperature trap-to-trap distillation over NaF and stored over NaF at 77 K. Solid TlF (Ventron Alfa, 97%) was used as received. Thallium rod (B.D.H. 99.99%) was cleaned with abrasive paper and was freshly cut. Solids, for example, TlF and

Tl metal, were weighed in the glove box using an electronic balance (Sartorius Model 1205 MP). The error in weighing was estimated to be ± 0.004 g.

2:5:1 Preparation of Thallium Hexafluorophosphate.³⁰

A flamed out double limb reaction vessel was loaded with TlF (4.5 mmol) in the glove box. The reaction vessel was attached to the line, re-evacuated, and MeCN (5ml) and PF₅ (4.5 mmol) were distilled at 77 K, by vacuum distillation using liquid N₂ as a coolant. On warming to room temperature, a pale yellow solution was obtained which became colourless after overnight shaking. The solution phase was decanted into the empty limb of the vessel and a white solid was isolated after the removal of volatile material by vacuum distillation. The infra-red spectrum of the solid had bands at $\bar{\nu}_{\max}$ 840 cm⁻¹ and 560 cm⁻¹ assigned to PF₆⁻ but no bands due to coordinated MeCN were observed.

2:5:2 Preparation of Thallium Heptafluorotungstate(VI).⁶²

Thallium(I) fluoride (0.70 mmol) was loaded into a double limbed reaction vessel. MeCN (5ml) and WF₆ (2.10 mmol) were vacuum distilled at 77 K. The mixture was shaken overnight at room temperature. From the colourless solution so obtained, a white solid was isolated after removal of the volatile material. The infrared spectrum of the solid (Nujol Mull) contained a strong band at 620 cm⁻¹ assigned to WF₇⁻ and the bands due to coordinated MeCN were absent. The Raman spectrum contained characteristic bands at 710 (s), 615 (m) and 295 (s) due to WF₇⁻.

2:5:3 Preparation of Thallium Hexafluorotungstate(V).⁴⁴

Thallium metal (0.5 mmol) was placed in one limb of a reaction vessel and MeCN (5ml) and WF_6 (1.5mmol) were added by vacuum distillation. The reaction mixture was shaken for one hour at room temperature. A white solid was isolated from the resulting colourless solution after removal of the volatile material. The infrared spectrum of the solid (Nujol Mull) contained bands at 590 and 615 cm^{-1} assigned to WF_6^- and WF_7^- respectively, thus the solid was assumed to be a mixture of $TlWF_6$ and $TlWF_7$.

2:5:4 Preparation of Thallium(I) Hexafluoromolybdate(V).⁴⁸

$TlMoF_6$ was prepared by the oxidation of thallium metal with $NOMoF_6$.

(1) Preparation of $NOMoF_6$.¹²⁴ MeCN (5ml) was distilled into one limb of a previously evacuated and flamed out reaction vessel.

Nitric oxide (1.5 mmol) and MoF_6 (1 mmol) were distilled onto MeCN and the reaction mixture was allowed to warm to room temperature.

An orange solid was isolated from the resulting solution after removal of volatile material. The infrared spectrum of the solid (Nujol Mull) contained bands at 620 (ν_3) and 240 (ν_4) cm^{-1} corresponding to MoF_6^- and one band at 2340 cm^{-1} assigned to ' ν ' of NO^+ . The orange solid was thus identified as nitrosonium hexafluoromolybdate(V).

(2) Oxidation of thallium metal using $NOMoF_6$ as an oxidising agent.

Thallium metal (1 mmol) was loaded in one limb of the reaction vessel and $NOMoF_6$ (0.75 mmol) into the other. MeCN (5ml) was distilled onto $NOMoF_6$ and the resulting solution was transferred to the limb containing Tl metal which dissolved rapidly in the solution at room temperature, with the evolution of a colourless gas, NO. A mustard colour solid was isolated from the solution after removal of

volatile material. The infrared spectrum of the solid (Nujol Mull) contained bands at 635 (ν_3) and 255 (ν_4) cm^{-1} assigned to MoF_6^- . The bands due to coordinated MeCN were not present.

2:5:5 Preparation of Thallium(I) Hexafluorouranate(V).

TlUF_6 was obtained by the oxidation of thallium metal using NOUF_6 as an oxidising agent.

(1) Preparation of NOUF_6 .¹²⁴ Acetonitrile (5ml), nitric oxide (1.5 mmol) and UF_6 (1 mmol) were distilled into a reaction vessel. The reaction mixture was allowed to warm to room temperature. A pale green solid was isolated from the resulting pale green solution after removing the volatile material. The solid was identified as nitrosonium hexafluorouranate(V) by its infrared spectrum which showed bands at 520 (ν_3) and 2320 cm^{-1} assigned to UF_6^- and NO^+ respectively.

(2) Preparation of TlUF_6 . Thallium metal (1 mmol) and NOUF_6 (0.75 mmol) were loaded into each of the two limbs of the reaction vessel. MeCN (5ml) was distilled onto NOUF_6 and the resulting solution transferred to the limb containing Tl metal which reacted vigorously with the solution at room temperature evolving a colourless gas, NO. A pale green solid was isolated from the resulting pale green solution, after removal of volatile material. The infrared spectrum of the solid (Nujol Mull) contained a strong band at 520 (ν_3) cm^{-1} assigned to UF_6^- . No bands due to coordinated MeCN were observed. The electronic spectrum of the solid, in MeCN, showed the characteristic f-f transitions of a UF_6^- anion.⁴⁵ Therefore, the solid was characterized as thallium(I) hexafluorouranate(V).

2:5:6 Preparation of $\text{Tl}(\text{UF}_6)_3 \cdot 5\text{MeCN}$.⁴⁵

Thallium metal (2 mmol) was loaded into one limb of a reaction vessel. MeCN (5ml) and UF_6 (8 mmol) were added by vacuum distillation. The reaction mixture was shaken for one hour at room temperature. A pale green solid was isolated from the resulting green solution after removing the volatile material. The infrared spectrum of $\text{Tl}^{\text{III}}(\text{UF}_6)_3 \cdot 5\text{MeCN}$ contained bands due to coordinated MeCN, 2320 (comb.) 2295 $\nu(\text{CN})$ and 950 $\nu(\text{CC})$ and a strong band at 520 cm^{-1} due to UF_6^- .

2:5:7 Preparation of Mixed Thallium(I,III) Hexafluoromolybdate(V).

Thallium metal (2 mmol) was loaded in a reaction vessel. MeCN (5 ml) and MoF_6 (10 mmol) were distilled in and the mixture allowed to warm to room temperature. The reaction mixture was shaken overnight and an off-white solid was isolated from the pale yellow solution after removing the volatile material. The solid was identified as a mixture of thallium(I) and thallium(III) hexafluoromolybdate from a combination of ^{205}Tl n.m.r. spectroscopy, $^{205}\text{Tl}^{\delta} = -158$ ppm at 0.13 mol dm^{-3} and $^{205}\text{Tl}^{3+\delta} = 2051$ ppm at 0.13 mol dm^{-3} , and infrared spectroscopy, bands at 2322 (comb.) 2290 $\nu(\text{CN})$ and 950 $\nu(\text{CC})$ were assigned to coordinated MeCN and those at 640 (ν_3) and 250 (ν_4) cm^{-1} to MoF_6^- .

2:5:8 Preparation of Solutions for ^{205}Tl N.M.R. Spectroscopy.

Solutions of Tl(I) and Tl(III) complex fluoroanion salts, in MeCN, were prepared in the glove box. To minimize the error, the salts were sealed in frangible ampoules, weighed on an analytical balance outside the glove box. From the standard solutions so obtained, solutions of different concentrations were made by

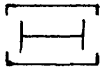
dilution using two microburettes in the glove box. The solutions were loaded into the vessels fitted with n.m.r. tubes. Thallium-205 n.m.r. spectra were obtained in 5 mm n.m.r. tubes at 298 K using a JEOL FX-90 spectrometer with a ^{205}Tl observation frequency of 51.62MHz for Tl^{I} and 51.74MHz for Tl^{III} . All ^{205}Tl resonance frequencies were referenced to the 'infinite dilution' resonance frequency of $^{205}\text{Tl}^+$ in water at 298 K (57.683833MHz)⁶⁸ such that the protons of TMS resonate at exactly 100MHz and calculated by using the formula given in equation (10).

$$\delta(\text{ppm}) = \frac{\overbrace{\text{H}}^{\text{ref.}} - \overbrace{\text{H}}^{\text{ref.}}}{\overbrace{\text{H}}^{\text{ref.}}} \times 10^6 \quad (10)$$

Downfield shifts are assigned positive values. The variation of ^{205}Tl chemical shifts in MeCN solutions of Tl^{I} and Tl^{III} salts, and in mixed oxidation state compounds, with increasing salt concentration, is given in Tables 4 to 9.

Table 5.

$^{205}\text{Tl}^+$ Resonance Frequencies and Chemical Shifts of TlMoF_6 at Different Salt Concentrations.

Concentrations (mol dm ⁻³)	 (MHz)	δ (ppm)	$\Delta V_{\frac{1}{2}}$ (Hz)
0.0417	57.671798	-208.6	1900
0.0695	57.672434	-197.9	1400
0.0973	57.672900	-189.5	580
0.139	57.673547	-178.3	570

$^{205}\text{Tl}^+$ Resonance Frequencies and Chemical Shifts of TlWF_6

0.041	57.670297	-234.6	56
0.069	57.670180	-236.6	61
0.096	57.670120	-237.7	86
0.137	57.670066	-238.6	98

Table 6.

$^{205}\text{Tl}^+$ Resonance Frequencies and Chemical Shifts of Tl^+UF_6^- in MeCN
at Different Salt Concentrations.

Concentration (mol. dm ⁻³)	ν (MHz)	δ (ppm)	$\Delta\nu_{\frac{1}{2}}$ (Hz)
0.044	57.671021	-206.5	200
0.048	57.672083	-203.7	200
0.073	57.672875	-189.0	230
0.09	57.673218	-184.0	280
0.101	57.673354	-181.6	310
0.147	57.674174	-164.5	400
0.15	57.674461	-162.5	400
0.20	57.675104	-151.3	470
0.27	57.675856	-138.3	470
0.34	57.676618	-125.1	620

Table 7.

$^{205}\text{Tl}^{3+}$ Resonance Frequencies and Chemical Shifts of $\text{Tl}^{\text{III}}(\text{UF}_6)_3 \cdot 5\text{MeCN}$
 at Different Salt Concentrations.

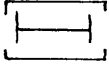
Concentration (mol. dm ⁻³)	 (MHz)	δ (ppm)	$\Delta V_{\frac{1}{2}}$ (Hz)
0.041	57.798715	1991.8	70
0.045	57.798751	1992.2	70
0.068	57.798781	1992.7	70
0.09	57.798822	1993.4	70
0.093	57.798829	1993.5	70
0.136	57.798868	1994.2	100
0.15	57.798885	1994.5	73
0.22	57.798939	1995.5	83
0.27	57.798977	1996.1	85
0.34	57.799028	1996.9	90

Table 8
 $^{205}\text{Tl}^+$ and $^{205}\text{Tl}^{3+}$ Resonance Frequencies and Chemical Shifts in the 1:1 Mixture, $\text{Tl}^{\text{I}}\text{UF}_6 + \text{Tl}^{\text{III}}(\text{UF}_6)_3 \cdot 5\text{MeCN}$
 at Different Concentrations.

Concentration (mol dm^{-3})	$^{205}\text{Tl}^+$ Signals			$^{205}\text{Tl}^{3+}$ Signals		
	ν (MHz)	δ (ppm)	$\Delta\nu_{\frac{1}{2}}$ (Hz)	ν (MHz)	δ (ppm)	$\Delta\nu_{\frac{1}{2}}$ (Hz)
0.045	57.673912	-172	300	57.809994	2187.1	75
0.075	57.675281	-148.3	310	57.810049	2188.1	60
0.105	57.676419	-128.5	550	57.810087	2188.7	65
0.15	57.678138	-98.7	720	57.810138	2189.6	80

Table 9.

$^{205}\text{Tl}^+$ and $^{205}\text{Tl}^{3+}$ Resonance Frequencies and Chemical Shifts in the Mixed Oxidation State Compound



Concentration g dm^{-3}	$^{205}\text{Tl}^+$ Signals			$^{205}\text{Tl}^{3+}$ Signals		
	 (MHz)	δ (ppm)	$\Delta V_{\frac{1}{2}}$ (Hz)	 (MHz)	δ (ppm)	$\Delta V_{\frac{1}{2}}$ (Hz)
43	57.672534	-195.9	200	57.801423	2039	210
71	57.673371	-181.4	450	57.801767	2045	240
99.5	57.674219	-166.7	600	57.802077	2050	250
143	57.674721	-158.0	1200	57.802144	2051	850

CHAPTER THREE

Substitution Reactions of the Solvated Fe^{II} Cation in Acetonitrile

3.1 Introduction

The chemistry of iron complexes is important both from an industrial and a biochemical point of view. Iron has a functional role in many living systems, for example oxygen transport to different parts of the human body through hemoglobin. In aqueous solution, Fe(III) is the most common oxidation state whereas Fe(II) is the stable oxidation state in acetonitrile. Iron(II) is known, in MeCN solution as the $[\text{Fe}(\text{NCMe})_6]^{2+}$ ion and is prepared by the oxidation of iron metal with oxidising agents such as NOBF_4 ,²¹ $\text{CF}_3\text{SO}_3\text{H}$,¹²⁵ MF_6 , (M = W or Mo) or NOPF_6 ,⁴⁷ and by Lewis acid-Lewis base reactions involving FeCl_2 and a Lewis acid chloride⁶¹ or anhydrous FeF_2 and PF_5 .⁴⁷ There is no definite evidence in the literature for the formation of $[\text{Fe}(\text{NCMe})_6]^{3+}$ although Fe(III) is known in complex ions such as FeCl_4^- .⁴⁷

The hexakis (acetonitrile) iron(II) cation is a convenient starting point for the development of the non-aqueous chemistry of iron(II) with simple ligands. The aim of this study is to investigate the substitution behaviour of the $[\text{Fe}(\text{NCMe})_6]^{2+}$ cation, in acetonitrile solution, using simple N,P and S-donor ligands such as NH_3 , NMe_3 , pyridine (py), $\text{P}(\text{OMe})_3$, PMe_3 , Me_2S and tetramethylthiourea(tmtu), and to study how far these simple ligands are able to stabilize iron(II) in acetonitrile solution.

3.1.1 Iron(II) Salts with Nitrogen Donor Ligands.

Iron(II) hexaammine salts, $[\text{Fe}(\text{NH}_3)_6]\text{X}_2$, (X = Cl, Br, I, ClO_4 or BF_4), are well known in the solid state but their chemistry in solution has been little studied. The phenomenon of phase transitions in these salts has been studied by the X-ray structural investigation.¹²⁶ The hexa-ammine compounds have been shown to build up 'octahedral' ions,

$[\text{Fe}(\text{NH}_3)_6]^{2+}$, with the terminal hydrogens forming hydrogen bonding with the anions. The quadrupole interaction of the ^{57}Fe nucleus for the complexes, $[\text{Fe}(\text{NH}_3)_6]\text{X}_2$ and $[\text{Fe}(\text{ND}_3)_6]\text{X}_2$ has been measured by Mössbauer spectrometry and varies in an appreciable amount when the H atoms are replaced by the D atoms.¹²⁷

The hexa-ammine iron(II) salts have been prepared either by the dry or the wet reactions. In the dry process, NH_3 is passed over the anhydrous iron(II) salt whereas in the wet process, NH_3 is made to flow through a freshly prepared solution of the iron(II) salt in ammoniated ethanol till the complex is precipitated which is washed with ammoniated alcohol and ether, and finally dried in an ammonia stream.¹²⁸ K.H. Schmidt and A. Müller have carried out a systematic investigation of skeletal infrared and Raman data of the octahedral iron(II) hexa-ammine salt, $\text{Fe}(\text{NH}_3)_6\text{Cl}_2$.¹²⁹ The metal-nitrogen stretching vibrational frequency for the complex, $[\text{Fe}(\text{NH}_3)_6]^{2+}$, occurs in the range 30 to 370 cm^{-1} . The ligand field splitting energies for hexa-ammine complexes of Mn(II), Fe(II) and Zn(II) have been measured thermochemically using the calorimetric technique.¹³⁰ It has been shown that the maximum difference in heat of solution between the normal crystalline lower amines and the high energy modifications of the lower amines of these salts, when expressed as k cal mole^{-1} of each hepta-ammine, are equivalent to the ligand field splitting energies of the hexa-ammine metal(II) ions.

The hexa(pyridine)iron(II) cation, $[\text{Fe}(\text{py})_6]^{2+}$, has been prepared by adding a solution of pyridine in ethanol to a suspension of FeCl_2 in ether.¹³¹ The compound has been characterized by electronic and infrared spectroscopy, and by the X-ray powder method. The structure of the complex, $[\text{Fe}(\text{py})_6][\text{Fe}_4(\text{CO})_{13}]$, has been determined by X-ray crystallography and is shown to be composed of discrete cations and anions.¹³² In the cation, $[\text{Fe}(\text{py})_6]^{2+}$, the Fe(II) has the regular

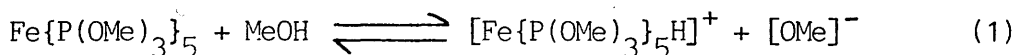
octahedral environment of six nitrogen atoms about it with the pyridine molecules lying in three mutually perpendicular planes. Recently the hexa(pyridine)iron(II) salt, $[\text{Fe}(\text{py})_6][\text{Picrate}]_2$, has been obtained in the form of brown green crystals by mixing alcoholic solutions of iron picrate and pyridine.¹³³ Iron(II) complexes with the ligand trimethylamine do not appear to have been reported previously.

3.1.2 Iron(II) Salts with Phosphorus Donor Ligands.

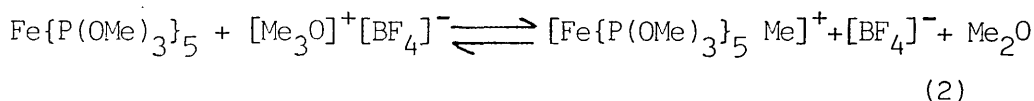
Iron-trimethyl phosphine complexes are known mainly in the form of low oxidation state compounds such as clusters.¹³⁴ Only a few simple iron-trimethyl phosphine complexes, such as $\text{Fe}(\text{PMe}_3)_2(\text{CO})_2\text{X}_2$,¹³⁵ ($\text{X} = \text{Cl}, \text{Br}$ or I) and $\text{Fe}(\text{PMe}_3)_3(\eta^4\text{-butadiene})$,¹³⁶ are known. The latter complex is prepared by the reduction of FeCl_2 in the presence of PMe_3 and butadiene. A number of five coordinate $\text{Ni}(\text{II})\text{-PMe}_3$ complexes of the general formula, $\text{NiX}_2(\text{PMe}_3)_3$, $[\text{NiX}(\text{PMe}_3)_4][\text{X}]$, ($\text{X} = \text{Cl}, \text{Br}$ or I) and $[\text{Ni}(\text{PMe}_3)_5][\text{BF}_4]_2$, have been characterized in CH_2Cl_2 or CHClF_2 solutions.¹³⁷ A number of cobalt-trimethylphosphine complexes have been reported. In the presence of trimethylphosphine anhydrous CoCl_2 is reduced by magnesium in tetrahydrofuran(THF) solution to form tetrakis (trimethylphosphine) cobalt(0).¹³⁸ The $\text{Co}(0)$ complex, $\text{Co}(\text{PMe}_3)_4$ reacts with anhydrous CoX_2 salts, ($\text{X} = \text{Cl}, \text{Br}$ or I) in etheral solution in the presence of PMe_3 forming $\text{Co}(\text{I})$ complexes, $\text{CoX}(\text{PMe}_3)_3$.¹³⁹ The oxidation of the $\text{Co}(0)$ complex by iodine results in the formation of the complex, $\text{CoI}(\text{PMe}_3)_3$. The tetrahedral $[\text{Co}(\text{PMe}_3)_4]^+$ cation is formed when $\text{CoX}(\text{PMe}_3)_3$ complexes are reacted with PMe_3 at low temperatures in CH_2Cl_2 solution. Trimethylphosphine complexes of cobalt(I), $[\text{Co}(\text{MeCN})(\text{C}_2\text{H}_4)(\text{PMe}_3)_3][\text{X}]$, ($\text{X} = \text{Br}$ or BPh_4), have been prepared by the reaction of $\text{CoBr}(\text{PMe}_3)_3$ with ethylene in acetonitrile either in the presence or absence of NaBPh_4 .¹⁴⁰ The

crystal structure of the complex $[\text{Co}(\text{MeCN})(\text{C}_2\text{H}_4)(\text{PMe}_3)_3][\text{BPh}_4]$ has been determined and contains a distorted trigonal bipyramid cation, $[\text{Co}(\text{MeCN})(\text{C}_2\text{H}_4)(\text{PMe}_3)_3]^+$ in which MeCN and PMe_3 are axial whereas C_2H_4 and two PMe_3 ligands are equatorial. Simple PMe_3 complexes such as $\text{MnX}_2(\text{PMe}_3)$ and $\text{MnX}_2(\text{PMe}_3)_2$, ($\text{X} = \text{Cl}, \text{Br}$ or I) have recently been prepared by the reaction of anhydrous MnX_2 salts with PMe_3 in toluene/ CH_2Cl_2 mixtures.¹⁴¹

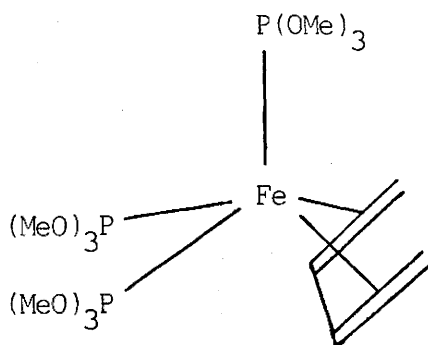
Iron-trimethyl phosphite species are widely reported principally due to the unusual steric and electronic properties of the ligand. The alkyl phosphites are less sterically demanding than the corresponding alkyl phosphines and possess greater π -acceptor ability due to the more electronegative substituents on phosphorus.¹⁴² The main work on iron-trimethyl phosphite complexes stems from the preparation of the neutral complex, $\text{Fe}\{\text{P}(\text{OMe})_3\}_5$, by sodium amalgam reduction of $\text{Fe}\{\text{P}(\text{OMe})_3\}_3\text{Cl}_2$, in the presence of excess trimethylphosphite.¹⁴³ The same species has been obtained by the sodium amalgam reduction of FeBr_2 in the presence of excess $\text{P}(\text{OMe})_3$ in tetrahydrofuran solution.¹⁴⁴ This species displays interesting behaviour both physically and chemically. It is fluxional in solution but at 168 K exhibits an A_2B_3 second order $^{31}\text{P}\{-^1\text{H}\}$ -n.m.r. spectrum corresponding to a trigonal bipyramid geometry.¹⁴⁵ The chemistry of this zero-valent species is dominated by its exceptionally electron rich properties. The relatively basic iron atom in the species, $\text{Fe}\{\text{P}(\text{OMe})_3\}_5$, gets protonated to form a six coordinate species when dissolved in methanol (equation 1).



The species can also be alkylated by reaction with $[\text{Me}_3\text{O}]^+[\text{BF}_4]^-$ as represented in equation 2.



The high electron density on the metal centre in $\text{Fe}\{\text{P}(\text{OMe})_3\}_5$ is also indicated by a facile one electron oxidation process in which silver(I) or tropylium salts react with the species, in acetonitrile solution, to give $[\text{Fe}\{\text{P}(\text{OMe})_3\}_5(\text{MeCN})]^{2+}$ through two consecutive one electron transfer reactions. The cationic iron(II) complexes, $[\text{Fe}\{\text{P}(\text{OMe})_3\}_5\text{X}]^+$ ($\text{X} = \text{Cl}, \text{Br}$ or I) have been obtained by the addition of $\text{P}(\text{OMe})_3$ to iron bis(tetrahydrofuran)dihalide complexes.¹⁴⁴ A ^{31}P - $\{^1\text{H}\}$ n.m.r. study of these six coordinate iron(II) species in methylene chloride solution yields the characteristic AB_4 spin system spectrum. Under somewhat more extreme conditions, it is possible to replace the halide ion in the complex, $[\text{Fe}\{\text{P}(\text{OMe})_3\}_5\text{X}]^+$ by $\text{P}(\text{OMe})_3$ yielding the species, $[\text{Fe}\{\text{P}(\text{OMe})_3\}_6]^{2+}$, precipitated from the solution by the addition of a similar sized dianion. The complex cation, $[\text{Fe}\{\text{P}(\text{OMe})_3\}_6]^{2+}$ has also been prepared as the tetraphenylborate, BPh_4^- , salt by refluxing anhydrous FeCl_2 and NaBPh_4 in the presence of excess $\text{P}(\text{OMe})_3$ for four hours in MeOH solution.¹⁴⁶ Five coordinate complexes of the type, $[\text{Fe}(\eta^4\text{-diene})\{\text{P}(\text{OMe})_3\}_3]$ have been prepared by Steven *et al.* for a variety of simple cyclic and acyclic dienes using metal evaporation techniques.¹⁴⁷



These species are fluxional and have been used to investigate the exchange mechanisms in five coordinate complexes. Iron(II)-phosphite complexes, $[\text{Fe}\{\text{BH}_3(\text{CN})\}_2\{\text{P}(\text{OMe})_3\}_4]$, have been obtained both metathetically and electrochemically.¹⁴⁸ The metathetical reaction

involves mixing of $\text{FeCl}_2 \cdot 2\text{H}_2\text{O}$, $\text{Na}[\text{BH}_3(\text{CN})]$ and $\text{P}(\text{OMe})_3$ in methanol or acetonitrile solution, whereas the electrochemical process involves anodic dissolution of iron in acetonitrile solutions of trimethylphosphite and $\text{Na}[\text{BH}_3(\text{CN})]$. Recently iron(II) trimethyl phosphite complexes of the composition, $[\text{FeX}(\text{CO})\{\text{P}(\text{OMe})_3\}_4][\text{BPh}_4]$, ($\text{X} = \text{H}, \text{Cl}$ or Br), have been reported in the literature.¹⁴⁹ These complexes are white diamagnetic solids, soluble in all polar solvents and are stable to air both as solids or in solution. The trimethyl phosphite ligands have a trans geometry both in solution and solid state.

Previous work carried out in this Department involved a study of the direct replacement of coordinated MeCN in the complex cation, $[\text{Fe}(\text{NCMe})_6]^{2+}$, by $\text{P}(\text{OMe})_3$ in acetonitrile.⁴⁷ The reaction involves a step-wise substitution of $\text{P}(\text{OMe})_3$ for coordinated MeCN and the course of the reaction has been followed by $^{31}\text{P}\{-^1\text{H}\}$ n.m.r. spectroscopy. The products isolated, after a week, are the diamagnetic yellow solid, $[\text{Fe}(\text{NCMe})\{\text{P}(\text{OMe})_3\}_5][\text{PF}_6]_2$ and the dimethyl methyl phosphonate formed only in a small quantity. The $^{31}\text{P}\{-^1\text{H}\}$ n.m.r. spectrum of the cation is identical to that of the analogous SbF_6^- salt obtained from the oxidation of $\text{Fe}\{\text{P}(\text{OMe})_3\}_5$ by Ag^{I} or tropylium salts.¹⁴⁴ Most of the intermediate steps in the reaction have been observed from a combination of $^{31}\text{P}\{-^1\text{H}\}$ n.m.r. and electronic spectroscopy. The kinetics of low spin $[\text{Fe}\{\text{P}(\text{OMe})_3\}_2(\text{NCMe})_4]^{2+}$ formation are consistent with an interchange mechanism occurring via an outer sphere complex.¹⁵⁰ In the present study, this work has been extended to include reactions of high spin iron(II) complexes having ligated ammonia, pyridine or trimethylamine, with trimethyl phosphite and trimethyl phosphine.

Overall the reactions of these high spin iron(II) cations with phosphorus donor ligands are very similar, however, three different types of behaviour can be distinguished. These may be rationalized

in terms of the different steric properties of the N- and P- donor ligands involved.

3:2 Results.

3:2:1 Preparation and Characterization of Iron(II) Cations with Nitrogen or Sulphur Donor Ligands.

Previous work has shown that coordinated MeCN in hexakis (acetonitrile) iron(II) cation, is replaced readily by pyridine(py) in the presence or absence of acetonitrile.¹⁵¹ The off white solid isolated from the reaction of $[\text{Fe}(\text{NCMe})_6][\text{PF}_6]_2$ with neat pyridine is identified as $[\text{Fe}(\text{py})_6][\text{PF}_6]_2$ on the basis of its analysis and infra-red spectrum. The infra-red spectrum of the solid, $[\text{Fe}(\text{py})_6][\text{PF}_6]_2$, contains bands due to coordinated pyridine, $\bar{\nu}_{\text{max}}$ 1603, 1219, 1160 and 1010 cm^{-1} and the PF_6^- anion, $\bar{\nu}_{\text{max}}$ 840 and 560 cm^{-1} . The bands due to coordinated MeCN are not present. The cation, $[\text{Fe}(\text{py})_6]^{2+}$ loses pyridine when the complex $[\text{Fe}(\text{py})_6][\text{PF}_6]_2$ dissolved in acetonitrile. The analysis of the off-white solid isolated from the resulting solution is consistent with its being $[\text{Fe}(\text{py})_5(\text{NCMe})][\text{PF}_6]_2$, however the presence of $[\text{Fe}(\text{py})_4(\text{NCMe})_2][\text{PF}_6]_2$ may not be excluded. The product obtained from the reaction of $[\text{Fe}(\text{NCMe})_6][\text{PF}_6]_2$ with pyridine in acetonitrile is analytically and spectroscopically identical to the product isolated from the solution of $[\text{Fe}(\text{py})_6][\text{PF}_6]_2$ in acetonitrile. These complexes are high spin and the magnetic moments determined by the Gouy balance method at 298 K, are 5.7 ± 0.2 B.M. The electronic spectra of the complexes, $[\text{Fe}(\text{py})_6][\text{PF}_6]_2$ or $[\text{Fe}(\text{py})_5(\text{NCMe})][\text{PF}_6]_2$, which may form an equilibrium mixture of cations, $[\text{Fe}(\text{py})_{6-x}(\text{NCMe})_x]^{2+}$, $x = 0$ to at least 2, in MeCN solution, consist of a broad asymmetric band, $\bar{\nu}_{\text{max}} = 12000 \text{ cm}^{-1}$ ($\epsilon = 13 \text{ dm}^3 \text{ mol}^{-1} \text{ cm}^{-1}$) with a shoulder at 10500 cm^{-1} ,

assigned to the ${}^5T_{2g} \longrightarrow {}^5E_g$ transition.

Preliminary work involving the reaction of ammonia with $[\text{Fe}(\text{NCMe})_6][\text{PF}_6]_2$, in acetonitrile solution,¹⁵² has been confirmed in the present work. An off-white solid was isolated from the reaction mixture after removal of the volatile material. The solid was identified as $[\text{Fe}(\text{NH}_3)_6][\text{PF}_6]_2$ from its analysis and infrared spectrum; bands at $\bar{\nu}_{\text{max}}$ 3400, 1220 and 630 cm^{-1} were assigned to coordinated NH_3 whereas those at $\bar{\nu}_{\text{max}}$ 840 and 560 cm^{-1} corresponded to the PF_6^- anion. There was no evidence for the presence of coordinated MeCN. The cation, $[\text{Fe}(\text{NH}_3)_6]^{2+}$, was recovered unchanged after dissolution of the complex, $[\text{Fe}(\text{NH}_3)_6][\text{PF}_6]_2$ in acetonitrile, a situation similar to that observed in liquid NH_3 .¹³⁰ The electronic spectrum of the complex, $[\text{Fe}(\text{NH}_3)_6][\text{PF}_6]_2$ in acetonitrile solution, consisted of a broad asymmetric band, $\bar{\nu}_{\text{max}} = 12,400 \text{ cm}^{-1}$ ($\epsilon = 8 \text{ dm}^3 \text{ mol}^{-1} \text{ cm}^{-1}$) with a shoulder at 9,000 cm^{-1} and was consistent with the presence of a high spin iron(II). The band was assigned to the ${}^5T_{2g} \longrightarrow {}^5E_g$ transition. The magnetic moment of the complex determined by the Gouy balance method, was found to be 5.6 ± 0.1 B.M. at 298 K.

It has been shown in a preliminary study that the reaction of trimethylamine with $[\text{Fe}(\text{NCMe})_6][\text{PF}_6]_2$, in acetonitrile, has resulted in the formation of a pale brown solid.¹⁵² In the present work an off-white solid was isolated from the reaction of $[\text{Fe}(\text{NCMe})_6][\text{PF}_6]_2$ with Me_3N in the absence or the presence of MeCN. The solid was characterized as $[\text{Fe}(\text{NMe}_3)(\text{NCMe})_4][\text{PF}_6]_2$ from its microanalysis and the infrared spectrum which contained bands due to coordinated Me_3N , $\bar{\nu}_{\text{max}}$ 3250, 1478 and 1048 cm^{-1} , MeCN, $\bar{\nu}_{\text{max}}$ 2310 and 2285 cm^{-1} and the PF_6^- anion, $\bar{\nu}_{\text{max}}$ 840 and 560 cm^{-1} . Assuming the anion to be non-coordinated, iron(II) in the complex, $[\text{Fe}(\text{NMe}_3)(\text{NCMe})_4][\text{PF}_6]_2$, appears to be

pentacoordinated however, it should be hexacoordinated under normal conditions. Loss of one MeCN ligand during isolation of the solid is not surprising since MeCN is weakly bound to 3d bivalent metal cations. Thermogravimetric analysis of the solid compound, $[\text{Fe}(\text{NCMe})_6][\text{PF}_6]_2$, indicates that two MeCN ligands are lost at temperatures less than 353 K.¹⁵¹ This provides a good evidence for the weakly bound nature of MeCN to 3d metal cations. The magnetic moment of the complex, $[\text{Fe}(\text{NMe}_3)(\text{NCMe})_4][\text{PF}_6]_2$, has been determined by the Gouy balance method and has a value 5.6 ± 0.2 B.M. at 298 K. The electronic spectrum of the complex, in MeCN solution, consists of a broad asymmetric band, $\bar{\nu}_{\text{max}}$ 11,200 cm^{-1} ($\epsilon = 10 \text{ dm}^3 \text{ mol}^{-1} \text{ cm}^{-1}$) with a pronounced shoulder at 10,000 cm^{-1} . The band is assigned to the ${}^5\text{T}_{2g} \longrightarrow {}^5\text{E}_g$ transition and is consistent with the presence of a high spin octahedral iron(II) presumably $[\text{Fe}(\text{NMe}_3)(\text{NCMe})_5]^{2+}$.

The reaction of hexakis(acetonitrile) iron(II) hexafluorophosphate with tmtu, (mole ratio 1:6 or 1:8), in acetonitrile results in the formation of a light green solid. The presence of coordinated tmtu in these complexes is evident from the infrared spectra which contains bands at 1560 cm^{-1} (ν_{NCN}) and 1100 cm^{-1} ($\nu_{\text{C=S}}$) compared with 1520 and 1115 cm^{-1} in pure tmtu. The complex isolated from the reaction in which $\text{Fe}^{\text{II}}:\text{tmtu}$ mole ratio was 1:8, contains bands due to uncoordinated tmtu in its infrared spectrum whereas no such distinction can be made in the spectrum of the complex derived from mole ratio 1:6. A broad band at 835 cm^{-1} and a strong band at 560 cm^{-1} are assigned to the anion, PF_6^- . The electronic spectrum of the complex ($\text{Fe}^{\text{II}}:\text{tmtu} = 1:6$) in MeCN solution, consists of two bands at $\bar{\nu}_{\text{max}}$ 16900 ($\epsilon = 390 \text{ dm}^3 \text{ mol}^{-1} \text{ cm}^{-1}$) and 13000 cm^{-1} ($\epsilon = 280 \text{ dm}^3 \text{ mol}^{-1} \text{ cm}^{-1}$). The molar extinction coefficients for the two bands are estimated by assuming that all the six moles of tmtu ligands are coordinated to Fe^{II} , by replacing the MeCN molecules in the complex $[\text{Fe}(\text{NCMe})_6]^{2+}$.

A recent study has reported the formation of tetra, penta and hexa-coordinated high spin iron(II) complexes with substituted thioureas (N,N'-dimethyl thiourea, N,N'-diethyl thiourea and N,N'-di n-propyl thiourea) having perchlorate or tetrafluoroborate as counteranions.¹⁵³ These complexes have been prepared by adding stoichiometric amounts of the ligand to a concentrated solution of iron(II) salt in 1-butanol with different volumes of the solvent according to ligand solubility. The mixture is heated and stirred until all the ligand dissolved and then allowed to stand at 273 K until crystals are formed. The crystals are filtered out, washed with 1-butanol and dried in vacuo at room temperature. The electronic spectra of these complexes are recorded in the solid state as Nujol mulls. The d-d transitions for tetrahedral complexes are in the region, 6500 cm^{-1} whereas for octahedral complexes, they are in the region $9800\text{--}10300\text{ cm}^{-1}$. The use of involatile ligand, that is tmtu, causes the difficulty in precipitating or crystallizing the complex from acetonitrile solution. As a result a detailed study of the iron(II) tmtu complex has not been attempted in the present work. No reaction has been observed between $[\text{Fe}(\text{NCMe})_6]^{2+}$ and Me_2S with or without the presence of acetonitrile.

3:2:2 Replacement of Nitrogen Donor Ligands at Iron(II) by Trimethyl phosphite.

The reaction between $[\text{Fe}(\text{py})_6]^{2+}$ or $[\text{Fe}(\text{py})_{6-x}(\text{NCMe})_x]^{2+}$ and $\text{P}(\text{OMe})_3$, in acetonitrile solution, involves a step-wise substitution whose course has been followed by $^{31}\text{P}\text{-}\{^1\text{H}\}$ n.m.r. and electronic spectroscopy.¹⁵¹ Trimethyl phosphite reacts with $[\text{Fe}(\text{py})_6][\text{PF}_6]_2$ in acetonitrile, at room temperature to give a yellow, diamagnetic solid, $[\text{Fe}\{\text{P}(\text{OMe})_3\}_5(\text{py})][\text{PF}_6]_2$. The solution is initially red, rapidly becomes orange and then changes to pale yellow over a period of 24 hours.

The formation of the yellow diamagnetic solid, $[\text{Fe}\{\text{P}(\text{OMe})_3\}_5(\text{py})][\text{PF}_6]_2$, in substantial amount requires seven days. The $^{31}\text{P}\{-^1\text{H}\}$ n.m.r. spectrum of the cation, $[\text{Fe}\{\text{P}(\text{OMe})_3\}_5(\text{py})]^{2+}$, in CD_3CN , consists of an AB_4 spin system (Table 1) and the electronic spectrum (Table 2) consists of two bands assigned to $^1\text{A}_1 \longrightarrow ^1\text{A}_2$ and $^1\text{A}_1 \longrightarrow ^1\text{E}$ d-d transitions in C_{4v} symmetry by analogy with the spectrum of $[\text{Fe}(\text{CN})_5(\text{OH}_2)]^{3-}$ (ref.154). Most of the intermediate cations in this reaction have been identified from $^{31}\text{P}\{-^1\text{H}\}$ n.m.r. spectra of the reaction mixture with electronic spectroscopy providing supporting evidence. The n.m.r. assignments (Table 1) are made on the basis of the spin systems observed and for species giving rise to singlets, their appearance/disappearance behaviour with time.

The initial stages of the reaction are quite fast whereas the latter stages of the reaction are easily followed up by $^{31}\text{P}\{-^1\text{H}\}$ n.m.r. spectroscopy. The reaction between $[\text{Fe}(\text{py})_6]^{2+}$ and $\text{P}(\text{OMe})_3$, in acetonitrile, in the later stages is identical to that observed previously for $[\text{Fe}(\text{NCMe})_6]^{2+}$ (ref.47).

The first low spin cation to be formed in the reaction of $[\text{Fe}(\text{NCMe})_6]^{2+}$ with $\text{P}(\text{OMe})_3$ is $\text{cis}-[\text{Fe}\{\text{P}(\text{OMe})_3\}_2(\text{NCMe})_4]^{2+}$ identified by its $^{31}\text{P}\{-^1\text{H}\}$ n.m.r. and electronic spectra.^{47, 150} In the reaction between $[\text{Fe}(\text{py})_6]^{2+}$ and $\text{P}(\text{OMe})_3$, in acetonitrile solution, however, no $^{31}\text{P}\{-^1\text{H}\}$ n.m.r. signals attributable to bis(trimethylphosphite) cations are observed even when the reactants are mixed in an n.m.r. tube at 195K. Formation of a low spin species was observed by stopped-flow electronic spectroscopy, a technique that is described in chapter 6.

The reaction between $[\text{Fe}(\text{py})_6]^{2+}$ and $\text{P}(\text{OMe})_3$ was studied under pseudo first order conditions, the concentration of $\text{P}(\text{OMe})_3$ was at least 100 fold in excess over the concentration of $[\text{Fe}(\text{py})_6]^{2+}$. The traces from the reaction of $[\text{Fe}(\text{py})_6]^{2+}$ with $\text{P}(\text{OMe})_3$, were recorded

Table 1.

 ^{31}P - $\{^1\text{H}\}$ N.M.R. Data for Iron(II) Trimethyl Phosphite Cations.

Cation	Spin System	Chemical Shifts \bar{a} (p.p.m)		Coupling constant $J_{AB}(\text{Hz})$
		δ_A	δ_B	
fac-[FeP ₃ (py) ₃] ²⁺	A ₃	155.6	-	
mer-[FeP ₃ (py) ₃] ²⁺	AB ₂	156.1	143.3	131
cis-[FeP ₄ (py) ₂] ²⁺	A ₂ B ₂	157.6	146.4	137
[FeP ₅ (py)] ²⁺	AB ₄	156.0	148.4	131
trans-[FeP ₂ $\overset{\cdot}{\text{N}}\text{N}_3$] ²⁺	B ₂	-	145.2	
cis-[FeP ₂ $\overset{\cdot}{\text{N}}\text{N}_3$] ²⁺	A ₂	155.9	-	
fac-[FeP ₃ $\overset{\cdot}{\text{N}}\text{N}_2$] ²⁺	A ₃	154.2	-	
mer-[FeP ₃ $\overset{\cdot}{\text{N}}\text{N}_2$] ²⁺	AB ₂	157.5	147.1	130
cis-[FeP ₄ $\overset{\cdot}{\text{N}}\text{N}$] ²⁺	A ₂ B ₂	157.6	146.6	137
trans-[FeP ₄ $\overset{\cdot}{\text{N}}\text{N}$] ²⁺	B ₄	-	146.9	
[FeP ₅ $\overset{\cdot}{\text{N}}$] ²⁺	AB ₄	156.7	148.1	134
cis-[FeP ₄ (NH ₃) ₂] ²⁺	A ₂ B ₂	165.4	149.8	130

 \bar{a} To low field of 85% H₃PO₄P = P(OMe)₃; py = pyridine; $\overset{\cdot}{\text{N}}$ = Me₃N; N = MeCN

Table 2.

Electronic Spectra ^a of $[\text{Fe}\{\text{P}(\text{OMe})_3\}_5\text{L}]^{2+}$, L = py or NMe_3 Cations.

Cation	$\nu_{\text{max}} (\text{cm}^{-1})$	
	${}^1\text{A}_1 \longrightarrow {}^1\text{E}$	${}^1\text{A}_1 \longrightarrow {}^1\text{A}_2$
$[\text{Fe}\{\text{P}(\text{OMe})_3\}_5(\text{py})]^{2+}$	26,700 (300) ^b	32,600 (250)
$[\text{Fe}\{\text{P}(\text{OMe})_3\}_5(\text{NMe}_3)]^{2+}$	27,900 (360)	32,600 (300)
$[\text{Fe}\{\text{P}(\text{OMe})_3\}_5(\text{NCMe})]^{2+}$ ^c	26,700 (370)	32,700 (250)
$[\text{Fe}(\text{CN})_5(\text{OH}_2)]^{3-}$ ^d	22,520 (444)	30,300 (100)

^a Assignments in C_{4v} symmetry.

^b Molar extinction coefficients ($\text{dm}^3 \text{mol}^{-1} \text{cm}^{-1}$)

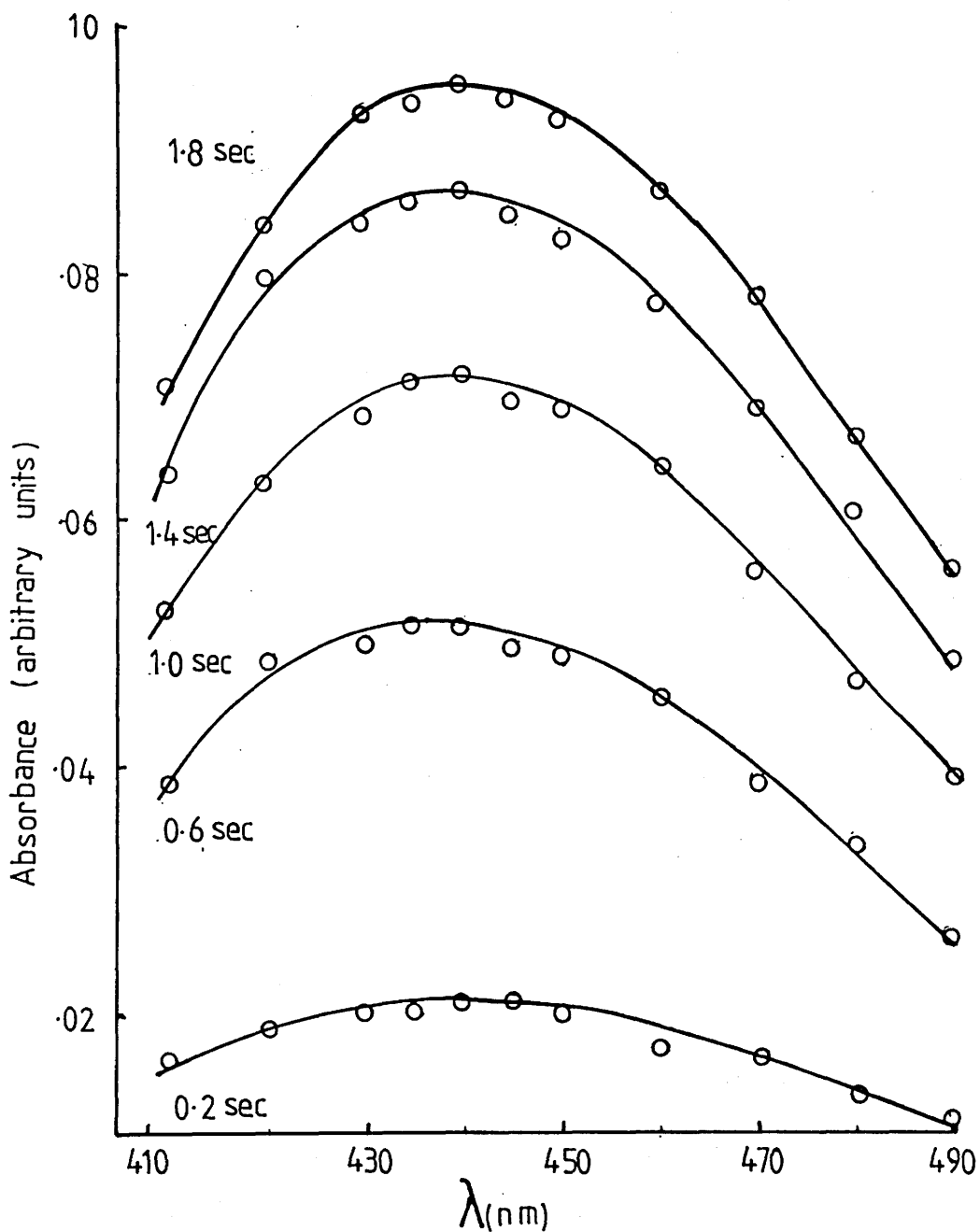
^c Reference 47.

^d Reference 154

over the region 17000 to 33000 cm^{-1} . The electronic spectrum of the 1st. low spin iron(II) bis(trimethylphosphite) species was obtained by plotting the change in optical density as a function of wave length. The results of an experiment using solutions $4 \times 10^{-3} \text{ mol dm}^{-3}$ in Fe(II) and $5 \times 10^{-1} \text{ mol dm}^{-3}$ in $\text{P}(\text{OMe})_3$ are plotted in Figure 1. The electronic spectrum showed a maximum absorption at $\bar{\nu}_{\text{max}} = 22,700 \text{ cm}^{-1}$ with a molar extinction coefficient, $\epsilon = 350 \text{ dm}^3 \text{ mol}^{-1} \text{ cm}^{-1}$, and is very similar to that observed for $[\text{Fe}\{\text{P}(\text{OMe})_3\}_2(\text{NCMe})_4]^{2+}$, $\bar{\nu}_{\text{max}} = 23,000 \text{ cm}^{-1}$ and $\epsilon = 320 \text{ dm}^3 \text{ mol}^{-1} \text{ cm}^{-1}$, under identical conditions.¹⁵⁰ This spectrum was found to be in good agreement with the spectrum of the first species observed in the conventional electronic spectroscopic study. The disappearance of this species as followed by electronic spectroscopy is first order in trimethyl phosphite concentration. Disappearance of the di-substituted species results in the formation of $\text{fac-}[\text{Fe}\{\text{P}(\text{OMe})_3\}_3(\text{py})_3]^{2+}$ which then undergoes further substitution. The rearrangement $\text{fac} \longrightarrow \text{mer}[\text{Fe}\{\text{P}(\text{OMe})_3\}_3(\text{py})_3]^{2+}$ is observed and there is a marked preference for $\text{cis-}[\text{Fe}\{\text{P}(\text{OMe})_3\}_4(\text{py})_2]^{2+}$ over the trans isomer. Approximately 20 hours are required for $\text{cis-}[\text{Fe}\{\text{P}(\text{OMe})_3\}_4(\text{py})_2]^{2+}$ isomer to become a major component of the reaction mixture and some of this species is still present after seven days.¹⁵¹

The compound $[\text{Fe}(\text{NMe}_3)(\text{NCMe})_4][\text{PF}_6]_2$, reacts with trimethyl phosphite, in acetonitrile at room temperature to form a red solution whose colour changes rapidly to orange and then to yellow over a period of 24 hours. A yellow diamagnetic solid, $[\text{Fe}\{\text{P}(\text{OMe})_3\}_5(\text{NMe}_3)]-[\text{PF}_6]_2$ was isolated from this solution after seven days. The $^{31}\text{P}\{-^1\text{H}\}$ n.m.r. spectrum of the cation, $[\text{Fe}\{\text{P}(\text{OMe})_3\}_5(\text{NMe}_3)]^{2+}$, in CD_3CN , consisted of an AB_4 spin system (Table 1). The reaction of trimethyl phosphite with $[\text{Fe}(\text{NMe}_3)(\text{NCMe})_5]^{2+}$, in acetonitrile proceeds via a step-wise substitution of $\text{P}(\text{OMe})_3$ for coordinated MeCN . The step-wise

Figure 1. Formation of the 1st. Low Spin Fe^{II} bis(trimethylphosphite) Species in the [Fe(py)₆]²⁺ and P(OMe)₃ Reaction as Observed by Stopped-Flow.



nature of the substitution reaction is demonstrated by the $^{31}\text{P}-\{^1\text{H}\}$ n.m.r. study of the reaction mixture $[\text{Fe}(\text{NMe}_3)(\text{NCMe})_5]^{2+}$ and $\text{P}(\text{OMe})_3$. A number of species which would give rise to a single peak in the $^{31}\text{P}-\{^1\text{H}\}$ n.m.r. spectrum, are involved and this could lead to ambiguity in assigning a particular single peak to a specific isomer. This problem, however, was overcome by correlating the appearance or disappearance of the singlet with the appearance of the second order multiplet spectra which were also involved and could be assigned unambiguously to a specific isomer. For example the $^{31}\text{P}-\{^1\text{H}\}$ n.m.r. spectrum obtained immediately after mixing the reactants at 243 K consists of two singlets at 145.2 and 155.9 ppm, which on the basis of their chemical shifts are assigned to trans and cis- $[\text{Fe}\{\text{P}(\text{OMe})_3\}_2(\text{NMe}_3)(\text{NCMe})_3]^{2+}$ isomers respectively (Figure 2). Over the first few minutes of the reaction, the intensity of the former singlet decreases, that assigned to the cis-isomer increases and a new singlet tentatively assigned to fac- $[\text{Fe}\{\text{P}(\text{OMe})_3\}_3(\text{NMe}_3)(\text{NCMe})_2]^{2+}$ on the basis of its chemical shift (Table 1), is observed (Figure 2.). It is necessary to assume that the three nitrogen ligands in fac- $[\text{Fe}\{\text{P}(\text{OMe})_3\}_3(\text{NMe}_3)(\text{NCMe})_2]^{2+}$ are equivalent on the n.m.r. time scale as a result of rapid exchange between NMe_3 and MeCN . The singlet assigned to fac- $[\text{Fe}\{\text{P}(\text{OMe})_3\}_3(\text{NMe}_3)(\text{NCMe})_2]^{2+}$ was replaced rapidly by AB_2 and A_2B_2 multiplet spectra which were assigned to mer- $[\text{Fe}\{\text{P}(\text{OMe})_3\}_3(\text{NMe}_3)(\text{NCMe})_2]^{2+}$ and cis- $[\text{Fe}\{\text{P}(\text{OMe})_3\}_4(\text{NMe}_3)(\text{NCMe})]^{2+}$ isomers respectively. A singlet assigned to the isomer, trans- $[\text{Fe}\{\text{P}(\text{OMe})_3\}_4(\text{NMe}_3)(\text{NCMe})]^{2+}$ was also observed and marked by an asterisk in Figure 3. In addition to the signals due to the species listed in Table 1, a broad singlet is observed due to the exchange of free trimethyl phosphite with $\text{P}(\text{OMe})_3$ associated with the metal ion. This exchange can be slowed down by reducing the temperature of the reaction mixture.

Figure 2. Representative $^{31}\text{P}\{-^1\text{H}\}$ N.M.R. Spectra for the Reaction of $[\text{Fe}(\text{NMe}_3)(\text{NCMe})_5]^{2+}$ with $\text{P}(\text{OMe})_3$.

(a) after 5 minutes at 243K.

(b) after 30 minutes at 293K.

cis- $[\text{Fe}\{\text{P}(\text{OMe})_3\}_2(\text{NMe}_3)(\text{NCMe})_3]^{2+}$, A_2

trans- $[\text{Fe}\{\text{P}(\text{OMe})_3\}_2(\text{NMe}_3)(\text{NCMe})_3]^{2+}$, B_2

fac- $[\text{Fe}\{\text{P}(\text{OMe})_3\}_3(\text{NMe}_3)(\text{NCMe})_2]^{2+}$, A_3

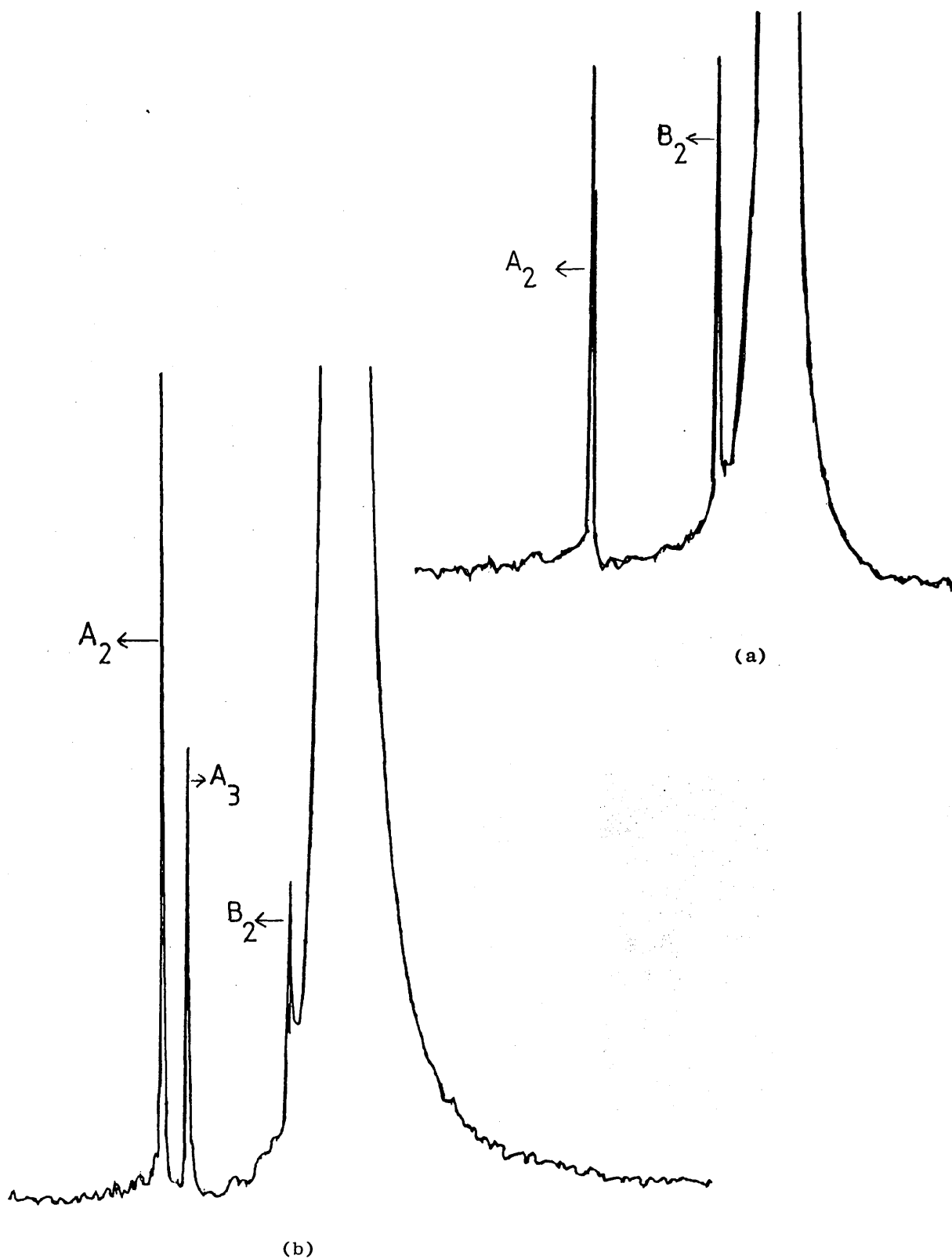
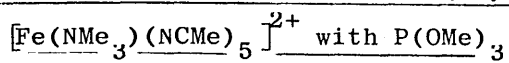
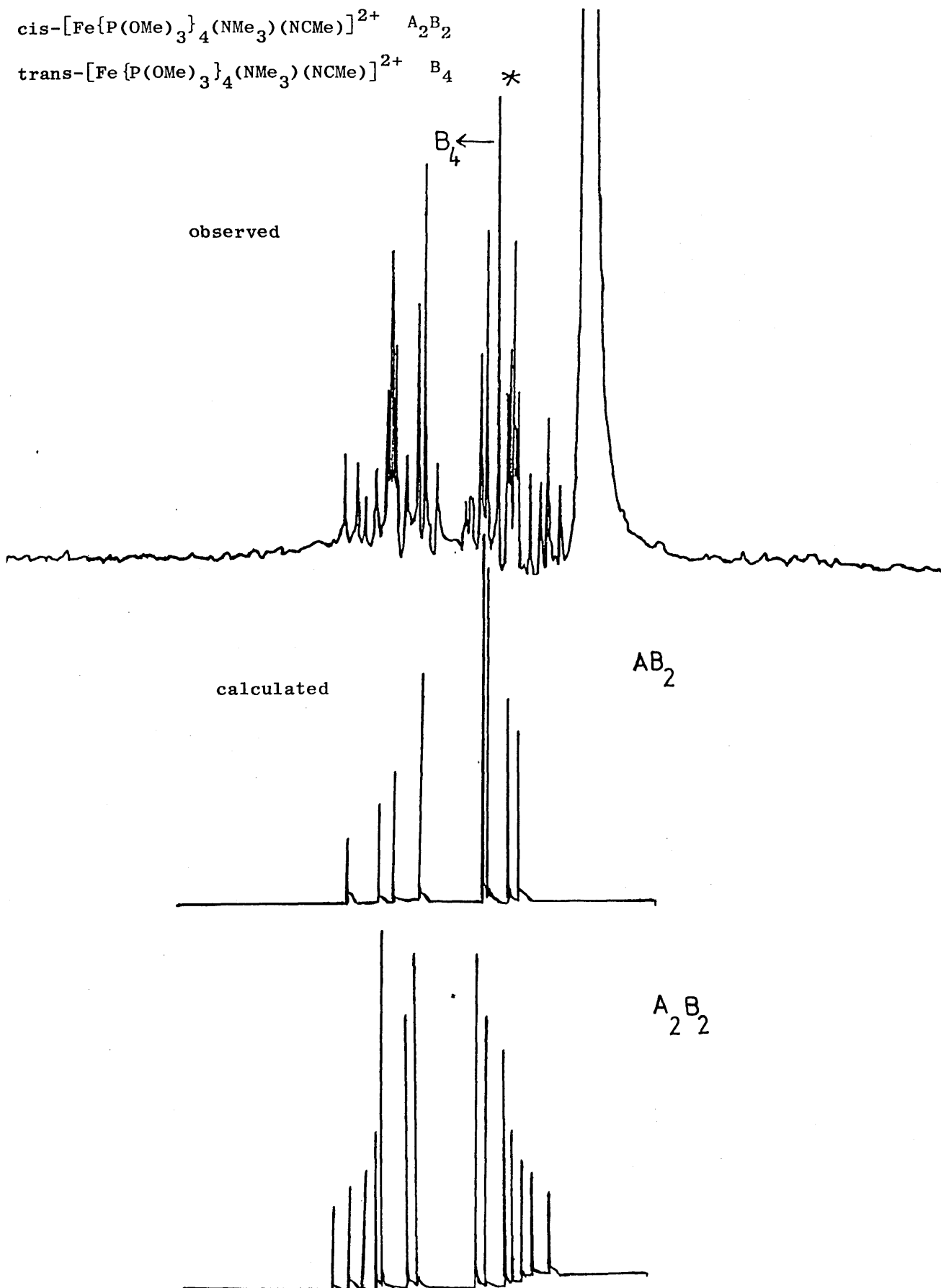
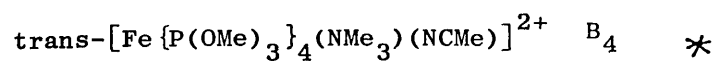
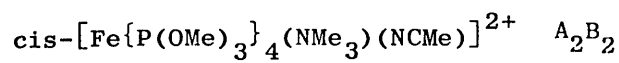
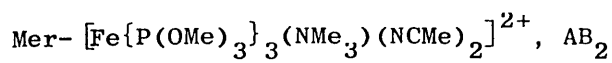


Figure 3. Observed and Calculated $^{31}\text{P}\{-^1\text{H}\}$ N.M.R. Spectra for the Reaction of



after 3 hours at 298K.



As the theory behind second order spectra is well established,¹⁵⁵ it is possible to calculate spectra for particular values of chemical shift and coupling constant. Figure 4 shows calculated AB₄ spectrum along with the spectrum of the product, [Fe{P(OMe)₃}₅(NMe₃)]-[PF₆]₂, isolated after seven days of the reaction. A comparison of calculated frequencies of transition with experimentally observed results is listed in Table 3, for AB₂, A₂B₂ and AB₄ spectra. Representative spectra at different reaction times are illustrated in Figures 2,3 and 4. The ³¹P chemical shifts of the trimethyl phosphite complexes exhibit a shift to lower field with respect to free P(OMe)₃. The range of shifts fall into two distinct groups: complexes which have P(OMe)₃ trans to NMe₃ or NCMe, have ³¹P chemical shifts in the range +15 to +20 ppm from free P(OMe)₃ and the complexes having P(OMe)₃ trans to P(OMe)₃ have ³¹P chemical shifts in the range +5 to +10 ppm.

Under the conditions of the experiment, the substitution of the first P(OMe)₃ molecule for coordinated MeCN in the complex, [Fe(NMe₃)(NCMe)₅]²⁺, seemed to be too fast to be observed and no spectroscopic evidence for the species [Fe{P(OMe)₃}₁(NMe₃)(NCMe)₄]²⁺ was evident even when a large excess of Fe^{II} over P(OMe)₃ was used.

The first low spin iron(II) bis(trimethylphosphite) species, trans and cis-[Fe{P(OMe)₃}₂(NMe₃)(NCMe)₃]²⁺ were both observed together in ³¹P-¹H n.m.r. The cis isomer can undergo substitution directly forming the species, fac-[Fe{P(OMe)₃}₃(NMe₃)(NCMe)₂]²⁺, whereas the formation of fac-[Fe{P(OMe)₃}₃(NMe₃)(NCMe)₂]²⁺ from trans-[Fe{P(OMe)₃}₂(NMe₃)(NCMe)₃]²⁺ probably requires rearrangement of the pentacoordinated species, [Fe{P(OMe)₃}₂(NMe₃)(NCMe)₂]²⁺ generated from the trans isomer by the loss of one MeCN ligand. The decay of the cis-isomer to produce fac-[Fe{P(OMe)₃}₃(NMe₃)(NCMe)₂]²⁺ is fast

Figure 4. Observed and Calculated $^{31}\text{P}\{-^1\text{H}\}$ N.M.R. Spectra for the Reaction of $[\text{Fe}(\text{NMe}_3)(\text{NMe})_5]^{2+}$ with $\text{P}(\text{OMe})_3$

after seven days

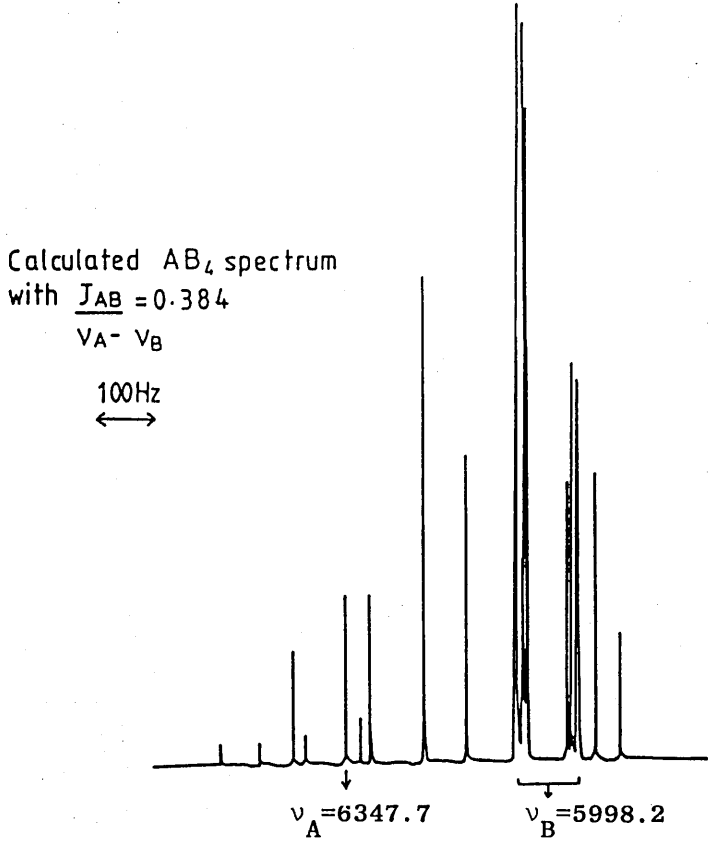
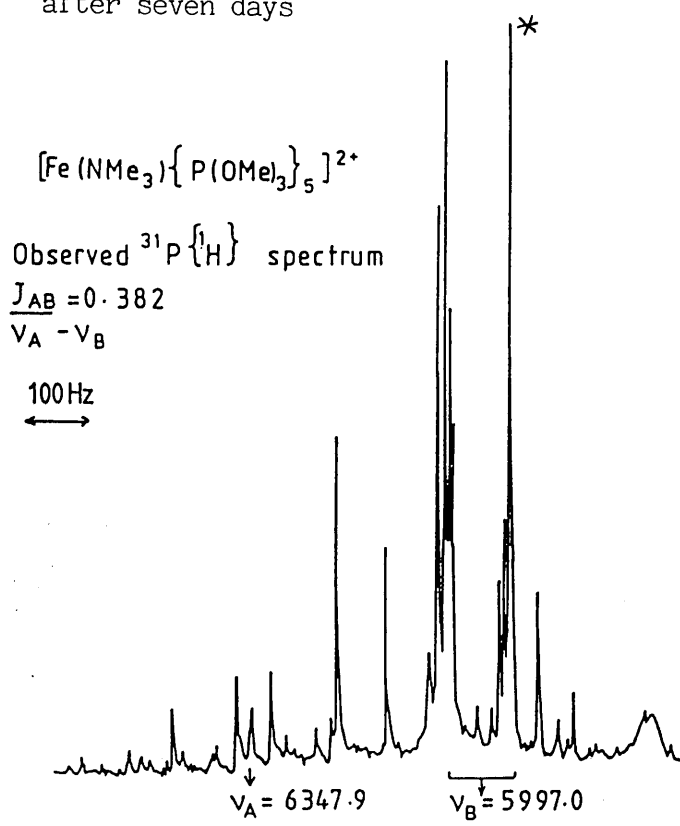


Table 3.

Observed and Calculated Frequencies of Second Order Spectra for AB_2 , A_2B_2 and AB_4 Systems.

AB_2 data from $\text{mer-}[\text{Fe}\{\text{P}(\text{OMe})_3\}_3(\text{NMe}_3)(\text{NCMe})_2]^{2+}$,

A_2B_2 from $\text{cis-}[\text{Fe}\{\text{P}(\text{OMe})_3\}_4(\text{NMe}_3)(\text{NCMe})]^{2+}$ and AB_4 from

$[\text{Fe}\{\text{P}(\text{OMe})_3\}_5(\text{NMe}_3)]^{2+}$

AB_2	
obs.	calc.
5879.3	5879.7
5920.4	5918.9
5999.4	6000.3
6039.2	6040.5
6265.9	6265.8
6379.1	6379.1
6408.4	6408.3
6568.6	6568.4

A_2B_2	
obs.	calc.
a	5532.2
5764.4	5763.6
5810.7	5809.2
5924.4	5923.7
5939.5	5939.5
6039.2	6039.4
6061.6	6061.3
6269.5	6269.7
6293.8	6292.7
6391.6	6391.6
6408.4	6407.4
6453.6	6452.7
6522.3	6522.0
6568.6	6568.5
a	6798.8

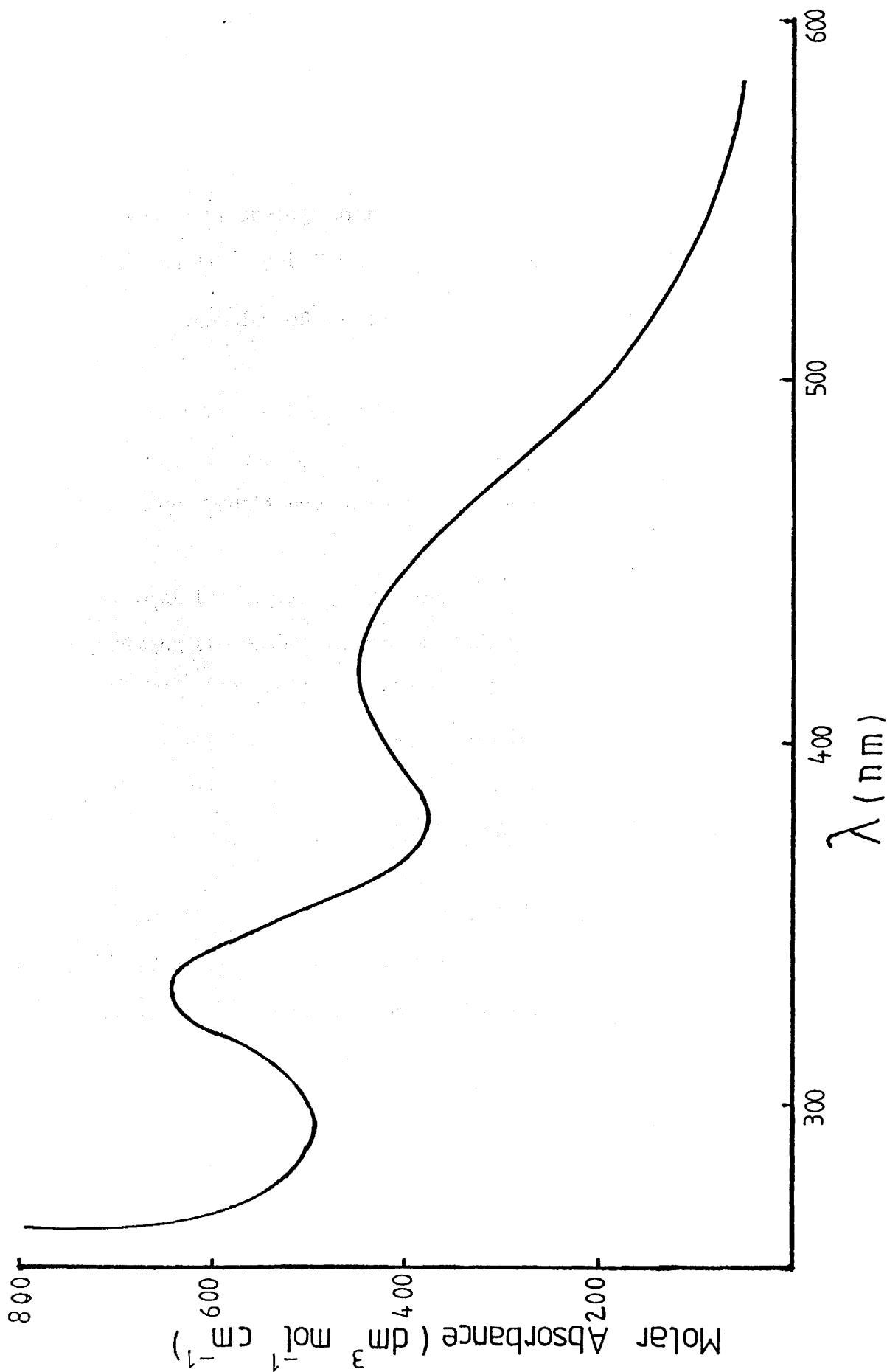
AB_4	
obs.	calc.
5853.0	5853.0
5904.0	5903.3
5941.0	5940.5
5950.9	5950.7
5958.6	5958.3
6037.0	6036.8
6042.4	6042.6
6048.5	6047.9
6060.4	6059.9
6063.2	6062.5
6139.8	6139.0
6247.7	6246.8
6347.9	6347.8
6369.0	6368.4
6398.0	6397.3
6481.0	6480.2
a	6569.7

a. too weak to be observed.

being complete in about 30 minutes at room temperature. The fac-isomer is then converted to mer-[Fe{P(OMe)₃}₃(NMe₃)(NCMe)₂]²⁺ presumably due to its rearrangement, and to cis-[Fe{P(OMe)₃}₄(NMe₃)(NCMe)₂]²⁺. The mer-[Fe{P(OMe)₃}₃(NMe₃)(NCMe)₂]²⁺ undergoes further substitution forming trans-[Fe{P(OMe)₃}₄(NMe₃)(NCMe)₂]²⁺ which is the dominant intermediate in the later stages of the reaction, only four hours being necessary for this species to be formed. The final product, [Fe{P(OMe)₃}₅NMe₃]²⁺, can be formed from fac-[Fe{P(OMe)₃}₃(NMe₃)(NCMe)₂]²⁺ via the three possible routes as described in the discussion and requires only 24 hours to be formed at room temperature. This is effectively the final product of the substitution reaction. There is no evidence for the formation of the species, [Fe{P(OMe)₃}₆]²⁺, even after several weeks of the reaction. Thus the reaction can be considered complete at the five substitution stage.

The substitution of coordinated MeCN by P(OMe)₃ in the complex, [Fe(NMe₃)(NCMe)₅]²⁺ was followed by conventional electronic spectroscopy. The decay of the disubstituted species, [Fe{P(OMe)₃}₂(NMe₃)(NCMe)₃]²⁺ was found to be first order in [P(OMe)₃]. The electronic spectroscopy provides supporting evidence for the complexes, [Fe{P(OMe)₃}_n(NMe₃)(NCMe)_{5-n}]²⁺, (n = 2-5), identified by ³¹P-¹H n.m.r. to be low spin. Two bands were observed for each of the species but a definite assignment was not possible because of the presence of more than one species in solution at the same time. Two sets of isosbestic points were observed but they were not well defined due to the reason given above. By analogy with the ³¹P-¹H n.m.r. study the first species observed by conventional electronic spectroscopy may be the mixture of cis and trans-[Fe{P(OMe)₃}₂(NMe₃)(NCMe)₃]²⁺, $\bar{\nu}_{\max}$ 23500 ($\epsilon = 400 \text{ dm}^3 \text{ mol}^{-1} \text{ cm}^{-1}$) and 29400 cm^{-1} ($\epsilon = 600 \text{ dm}^3 \text{ mol}^{-1} \text{ cm}^{-1}$) (Figure 5). Although the ratio of the two isomers can not be

Figure 5. Electronic Spectrum of the 1st. Low Spin Species,
 $[\text{Fe}\{\text{P}(\text{OMe})_3\}_2(\text{NMe}_3)(\text{NCMe})_3]^{2+}$ as Observed by Conventional
Electronic Spectroscopy.



determined, it seems reasonable that the mixture contains predominantly the cis isomer as is evident from the $^{31}\text{P}\text{-}\{^1\text{H}\}$ n.m.r. study. The electronic spectrum of the final product, $[\text{Fe}\{\text{P}(\text{OMe})_3\}_5(\text{NMe}_3)]^{2+}$, consists of two bands at $\bar{\nu}_{\text{max}}$ 27900 ($\epsilon = 360 \text{ dm}^3 \text{ mol}^{-1} \text{ cm}^{-1}$) and 32600 cm^{-1} ($\epsilon = 300 \text{ dm}^3 \text{ mol}^{-1} \text{ cm}^{-1}$) assigned to the $^1\text{A}_1 \longrightarrow ^1\text{A}_2$ and $^1\text{A}_1 \longrightarrow \text{E}$ d-d transitions (Figure 6) of the low spin d^6 system in C_{4v} symmetry by analogy with the electronic spectrum of the complex $[\text{Fe}(\text{CN})_5(\text{H}_2\text{O})]^{3-}$ (ref.154).

The formation of the first low spin species, $[\text{Fe}\{\text{P}(\text{OMe})_3\}_2(\text{NMe}_3)\text{-(NMe)}_3]^{2+}$ was observed by a stopped-flow study. The traces from the reaction of $[\text{Fe}(\text{NMe}_3)(\text{NMe})_5]^{2+}$ with $\text{P}(\text{OMe})_3$ were recorded over the region, $18000\text{--}32000 \text{ cm}^{-1}$. The reaction was studied under pseudo first order conditions, concentration of $\text{P}(\text{OMe})_3$ was at least in a hundred fold excess over the concentration of Fe^{II} . The electronic spectrum of the species, $[\text{Fe}\{\text{P}(\text{OMe})_3\}_2(\text{NMe}_3)(\text{NMe})_3]^{2+}$ was obtained by plotting the change in optical density as a function of wave length (Figure 7). The calculation of optical density from the trace of the reaction recorded at a particular wave length using stopped-flow method, is explained in chapter 6. The results of the experiment are plotted in Figure 7. The solutions used had the concentrations, $\text{Fe}^{\text{II}} = 4.0 \times 10^{-3} \text{ mol dm}^{-3}$ and $\text{P}(\text{OMe})_3 = 0.5 \text{ mol dm}^{-3}$. The electronic spectrum showed a maximum absorption at $\bar{\nu}_{\text{max}}$ 22700 cm^{-1} ($\epsilon = 340 \text{ dm}^3 \text{ mol}^{-1} \text{ cm}^{-1}$), but within the time of mixing the reagents to obtain a spectrum by conventional means, the spectrum changed slightly, $\bar{\nu}_{\text{max}}$ 23500 cm^{-1} ($\epsilon = 400 \text{ dm}^3 \text{ mol}^{-1} \text{ cm}^{-1}$). By analogy with the $^{31}\text{P}\text{-}\{^1\text{H}\}$ n.m.r. spectra, the species observed in the stopped-flow study is assumed to be a mixture of trans and cis- $[\text{Fe}\{\text{P}(\text{OMe})_3\}_2(\text{NMe}_3)(\text{NMe})_3]^{2+}$.

Figure 6. Electronic Spectrum of $[\text{Fe}\{\text{P}(\text{OMe})_3\}_5(\text{NCMe})]^{2+}$ in Acetonitrile.

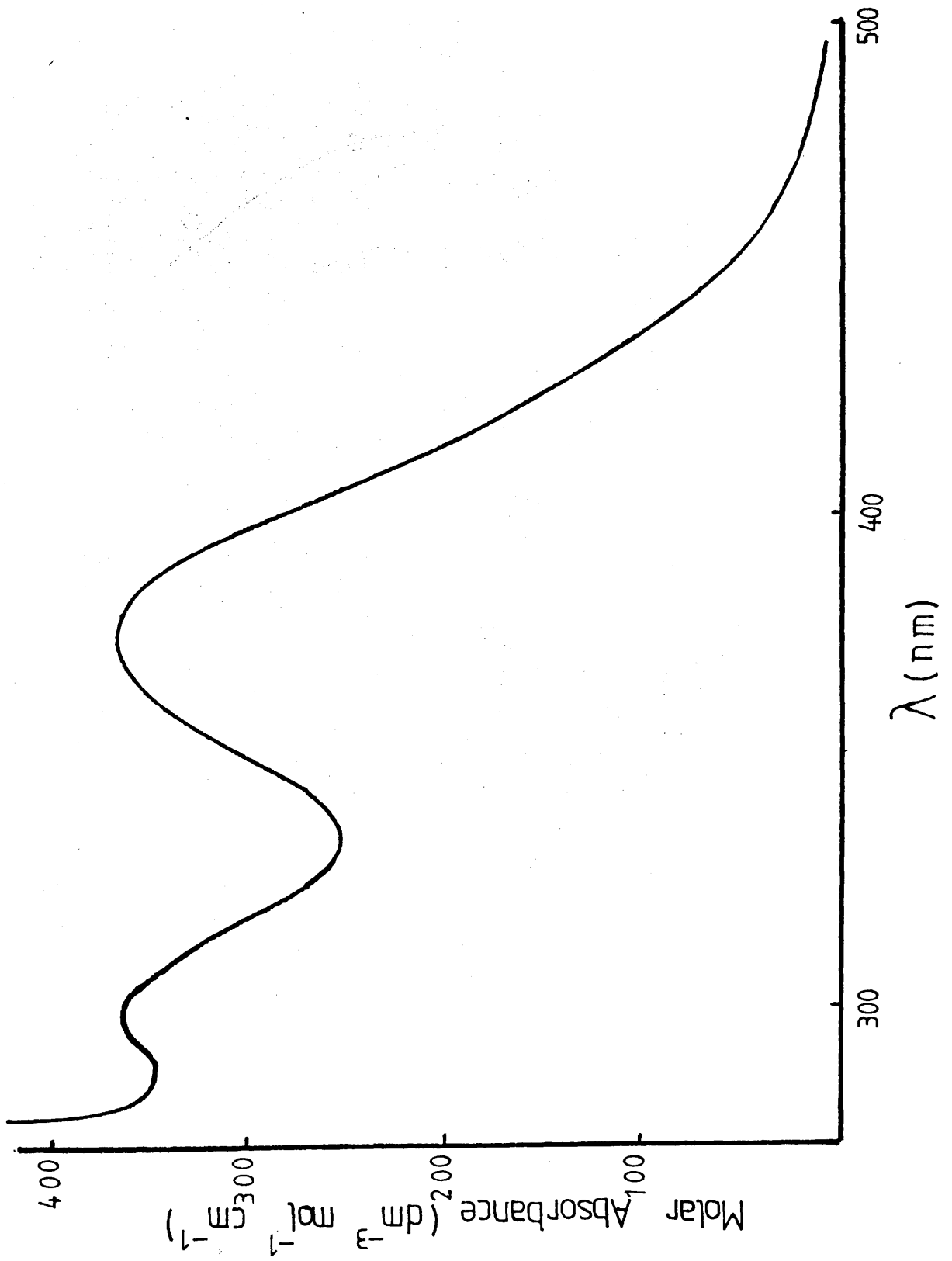
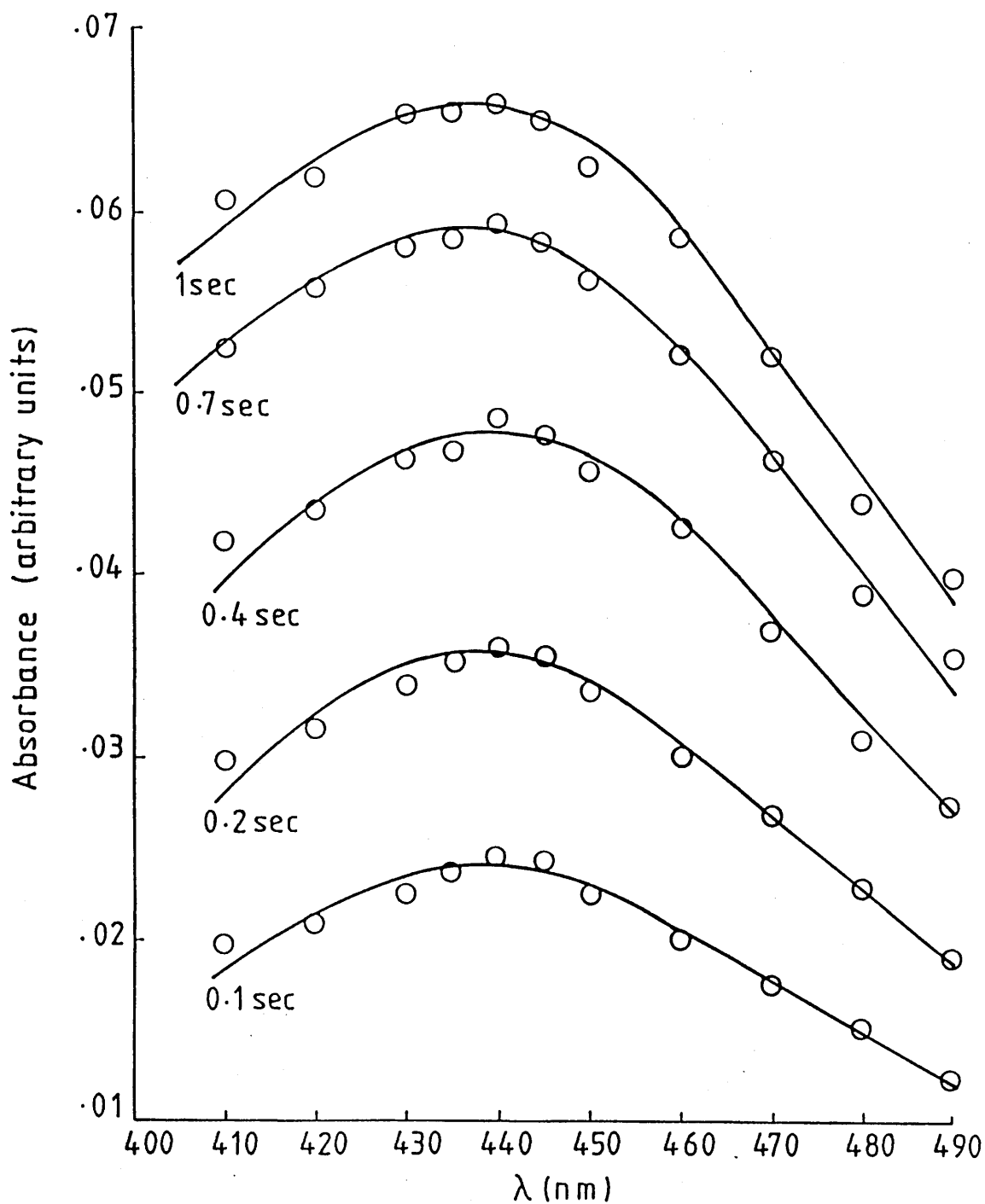


Figure 7. Formation of the 1st. Low Spin Species $[\text{Fe}\{\text{P}(\text{OMe})_3\}_2(\text{NMe}_3)(\text{NCMe})_3]^{2+}$ as observed by Stopped-Flow.



3:2:3 Replacement of Nitrogen Donor Ligands at Iron(II) by Trimethyl Phosphine.

Trimethyl phosphine reacts with hexakis(acetonitrile) iron(II), hexa(pyridine) iron(II) and trimethylamine tetrakis(acetonitrile) iron(II), hexafluorophosphate salts, in acetonitrile, at room temperature to form red solutions from which red diamagnetic solids, predominantly, $[\text{Fe}(\text{PMe}_3)_3\text{L}_3][\text{PF}_6]_2$, (L = MeCN or py) or $[\text{Fe}(\text{PMe}_3)_3(\text{NMe}_3)(\text{NCMe})_2][\text{PF}_6]_2$, were isolated. The solids were studied by $^{31}\text{P}-\{^1\text{H}\}$ and ^1H n.m.r. spectroscopy. The spectra indicated that the cations in which PMe_3 ligands have a facial configuration are the major species in each case. The $^{31}\text{P}-\{^1\text{H}\}$ n.m.r. spectra (Table 4) in each case consisted of a sharp strong singlet, a weak AB_2 and a very weak A_2B_2 complex multiplets. A representative spectrum along with the calculated spectra for the $[\text{Fe}(\text{NCMe})_6]^{2+}$ and PMe_3 system, is shown in Figure 8. The strong singlet from its chemical shift was assigned to the fac-isomer, $[\text{Fe}(\text{PMe}_3)_3\text{L}_3]^{2+}$, (L = MeCN or pyridine) or $[\text{Fe}(\text{PMe}_3)_3(\text{NMe}_3)(\text{NCMe})_2]^{2+}$, the AB_2 multiplet to that of the corresponding mer-isomer and the A_2B_2 complex order spectra, to the cis-isomers, $[\text{Fe}(\text{PMe}_3)_4\text{L}_2]^{2+}$ or $[\text{Fe}(\text{PMe}_3)_4(\text{NMe}_3)(\text{NCMe})]^{2+}$. The ^1H n.m.r. spectra of all these systems also suggested that the fac-isomer was the dominant isomer in all the cases. The ^1H n.m.r. signals observed in all the above systems were sharp, suggesting a rapid exchange among the nitrogen donor ligands. This is consistent with the observation of a singlet for the species, fac- $[\text{Fe}(\text{PMe}_3)_3(\text{NMe}_3)(\text{NCMe})_2]^{2+}$, in its $^{31}\text{P}-\{^1\text{H}\}$ n.m.r. spectrum. Three types of ^1H chemical shifts were observed in the ^1H n.m.r. spectra of the above systems as follows:

CH_3 protons of MeCN and Me_3N , $\delta = 1.96$ ppm

CH_3 protons of PMe_3 trans to P-donor ligands, $\delta = 1.53$ ppm

CH_3 protons of PMe_3 trans to N-donor ligands, $\delta = 1.35$ ppm

Table 4.

 ^{31}P - $\{^1\text{H}\}$ N.M.R. Data for Iron(II) Trimethyl Phosphine Cations.

Cation	Spin System	Chemical Shifts ^a (p.p.m)		Coupling constant $J_{AB}(\text{Hz})$
		δ_A	δ_B	
fac-[FeP ₃ N ₃] ²⁺	A ₃	19.5		
mer-[FeP ₃ N ₃] ²⁺	AB ₂	20.1	10.4	56
cis-[FeP ₄ N ₂] ²⁺	A ₂ B ₂	13.3	2.7	51
fac-[FeP ₃ (py) ₃] ²⁺	A ₃	19.5		
mer-[FeP ₃ (py) ₃] ²⁺	AB ₂	20.1	10.4	56
cis-[FeP ₄ (py) ₂] ²⁺	A ₂ B ₂	13.3	2.7	51
fac-[FeP ₃ $\overset{\cdot}{\text{N}}\text{N}_2$] ²⁺	A ₃	19.6		
mer-[FeP ₃ $\overset{\cdot}{\text{N}}\text{N}_2$] ²⁺	AB ₂	20.1	10.4	56
cis-[FeP ₄ $\overset{\cdot}{\text{N}}\text{N}$] ²⁺	A ₂ B ₂	13.3	2.7	51
fac-[FeP ₃ (NH ₃) ₃] ²⁺	A ₃	19.5		
fac-[FeP ₃ (NH ₃) ₂ N] ²⁺	A ₂ B	18.9	21.9	80
mer-[FeP ₃ (NH ₃) ₃] ²⁺	AB ₂	20.1	10.4	55
cis-[FeP ₄ (NH ₃) ₂] ²⁺	A ₂ B ₂	13.3	2.7	51

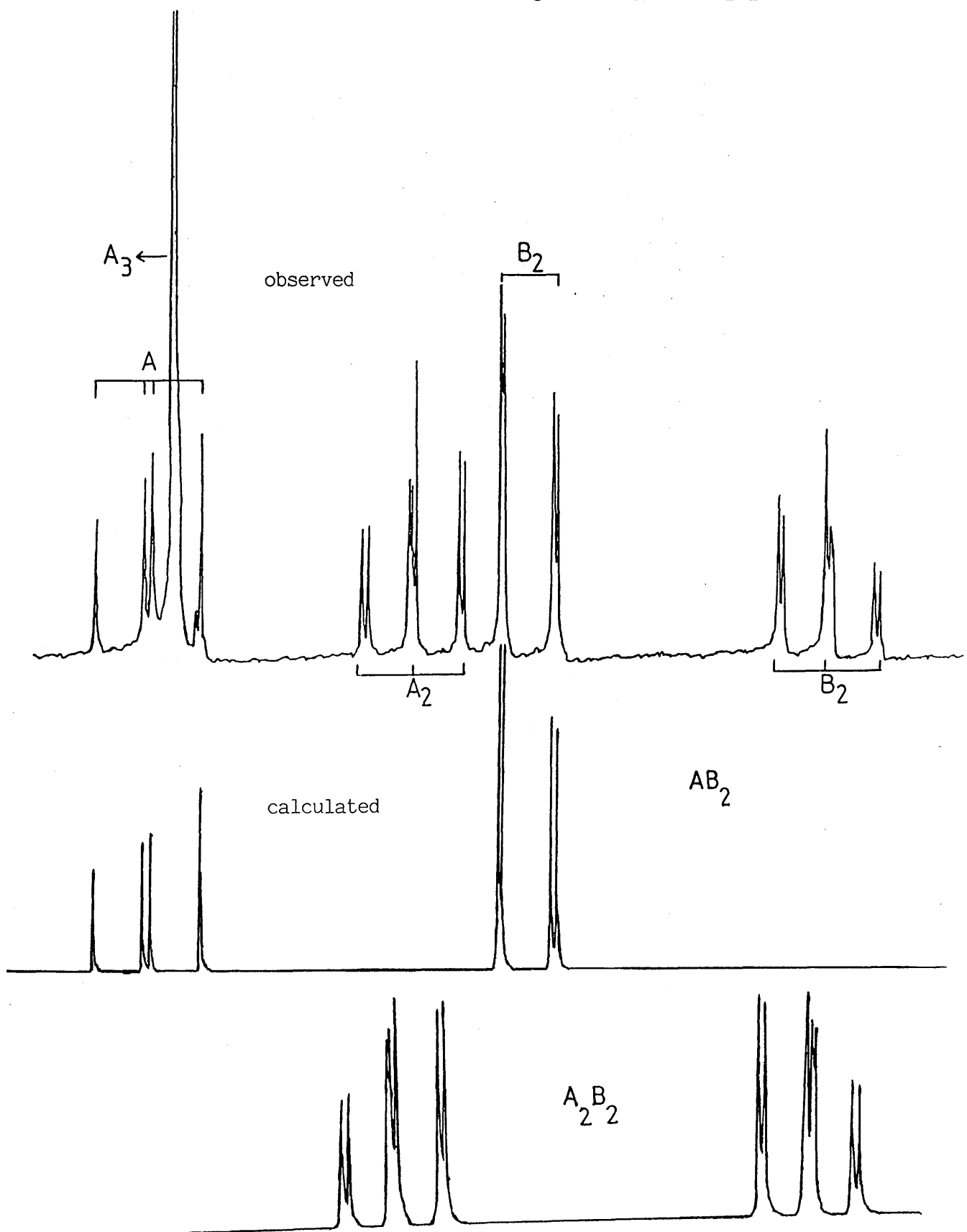
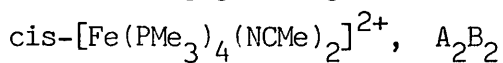
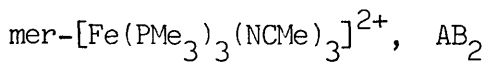
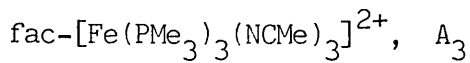
^a To low field of 85% H₃PO₄P = PMe₃;

N = MeCN;

py = pyridine;

 $\overset{\cdot}{\text{N}}$ = Me₃N

Figure 8. Observed and Calculated Spectra for the Reaction of $[\text{Fe}(\text{NCMe})_6]^{2+}$ with PMe_3 .



The cations, $\text{mer-}[\text{Fe}(\text{PMe}_3)_3\text{L}_3]^{2+}$, (L = MeCN or pyridine) or $\text{mer-}[\text{Fe}(\text{PMe}_3)_3(\text{NMe}_3)(\text{NCMe})_2]^{2+}$ in which the relative positions of NMe_3 and MeCN were not determined, were identified from their AB_2 spin system. These cations were present only in minor amounts. The cations, $\text{cis-}[\text{Fe}(\text{PMe}_3)_4\text{L}_2]^{2+}$ (L = MeCN or py) or $\text{cis-}[\text{Fe}(\text{PMe}_3)_4(\text{NMe}_3)(\text{NCMe})]^{2+}$, were identified from the A_2B_2 spin systems observed and formed only in trace quantities.

The electronic spectra of the products isolated from the reaction of PMe_3 with Fe^{II} nitrogen donor cations, in MeCN consisted of two bands (Table 5), assigned to the ${}^1\text{A}_1 \longrightarrow {}^1\text{A}_2$ and ${}^1\text{A}_1 \longrightarrow {}^1\text{E}$ d-d transitions of a low spin d^6 system in $\text{C}_{3\text{V}}$ symmetry by analogy with the electronic spectrum of the complex, $[\text{Co}(\text{NH}_3)_3(\text{H}_2\text{O})_3]^{3+}$ (ref. 156).

The reaction between hexa-ammine iron(II) hexafluorophosphate, $[\text{Fe}(\text{NH}_3)_6][\text{PF}_6]_2$, and PMe_3 in acetonitrile was similar to those described above but the ${}^{31}\text{P}$ - $\{^1\text{H}\}_{\text{n.m.r.}}$ spectrum of the product (Figure 9) showed the presence of two major species. The fac-isomer $[\text{Fe}(\text{PMe}_3)_3(\text{NH}_3)_3]^{2+}$ was identified from the singlet arising due to its A_3 spin system and the other species gave rise to an A_2B spectrum with a facial arrangement of PMe_3 , indicated by the ${}^{31}\text{P}$ chemical shifts (Table 4). The electronic spectrum of the solid isolated from the reaction of $[\text{Fe}(\text{NH}_3)_6]^{2+}$ with PMe_3 in acetonitrile, was very similar to those obtained from the reaction of other Fe^{II} salts with PMe_3 (Table 5) and the infrared spectrum contained bands due to coordinated MeCN as well as due to NH_3 and PMe_3 . The ${}^1\text{H}$ n.m.r. spectrum of the solid in CD_3CN contained a relatively broad signal assigned to the methyl protons of MeCN implying that the exchange between NH_3 and MeCN is slow on the n.m.r. time scale. These observations are consistent with the presence of the isomer,

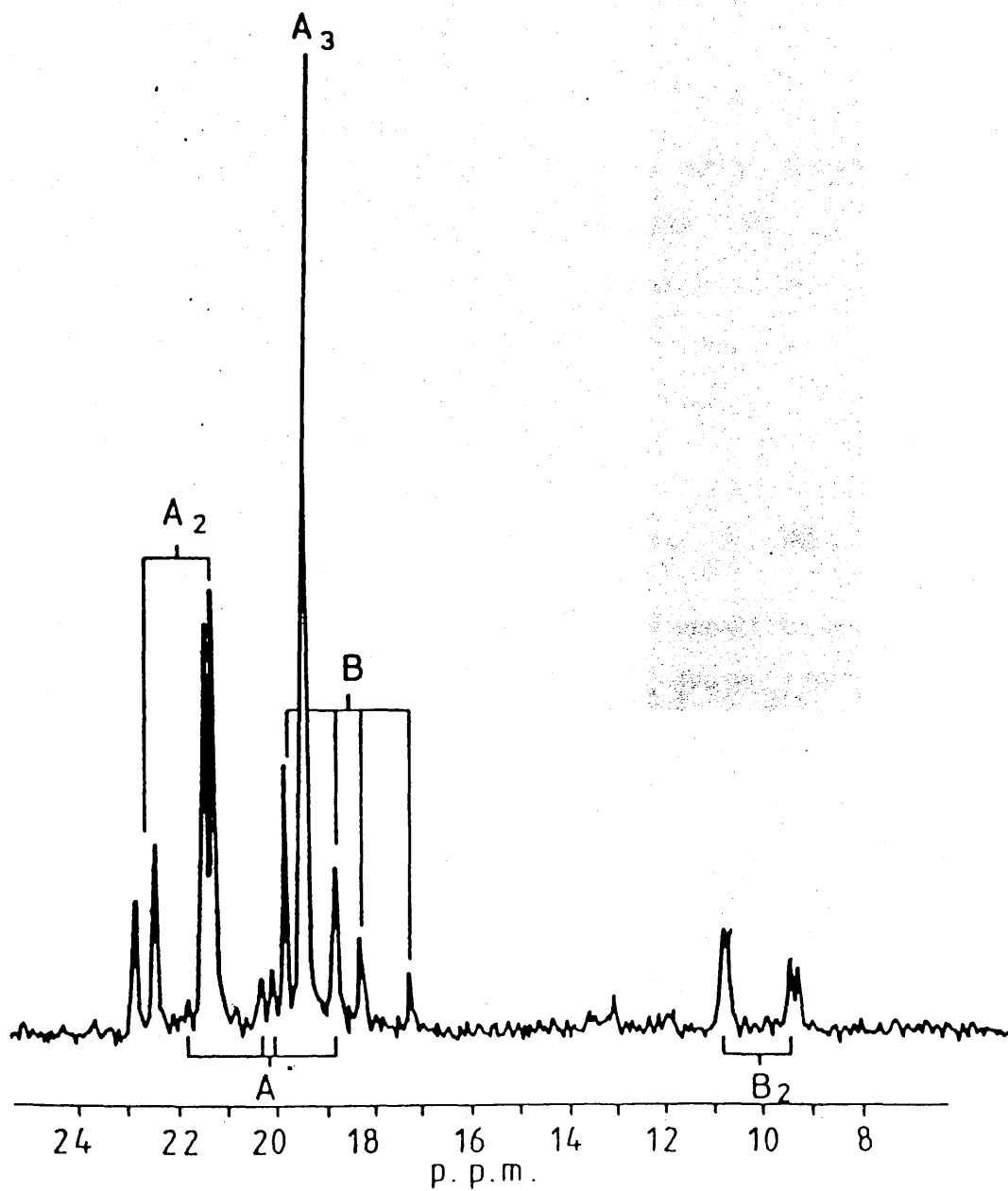
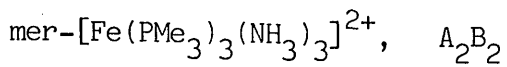
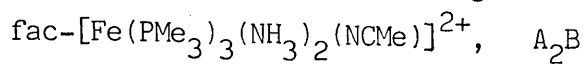
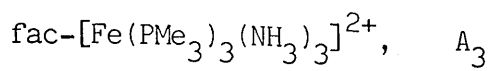
Table 5.

Electronic Spectra ^a of Iron(II) Trimethyl Phosphine Cations.

Cation	$\bar{\nu}_{\max}$ (cm ⁻¹)	
	¹ A ₁ → E	¹ A ₁ → ¹ A ₂
[Fe(PMe ₃) ₃ (NCMe) ₃] ²⁺	21,500 (250) ^b	27,900 (300)
[Fe(PMe ₃) ₃ (py) ₃] ²⁺	21,600 (260)	28,400 (350)
[Fe(PMe ₃) ₃ (NH ₃) ₃] ²⁺	21,200 (300)	27,600 (310)
+ [Fe(PMe ₃) ₃ (NH ₃) ₂ (NCMe)] ²⁺		
[Fe(PMe ₃) ₃ (NMe ₃)(NCMe) ₂] ²⁺	21,500 (260)	27,900 (350)
[Co(NH ₃) ₃ (OH ₂) ₃] ³⁺ ^c	18,950 (180)	27,500 (160)

^a Assignments in C_{3v} symmetry^b Molar extinction coefficients (dm³ mol⁻¹ cm⁻¹)^c Reference 156

Figure 9. The ^{31}P - $\{^1\text{H}\}$ N.M.R. Spectrum of the Product Isolated from the $[\text{Fe}(\text{NH}_3)_6]^{2+}$ and PMe_3 Reaction.



fac-[Fe(PMe₃)₃(NH₃)₂(NMe₃)]²⁺. The other species formed during the reaction were mer-[Fe(PMe₃)₃(NH₃)₃] and cis-[Fe(PMe₃)₄(NH₃)₂]²⁺ identified from their AB₂ and A₂B₂ spin systems. The former species was present in minor amounts whereas the latter was present in trace quantities.

Attempts to follow these reactions by low temperature ³¹P-¹H)n.m.r. or electronic spectroscopy were not successful as the reactions were complete within the time of mixing.

3:3 Discussion

Iron(II) cations with simple nitrogen donor ligands, [Fe(NH₃)₆]²⁺, [Fe(py)₆]²⁺, [Fe(py)_{6-x}(NMe₃)_x]²⁺ and [Fe(NMe₃)(NMe₃)₅]²⁺, have properties consistent with octahedral or distorted octahedral environments around the iron atom. The arrangement of these simple nitrogen donor ligands on the basis of their ligand field towards iron(II) (Table 6) can be represented as



All the above iron(II) cations are moisture sensitive both in the solid state and in solution. The cation, [Fe(NH₃)₆]²⁺, retains its identity when dissolved in MeCN whereas the cation, [Fe(py)₆]²⁺, loses pyridine in MeCN forming presumably an equilibrium mixture of cations, [Fe(py)_{6-x}(NMe₃)_x]²⁺, (x = 0 to at least 2). The reaction of trimethylamine with [Fe(NMe₃)₆]²⁺ in the presence or absence of MeCN, results in the ligation of only one NMe₃ molecule. The difference in the behaviour of NMe₃ and other simple amines as ligands towards metal centre have been reported in the literature. The ligand, NMe₃, is thermodynamically inferior to mono and dimethyl amine with respect to complex formation towards copper(II) in

Table 6.

Electronic Spectra of High Spin Iron II Cations.

Cation	V_{\max} (cm ⁻¹) $5T_{2g} \longrightarrow 5E_g$	
[Fe(NCMe) ₆] ²⁺ <u>a</u>	11,100 (10) <u>b</u>	9,700 (sh)
[Fe(NMe ₃)(NCMe) ₅] ²⁺	11,200 (10)	10,000 (sh)
[Fe(py) _{6-x} (NCMe) _x] ²⁺ <u>c</u>	12,000 (13)	10,500 (sh)
[Fe(NH ₃) ₆] ²⁺	12,400 (8)	9,000 (sh)

a Reference 47

b Molar extinction coefficients (dm³ mol⁻¹ cm⁻¹)

c [Fe(py)₆]²⁺ dissolved in MeCN.

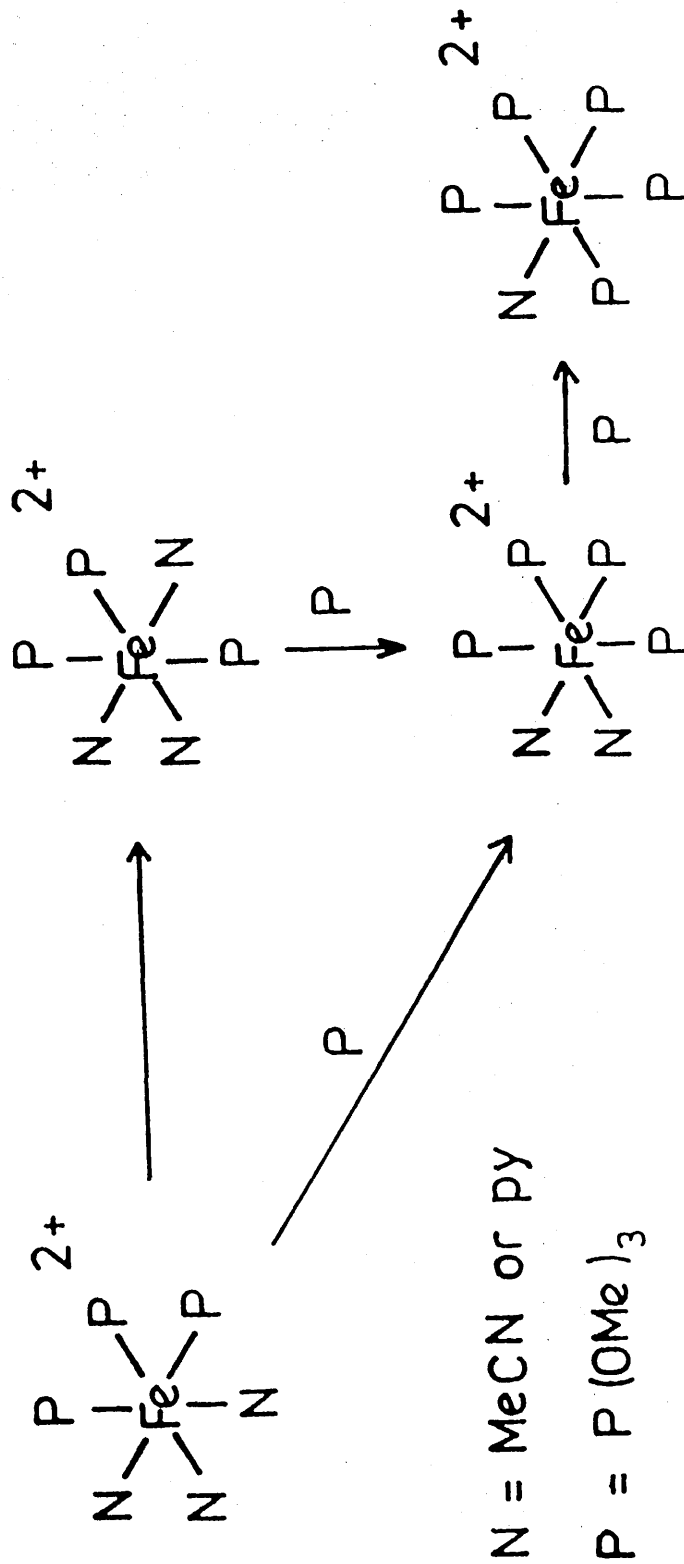
methanol.¹⁵⁷ The main form in which Cu^{II} exists in methanol is $[\text{Cu}(\text{MeOH})_6]^{2+}$. The replacement of MeOH by amine molecules has been studied spectrophotometrically and the data obtained have been used to calculate the composition and the stability constants of the complexes in solution. Thus it has been found that the main species present in solution are those which have four amine molecules coordinated to Cu^{II} in case of MeNH_2 , three in Me_2NH and only two in case of Me_3N . The equilibria and kinetics of the hexaaquanickel(II) cation, $[\text{Ni}(\text{H}_2\text{O})_6]^{2+}$, reacting with NH_3 , MeNH_2 , Me_2NH and Me_3N , have been investigated at 298 K by means of potentiometric titrations.¹⁵⁸ The rate constants for the formation of 1:1 complexes, $[\text{Ni}(\text{NR}_3)(\text{H}_2\text{O})_5]^{2+}$ ($\text{NR}_3 = \text{NH}_3$, MeNH_2 , Me_2NH or Me_3N) have been found to decrease with increasing alkyl substitution. The above two examples indicate the more sterically demanding nature of Me_3N as compared with NH_3 or simple primary and secondary amines. These observations are consistent with the behaviour of $[\text{Fe}(\text{NCMe})_6]^{2+}$ towards NH_3 and NMe_3 and thus emphasize the importance of the steric properties of NMe_3 in determining the stoichiometry of the complexes isolated.

The reaction of $[\text{Fe}(\text{NCMe})_6]^{2+}$ with tmtu, in MeCN solution, results in the formation of a complex in which the presence of coordinated tmtu is confirmed beyond any doubt from the infrared spectrum. The electronic spectrum of the complex in MeCN solution, does suggest the presence of an octahedral low spin iron(II), whereas a similar Fe^{II} dmtu complex is shown to be high spin from its solid state electronic spectrum and magnetic moment.¹⁵³ Apparently the substitution of the two hydrogen atoms in N,N'-dimethylthiourea with two methyl groups results in an increase in the ligand field, $\bar{\nu}_{\text{max}}$ for $[\text{Fe}(\text{DMTU})_6][\text{ClO}_4]_2$ is $10,000 \text{ cm}^{-1}$ compared with 13000 cm^{-1} for the Fe^{II} tmtu complex. As the magnetic moment of the Fe^{II} tmtu complex has not been determined in the present study hence nothing can be said

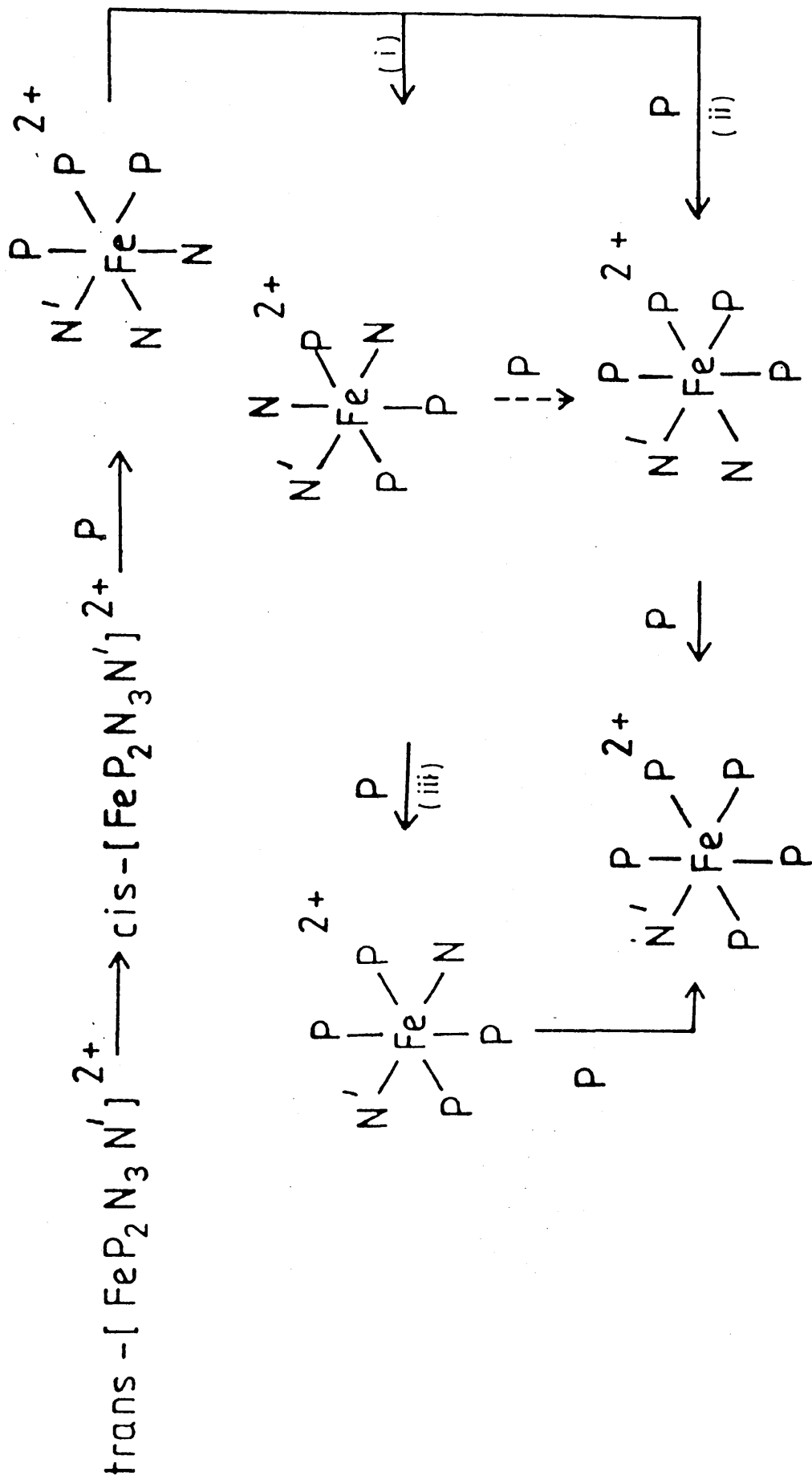
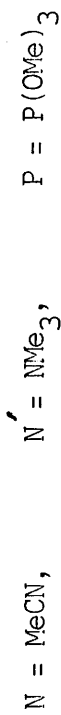
with certainty about the magnetic properties of the complex. The formation of an intermediate spin complex or the presence of more than one species in MeCN solution, may also be regarded as alternate suggestions. The lack of reactivity of Me_2S towards $[\text{Fe}(\text{NCMe})_6]^{2+}$ in MeCN solution, may be explained on the basis of the electronic properties of the ligand. Sterically Me_2S should be a better ligand than $\text{N,N}'$ -dimethylthiourea and tetramethylthiourea but electronically it seems to be a poor sigma donor. As a result it can not compete with MeCN ligands towards iron(II).

The pathways deduced for the reaction of trimethyl phosphite with iron(II) cations, $[\text{Fe}(\text{py})_6]^{2+}$ and $[\text{Fe}(\text{NMe}_3)(\text{NCMe})_5]^{2+}$, are represented in schemes 1 and 2 respectively. The reaction between $[\text{Fe}(\text{py})_6]^{2+}$ and $\text{P}(\text{OMe})_3$ in the latter stages is essentially identical to that observed previously for $[\text{Fe}(\text{NCMe})_6]^{2+}$ (ref.47) but no ^{31}P - $\{^1\text{H}\}$ n.m.r. signals attributable to bis(trimethyl phosphite) cations are observed even when the reactants are mixed in an n.m.r. tube at 195 K, presumably due to rapid exchange involving cations such as $[\text{Fe}\{\text{P}(\text{OMe})_3\}_2(\text{py})_4]^{2+}$ and $[\text{Fe}\{\text{P}(\text{OMe})_3\}_2(\text{py})_3(\text{NCMe})]^{2+}$. Formation of a low spin species is, however, observed by stopped flow electronic spectroscopy, the visible spectrum, $\bar{\nu}_{\text{max}} = 22,700 \text{ cm}^{-1}$ ($\epsilon = 350 \text{ dm}^3 \text{ mol}^{-1} \text{ cm}^{-1}$), being very similar to that observed for the cation, $[\text{Fe}\{\text{P}(\text{OMe})_3\}_2(\text{NCMe})_4]^{2+}$ (ref. 150) under identical conditions. The rearrangement fac. \longrightarrow mer $[\text{Fe}\{\text{P}(\text{OMe})_3\}_3(\text{py})_3]^{2+}$ is observed and there is a marked preference for cis $[\text{Fe}\{\text{P}(\text{OMe})_3\}_4(\text{py})_2]^{2+}$ over the trans isomer. Approximately 20 hours are required for cis $[\text{Fe}\{\text{P}(\text{OMe})_3\}_4(\text{py})_2]^{2+}$ isomer to become a major component of the reaction mixture and some of this species is still present after seven days. In comparison the reaction between $[\text{Fe}(\text{NMe}_3)(\text{NCMe})_5]^{2+}$ and $\text{P}(\text{OMe})_3$ proceeds by a different pathway (Scheme 2). The stopped-flow visible electronic spectrum of a

Scheme 1. Proposed Pathways for the Latter Stages of the $[\text{Fe}(\text{py})_6]^{2+}$ and $\text{P}(\text{OMe})_3$ Reaction.



Scheme 2. Proposed Pathways for the $[\text{Fe}(\text{NMe}_3)(\text{NCMe})_5]^{2+}$ and $\text{P}(\text{OMe})_3$ Reaction.



mixture of $[\text{Fe}(\text{NMe}_3)(\text{NCMe})_5]^{2+}$ and $\text{P}(\text{OMe})_3$, $\bar{\nu}_{\text{max}} = 22700 \text{ cm}^{-1}$ ($\epsilon = 340 \text{ dm}^3 \text{ mol}^{-1} \text{ cm}^{-1}$), is similar to those observed for $[\text{FeL}_6]^{2+}$ (L = MeCN or py) and $\text{P}(\text{OMe})_3$ systems but within the time of mixing the reagents to obtain a spectrum by conventional means, the spectrum changes slightly, $\bar{\nu}_{\text{max}} = 23500 \text{ cm}^{-1}$ ($\epsilon = 400 \text{ dm}^3 \text{ mol}^{-1} \text{ cm}^{-1}$). By analogy with the $^{31}\text{P}\text{-}\{^1\text{H}\}$ n.m.r.study, the species whose formation are observed in stopped-flow and decay in conventional electronic spectroscopy, are formulated as a mixture of trans and cis- $[\text{Fe}\{\text{P}(\text{OMe})_3\}_2(\text{NMe}_3)(\text{NCMe})_3]^{2+}$. The species, cis- $[\text{Fe}\{\text{P}(\text{OMe})_3\}_2(\text{NMe}_3)(\text{NCMe})_3]^{2+}$ on further substitution forms fac- $[\text{Fe}\{\text{P}(\text{OMe})_3\}_3(\text{NMe}_3)(\text{NCMe})_2]^{2+}$. The final product, $[\text{Fe}\{\text{P}(\text{OMe})_3\}_5(\text{NMe}_3)]^{2+}$ can be formed from fac- $[\text{Fe}\{\text{P}(\text{OMe})_3\}_3(\text{NMe}_3)(\text{NCMe})_2]^{2+}$ via the three possible routes as shown in scheme 2. Out of these three routes, two are observed for the reactions involving $[\text{Fe}(\text{NCMe})_6]^{2+}$ or $[\text{Fe}(\text{py})_{6-x}(\text{NCMe})_x]^{2+}$ and $\text{P}(\text{OMe})_3$. The third route in which the cation, trans- $[\text{Fe}\{\text{P}(\text{OMe})_3\}_4(\text{NMe}_3)(\text{NCMe})]^{2+}$, is involved, has been observed only in the reaction of $[\text{Fe}(\text{NMe}_3)(\text{NCMe})_5]^{2+}$ with $\text{P}(\text{OMe})_3$. In this system, trans- $[\text{Fe}\{\text{P}(\text{OMe})_3\}_4(\text{NMe}_3)(\text{NCMe})]^{2+}$ is the dominant intermediate in the later stages of the reaction, only four hours being necessary for this state to be achieved and some of it is still present in the final product. The peak marked with an asterisk in Figure 5 is assigned to trans- $[\text{Fe}\{\text{P}(\text{OMe})_3\}_4(\text{NMe}_3)(\text{NCMe})]^{2+}$. It is, therefore, suggested that the pathway involving this isomer is dominant in the reaction of $[\text{Fe}(\text{NMe}_3)(\text{NCMe})_5]^{2+}$ with $\text{P}(\text{OMe})_3$.

The reaction between $[\text{Fe}(\text{NH}_3)_6]^{2+}$ and $\text{P}(\text{OMe})_3$ appears to be similar to those described above but little detailed information could be obtained. The only cation positively identified by $^{31}\text{P}\text{-}\{^1\text{H}\}$ n.m.r. spectroscopy is cis- $[\text{Fe}\{\text{P}(\text{OMe})_3\}_4(\text{NH}_3)_2]^{2+}$ (Table 1) but the salt can not be isolated free of bulk $\text{P}(\text{OMe})_3$,¹⁵¹ suggesting the possibility of an outer-sphere interaction via N-H...O(Me) hydrogen bonding.

The step-wise substitution of coordinated MeCN by $P(OMe)_3$ in the complex, $[Fe(NMe_3)(NCMe)_5]^{2+}$ has been followed by conventional electronic spectroscopy. Two bands are observed for each of the species but a definite assignment is not possible as more than one species are present in solution at the same time. The bands are assigned to the ${}^1A_1 \longrightarrow {}^1A_2$ and ${}^1A_1 \longrightarrow E$, d-d transitions of the low spin d^6 system in C_{4V} symmetry by analogy with the electronic spectrum of $[Fe(CN)_5(H_2O)]^{3-}$ (ref.154). Substitution reactions of low spin (d^6) iron(II) complexes are generally slow and the complexes are called 'substitution inert'. The lowering of the rate of reaction relative to high spin Fe^{II} has been rationalised in terms of a large increase in the net ligand field activation energy in going from high spin d^6 ($t_{2g}^4 e_g^2$) to low spin d^6 ($t_{2g}^6 e_g^0$). The high ligand field splitting caused by alkyl phosphites is not explained in terms of σ -donor character alone. It is attractive to propose that extra stability of the 1A_1 level takes place via a metal phosphorus π -bonding interactions. The molar extinction coefficients of the two bands observed for the Fe^{II} -trimethylphosphite species are rather large for d-d transitions but are in keeping with values of the species, $[Fe\{P(OMe)_3\}_5(NCMe)]^{2+}$ observed previously.¹⁵⁰ The bands may be borrowing intensity from the charge transfer bands which are visible at higher energy $> 37000\text{ cm}^{-1}$. In the complexes, $[Fe\{P(OMe)_3\}_n(NMe_3)(NCMe)_{5-n}]^{2+}$, ($n = 2-5$) reduction in symmetry from O_h to C_{4V} play an important role by relaxing the selection rules and allowing the 'mixing in' of orbitals of different quantum numbers.

There are two main classes of mechanisms, dissociative and associative, each of the two is further subdivided to give the following four mechanisms, dissociative (D), dissociative interchange (I_d), associative interchange (I_a) and associative (A). These

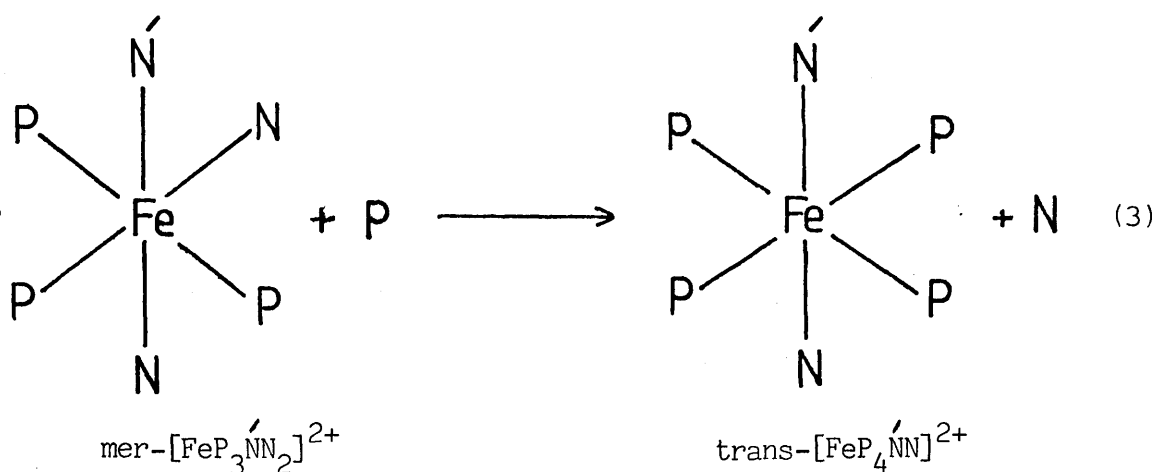
mechanisms have been discussed in detail in chapter 1. The mechanisms for solvent exchange involving metal ions have been extensively studied ranging from beryllium(II) to uranium(VI) in different solvents.¹⁵⁹ The bivalent first row transition metal ions have been the most intensively studied and the mechanisms are deduced from various types of experimental work, for example the determination of activation volumes by high pressure n.m.r. techniques. For the $[M(\text{Solvent})_6]^{2+}$ species in water¹⁶⁰ and methanol¹⁶¹, the activation mode changes from associative (A) for Mn^{2+} to dissociative (D) for Fe^{2+} with the transition state becoming increasingly dissociative for Co^{2+} and Ni^{2+} . This trend in mechanistic variation appears to persist in other solvents also.¹⁶² The activation parameters, that is ΔV^* , ΔH^* and ΔS^* , for the exchange of MeCN solvent on Mn^{II} , Fe^{II} , Co^{II} and Ni^{II} determined by using nitrogen-14FT NMR linebroadening measurements, indicate a progressive change from associative to predominantly dissociative activation in going from Mn^{II} to Ni^{II} .¹⁶³ A recent study of the exchange of bulk acetic acid molecules and the molecules bound to metal cations, Mn^{II} , Fe^{II} , Co^{II} and Ni^{II} , by using oxygen-17 line-broadening method, indicates that the dissociative character of the activation process increases with increasing atomic number.⁷⁹ The above described situations mostly involve measurement of the volumes of activation for solvent exchange at Mn^{II} , Fe^{II} , Co^{II} and Ni^{II} . The ratio of the volume of activation to the solvent partial molar volume, $\Delta V^*/V_0$ has been found to be negative for Mn^{II} about zero for Fe^{II} and positive for Co^{II} and Ni^{II} . For a dissociative process this ratio should be +1 and for an associative process it should be -1. Interchange processes should have values which fall between these limits. On the basis of the results for solvent exchange at the M^{2+} ions, it is predicted that Mn^{II} would react via an I_a mechanism, Co^{II} and Ni^{II} would react via an I_d

mechanism and Fe^{II} which is on the border line may react via I_a or I_d depending upon the nature of the ligand involved in the substitution reactions.

The rate constants measured for a series of substitution reactions of the low spin aquo-pentacyanoferrate(II) ion, $[\text{Fe}(\text{CN})_5(\text{H}_2\text{O})]^{3-}$, with a variety of ligands such as aromatic nitrogen heterocycles and thiourea or N-substituted thioureas suggest that a dissociative mechanism is operative in these reactions.¹⁶⁴ Similarly the substitution at the low spin iron(II) in the species, $[\text{Fe}(\text{CN})_5\text{L}]^{3-}$, (L = 3,5-dimethylpyridine) with a variety of charged and uncharged ligands occurs via a dissociative mechanism.¹⁶⁵ By analogy with the solvent exchange behaviour of the 3d metal cations, $[\text{M}(\text{Solvent})_6]^{2+}$, and the substitution reactions of low spin iron(II) $[\text{Fe}(\text{CN})_5\text{L}]^{3-}$, (L = H_2O or 3,5-dimethylpyridine), it is not unreasonable to assume that the reactions described above proceed via a dissociative interchange, I_d , mechanism in which the identity of the spectator ligands will be important.

The effect of ligated NMe_3 on the observed reaction path is considered to be due to the fact that it is sterically more demanding than either pyridine or MeCN. Replacement of an N-H by a N-Me substituent can have a pronounced effect on the rates of substitution reactions, for example the enhanced rates of base hydrolysis observed for $[\text{M}(\text{NH}_2\text{Me})_5(\text{OSO}_2\text{CF}_3)]^{2+}$, (M = Co, Rh and Cr) compared with their penta-ammine analogues,¹⁶⁶ and the greater lability of $[\text{M}(\text{dma})_6]^{2+}$ (dma = N,N-dimethylacetamide) towards solvent exchange as compared with their N,N-dimethyl and N,N-diethyl formamide analogues.¹⁵⁹ Coordinated \rightleftharpoons bulk MeCN solvent exchange rates have not been determined in the present work as it was outside the scope of the project. In view of the very fast exchange rates to be expected such determinations

are of little importance. Also a detailed kinetic analysis has not been attempted in the present work due to the presence of concurrent reactions occurring at apparently similar rates. However the different pathways observed starting from $[\text{Fe}(\text{NMe}_3)(\text{NCMe})_5]^{2+}$ and $\text{P}(\text{OMe})_3$ could be the result of labilization of MeCN by Me_3N in the cis-position in the later stages of this reaction. This is evident in the formation of $\text{trans}-[\text{Fe}\{\text{P}(\text{OMe})_3\}_4(\text{NMe}_3)(\text{NCMe})]^{2+}$ from $\text{mer}-[\text{Fe}\{\text{P}(\text{OMe})_3\}_3(\text{NMe}_3)(\text{NCMe})_2]^{2+}$



The labilization of MeCN by Me_3N in the cis position is not the only factor in determining the different behaviour observed. If this would be the case then substantial amounts of $[\text{Fe}\{\text{P}(\text{OMe})_3\}_5\text{NMe}_3]^{2+}$ would have formed rapidly via the formation of $\text{cis}-[\text{Fe}\{\text{P}(\text{OMe})_3\}_4(\text{NMe}_3)(\text{NCMe})]^{2+}$. This step was observed to be slow and consistent with the steric requirement of the trimethyl phosphite ligand.

The replacement of nitrogen donor ligands at iron(II) cations $[\text{FeL}_6]^{2+}$, ($\text{L} = \text{MeCN}$, pyridine or NH_3) or $[\text{Fe}(\text{NMe}_3)(\text{NCMe})_5]^{2+}$, by trimethyl phosphine has been observed to be very fast in comparison with trimethyl phosphite. The reactions are complete within the time of

mixing the reactants. The substitution reactions of the iron(II) cations with trimethyl phosphine in MeCN at room temperature, result in the formation of low spin Fe^{II} cations containing three ligated PMe_3 molecules (Scheme 3). The complexes having four ligated PMe_3 molecules are only present in trace quantities. In contrast four MeCN ligands in the cation, $[\text{Fe}(\text{NCMe})_6]^{2+}$, can be replaced readily using bidentate $\text{Ph}_2\text{PCH}_2\text{CH}_2\text{PPh}_2$ or tetradentate $\text{P}(\text{CH}_2\text{CH}_2\text{PPh}_2)_3$ ligands.¹⁶⁷

In recent years it has become accepted that in the chemistry of phosphorus ligands, steric effects are at least as important as electronic effects and in some cases may dominate.¹⁶⁸ Reactions of phosphorus ligands with nickel(0) have been rationalised in terms of a steric parameter termed 'ligand cone angle'.¹⁶⁹ This concept is based upon the observation that the order of decreasing binding ability of the phosphorus ligands is a reflection of the increasing steric crowding around the bonding face of the phosphorus, as revealed by molecular models. Cone angles are measured by constructing atomic models, and the minimum cone angle, θ , for symmetric ligands may be defined as the apex angle of a cylindrical cone, centered 2.28 \AA or 2.57 cm from the centre of the phosphorus atom, which just touches the Van der Waal's radii of the outermost atoms of the model as represented in Figure 10.

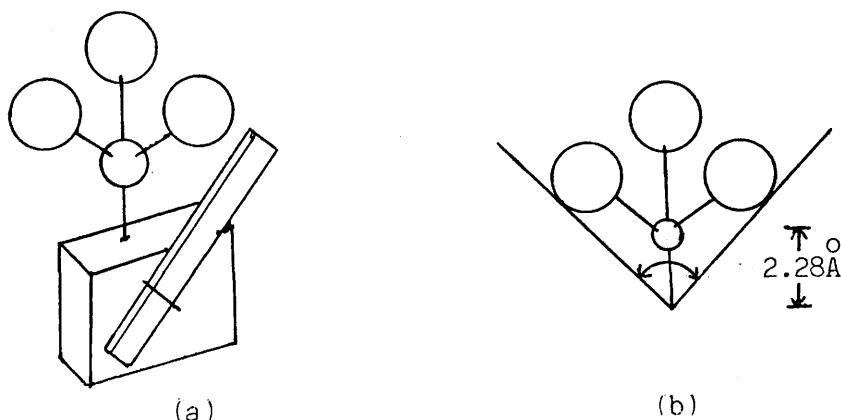
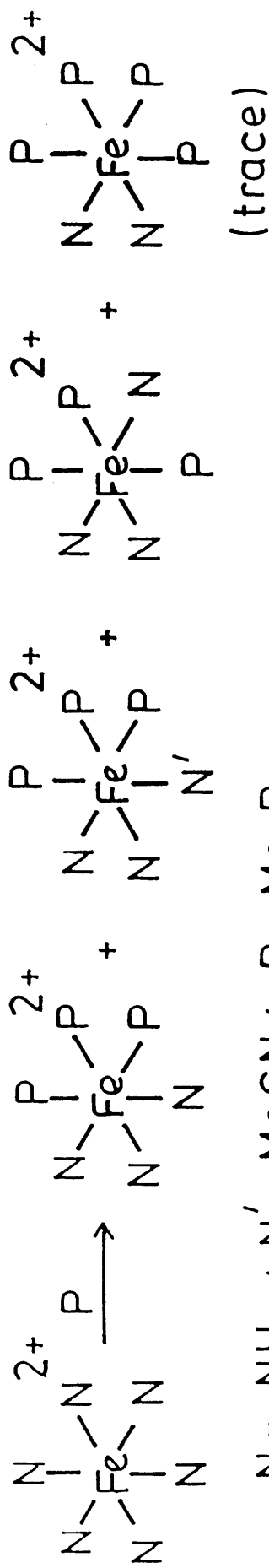
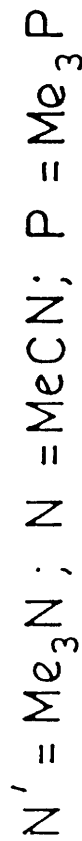
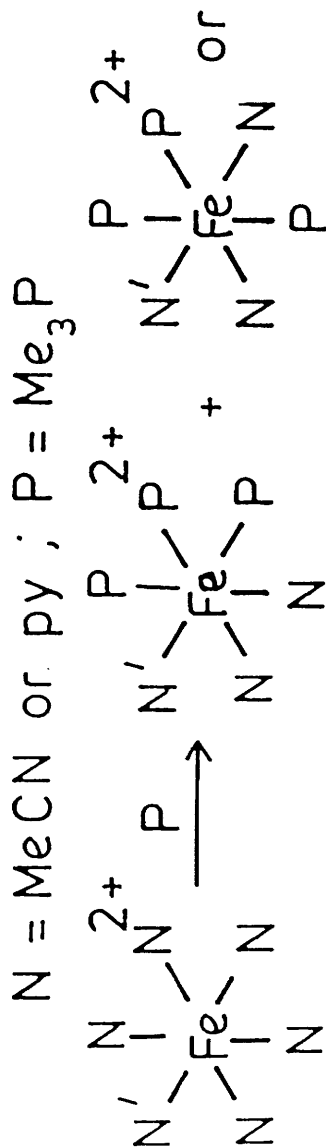
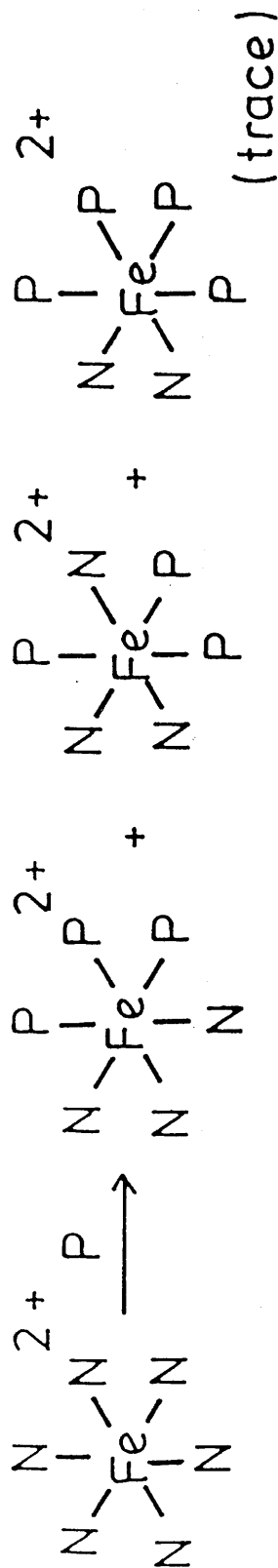


Figure 10. a) Ligand cone angle measuring device; b) the ligand cone angle

Scheme 3. Proposed Pathways for the Reaction of Fe^{II} -Nitrogen Donor Cations with PMe_3 .



The measurement of such angles for ligands of fixed geometry is relatively easy but more complex ligands cause problems due to their greater flexibility. Cone angles for the two ligands, $\text{P}(\text{OMe})_3$ and PMe_3 , used in the present study, are 107° and 117° respectively. Electronically, PMe_3 is expected to be a better sigma donor to Fe^{II} than $\text{P}(\text{OMe})_3$ but it has a larger steric requirement. Formation of less highly substituted products in the reactions of Fe^{II} cations with PMe_3 can be rationalized on this basis. The outcome of these reactions is determined entirely by PMe_3 . The identity of the nitrogen donor ligand is important only in reactions involving exchange between the N-donor ligand and the solvent MeCN. The fast exchange between MeCN and Me_3N or pyridine may be the result of the similar ligand field splitting energies of the ligands involved. The ligand field splitting energy of NH_3 is higher than that of MeCN. This results in a greater loss of ligand field stabilization energy on dissociation as a result of which the exchange between NH_3 and MeCN becomes slow.

3:4 Conclusions

Coordinated acetonitrile in the hexakis (acetonitrile) iron(II) cation is replaced readily by ammonia or pyridine at room temperature to give $[\text{FeL}_6]^{2+}$, ($\text{L} = \text{NH}_3$ or pyridine). In comparison only one trimethylamine ligand is coordinated to iron(II) under identical conditions thus emphasizing the importance of the steric properties of NMe_3 ligand. The arrangement of simple nitrogen donor ligands, on the basis of their ligand field towards iron(II), is represented as $\text{NH}_3 > \text{pyridine} > \text{NMe}_3 > \text{MeCN}$. Substitution of $\text{P}(\text{OMe})_3$ for pyridine in $[\text{Fe}(\text{py})_6]^{2+}$ and for MeCN in $[\text{Fe}(\text{NMe}_3)(\text{NCMe})_5]^{2+}$, in acetonitrile solution proceeds via a stepwise ligand substitution reaction. The pathways deduced for these reactions depend upon the

identity of the nitrogen donor ligand. The first step of substitution at the high spin iron(II) cations, $[\text{Fe}(\text{py})_6]^{2+}$ or $[\text{Fe}(\text{NMe}_3)(\text{NCMe})_5]^{2+}$, is relatively fast and the transition from high to low spin Fe(II) occurs with the formation of the bis(trimethylphosphite) species. Although the kinetic measurements have not been attempted in the present work, the reactions are presumed to proceed via the dissociative mechanism by analogy with the solvent exchange behaviour of 3d metal cations, $[\text{M}(\text{Solvent})_6]^{2+}$, and the reactions of low spin complexes of iron(II) with a variety of ligands. The slow rate of the reactions is a function of the steric requirement of $\text{P}(\text{OMe})_3$. The substitution of $\text{P}(\text{OMe})_3$ for the nitrogen donor ligands at the high spin iron(II) cations, can be achieved up to five ligated $\text{P}(\text{OMe})_3$ molecules. Replacement of nitrogen donor ligands at iron(II) cations, $[\text{FeL}_6]^{2+}$, $\text{L} = \text{MeCN}$, pyridine and NH_3 or $[\text{Fe}(\text{NMe}_3)(\text{NCMe})_5]^{2+}$, by trimethyl phosphine is very fast and the reactions were complete within the time of mixing. The substitution of PMe_3 for the nitrogen donor ligands at iron(II) cations, can be achieved up to three ligated PMe_3 molecules. This shows that both steric and electronic properties of the phosphorus ligands are important in determining the outcome of the reactions.

3:5 Experimental

All operations were carried out in a Pyrex Vacuum line or a N_2 -atmosphere glove box (Lintott, $\text{H}_2\text{O} < 5\text{ppm}$). Ammonia gas (B.O.C.Ltd) was dried and purified by repeated low temperature distillation over freshly cut sodium in vacuo and was stored over sodium metal at 77 K. Trimethyl amine (Matheson Ltd) was purified by repeated distillation over P_2O_5 under vacuum and stored over freshly sublimed P_2O_5 at 77 K. Pyridine (BDH Analar) was distilled from NaOH pellets, collected over 4A molecular sieves, degassed and stored over activated 4A sieves.

Trimethyl phosphite (BDH) was distilled, degassed, dried over sodium metal and stored over activated 4A molecular sieves.

Trimethyl phosphine was obtained by thermal decomposition of its silver iodide complex (Aldrich) ≤ 473 K in vacuo. Acetonitrile (Rathburn Ltd., HPLC Grade S) was purified using a published procedure.¹⁶ FeF_2 (Ozark-Mahoning) was used as received.

Instrumentation was as follows: Raman, Spex Ramalog with 520.8 or 647.1 nm excitation; i.r. PE580 or PE983 with 3600 data station; electronic, Beckman 5270 or Lambda 9 Perkin Elmer; stopped flow, Hi-Tech SF-3L system with SFL-36 evacuable flow module and dry Ar line; n.m.r., varien XL-100 at 40.5 MHz (^{31}P), Bruker WP 200 (^1H); atomic absorption, PE 306. Microanalyses were by Malissa and Reuter, Federal Republic of Germany. Iron and nitrogen were determined also by atomic absorption and Kjeldahl methods respectively.

3:5:1 Preparation of Hexakis(acetonitrile)iron(II) Hexafluorophosphate.⁴⁷

In a double limbed reaction vessel, FeF_2 (3mmol) was loaded in one of the limbs in the dry box. Acetonitrile (5ml) and PF_5 (5mmol) were distilled in, at 77 K. The reaction mixture was allowed to warm to room temperature and shaken for 24 hours at room temperature. A white solid was isolated from the resulting pale yellow solution, after removing the volatile material. The infra-red spectrum of the solid had bands due to coordinated acetonitrile, $\bar{\nu}_{\text{max}}$, 2320, 2295 and 941 cm^{-1} and due to PF_6^- at 835 and 560 cm^{-1} , assigned to ν_3 and ν_4 respectively.

3:5:2 Reactions of Hexakis(acetonitrile)iron(II) Hexafluorophosphate in Acetonitrile:- (a) with Pyridine.¹⁵¹

The complex, $[\text{Fe}(\text{NCMe})_6][\text{PF}_6]_2$ (0.42 mmol) was added to one limb of a reaction vessel and pyridine (5ml) was distilled in at 77 K.

The vessel was warmed to room temperature and shaken for about half an hour to ensure thorough mixing. An off-white solid was isolated from the resulting pale yellow solution after removal of the volatile material. The infra-red spectrum of the solid contained bands due to coordinated pyridine, $^{170} \bar{\nu}_{\max}$ 1603, 1219, 1160 and 1010 cm^{-1} , and bands at $\bar{\nu}_{\max}$ 840 and 560 cm^{-1} (ν_3 and ν_4 respectively) due to PF_6^- .¹⁷¹

(b) With Ammonia:

The compound, $[\text{Fe}(\text{NCMe})_6][\text{PF}_6]_2$ (0.42 mmol) was loaded in a double limb reaction vessel in the glove box. Acetonitrile (5ml) and NH_3 (3 mmol) were distilled and the mixture was allowed to warm to room temperature. The reaction mixture was shaken thoroughly to ensure complete reaction. From the yellow solution so obtained, an off-white solid was isolated after removal of the volatile material. The infra-red spectrum of the solid contained bands due to coordinated NH_3 , $^{172} \bar{\nu}_{\max}$, 3400, 3310, 1620 and 1220 cm^{-1} , and PF_6^- bands at $\bar{\nu}_{\max}$ 840 and 560 cm^{-1} (ν_3 and ν_4 respectively). Bands due to coordinated MeCN were absent. The compound was identified by its infra-red spectrum and analysis of Fe and N (Table 8) as hexa-ammine iron(II) hexafluorophosphate.

(c) With Trimethylamine:

The compound, $[\text{Fe}(\text{NCMe})_6][\text{PF}_6]_2$ (0.42 mmol) was dissolved in acetonitrile (5ml) and Me_3N (2.5 mmol) was added by distillation. The mixture warmed to room temperature and shaken for about fifteen minutes. An off-white solid was isolated from the resulting pale yellow solution after the removal of volatile material. The infra-red spectrum of the solid showed the presence of coordinated Me_3N ,¹⁷³ MeCN¹⁷⁴ and the PF_6^- anion. The solid state infra-red spectrum is listed in Table 7. Bands in the infra-red spectrum were assigned to

Table 7.

Infra-Red Spectrum of the Complex $[\text{Fe}(\text{NMe}_3)(\text{NCMe})_4][\text{PF}_6]_2$

Wavenumber (cm^{-1})	Assignment	Corresponding Band of free ligand (cm^{-1}) 173, 174
3250 (m)	CH str. (Me_3N)	2950
3010 (m)	CH str. (MeCN)	3003
2945 (m)	CH str. (MeCN)	2944
2320 (s)	CN comb. (MeCN)	2293
2290 (s)	$\text{C}\equiv\text{N}$ str.	2254
1478 (m)	CH_3 rock. (Me_3N)	1460
1048 (m)	CN str. (Me_3N)	1043
1040 (m)	CH_3 rock. (MeCN)	1047
978 (m) } 940 (m) }	C-C str.] C-C str.]	917
840 (v.s)	$\nu_3(\text{PF}_6^-)$ <u>a</u>	-
560 (v.s)	$\nu_4(\text{PF}_6^-)$ <u>a</u>	-

v.s. = very strong,

s = strong

m = medium

a Assigned by comparison with the i.r. spectrum of KPF_6 . 171

PF_6^- and coordinated ligands (NMe_3 and MeCN) by comparison with the i.r. spectrum of KPF_6 ¹⁷¹ and free NMe_3 and MeCN . The solid was identified from its i.r. spectrum and microanalysis (Table 8) as trimethylamine tetrakis(acetonitrile)iron(II) hexafluorophosphate.

Reactions between $[\text{Fe}(\text{NCMe})_6][\text{PF}_6]_2$ and NMe_3 , mole ratio 1:10 or 1:20, in the presence or absence of MeCN resulted in the formation of off-white solids spectroscopically and analytically identical to the complex, $[\text{Fe}(\text{NMe}_3)(\text{NCMe})_4][\text{PF}_6]_2$. The electronic spectrum of the complex, $[\text{Fe}(\text{NMe}_3)(\text{NCMe})_4][\text{PF}_6]_2$, in acetonitrile, contained a broad band at $11,200 \text{ cm}^{-1}$ ($\epsilon = 10 \text{ dm}^3 \text{ mol}^{-1} \text{ cm}^{-1}$) with a pronounced shoulder at $10,000 \text{ cm}^{-1}$ characteristic of high spin iron(II) ion in a distorted octahedral environment, presumably due to the cation, $[\text{Fe}(\text{NMe}_3)(\text{NCMe})_5]^{2+}$.

(d) With Tetramethyl thiourea:

The compound, $[\text{Fe}(\text{NCMe})_6][\text{PF}_6]_2$ (0.4 mmol) was loaded in one limb of a reaction vessel and tetramethyl thiourea (2.4mmol or 3.2mmol) into the other. MeCN (5ml) was distilled onto tetramethyl thiourea and the resulting colourless solution was transferred to the limb containing $[\text{Fe}(\text{NCMe})_6][\text{PF}_6]_2$. A dark green solution was formed after thorough shaking from which a light green solid was isolated after removing the volatile material. The infra-red spectrum of the solid isolated from mole ratio $\text{Fe}^{\text{II}}:\text{tmtu} = 1:6$, contained bands due to coordinated tetramethyl thiourea (tmtu),¹⁷⁵ $1550 (\nu\text{NCN})$, $1265 (\nu\text{CH}_3\text{-N})$, $1100 (\nu\text{C=S})$, $1050 (\text{CH}_3 \text{ rocking})$ and 870 cm^{-1} (CN torsion) compared with the bands, 1520 , 1260 , 1120 , 1060 and 880 cm^{-1} in pure tetramethyl thiourea. The bands at 835 and 560 cm^{-1} were assigned to PF_6^- . Bands due to coordinated MeCN were absent. The i.r. spectrum of the product isolated from $\text{Fe}^{\text{II}}:\text{tmtu} = 1:8$ also contained bands due to uncoordinated tmtu at 1480 , 1200 and 1150 cm^{-1} in

Table 8.

Analytical data ^a for iron(II) complexes.

Complex	Colour	Analysis (%)					
		C	H	F	Fe	N	P
$[\text{Fe}(\text{NMe}_3)(\text{NCMe})_4][\text{PF}_6]_2$	off-white	23.1 (23.2)	3.5 (3.6)	40.1 (40.1)	9.9 (9.8)	12.4 (12.4)	10.8 (10.9)
$[\text{Fe}(\text{NH}_3)_6][\text{PF}_6]_2$	off-white				12.3 (12.5)	18.6 (18.8)	
$[\text{Fe}\{\text{P}(\text{OMe})_3\}_5(\text{NMe}_3)][\text{PF}_6]_2$ ^b	yellow	20.5 (21.0)	5.0 (5.2)	23.0 (22.3)	5.7 (5.5)	2.0 (1.4)	22.4 (21.2)
$[\text{Fe}(\text{PMe}_3)_3(\text{NCMe})_3][\text{PF}_6]_2$	red	26.0 (25.8)	5.0 (5.1)	32.5 (32.7)	8.2 (8.0)	6.2 (6.0)	22.0 (22.2)
$[\text{Fe}(\text{PMe}_3)_3(\text{NH}_3)_2(\text{NCMe})][\text{PF}_6]_2$ +	red	20.0 (20.4)	5.6 (5.5)	35.9 (35.0)		6.6 (6.4)	24.5 (23.8)
$[\text{Fe}(\text{PMe}_3)_3(\text{NH}_3)_3][\text{PF}_6]_2$		(17.3)	(5.7)	(36.4)		(6.7)	(24.8)

^a Required values are given in parentheses.

^b Trans- $[\text{Fe}\{\text{P}(\text{OMe})_3\}_4(\text{NMe}_3)(\text{NCMe})][\text{PF}_6]_2$ present as a minor product.

addition to the bands mentioned above. The electronic spectrum of the solid isolated from $\text{Fe}^{\text{II}}:\text{tmtu} = 1:6$, in MeCN solution, consisted of two bands at $\bar{\nu}_{\text{max}} 16,900$ ($\epsilon = 390 \text{ dm}^3 \text{ mol}^{-1} \text{ cm}^{-1}$) and 13000 cm^{-1} ($\epsilon = 280 \text{ dm}^3 \text{ mol}^{-1} \text{ cm}^{-1}$). From the infra-red and electronic spectra, the compound was assumed to be hexakis(tetramethylthiourea) iron(II)hexafluorophosphate. The microanalysis of the compound was not attempted because of the difficulty in obtaining the complex free from the unreacted ligand.

(e) With Dimethyl sulphide:

Me_2S (5 mmol) was added to $[\text{Fe}(\text{NCMe})_6][\text{PF}_6]_2$ (0.4 mmol) in the absence or presence of MeCN (4ml). After shaking overnight, a white solid was isolated by removing the volatile material. The infra-red and electronic spectra of the solid were identical to those of the compound, $[\text{Fe}(\text{NCMe})_6][\text{PF}_6]_2$.

3:5:3 Reaction of $[\text{Fe}(\text{NMe}_3)(\text{NCMe})_4][\text{PF}_6]_2$ with Trimethylphosphite in Acetonitrile.

A mixture of $[\text{Fe}(\text{NMe}_3)(\text{NCMe})_4][\text{PF}_6]_2$, (0.35 mmol), trimethyl phosphite (10 mmol) and MeCN (5ml) was allowed to warm from 77 K to room temperature. The solution had a deep red colour at room temperature which over a period of half an hour to about one hour, changed to orange. Finally the solution became yellow after about 24 hours. The rate of the reaction as marked by the colour changes, was very dependent upon the concentration of $\text{P}(\text{OMe})_3$. A yellow solid was isolated from the solution after one week by removing the volatile material. The solid was characterized from the spectroscopic data and microanalysis as predominantly trimethylamine pentakis-(trimethyl phosphite) iron(II) hexafluorophosphate. The result of analysis together with the required values are listed in Table 8.

The result of the analysis is not in good agreement with the required values because of the presence of complexes of a lower degree of substitution as shown by $^{31}\text{P}-\{^1\text{H}\}$ n.m.r. spectroscopy. The major signal in the $^{31}\text{P}-\{^1\text{H}\}$ n.m.r. spectrum of the solid product, in CD_3CN , was the expected AB_4 pattern of $[\text{Fe}\{\text{P}(\text{OMe})_3\}_5(\text{NMe}_3)]^{2+}$ but there was also present a singlet due to the cation $\text{trans}-[\text{Fe}\{\text{P}(\text{OMe})_3\}_4(\text{NMe}_3)(\text{NCMe})]^{2+}$. The infra-red spectrum indicated the presence of coordinated $\text{P}(\text{OMe})_3$, $^{176}\text{NMe}_3$ and PF_6^- , and is listed in Table 9. The electronic spectrum in MeCN solution consisted of two bands at $\bar{\nu}_{\text{max}} 27,900 \text{ cm}^{-1}$ ($\epsilon = 360 \text{ dm}^3 \text{ mol}^{-1} \text{ cm}^{-1}$) and $32,600 \text{ cm}^{-1}$ ($\epsilon = 300 \text{ dm}^3 \text{ mol}^{-1} \text{ cm}^{-1}$).

$^{31}\text{P}-\{^1\text{H}\}$ n.m.r. Study.

The reaction between trimethylamine tetrakis(acetonitrile) iron(II) hexafluorophosphate and $\text{P}(\text{OMe})_3$ was followed by $^{31}\text{P}-\{^1\text{H}\}$ n.m.r. The reaction was studied using CD_3CN as a solvent with $[\text{Fe}^{\text{II}}] = 0.12 \text{ mol dm}^{-3}$ and $[\text{Fe}^{\text{II}}]:[\text{P}(\text{OMe})_3]$ varied from 1:5 to 1:20. The solid complex was loaded in a reaction vessel fitted with an n.m.r. tube in the glove box. The solvent, CD_3CN was distilled and the solid dissolved in it. $\text{P}(\text{OMe})_3$ was then distilled at 77 K and the mixture was warmed until liquid (about 243 K). The mixture was shaken and a portion of it was transferred to the n.m.r. tube which was sealed off. Alternatively $\text{P}(\text{OMe})_3$ was injected directly using a syringe and septum cap to an n.m.r. tube containing the Fe^{II} solution at 243 K.

On warming from 77 K to 243 K, a red solution was formed and the $^{31}\text{P}-\{^1\text{H}\}$ n.m.r. spectrum at this temperature showed three singlets, one due to $\text{P}(\text{OMe})_3$ broadened by exchange. As the temperature was allowed to rise, one of the singlets decreased in intensity, the intensity of the other increased and a new singlet

Table 9.

Infra-Red Spectrum of the Complex $[\text{Fe}\{\text{P}(\text{OMe})_3\}_5(\text{NMe}_3)][\text{PF}_6]_2$

Wavenumber (cm^{-1})	Assignment 173,176
3250 (m)	CH str. (Me_3N)
3005 (w)	CH_3 asym.str. $[\text{P}(\text{OMe})_3]$
2960 (m)	CH_3 sym.str. $[\text{P}(\text{OMe})_3]$
2855 (m)	CH_3 deform. $[\text{P}(\text{OMe})_3]$
1490 (m)	CH_3 rock. (Me_3N)
1465 (m)	CH_3 rock. (Me_3N)
1180 (s)	CH_3 rock. $[\text{P}(\text{OMe})_3]$
1040 (v.s)	$\text{P}(\text{OC})_3$ asym.str.
840 (s)	$\nu_3(\text{PF}_6^-)$ ^a
790 (s)	$\text{P}(\text{O})_3$ sym.str.
725 (s)	$\text{P}(\text{O})_3$ asym.str.
560 (s)	$\nu_4(\text{PF}_6^-)$ ^a
515 (m)	$\text{P}(\text{OC})_3$ asym. bend.

w = weak, m = medium, s = strong, v.s. = very strong

^a Assigned by comparison with the i.r. spectrum of KPF_6 .¹⁷¹

appeared in the spectrum. The two singlets, in the first spectrum, were assigned to trans and cis- $[\text{Fe}\{\text{P}(\text{OMe})_3\}_2(\text{NMe}_3)(\text{NCMe})_3]^{2+}$ on the basis of their chemical shifts. The singlet appearing after increase in temperature was tentatively assigned to fac- $[\text{Fe}\{\text{P}(\text{OMe})_3\}_3(\text{NMe}_3)(\text{NCMe})_2]^{2+}$ on the basis of its chemical shift. This singlet was replaced rapidly by AB_2 and A_2B_2 multiplets assigned to mer- $[\text{Fe}\{\text{P}(\text{OMe})_3\}_3(\text{NMe}_3)(\text{NCMe})_2]^{2+}$ and cis- $[\text{Fe}\{\text{P}(\text{OMe})_3\}_4(\text{NMe}_3)(\text{NCMe})]^{2+}$, and a singlet, assigned to the cation, trans- $[\text{Fe}\{\text{P}(\text{OMe})_3\}_4(\text{NMe}_3)(\text{NCMe})]^{2+}$. The relative amount of $\text{P}(\text{OMe})_3$ had reduced during this time. In latter stages of the substitution reaction, trans- $[\text{Fe}\{\text{P}(\text{OMe})_3\}_4(\text{NMe}_3)(\text{NCMe})]^{2+}$ was the dominant isomer with a significant amount of $[\text{Fe}\{\text{P}(\text{OMe})_3\}_5(\text{NMe}_3)]^{2+}$ as shown by its AB_4 spectrum. After one week, the major product was $[\text{Fe}\{\text{P}(\text{OMe})_3\}_5(\text{NMe}_3)]^{2+}$ along with some amount of trans- $[\text{Fe}\{\text{P}(\text{OMe})_3\}_4(\text{NMe}_3)(\text{NCMe})]^{2+}$. No evidence was observed for the species, $[\text{Fe}\{\text{P}(\text{OMe})_3\}_6]^{2+}$ even after several weeks at room temperature.

The reaction was also followed by ^1H n.m.r. spectroscopy but the results were very difficult to interpret due to the smaller range of chemical shifts being studied.

Stopped-flow Study

The first step in the substitution reactions of Fe^{II} cations, $[\text{Fe}(\text{py})_6]^{2+}$ and $[\text{Fe}(\text{NMe}_3)(\text{NCMe})_5]^{2+}$ with $\text{P}(\text{OMe})_3$ was followed by stopped-flow spectrophotometry. This involved MeCN solutions in which $[\text{Fe}^{\text{II}}] = 4 \times 10^{-3} \text{ mol dm}^{-3}$ and $[\text{P}(\text{OMe})_3] = 0.5 \text{ mol dm}^{-3}$ thus ensuring the pseudo first order conditions of the reactions. The solutions were made in the glove box by dissolving the appropriate amounts of the solid in a known volume of the solvent generally 25ml. The solution of $\text{P}(\text{OMe})_3$ in MeCN was made by mixing the known weight

of $\text{P}(\text{OMe})_3$ with MeCN and then making the volume of the solution to 25ml by adding more MeCN. The solutions were made quickly to minimise loss of the solvent and $\text{P}(\text{OMe})_3$ by evaporation. The stopped-flow apparatus was thermostatted to $25.0 \pm 0.1^\circ\text{C}$. Visible spectra of the transient intermediates were obtained from point by point (10nm interval) determination of absorbance changes following stopped-flow mixing of MeCN solutions of Fe^{II} with that of $\text{P}(\text{OMe})_3$ solution. The detail of the stopped-flow method is described in chapter 6.

Conventional Spectrophotometric Studies.

The later stages of the reaction between $[\text{Fe}(\text{NMe}_3)(\text{NCMe})_5]^{2+}$ and $\text{P}(\text{OMe})_3$ were also followed by conventional electronic spectroscopy. This involved solutions of $[\text{Fe}(\text{NMe}_3)(\text{NCMe})_5]^{2+}$ and $\text{P}(\text{OMe})_3$ in acetonitrile with $[\text{Fe}^{\text{II}}] = 4 \times 10^{-3} \text{ mol dm}^{-3}$ and $[\text{P}(\text{OMe})_3]$ in the range $0.1\text{-}0.8 \text{ mol dm}^{-3}$. The reaction mixtures were made by distilling a weighed amount of $\text{P}(\text{OMe})_3$ into flasks with a Spectrosil cell side arm. These flasks had been loaded with solutions of $[\text{Fe}(\text{NMe}_3)(\text{NCMe})_5]^{2+}$ in the dry box. The total volume of the solution was kept constant, that is 5ml. Allowance was made for the volume of $\text{P}(\text{OMe})_3$ to be added but the volume of mixing was assumed to be negligible within the limits of the experiment. Alternatively weighed amount of $\text{P}(\text{OMe})_3$ was distilled into frangible ampoules which were sealed and then loaded into the flasks having Spectrosil cell side arm. The reaction mixtures were held at 77 K until required and then rapidly warmed before being placed in a thermostatted cell holder. The frangible ampoules were broken before the cell was placed in the thermostatted cell holder. The temperature was adjusted at $25 \pm 0.1^\circ\text{C}$. The spectra were recorded initially at 3 minute intervals; the time interval was enlarged as the changes in the spectrum became less observable. The first spectrum consisted

of two bands at $23,500 \text{ cm}^{-1}$ ($\epsilon = 400 \text{ dm}^3 \text{ mol}^{-1} \text{ cm}^{-1}$) and $29,400 \text{ cm}^{-1}$ ($\epsilon = 600 \text{ dm}^3 \text{ mol}^{-1} \text{ cm}^{-1}$) which decayed via a series of three isosbestic points. The isosbestic points were not well defined because of the presence of a number of species in the reaction mixture at the same time.

3:5:4 Reactions of Trimethylphosphine in Acetonitrile:-

(a) With hexakis(acetonitrile)iron(II) hexafluorophosphate.

The compound, $[\text{Fe}(\text{NCMe})_6][\text{PF}_6]_2$ (0.3 mmol) was dissolved in MeCN (5ml) and PMe_3 (2mmol) was distilled. On warming to room temperature, a red solution was formed. Removal of volatile material left a red solid whose i.r. spectrum indicated the presence of coordinated PMe_3 ¹⁷⁷ and MeCN, and bands due to the PF_6^- anion. The i.r. spectrum of the solid is listed in Table 10. The $^{31}\text{P}-\{^1\text{H}\}$ n.m.r. spectrum of the solid in CD_3CN solutions consisted of a strong singlet, a weak AB_2 and a very weak A_2B_2 multiplet. A comparison of the observed and calculated frequencies of the AB_2 and A_2B_2 systems is given in Table 11. The observed and calculated spectra are shown in Figure 8. The product isolated from a reaction mixture of $[\text{Fe}(\text{NCMe})_6][\text{PF}_6]_2$ (0.3mmol), MeCN (5ml) and PMe_3 (2mmol) which had been left for about 24 hours at room temperature, was spectroscopically identical to the solid described above. The compound was identified by its spectra and microanalysis (Table 8) as predominantly tris(acetonitrile) tris(trimethylphosphine) iron(II) hexafluorophosphate. The very weak A_2B_2 multiplet in the $^{31}\text{P}-\{^1\text{H}\}$ n.m.r. spectrum, was observed due to the species, $\text{cis}-[\text{Fe}(\text{PMe}_3)_4(\text{NCMe})_2]^{2+}$ which was present only in trace quantities as indicated from the microanalysis. The electronic spectrum of the solid in MeCN solution consisted of two bands at $\bar{\nu}_{\text{max}} 21,500 \text{ cm}^{-1}$

($\epsilon = 250 \text{ dm}^3 \text{ mol}^{-1} \text{ cm}^{-1}$) and $27,900 \text{ cm}^{-1}$ ($\epsilon = 300 \text{ dm}^3 \text{ mol}^{-1} \text{ cm}^{-1}$).

(b) With hexapyridine iron(II) hexafluorophosphate.

The complex, $[\text{Fe}(\text{py})_6][\text{PF}_6]_2$ (0.3mmol) was loaded into a double limb reaction vessel, and MeCN (5ml) was distilled in at 77 K. The compound was dissolved in MeCN and PMe_3 (2mmol) was distilled. The reaction mixture was allowed to warm to room temperature when a red solution was formed. There was no change in the colour of the solution even after 24 hours. A red solid was isolated from the solution after the volatile material was removed. The infra-red spectrum of the solid showed bands due to coordinated PMe_3 , pyridine and the bands due to the PF_6^- anion. The infra-red spectrum of the solid is listed in Table 12. The $^{31}\text{P}\{-^1\text{H}\}$ n.m.r. spectrum of the solid in CD_3CN solution consisted of a strong singlet, a weak AB_2 and a very weak A_2B_2 multiplet. A comparison of the observed and calculated frequencies for AB_2 and A_2B_2 systems is given in Table 13. By analogy with the product isolated in the reaction of $[\text{Fe}(\text{NCMe})_6][\text{PF}_6]_2$ and PMe_3 , the compound was identified as predominantly tris(pyridine), tris(trimethylphosphine) iron(II) hexafluorophosphate. The very weak A_2B_2 multiplet observed in the $^{31}\text{P}\{-^1\text{H}\}$ n.m.r. spectrum was assigned to the species, $\text{cis-}[\text{Fe}(\text{PMe}_3)_4(\text{py})_2]^{2+}$ which was present only in trace quantities. The electronic spectrum of the solid in MeCN solution consisted of two bands at $\bar{\nu}_{\text{max}} 21,600 \text{ cm}^{-1}$, ($\epsilon = 260 \text{ dm}^3 \text{ mol}^{-1} \text{ cm}^{-1}$) and $28,400 \text{ cm}^{-1}$, ($\epsilon = 350 \text{ dm}^3 \text{ mol}^{-1} \text{ cm}^{-1}$).

(c) With trimethylamine tetrakis(acetonitrile)iron(II) hexafluorophosphate.

The compound, $[\text{Fe}(\text{NMe}_3)(\text{NCMe})_4][\text{PF}_6]_2$, (0.3mmol) was loaded in a vessel in the dry box, and MeCN (5ml) was distilled in at 77 K. The compound was dissolved in MeCN and PMe_3 (2mmol) was added by vacuum distillation. On warming to room temperature, a red solution was

Table 12.

Infra-Red Spectrum of the complex $[\text{Fe}(\text{PMe}_3)_3(\text{py})_3][\text{PF}_6]_2$

Wavenumber (cm^{-1})	Assignment
1660 (w)	1+6 b coord. pyridine
1600 (m)	8 a coord. pyridine
1310 (s)	CH sym.bend (PMe_3)
1295 (s)	CH sym.bend (PMe_3)
1220 (m)	9 a coord. pyridine
1140 (m)	15 coord. pyridine
1065 (m)	18 a coord. pyridine
1040 (m)	12 coord. pyridine
975 (s)	CH_3 rock. (PMe_3)
950 (s)	CH_3 rock. (PMe_3)
845 (v.s)	$\nu_3(\text{PF}_6^-)$ ^a
725 (s)	P-C asym. str.
670 (m)	P-C sym. str.
560 (s)	$\nu_4(\text{PF}_6^-)$ ^a

w = weak, m = medium, s = strong, v.s = very strong

^a Assigned by comparison with the i.r. spectrum of KPF_6 .¹⁷¹

Table 13.

Observed and Calculated Frequencies of Second Order Spectra for
AB₂ and A₂B₂ Systems.

AB₂ data from mer-[Fe(PMe₃)₃(py)₃]²⁺ and A₂B₂ from cis-[Fe(PMe₃)₄(py)₂]²⁺

AB ₂	
obs.	calc.
388.6	388.6
393.5	393.3
445.2	445.1
448.1	448.2
763.5	763.3
815.1	815.1
823.10	823.0
874.8	874.7

A ₂ B ₂	
obs.	calc.
51.7	51.6
58.2	58.1
101.2	101.0
103.8	103.8
108.3	108.5
153.2	153.1
158.3	158.3
488.0	488.0
493.0	493.1
538.0	538.0
542.5	542.5
545.0	545.2
588.0	588.2
594.5	594.6

formed whose colour did not change even after 24 hours. A red solid was isolated from the solution after the removal of volatile material. The i.r. spectrum of the solid indicated the presence of coordinated PMe_3 , NMe_3 and MeCN and bands due to the PF_6^- anion were also present. The i.r. spectrum of the complex in the solid state is listed in Table 14. The $^{31}\text{P}\{-^1\text{H}\}$ n.m.r. spectrum of the solid in CD_3CN solution consisted of a strong singlet, a weak AB_2 multiplet and a very weak A_2B_2 multiplet. The ^1H n.m.r. spectrum consisted of signals due to CH_3 protons of MeCN and Me_3N , CH_3 protons of PMe_3 trans to MeCN or Me_3N and CH_3 protons of PMe_3 trans to PMe_3 . The singlets due to the CH_3 protons of MeCN and Me_3N were sharp suggesting a rapid exchange among MeCN and Me_3N . This was consistent with the $^{31}\text{P}\{-^1\text{H}\}$ n.m.r. study of the compound, in CD_3CN solution. By analogy with the product isolated in the reaction between $[\text{Fe}(\text{NCMe})_6][\text{PF}_6]_2$ and PMe_3 , the compound was identified as predominantly trimethylamine bis(acetonitrile) tris(trimethylphosphine) iron(II) hexafluorophosphate. The A_2B_2 multiplet observed in the $^{31}\text{P}\{-^1\text{H}\}$ n.m.r. spectrum of the solid was assigned to the species, $\text{cis-}[\text{Fe}(\text{PMe}_3)_4(\text{NMe}_3)(\text{NCMe})]^{2+}$ which was present only in trace quantities. The electronic spectrum of the solid in MeCN solution consisted of two bands at $\bar{\nu}_{\text{max}} 21,500 \text{ cm}^{-1}$, ($\epsilon = 260 \text{ dm}^3 \text{ mol}^{-1} \text{ cm}^{-1}$) and $27,900 \text{ cm}^{-1}$ ($\epsilon = 350 \text{ dm}^3 \text{ mol}^{-1} \text{ cm}^{-1}$).

(d) With hexa-ammine iron(II) hexafluorophosphate.

The complex $[\text{Fe}(\text{NH}_3)_6][\text{PF}_6]_2$ (0.3mmol) was dissolved in MeCN (5ml) and PMe_3 (2mmol) was added by vacuum distillation. The reaction mixture was allowed to warm to room temperature when a red solution was formed. The solution did not change its colour even when left for 24 hours. A red solid was isolated from the solution after the volatile material was removed. The infra-red spectrum of the solid indicated the

Table 14.

Infra-Red Spectrum of the complex $[\text{Fe}(\text{PMe}_3)_3(\text{NMe}_3)(\text{NCMe})_2][\text{PF}_6]_2$

Wavenumber (cm^{-1})	Assignment ^{173,174,177}
3240 (m)	CH str. (Me_3N)
3005 (m)	CH str. (MeCN)
2940 (m)	CH str. (MeCN)
2330 (w)	CN comb.
2295 (w)	C≡N str.
1432 (s)	CH asym.bend (PMe_3)
1310 (s)	CH sym.bend (PMe_3)
1295 (s)	CH sym.bend (PMe_3)
1042 (w)	CH_3 rock (MeCN)
978 (s)	CH_3 rock. (PMe_3)
950 (v.s)	CH_3 rock. (PMe_3)
840 (v.s)	$\nu_3(\text{PF}_6^-)$ ^a
725 (s)	P-C asym.str.
670 (m)	P-C sym.str.
560 (s)	$\nu_4(\text{PF}_6^-)$ ^a

w = weak, m = medium, s = strong, v.s = very strong

^a Assigned by comparison with the i.r. spectrum of KPF_6 .¹⁷¹

presence of coordinated PMe_3 , $\bar{\nu}_{\text{max}}$, 1310, 1295, 975, 950, 725 and 670 cm^{-1} , NH_3 , $\bar{\nu}_{\text{max}}$, 3380, 3300, 1630 and 1215 cm^{-1} and MeCN , $\bar{\nu}_{\text{max}}$ 2330 and 2280 cm^{-1} . The bands at 840 and 560 cm^{-1} were assigned to ν_3 and ν_4 of PF_6^- anion. The $^{31}\text{P}\{-^1\text{H}\}$ n.m.r. spectrum of the solid in CD_3CN consisted of a strong singlet, an A_2B multiplet, a weak AB_2 multiplet and a very weak A_2B_2 multiplet. A comparison of the observed and calculated frequencies of the various systems observed is given in Table 15. The ^1H n.m.r. spectrum of the solid in CD_3CN contained a relatively broad signal assigned to the methyl protons of MeCN which showed that the exchange between MeCN and NH_3 was slow on the n.m.r. time scale. This was consistent with the observation of the A_2B multiplet in the $^{31}\text{P}\{-^1\text{H}\}$ n.m.r. spectrum assigned to the species $\text{fac}[\text{Fe}(\text{PMe}_3)_3(\text{NH}_3)_2(\text{NCMe})]^{2+}$. The compound was identified from its spectra and microanalysis as a mixture of triammine tris(trimethylphosphine) iron(II) hexafluorophosphate and acetonitrile bis ammine tris(trimethylphosphine) iron(II) hexafluorophosphate. The result of analysis together with the required values for $[\text{Fe}(\text{PMe}_3)_3(\text{NH}_3)_3][\text{PF}_6]_2$ and $[\text{Fe}(\text{PMe}_3)_3(\text{NH}_3)_2(\text{NCMe})][\text{PF}_6]_2$ are given in Table 8. The A_2B_2 multiplet observed in the $^{31}\text{P}\{-^1\text{H}\}$ n.m.r. spectrum was assigned to the species $\text{cis}[\text{Fe}(\text{PMe}_3)_4(\text{NH}_3)_2]^{2+}$ which was present in trace quantities. The electronic spectrum of the solid in MeCN consists of two bands at $\bar{\nu}_{\text{max}}$ $21,200 \text{ cm}^{-1}$, ($\epsilon = 300 \text{ dm}^3 \text{ mol}^{-1} \text{ cm}^{-1}$) and $27,600 \text{ cm}^{-1}$. ($\epsilon = 310 \text{ dm}^3 \text{ mol}^{-1} \text{ cm}^{-1}$).

Table 15.

Observed and Calculated Frequencies of Second Order Spectra for A_2B , AB_2 and A_2B_2 Systems.

A_2B data from fac- $[Fe(PMe_3)_3(NH_3)_2(NCMe)]^{2+}$, AB_2 from mer- $[Fe(PMe_3)_3(NH_3)_3]^{2+}$ and A_2B_2 from cis- $[Fe(PMe_3)_4(NH_3)_2]^{2+}$

A_2B	
obs.	calc.
703.5	703.2
743.5	743.2
765.0	765.0
805.0	805.1
864.8	864.8
869.6	869.5
909.6	909.6
926.5	926.5

AB_2	
obs.	calc.
388.3	388.4
393.0	393.1
445.0	445.0
447.7	447.7
765.0	764.9
815.0	815.0
823.0	822.8
874.5	874.5

A_2B_2	
obs.	calc.
51.2	50.96
58.0	57.93
101.0	100.9
103.5	103.2
107.7	107.6
152.8	152.5
158.0	157.7
487.6	487.5
492.7	492.6
537.5	537.5
542.0	542.0
544.7	544.8
587.7	587.7
594.2	594.2

CHAPTER Four

Redox and Substitution Reactions of
Solvated Cu^{II} and Cu^I , and Solvated
 Tl^{III} and Tl^I Cations in Acetonitrile

4:1 Introduction.

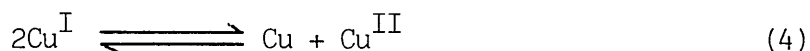
There has been a great deal of interest in the redox chemistry of transition and post transition metal ions over the past several years. On the basis of the published half-wave potentials for the couple solvated Cu^{2+} -solvated Cu^+ in acetonitrile, ($E_{\frac{1}{2}} = +0.75\text{V}$), the solvated Cu^{2+} is regarded as a strong oxidising agent in MeCN.⁸⁴ The reactions of Tl^{III} and Tl^{I} studied in MeCN imply that the solvated Tl^{3+} is a stronger oxidising agent than solvated Cu^{2+} although the half-wave potential, $E_{\frac{1}{2}}$, for the $\text{Tl}^{\text{III}}-\text{Tl}^{\text{I}}$ couple could not be determined.⁴⁶ The aim of the work described in this chapter is the synthetic study of the redox and substitution behaviour of solvated $\text{Cu}(\text{II})$ and $\text{Cu}(\text{I})$, and solvated $\text{Tl}(\text{III})$ and $\text{Tl}(\text{I})$ cations in acetonitrile solution excluding moisture and oxygen. The ligands used are the simple nitrogen, phosphorus and sulphur donor species such as trimethylamine (Me_3N), trimethylphosphine (Me_3P), dimethylsulphide (Me_2S) and tetramethylthiourea (tmtu). These ligands were used because of the reasons described in chapter 1. The reduced form of the metal cations and the oxidised form of the ligands were identified using various spectroscopic techniques.

4:1:1 Redox Chemistry of Copper:

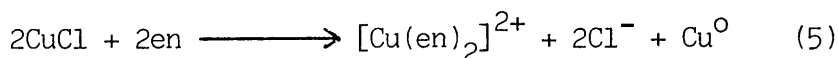
Copper is one of the most widely studied elements and its redox chemistry has been investigated both in aqueous and non-aqueous solvents as reaction media. The divalent oxidation state of copper is the more extensively studied state as it is the most stable oxidation state in aqueous solution. The relative stabilities of the Cu^{I} and Cu^{II} states, in aqueous solution, are indicated by the standard reduction potential data given in equations (1) to (3).⁸²



The much larger heat of hydration of Cu^{II} compared with Cu^{I} , possibly due to the higher charge and greater coordination number, makes the hydrated $\text{Cu}(\text{II})$ ion the more stable oxidation state in aqueous solution.¹⁷⁸ However a number of $\text{Cu}(\text{I})$ cationic or anionic complexes are stable in aqueous medium. These have been described in chapter 1. The equilibrium (equation 4)



can readily be displaced in either direction. Thus $\text{Cu}(\text{II})$ reacts with CN^- or I^- ions to give the $\text{Cu}(\text{I})$ compounds whereas CuCl reacts with ethylenediamine(en) in aqueous potassium chloride solution to form the $\text{Cu}(\text{II})$ state (equation 5).



The electronic configuration of the Cu^{2+} ion in the outermost shell is d^9 . This makes the Cu^{2+} ion subject to Jahn-Teller distortion when placed in a cubic environment and has a pronounced effect on its stereochemistry.¹⁷⁹ A typical example is the $\text{Cu}(\text{II})$ hexa-aqua ion, $[\text{Cu}(\text{H}_2\text{O})_6]^{2+}$, whose electronic spectrum consists of a broad asymmetric band with a shoulder on the low energy side. This asymmetric band results from a tetragonal distortion of the complex cation in solution with two of the water molecules being farther from the metal centre than the other four. Thus $\text{Cu}(\text{II})$ complexes exhibit a variety of geometries ranging from a distorted octahedron, $[\text{Cu}(\text{H}_2\text{O})_6]^{2+}$, through trigonal bipyramid, $[\text{Cu}(\text{bipy})_2\text{I}]^+$,¹⁸⁰ (bipy = bipyridyl) to a flattened

tetrahedral structure, $[\text{CuCl}_4]^{2-}$.¹⁸¹

The favoured oxidation state of copper in MeCN solution is the +1 state because of the effective solvation of the Cu^+ ion by MeCN as described in chapter 2. Copper(II) in MeCN thus behaves as a moderately good oxidising agent. The solvated Cu^{II} and Cu^{I} cations in MeCN have been well characterized and are obtained by a variety of synthetic routes.^{182,183} The Cu(II) salt has been isolated from MeCN solution as the solid $[\text{Cu}(\text{NCMe})_5][\text{PF}_6]_2$ but the electronic spectrum in MeCN solution suggests the presence of the tetragonally distorted $[\text{Cu}(\text{NCMe})_6]^{2+}$ ion.

An important contribution to copper chemistry is the role that biological copper has played in stimulating research into the inorganic chemistry of copper. The structural chemistry of two copper proteins, that is plastocyanin¹⁸⁴ and azurin,¹⁸⁵ showed that these proteins contain a tetrahedral copper stereo-chemistry involving two nitrogen atoms from two separate histidine groups and two sulphur atoms from a cysteine thiol and a methionine thioether. Copper(II) ions in proteins are classified into three types.¹⁸⁶ Type I and type II copper ions are isolated from other copper ions thus functioning as mononuclear complexes whereas type III copper ions have a binuclear structure which makes them non-detectable in an e.p.r. experiment. The low molecular weight proteins such as plastocyanin and azurin contain a copper(II) ion in type I form. All the Cu(II) ions in proteins have relatively high redox potentials and are readily reduced to Cu(I) by ascorbic acid, hydroquinones and catechols.

The mechanism of electron transfer in the bioinorganic species is a subject of great interest. A number of studies have been carried out to investigate the oxidation of the reduced form of the protein with inorganic complexes as the redox partners, for example Co(III)

with various substituted 1,10-phenanthroline ligands.¹⁸⁷ The kinetics of the oxidation reaction are consistent with an association of the protein and the inorganic complex prior to electron transfer. M.Ostern *et al.* have studied the oxidation of the reduced glutathione by Cu(II).¹⁸⁸ Glutathione is a peptide found in the erythrocytes of blood and has a number of functions including protection of hemoglobin against oxidation by hydrogen peroxide. It has been observed that Cu²⁺ ion in aqueous basic solution (pH ≈ 11) oxidises reduced glutathione (GSH) to the oxidised glutathione (GSSG) and itself is reduced to Cu(I). This redox reaction results in the colour change of the solution from blue to yellow along with the disappearance of the d-d band.



The reduction is supposed to take place through the formation of an intermediate in which a GSH molecule is bonded to Cu(II) via sulphur and nitrogen donors.

The cation $[\text{Cu}(\text{NCMe})_6]^{2+}$ is a convenient starting point for studying the redox chemistry of Cu(II) in MeCN. Previous work has shown that $[\text{Cu}(\text{NCMe})_6]^{2+}$ in MeCN reacts with an excess of $\text{P}(\text{OMe})_3$ to produce $[\text{Cu}\{\text{P}(\text{OMe})_3\}_4]^+$ and dimethyl methyl phosphonate.¹⁸⁹ The decay of the purple intermediate believed to be a copper(II)-phosphite complex, $[\text{Cu}\{\text{P}(\text{OMe})_3\}_x(\text{NCMe})_{6-x}]^{2+}$, ($x = 1$ to 4) has been followed by stop-flow spectrophotometry.⁸⁴ The present work involves a synthetic study of the redox and substitution reactions of $[\text{Cu}(\text{NCMe})_6]^{2+}$ in MeCN using Me_3N , Me_3P , Me_2S and tmtu as ligands. These ligands have been selected because they cannot be conveniently used in aqueous solution.

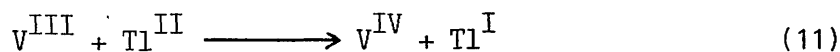
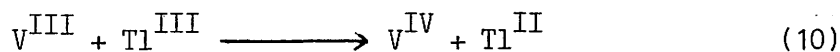
Trimethyl amine and dimethyl sulphide have been shown to behave in a similar way in a number of redox reactions. For example K.L.

4:1:2 Redox Chemistry of Thallium

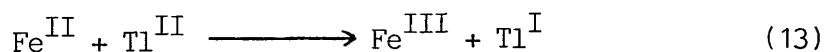
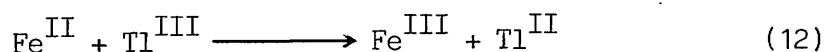
Thallium is one of the post transition elements whose redox chemistry has been the subject of great interest. The electrode potential data indicate that Tl(I) is much more stable than Tl(III) in



aqueous solution and that Tl(III) compounds can act as oxidising agents. Redox reactions of Tl(III) in aqueous acidic solutions have been intensively studied and appear to be two electron transfer processes. The kinetics of a large number of one- and two-equivalent redox reactions have been reported.¹⁹³ For example the reaction of Tl^{III} with V^{III} in acid perchlorate solution is first order with respect to both $[\text{V}^{\text{III}}]$ and $[\text{Tl}^{\text{III}}]$ and a mechanism involving Tl^{II} has been proposed.

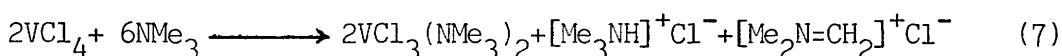


The oxidation of Fe^{II} by Tl^{III} in aqueous perchloric acid has been studied by G.S. Lawrence and co-workers¹⁹⁴ and is represented in equations (12) and (13).



Reactions between Tl^{II} and Fe^{II} (equation 13) has been proposed as the fast step in the oxidation of Fe^{II} by Tl^{III} whereas the rate determining step is the reaction in which Tl^{II} is produced (equation 12). The rate constant for the reaction represented by equation 13 has been

Baker and co-workers have found that under anhydrous conditions, vanadium(V)oxytrichloride (VOCl_3) is reduced by an excess of trimethylamine or dimethylsulphide.¹⁹⁰ The reduction products are vanadium(IV) complexes of the composition $\text{VOCl}_2(\text{NMe}_3)_2$ and $\text{VOCl}_2(\text{SMe}_2)_2$. The oxidation product from the Me_3N reaction is trimethylammonium chloride whereas the product from the Me_2S reaction has not been identified. The complexes, $\text{VOCl}_2(\text{NMe}_3)_2$ and $\text{VOCl}_2(\text{SMe}_2)_2$ have been shown to have a distorted trigonal bipyramid structure. The redox reaction involving VCl_4 and Me_3N has been investigated by R. Kiesel and E.P. Schram.¹⁹¹ The condensation of VCl_4 onto excess liquid Me_3N followed by warming the reaction mixture from 151 K to 298 K resulted in the redox reaction summarized in equation (7).



The species, $[\text{Me}_2\text{N}=\text{CH}_2]^+\text{Cl}^-$, has not been isolated but is suggested to be one of the products as the infrared spectrum of the solid indicates the presence of strong bands at $\bar{\nu}_{\text{max}} 1696 \text{ cm}^{-1}$ (C=N str) and 3120 cm^{-1} (CH_2 str).

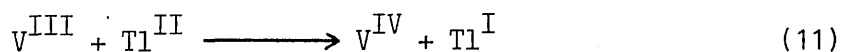
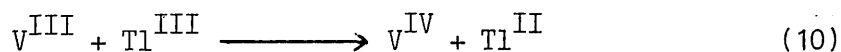
The reduction of gold(III) to gold(I) by Me_2S in aqueous methanol has been reported by G. Annibale and co-workers.¹⁹² It has been observed that $[\text{AuCl}_4]^-$ reacts with an excess of Me_2S in methanol solution in a two step reaction. In the first step substitution reactions leading to the formation of the disubstituted species, $[\text{AuCl}_2(\text{Me}_2\text{S})_2]^+$, are involved. The intermediate Au(III) complex, $[\text{AuCl}_2(\text{Me}_2\text{S})_2]^+$, in the second step, reacts with an extra molecule of Me_2S to form the gold(I) species, $[\text{AuCl}(\text{Me}_2\text{S})]$, and dimethyl sulphoxide.

4:1:2 Redox Chemistry of Thallium

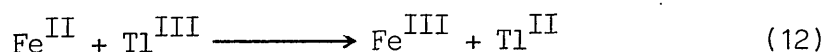
Thallium is one of the post transition elements whose redox chemistry has been the subject of great interest. The electrode potential data indicate that Tl(I) is much more stable than Tl(III) in



aqueous solution and that Tl(III) compounds can act as oxidising agents. Redox reactions of Tl(III) in aqueous acidic solutions have been intensively studied and appear to be two electron transfer processes. The kinetics of a large number of one- and two-equivalent redox reactions have been reported.¹⁹³ For example the reaction of Tl^{III} with V^{III} in acid perchlorate solution is first order with respect to both $[\text{V}^{\text{III}}]$ and $[\text{Tl}^{\text{III}}]$ and a mechanism involving Tl^{II} has been proposed.



The oxidation of Fe^{II} by Tl^{III} in aqueous perchloric acid has been studied by G.S. Lawrence and co-workers¹⁹⁴ and is represented in equations (12) and (13).



Reactions between Tl^{II} and Fe^{II} (equation 13) has been proposed as the fast step in the oxidation of Fe^{II} by Tl^{III} whereas the rate determining step is the reaction in which Tl^{II} is produced (equation 12). The rate constant for the reaction represented by equation 13 has been

measured and its comparison with that of the rate constant of the reaction represented in equation 12 gives a value of +0.37V for the standard reduction potential of the $Tl^{III}-Tl^{II}$ couple. The present study involves the redox reactions of $[Tl(NCMe)_6]^{3+}$ in MeCN with a number of ligands such as Me_3N , Me_3P and Me_2S . The oxidation states of thallium, Tl^{3+} and Tl^+ , in MeCN solution are readily differentiated from their ^{205}Tl chemical shifts as described in chapter 2.

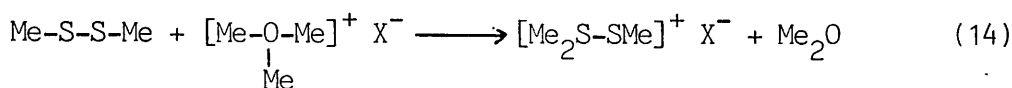
4:2 Results

4:2:1 Reactions of Dimethyl Sulphide with Solvated Cu^I and Cu^{II} Cations in MeCN.

The reaction of dimethyl sulphide with $[Cu(NCMe)_4][PF_6]$ in the presence or absence of MeCN resulted in the formation of a white solid. The infrared spectrum of the solid, $\bar{\nu}_{max}$ 2290 (CN comb), 2265 (C≡N str), 1030 (CH_3 rock), 835 ($\nu_3 PF_6^-$) and 560 cm^{-1} ($\nu_4 PF_6^-$), was identical to that of the complex, $[Cu(NCMe)_4][PF_6]$. There was no evidence in the infrared spectrum for the coordination of Me_2S .

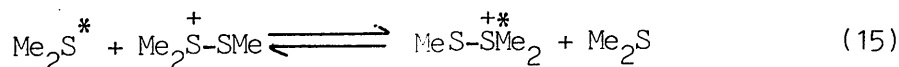
The species, $[Cu(NCMe)_6]^{2+}$, in acetonitrile solution, undergoes a redox reaction with Me_2S . A dark green intermediate was formed initially whose decay depended upon the concentration of Me_2S used. The decay was rapid when a large excess of Me_2S was used. The final solution was colourless and an off-white solid was obtained from this solution after the volatile material was removed. The infrared spectrum of the solid, isolated from the reaction of $[Cu(NCMe)_5][PF_6]_2$ with Me_2S in MeCN, consisted of bands corresponding to the salt, $[Cu(NCMe)_4][PF_6]$. There were additional bands in the regions of the spectrum where CH stretch and CH_3 rocking were expected, and a band at $\bar{\nu}_{max}$ 280 cm^{-1} was assumed to be due to the S-S stretching mode. It is, therefore, suggested that the Cu^I

salt is generated from the reduction of $[\text{Cu}(\text{NCMe})_6]^{2+}$ whereas the oxidation of Me_2S may have resulted in the formation of an S-S bonded species. The species containing S-S bond have been reported in the literature. The cation, $[\text{Me}_2\text{S-SMe}_2]^{2+}$, appears to be unknown under normal conditions but the species, $[\text{Me}_2\text{S-SMe}]^+$, has been obtained as the 2,4,6-trinitrobenzenesulphonate¹⁹⁵ PF_6^- ,¹⁹⁶ and BF_4^- ¹⁹⁷ salts by the reaction of dimethyl disulphide with the corresponding trimethyloxonium salt in MeCN solution.



X = 2,4,6-trinitrobenzenesulphonate, PF_6^- and BF_4^-

The ^1H n.m.r. spectra of the salts, $[\text{Me}_2\text{S-SMe}][\text{X}]$, in CD_3CN or MeNO_2 , consist of two sharp singlets (relative intensities 2:1) at 3.2 and 2.8 ppm. The larger singlet corresponds to the resonance of the two methyl groups attached to the sulphonium sulphur ($\text{Me}_2\overset{+}{\text{S}}-$) whereas the smaller singlet to the resonance of the methyl group attached to the sulphenyl sulphur ($\text{MeS}-$). The ^1H n.m.r. spectrum of a 1:1 mixture of $[\text{Me}_2\text{S-SMe}][\text{BF}_4^-]$ and Me_2S in CD_3CN at 273 K consists of two sharp singlets (relative intensities 1:4) at 2.8 and 2.65 ppm. The resonances due to the methyl groups of the sulphide and those of the sulphonium group collapse into a single sharp resonance (2.65 ppm) centred half way between the original positions of the $\text{Me}_2\overset{+}{\text{S}}-$ (3.2 ppm) and Me_2S (2.1 ppm) resonances. Thus the methyl groups of the sulphide and those attached to the sulphonium sulphur ($\text{Me}_2\overset{+}{\text{S}}-$) are undergoing exchange of environment as represented in equation 15.



The compound, $[\text{Me}_2\text{S-SMe}][\text{BF}_4^-]$, was prepared according to the

literature method.¹⁹⁷ The ^1H n.m.r. spectra of the salt $[\text{Me}_2\text{S-SMe}][\text{BF}_4]$, (Figure 1) and that of a 1:1 mixture of $[\text{Me}_2\text{S-SMe}][\text{BF}_4]$ and Me_2S in CD_3CN were in good agreement with the spectra reported in the literature. The infrared spectrum of the solid, $[\text{Me}_2\text{S-SMe}][\text{BF}_4]$, is listed in Table 1. The band at $\bar{\nu}_{\text{max}} 300 \text{ cm}^{-1}$ was presumed to arise from the S-S stretching mode. The Raman spectrum of the solid was not recorded as the salt burned in the laser beam.

The ^1H n.m.r. spectrum of the solid isolated from the reaction of $[\text{Cu}(\text{NCMe})_6]^{2+}$ and Me_2S , in CD_3CN , consisted of two sharp singlets (relative intensities 2:3) at 2.9 and 2.3 ppm. By analogy with the ^1H n.m.r. spectrum of the cation, $[\text{Me}_2\text{S-SMe}]^+$, the smaller singlet corresponds to the resonance of the two methyl groups of the Me_2S^+ fragment whereas the larger singlet originates from the methyl protons of the CH_3S^- part of the cation, $[\text{Me}_2\text{S-SMe}]^+$, and the MeCN ligands coordinated to Cu^{I} and exchanging with CD_3CN . To record a ^1H n.m.r. spectrum with resonances originating only from the protons of the cation, $[\text{Me}_2\text{S-SMe}]^+$, the MeCN molecules in the species, $[\text{Cu}(\text{NCMe})_6]^{2+}$ were exchanged with CD_3CN prior to its reaction with Me_2S . The ^1H n.m.r.

spectrum of the product obtained from the reaction of $[\text{Cu}(\text{CD}_3\text{CN})_6]^{2+}$ and Me_2S , in CD_3CN , consisted of two singlets (relative intensities 2:1) at 2.95 and 2.35 ppm (Figure 1) confirming the assignment made above. Thus in the redox reaction of Me_2S and $[\text{Cu}(\text{NCMe})_6]^{2+}$, the oxidised form of Me_2S may be formulated as $[\text{Me}_2\text{S-SMe}]^+$. This formulation is based on the evidence obtained from the infrared and ^1H n.m.r. spectra. In addition to the species described above, the material distilled at 183 K from the reaction mixture of $[\text{Cu}(\text{NCMe})_6]^{2+}$ and Me_2S , was identified as ethane by gas chromatography. The overall reaction of $[\text{Cu}(\text{NCMe})_5][\text{PF}_6]_2$ with Me_2S in MeCN, is summarized in equation 16.

Figure 1. ^1H N.M.R. Spectra of the Salts, $[\text{Me}_2\text{S-SMe}][\text{X}]$,
 $\text{X} = \text{BF}_4^-$, PF_6^- , and UF_6^- , in CD_3CN .

(a) $[\text{Me}_2\text{S-SMe}][\text{BF}_4^-]$

(b) $[\text{Me}_2\text{S-SMe}][\text{PF}_6^-]$

(c) $[\text{Me}_2\text{S-SMe}][\text{UF}_6^-]$

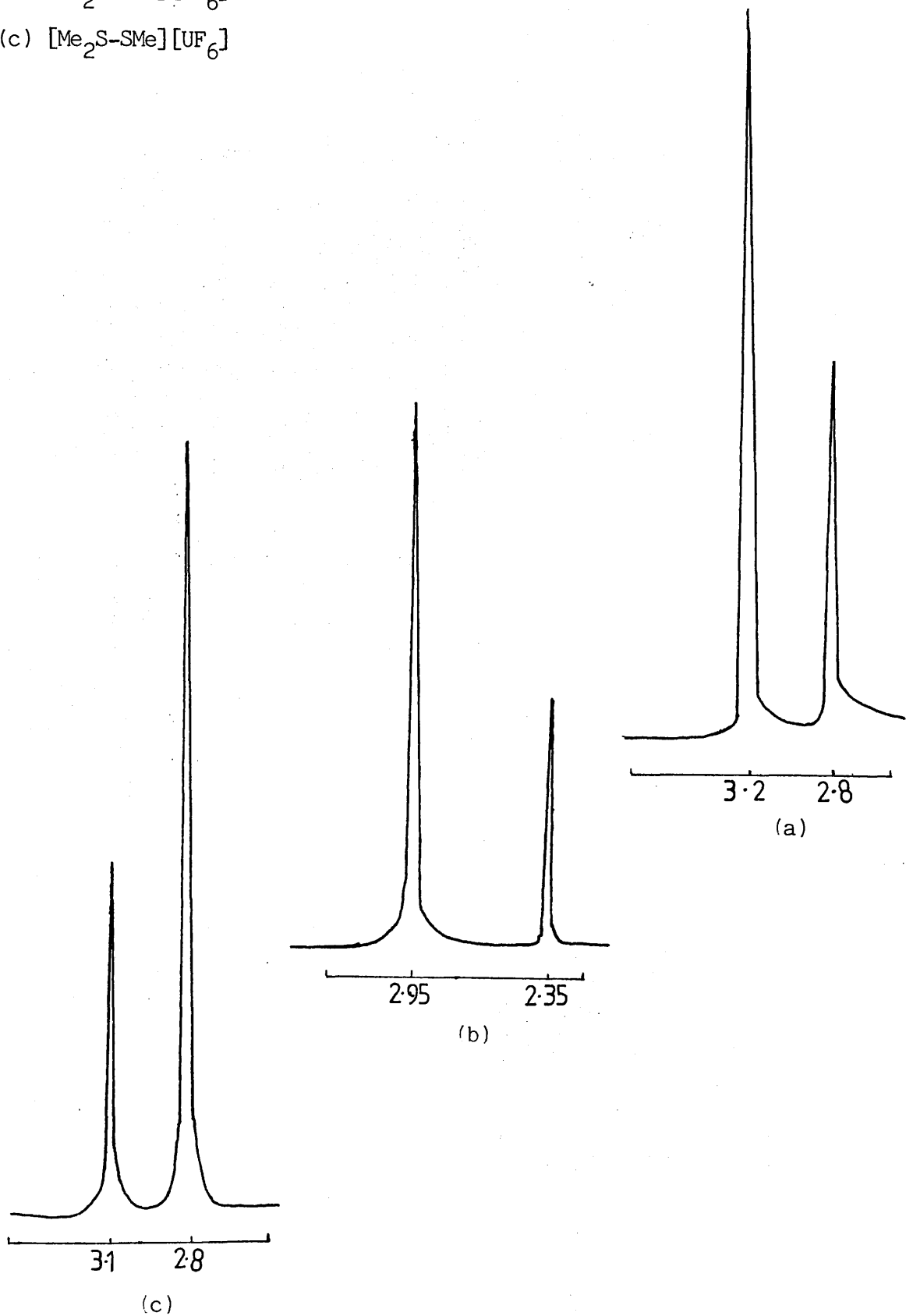
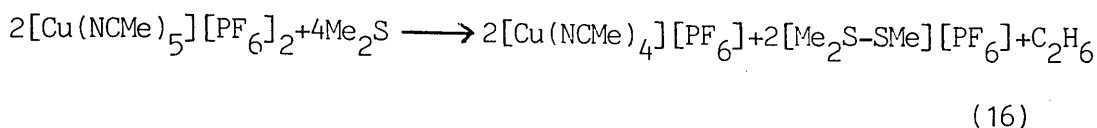


Table 1.

Infrared Spectrum of the Compound [Me₂S-SMe][BF₄]

wavenumber (cm ⁻¹)	Assignment
3040 (m)	CH str
2940 (m)	CH str
1425 (s)	CH ₃ deg.def.
1348 (m)	CH ₃ sym.def.
1085 (m)	CH ₃ rock
980 (s)	BF ₄ ⁻
765 (m)	C-S str.
690 (m)	C-S str.
670 (m)	C-S str.
520 (s)	BF ₄ ⁻
300 (m)	S-S str.

s = strong; m = medium

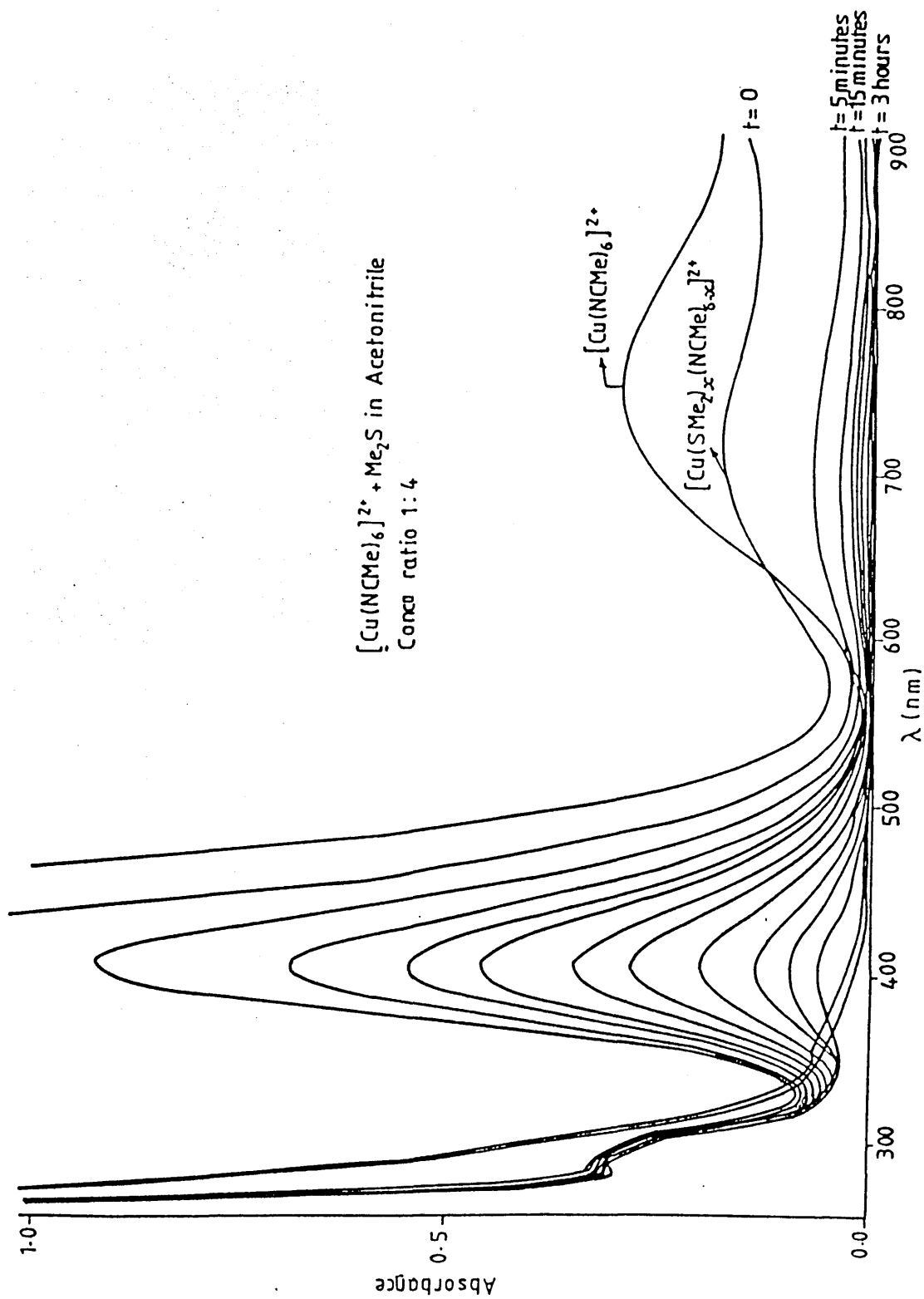


The decay of the green intermediate formed in the redox reaction of $[\text{Cu}(\text{NCMe})_6]^{2+}$ and Me_2S , can be followed by conventional electronic spectroscopy only when $[\text{Cu}^{\text{II}}]:[\text{Me}_2\text{S}] < 1:5$. The resultant spectra using solutions $5.0 \times 10^{-4} \text{ mol dm}^{-3}$ in $\text{Cu}(\text{II})$ and $2.0 \times 10^{-3} \text{ mol dm}^{-3}$ in Me_2S , a concentration ratio, $[\text{Cu}^{\text{II}}]:[\text{Me}_2\text{S}] = 1:4$, are shown in Figure 2. It was observed that the position of the Cu^{II} band was shifted from $13,300 \text{ cm}^{-1}$ to $14,300 \text{ cm}^{-1}$ upon mixing of Me_2S with $[\text{Cu}(\text{NCMe})_6]^{2+}$ in MeCN and a new band appeared at $\bar{\nu}_{\text{max}} 24,300 \text{ cm}^{-1}$. The intensity of the two bands decreased with the passage of time, the band at $\bar{\nu}_{\text{max}} 14300 \text{ cm}^{-1}$ disappeared much more quickly than the one at $\bar{\nu}_{\text{max}} 24300 \text{ cm}^{-1}$. The disappearance of the former band in the reaction of $[\text{Cu}(\text{NCMe})_6]^{2+}$ with Me_2S (concentration ratio = 1:4) required 30 minutes whereas approximately three hours were required for the disappearance of the latter band.

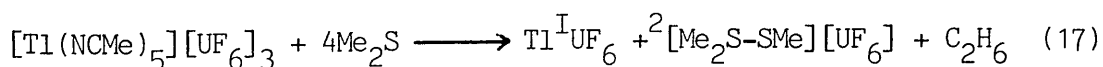
4:2:2 Reactions of Dimethylsulphide with Solvated Tl^{I} and Tl^{III} Cations in MeCN.

The reaction of dimethyl sulphide with $\text{Tl}^{\text{I}}\text{UF}_6$ in MeCN solution at room temperature resulted in the formation of a light green solid. The infrared spectrum of the solid was identical to that of $\text{Tl}^{\text{I}}\text{UF}_6$ and there was no evidence for the coordination of Me_2S . The species, $[\text{Tl}(\text{NCMe})_6]^{3+}$, in MeCN solution underwent a redox reaction when reacted with Me_2S . A lemon yellow intermediate was formed initially which decayed rapidly forming a light green solution. The infrared spectrum of the solid isolated from the reaction mixture of $[\text{Tl}^{\text{III}}(\text{NCMe})_5][\text{UF}_6]_3$ and Me_2S in MeCN, consisted of bands at $\bar{\nu}_{\text{max}}$ 3030, 2940 (CH str), 1315 (CH_3 def.), 1050, 995 (CH_3 rock), 690 (C-S str),

Figure 2. Consecutive Electronic Spectra for the Reaction of $[\text{Cu}(\text{NCMe})_6]^{2+}$ with Me_2S .



510 (UF_6^-) and a band at $\bar{\nu}_{\text{max}} 285 \text{ cm}^{-1}$ presumably due to the S-S stretching mode. Bands due to coordinated MeCN were absent. The Raman spectrum of the solid was not recorded as the salt burned in the laser beam. The ^{205}Tl n.m.r. spectrum of the solid in MeCN solution contained a signal at, $\delta = -140 \text{ ppm}$, showing the presence of Tl^{I} in the solid. The electronic absorption spectrum of the solid in MeCN solution showed characteristic absorptions of the UF_6^- anion at $\bar{\nu}_{\text{max}} 7300, 7430, 7580$ and 7940 cm^{-1} , and was in good agreement with the spectra of the salts containing the UF_6^- anion.¹⁹⁸ Therefore, one of the products in the solid isolated from the reaction of $[\text{Tl}^{\text{III}}(\text{NCMe})_5][\text{UF}_6]_3$ and Me_2S , was identified as $\text{Tl}^{\text{I}}\text{UF}_6$. The ^1H and ^{13}C n.m.r. spectra of the solid in CD_3CN , each consisted of two singlets (relative intensities, 1:2) at 3.1 and 2.8 ppm (Figure 1), and 31.7 and 27.8 ppm respectively. The ^1H n.m.r. spectrum of a 1:1 mixture of the solid obtained from the reaction of Me_2S with $[\text{Tl}^{\text{III}}(\text{NCMe})_5][\text{UF}_6]_3$ and Me_2S in CD_3CN at 298 K consisted of two singlets (relative intensities, 1:4) at 2.7 and 2.4 ppm, a situation similar to that of a 1:1 mixture of $[\text{Me}_2\text{S-SMe}][\text{BF}_4]$ and Me_2S as described above. Therefore, the oxidised form of Me_2S formed in the above described redox reaction was formulated as $[\text{Me}_2\text{S-SMe}]^+$. The material distilled at 183 K from the reaction mixture of $[\text{Tl}(\text{NCMe})_6]^{3+}$ and Me_2S , was identified as ethane by gas chromatography. The overall reaction of $[\text{Tl}^{\text{III}}(\text{NCMe})_5][\text{UF}_6]_3$ with Me_2S in MeCN is summarized in equation 17.



The redox reaction between $[\text{Tl}^{\text{III}}(\text{NCMe})_5][\text{UF}_6]_3$ and Me_2S in MeCN solution was studied by ^{205}Tl n.m.r. spectroscopy. A 1:1 mixture of $[\text{Tl}^{\text{III}}]$ and $[\text{Me}_2\text{S}]$ in MeCN showed the ^{205}Tl resonances both due to Tl^{I} and Tl^{III} , $\delta(^{205}\text{Tl}^{\text{I}}) = -121.2$ and $\delta(^{205}\text{Tl}^{\text{III}}) = +2015 \text{ ppm}$ whereas

mixtures of Tl^{III} and Me_2S with concentration ratios 1:2 and 1:4 indicated the ^{205}Tl resonances only due to Tl^{I} , $\delta(^{205}\text{Tl})$ were -172.6 and -185.1 ppm respectively. This difference in the ^{205}Tl chemical shift values is due to the different environment around the thallium nuclei, and is consistent with the results described in chapter 2.

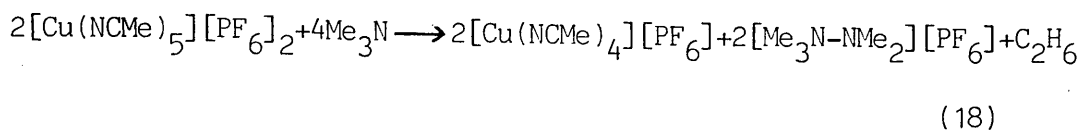
4:2:3 Reactions of Trimethylamine with Solvated Cu^{I} and Cu^{II} Cations in MeCN.

The reaction of trimethylamine with $[\text{Cu}(\text{NCMe})_4][\text{PF}_6]$ in the presence or absence of MeCN resulted in the formation of a white solid. The infrared spectrum of the solid was identical to that of the complex, $[\text{Cu}(\text{NCMe})_4][\text{PF}_6]$ and there was no evidence for coordinated Me_3N .

The cation, $[\text{Cu}(\text{NCMe})_6]^{2+}$, in MeCN solution when reacted with Me_3N underwent a redox reaction. A dark green intermediate was formed initially whose decay depended upon the concentration of Me_3N used. The final solution was colourless and an off-white solid was isolated from this solution after removal of the volatile material. The infrared spectrum of the solid obtained from the reaction of Me_3N and $[\text{Cu}(\text{NCMe})_5][\text{PF}_6]_2$, contained bands corresponding to the complex, $[\text{Cu}(\text{NCMe})_4][\text{PF}_6]$. Additional bands were present in the regions of the spectrum where CH stretch and CH_3 rocking were expected. The bands at $\bar{\nu}_{\text{max}}$ 980 and 315 cm^{-1} were presumed to be due to the N-N stretching and bending modes respectively by analogy with the infrared spectra of the N_2H_5^+ salts. In the infrared spectra of the N_2H_5^+ salts,¹⁹⁹ the N-N stretching mode is observed in the region, $960\text{--}995 \text{ cm}^{-1}$ whereas the N-N bending mode occurs at $285\text{--}335 \text{ cm}^{-1}$. By analogy with the $[\text{Cu}(\text{NCMe})_6]^{2+}$ and Me_2S redox reaction, it was possible that Cu^{II} in the above described reaction

was reduced to Cu^{I} and Me_3N oxidised to a species possibly formulated as $[\text{Me}_3\text{N-NMe}_2]^+$. A number of reactions involving the oxidation of Me_3N have been reported in the literature but the formation of the species, $[\text{Me}_3\text{N-NMe}_2]^+$ has not been previously described. It has been shown that Me_3N reduces Cu^{II} to Cu^{I} in the gas phase and itself is oxidised to the dimethylmethylen ammonium cation.²⁰⁰ The cation, $[\text{Me}_2\text{N=CH}_2]^+$, has been identified by the 1690 cm^{-1} (C=N str) absorption in the infrared spectrum.

The ^1H n.m.r. spectrum of the solid obtained from the reaction of $[\text{Cu}(\text{NCMe})_6]^{2+}$ and Me_3N , in CD_3CN consisted of two sharp singlets (relative intensities 3:4) at 2.80 and 1.95 ppm. By analogy with the ^1H n.m.r. spectrum of the cation, $[\text{Me}_2\text{S-SMe}]^+$, the smaller singlet was assigned to the resonances of the three methyl groups of the Me_3N^+ -fragment and the larger singlet to the resonances of the methyl protons of the Me_2N - part of the cation, $[\text{Me}_3\text{N-NMe}_2]^+$ and the MeCN ligands coordinated to Cu^{I} and exchanging with CD_3CN . A ^1H n.m.r. spectrum with resonances originating only from the protons of the cation, $[\text{Me}_3\text{N-NMe}_2]^+$, was recorded by using the solid isolated from the reaction of $[\text{Cu}(\text{CD}_3\text{CN})_6]^{2+}$ with Me_3N in CD_3CN . The species, $[\text{Cu}(\text{CD}_3\text{CN})_6]^{2+}$, was obtained by exchanging the MeCN molecules of $[\text{Cu}(\text{NCMe})_6]^{2+}$ with CD_3CN . The ^1H n.m.r. spectrum of the solid isolated in the above reaction, in CD_3CN , consisted of two singlets (relative intensities, 3:2) at 2.75 and 1.90 ppm, thus confirming the assignments made above. Therefore, the oxidised form of Me_3N in the redox reaction of $[\text{Cu}(\text{NCMe})_6]^{2+}$ and Me_3N , may be formulated as $[\text{Me}_3\text{N-NMe}_2]^+$. In addition to the species described above, the material distilled at 183 K from the reaction mixture of $[\text{Cu}(\text{NCMe})_6]^{2+}$ and Me_3N , was identified as ethane by gas chromatography. The overall reaction of $[\text{Cu}(\text{NCMe})_5][\text{PF}_6]_2$ with Me_3N in MeCN, is summarized in equation 18.



The decay of the green intermediate formed in the redox reaction of $[\text{Cu}(\text{NCMe})_6]^{2+}$ and Me_3N , can be followed by conventional electronic spectroscopy only when $[\text{Cu}^{\text{II}}]:[\text{Me}_3\text{N}] < 1:5$. The resultant spectra using solutions, $5.0 \times 10^{-4} \text{ mol dm}^{-3}$ in $\text{Cu}(\text{II})$ and $2.0 \times 10^{-3} \text{ mol dm}^{-3}$ in Me_3N , a concentration ratio, $[\text{Cu}^{\text{II}}]:[\text{Me}_3\text{N}] = 1:4$, were similar to the spectra recorded in the $[\text{Cu}(\text{NCMe})_6]^{2+}$ and Me_2S system. Two bands were observed at $\bar{\nu}_{\text{max}}$ 14400 and 24400 cm^{-1} , the intensity of the former band decreased much more rapidly than the latter band.

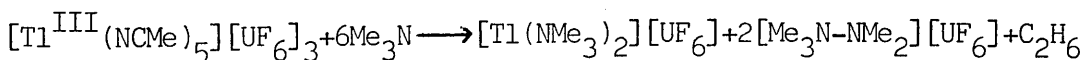
In order to determine the stoichiometry of the redox reactions involving $[\text{Cu}(\text{NCMe})_6]^{2+}$ and Me_2S or Me_3N (L), spectrophotometric titrations using $[\text{Cu}^{\text{II}}]:[\text{L}]$, 1:1, 1:2, 1:3, 1:4 and 1:10, were undertaken. It was observed that the reduction of Cu^{II} to Cu^{I} was not complete in the 1:1 and 1:2 mixtures, and the reaction was very slow. The redox reaction was comparatively fast in the 1:3 and 1:4 mixtures and approximately 3-4 hours were required for the complete reduction of Cu^{II} to Cu^{I} . The reduction of Cu^{II} to Cu^{I} in the 1:10 mixture was complete within the time of mixing hence could not be followed by conventional electronic spectroscopy.

4:2:4 Reactions of Trimethylamine with Solvated Tl^{I} and Tl^{III} Cations in MeCN.

The reaction of $\text{Tl}^{\text{I}}\text{UF}_6$ with Me_3N in MeCN solution resulted in the formation of a green precipitate. The infrared spectrum of the precipitate indicated bands due to coordinated Me_3N , $\bar{\nu}_{\text{max}}$ 3220 (CH str), 1475 (CH_3 rock), 1055 cm^{-1} (CN str) and the UF_6^- anion, $\bar{\nu}_{\text{max}}$ 520 cm^{-1} . From the infrared spectrum and the analysis of C, H

and N, the insoluble salt was identified as $[\text{Tl}(\text{NMe}_3)_2][\text{UF}_6]$. The salt was found to lose Me_3N on pumping under vacuum.

The cation, $[\text{Tl}(\text{NCMe})_6]^{3+}$, in MeCN solution underwent a redox reaction when reacted with Me_3N . A light green solution and a green precipitate were formed. The infrared spectrum of the insoluble salt was identical to the complex $[\text{Tl}(\text{NMe}_3)_2][\text{UF}_6]$, obtained from the reaction of $\text{Tl}^{\text{I}}\text{UF}_6$ with Me_3N . From the light green solution, a pale green solid was isolated after removal of the volatile material. The infrared spectrum of the solid consisted of bands at $\bar{\nu}_{\text{max}}$ 3215 (CH str), 1470 and 1250 (CH_3 rock), 1050 (CH str), 980 (N-N str), 520 (UF_6^-) and 320 cm^{-1} (N-N bend). An attempt to record the Raman spectrum was not successful as the compound decomposed in the laser beam. The ^1H n.m.r. spectrum of the solid in CD_3CN consisted of two singlets (relative intensities, 2:3) at 2.15 and 1.95 ppm. No ^{205}Tl resonance was observed from the MeCN solution of the pale green solid indicating the absence of both Tl^{I} and Tl^{III} . The electronic spectrum of the solid in MeCN solution showed characteristic absorptions of the UF_6^- anion at $\bar{\nu}_{\text{max}}$ 7300, 7428, 7582 and 7940 cm^{-1} . From a combination of infrared, ^1H n.m.r. and electronic spectra, the product was formulated as $[\text{Me}_3\text{N-NMe}_2][\text{UF}_6]$. The microanalysis of the compound, $[\text{Me}_3\text{N-NMe}_2][\text{UF}_6]$, was not attempted because of its ready decomposition both in the solid state and in MeCN solution. A material distilled at 183 K from the reaction mixture of $[\text{Tl}^{\text{III}}(\text{NCMe})_5][\text{UF}_6]_3$ and Me_3N in MeCN solution, was identified as ethane by gas chromatography. The overall reaction of Tl^{III} salt with Me_3N in MeCN solution is summarized in equation 19.



4:2:5 Reactions of Trimethylphosphine with Solvated Cu^{I} and Cu^{II} Cations in MeCN.

The reaction of trimethylphosphine with $[\text{Cu}(\text{NCMe})_4][\text{PF}_6^-]$ in MeCN solution resulted in the formation of an off-white solid. The infrared spectrum of the solid indicated the presence of coordinated PMe_3 and the PF_6^- anion. Bands due to coordinated MeCN were not present. The species was characterized by spectroscopy and by microanalysis as $[\text{Cu}(\text{PMe}_3)_4][\text{PF}_6^-]$. The infrared spectrum of the complex, $[\text{Cu}(\text{PMe}_3)_4][\text{PF}_6^-]$, is listed in Table 2. The $^{31}\text{P}\{-^1\text{H}\}$ n.m.r. spectrum of the solid in CD_3CN consisted of two sets of overlapping 1:1:1:1 quartets due to the coupling of the ^{31}P with a ^{63}Cu or ^{65}Cu nucleus. A 1:6:15:20:15:6:1 septet was observed for the PF_6^- anion due to the coupling of ^{31}P nucleus with six equivalent fluorine nuclei. The ^{31}P chemical shifts observed are -41.5 and -144.9 ppm with coupling constants of $J_{^{63}\text{Cu-P}} = 795$, $J_{^{65}\text{Cu-P}} = 851$ and $J_{\text{P-F}} = 707$ Hz. In comparison the coupling constants in the complex, $[\text{Cu}\{\text{P}(\text{OMe})_3\}_4][\text{PF}_6^-]$, are $J_{^{63}\text{Cu-P}} = 1221$, $J_{^{65}\text{Cu-P}} = 1311$ and $J_{\text{P-F}} = 707$ Hz.²⁰¹

The $^{31}\text{P}\{-^1\text{H}\}$ n.m.r. spectrum of the species, $[\text{Cu}(\text{PMe}_3)_4][\text{PF}_6^-]$, is represented in Figure 3. The resonances due to the coordinated PMe_3 in the $^{31}\text{P}\{-^1\text{H}\}$ n.m.r. spectrum were broad due to some residual quadrupolar relaxation caused by a lowering of the symmetry from T_d . This lowering of the symmetry is resulted from the asymmetric vibration of the Cu-P bonds and the ligand exchange reactions at Cu^{I} . Lowering the temperature of the solution caused the resonances to become sharp as it resulted in reducing the exchange.

The complex, $[\text{Cu}(\text{NCMe})_5][\text{PF}_6^-]_2$, in MeCN solution when reacted with PMe_3 underwent a redox reaction forming a pink intermediate which decayed rapidly. An attempt to record the electronic spectrum of the intermediate at 243 K by conventional electronic spectroscopy

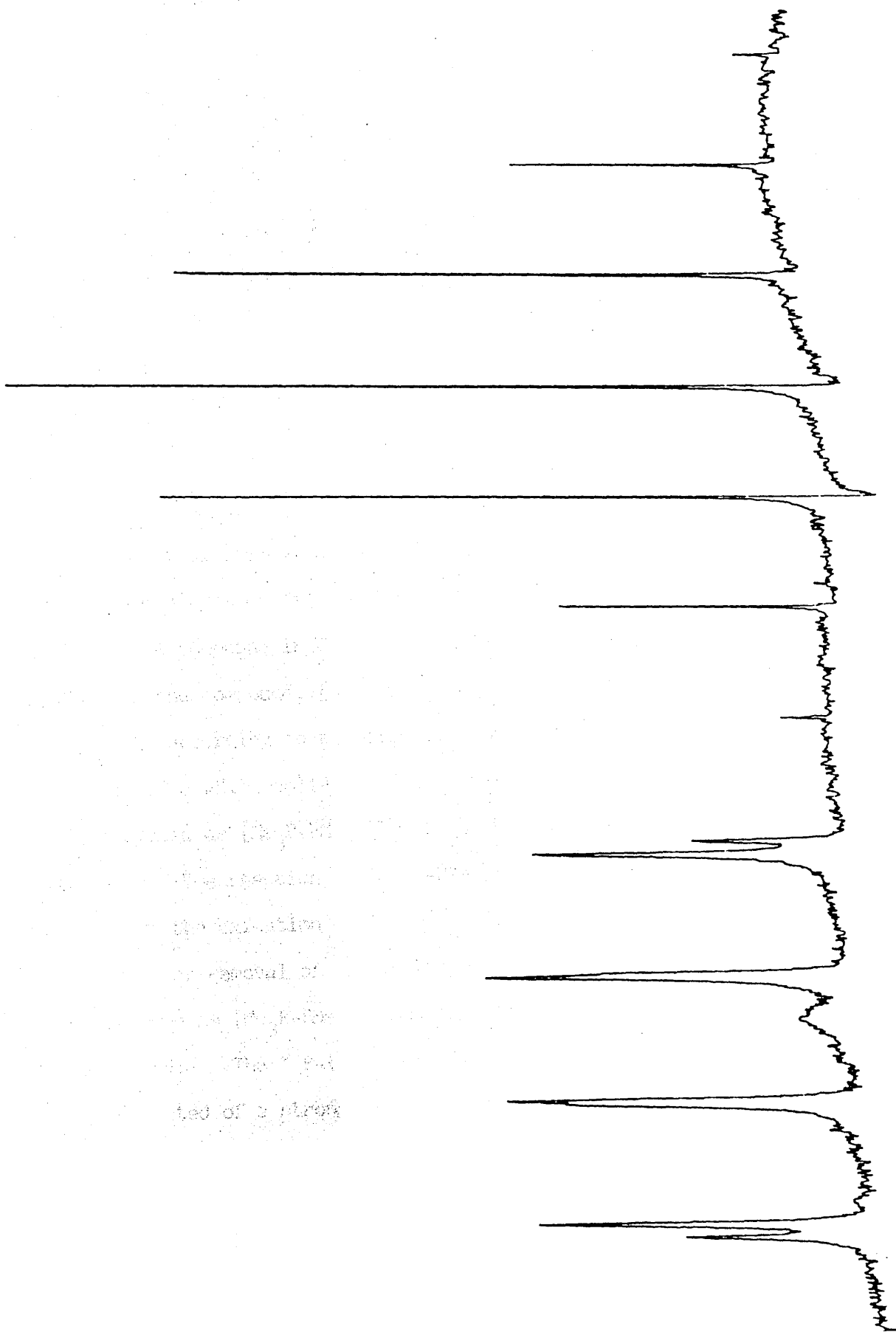
Table 2.

Infrared Spectrum of the Complex $[\text{Cu}(\text{PMe}_3)_4][\text{PF}_6^-]$

wavenumber (cm^{-1})	Assignment
2960 (m)	CH asym. str. (A_1)
2870 (m)	CH sym. str. (E)
1305 (s)	CH sym. bend (A_1)
1290 (s)	CH sym bend (E)
950 (v.s)	CH_3 rock (A_1)
880 (s)	CH_3 rock (E)
840 (v.s)	PF_6^- (ν_3)
726 (v.s)	PC asym. str. (E)
665 (m)	PC sym. str. (A_1)
560 (v.s)	PF_6^- (ν_4)

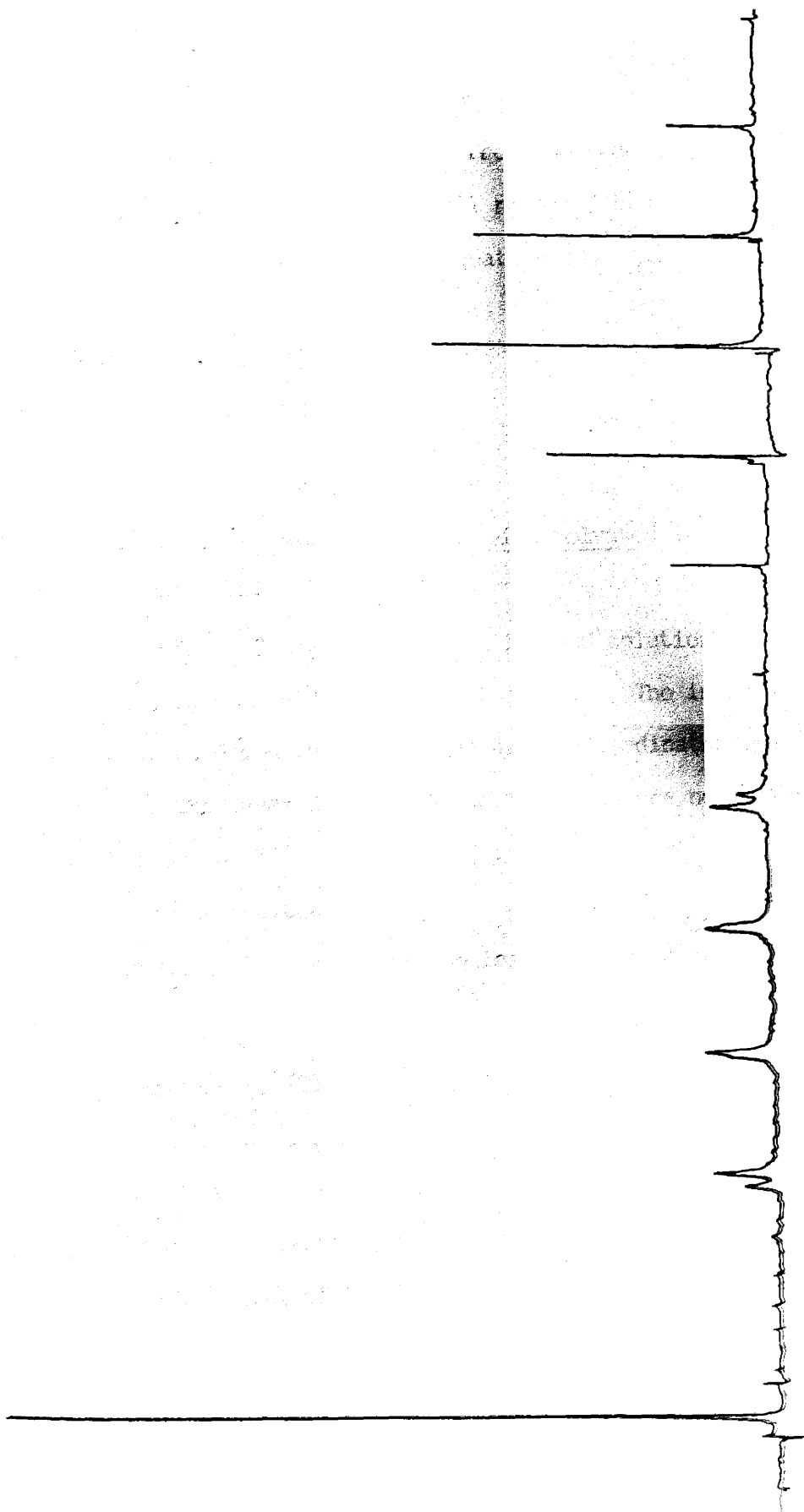
v.s. = very strong; s = strong; m = medium

Figure 3. $^{31}\text{P}\{-^1\text{H}\}$ N.M.R. Spectrum of the Salt, $[\text{Cu}(\text{PMe}_3)_4][\text{PF}_6]$

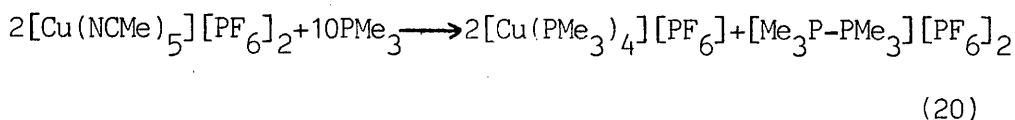


was unsuccessful. An off-white solid was isolated from the reaction mixture after removal of volatile material. The infrared spectrum of the solid indicated bands corresponding to the species, $[\text{Cu}(\text{PMe}_3)_4][\text{PF}_6]$. Additional bands were present in the regions of the spectrum where CH stretch, CH_3 rocking and P-C stretch were expected. A band at $\bar{\nu}_{\text{max}} 330 \text{ cm}^{-1}$ was assumed to be due to the P-P bending mode. The $^{31}\text{P}\{-^1\text{H}\}$ n.m.r. spectrum of the solid in CD_3CN was identical to that of the species, $[\text{Cu}(\text{PMe}_3)_4][\text{PF}_6]$ with the addition of a strong singlet with ^{31}P chemical shift, 27.5 ppm, (Figure 4). The species responsible for the strong singlet at 27.5 ppm in the $^{31}\text{P}\{-^1\text{H}\}$ n.m.r. spectrum was possibly the oxidised form of PMe_3 and was assumed to have a P-P bond. From a literature survey it has been found that cations containing P-P bonds have been known for some time. For example the cation, $[\text{Me}_3\text{P-PMe}_3]^{2+}$, has been obtained as the triiodide salt by reacting PMe_3 with iodine in MeCN.²⁰² The salt has been characterized by spectral and micro-analysis. The ^{31}P chemical shift of the compound in CD_3CN is 46.27 ppm.²⁰³ An attempt to synthesize the compound, $[\text{Me}_3\text{P-PMe}_3][\text{I}_3]_2$ by the reaction of PMe_3 with I_2 in MeCN, according to the literature method, resulted in the formation of a white solid. The solid was insoluble in MeCN and was formulated as $[\text{Me}_3\text{P-PMe}_3][\text{I}]_2$ from its micro-analysis and infrared spectrum. The reaction of $[\text{Me}_3\text{P-PMe}_3][\text{I}]_2$ with NOPF_6 in MeCN resulted in the oxidation of I^- ion to iodine. The off-white solid isolated after removal of the volatile material including I_2 , was characterized as $[\text{Me}_3\text{P-PMe}_3][\text{PF}_6]_2$ from its microanalysis and by spectroscopy. The $^{31}\text{P}\{-^1\text{H}\}$ n.m.r. spectrum of $[\text{Me}_3\text{P-PMe}_3][\text{PF}_6]_2$ in CD_3CN consisted of a strong singlet at 27.8 ppm with the addition of the peaks due to PF_6^- . The proton-coupled ^{31}P n.m.r. spectrum in CD_3CN consisted of a complex multiplet which could not be analysed. The infrared spectrum of the solid contained bands due to the $\text{Me}_3\text{P-}$

Figure 4. $^{31}\text{P}\{-^1\text{H}\}$ N.M.R. Spectrum of the Product Isolated from the Reaction of $[\text{Cu}(\text{NCMe})_5][\text{PF}_6]_2$ and PMe_3 .



group, the PF_6^- anion and a band at $\bar{\nu}_{\text{max}} 335 \text{ cm}^{-1}$ assumed to be due to the P-P bending mode. By analogy with the spectra of the compound, $[\text{Me}_3\text{P-PMe}_3][\text{PF}_6]_2$, the species formed from the oxidation of PMe_3 in the redox reaction of $[\text{Cu}(\text{NCMe})_5][\text{PF}_6]_2$ and PMe_3 , was formulated as $[\text{Me}_3\text{P-PMe}_3][\text{PF}_6]_2$. No evidence for ethane or any other small hydrocarbon was obtained from the reaction mixture of $[\text{Cu}(\text{NCMe})_6]^{2+}$ and PMe_3 . The overall reaction of $[\text{Cu}(\text{NCMe})_5][\text{PF}_6]_2$ with PMe_3 in MeCN is summarized in equation 20.

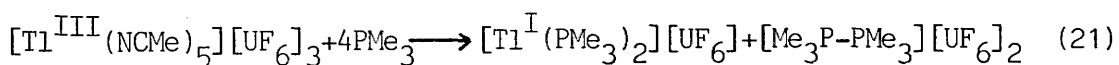


4:2:6 Reactions of Trimethylphosphine with Solvated Tl^{I} and Tl^{III} Cations in MeCN.

The reaction of Me_3P with $\text{Tl}^{\text{I}}\text{UF}_6$ in MeCN solution resulted in the formation of a blue green precipitate. The infrared spectrum of the precipitate consisted of bands due to coordinated PMe_3 and the UF_6^- anion. The bands due to coordinated MeCN were not observed. By analogy with the Tl^{I} salt obtained from the reaction of $\text{Tl}^{\text{I}}\text{UF}_6$ with Me_3N , the precipitate was formulated as $[\text{Tl}(\text{PMe}_3)_2][\text{UF}_6]$. The salt, $[\text{Tl}(\text{PMe}_3)_2][\text{UF}_6]$, was found to lose PMe_3 while pumped under vacuum.

The reaction of $[\text{Tl}^{\text{III}}(\text{NCMe})_5][\text{UF}_6]_3$ with PMe_3 in MeCN solution involved a redox step and resulted in the formation of a blue green precipitate and a light green solution. The infrared spectrum of the precipitate was identical to that of the product, $[\text{Tl}(\text{PMe}_3)_2][\text{UF}_6]$, formed in the reaction of $\text{Tl}^{\text{I}}\text{UF}_6$ with PMe_3 in MeCN. A pale green solid was isolated from the light green solution after removing the volatile material. The infrared spectrum of the solid indicated

the presence of bands due to the $\text{Me}_3\text{P-}$ group, the UF_6^- anion and a band at 328 cm^{-1} presumably due to the P-P bending mode. The Raman spectrum of the solid could not be recorded as the compound decomposed in the laser beam. The $^{31}\text{P-}\{^1\text{H}\}$ n.m.r. spectrum of the solid in CD_3CN consisted of a strong singlet at 65.0 ppm. This shifting of the ^{31}P resonance to the lower field with respect to the ^{31}P resonance in the species, $[\text{Me}_3\text{P-PMe}_3][\text{PF}_6]_2$, might be the effect of the paramagnetic anion, UF_6^- . The electronic spectrum of the pale green solid in MeCN solution consisted of the characteristic $f-f$ transitions of the UF_6^- anion. A ^{205}Tl n.m.r. study of the MeCN solution of the pale green solid did not show the presence of Tl^{I} or Tl^{III} . The pale green solid was thus formulated as $[\text{Me}_3\text{P-PMe}_3][\text{UF}_6]_2$ from a combination of infrared, electronic and $^{31}\text{P-}\{^1\text{H}\}$ n.m.r. spectra. The microanalysis of the compound was not attempted because of its ready decomposition both in the solid and solution state. No evidence was obtained for ethane or any other small hydrocarbon from the reaction mixture of $[\text{Tl}(\text{NCMe})_6]^{3+}$ and PMe_3 . The overall reaction of $[\text{Tl}^{\text{III}}(\text{NCMe})_5][\text{UF}_6]_3$ with PMe_3 in MeCN, is summarized in equation 21.



4:2:7 Reactions of Tetramethylthiourea with Solvated Cu^{I} and Cu^{II} Cations in MeCN.

The reaction of $[\text{Cu}(\text{NCMe})_4][\text{PF}_6]$ with tetramethylthiourea (tmtu) (concentration ratio, 1:4) in MeCN solution resulted in the formation of an off-white solid. The infrared spectrum of the solid indicated bands due to coordinated tmtu and the PF_6^- anion. Bands due to coordinated MeCN were absent. The ^1H n.m.r. spectrum of the solid in CD_3CN consisted of a strong sharp singlet at 3.2 ppm. The micro-

analysis of the compound was not attempted because of the difficulty in precipitating or crystallizing the complex from MeCN solution due to the non-volatile nature of the ligand, tmtu. A survey of the literature revealed that the complex, $[\text{Cu}(\text{tmtu})_3][\text{BF}_4]$, has been obtained by mixing aqueous solution of $\text{Cu}(\text{BF}_4)_2$ with tmtu at room temperature.²⁰⁴ The crystal structure of the compound has been determined by x-ray diffraction and consists of trigonal planar Cu^{I} monomers with some distortion arising from the steric interactions of the adjacent tmtu groups. The complex, $[\text{Cu}(\text{tmtu})_4][\text{ClO}_4]$, on the other hand, has been obtained by the reaction of $\text{Cu}(\text{ClO}_4)_2$ with tmtu in MeCN solution.²⁰⁵ By analogy with the Cu^{I} complexes, $[\text{Cu}(\text{tmtu})_4][\text{ClO}_4]$,²⁰⁵ $[\text{Cu}\{\text{P}(\text{OMe})_3\}_4][\text{PF}_6]$ ¹⁸⁹ and $[\text{Cu}(\text{PMe}_3)_4][\text{PF}_6]$, formed in acetonitrile solution, the salt obtained in the reaction of $[\text{Cu}(\text{NCMe})_4][\text{PF}_6]$ and tmtu in MeCN solution, was formulated as $[\text{Cu}(\text{tmtu})_4][\text{PF}_6]$.

The cation, $[\text{Cu}(\text{NCMe})_6]^{2+}$, in MeCN solution when reacted with tmtu underwent a redox reaction. A pink intermediate was formed initially which decayed rapidly forming a colourless solution. An off-white solid was isolated from this solution after removal of the volatile material. The infrared spectrum of the solid was identical to the complex, $[\text{Cu}(\text{tmtu})_4][\text{PF}_6]$, with the addition of a strong band at $\bar{\nu}_{\text{max}}$ 1625 and a medium band at 320 cm^{-1} . The ^1H n.m.r. spectrum of the solid in CD_3CN consisted of a broad singlet at 3.3 ppm. It has been reported in the literature that $\text{Cu}(\text{II})$ species, in reaction with substituted thioureas undergo redox reaction forming the $\text{Cu}(\text{I})$ complex and the oxidised ligand, as the final products. These reactions involve the formation of rose to purple coloured intermediates in both aqueous²⁰⁶ and non-aqueous solvents.²⁰⁵ The products formed in the reaction of Cu^{II} with tmtu in MeCN solution had been identified

as the Cu(I) salt and the species, $[(\text{Me}_2\text{N})_2\text{CS-SC}(\text{NMe}_2)_2]^{2+}$. The cation, $[(\text{Me}_2\text{N})_2\text{CS-SC}(\text{NMe}_2)_2]^{2+}$ has also been obtained as the salt, $[(\text{Me}_2\text{N})_2\text{CS-SC}(\text{NMe}_2)_2][\text{CF}_3\text{SO}_3]_2$, by the reaction of trifluoromethanesulphonic anhydride with tmtu in CH_2Cl_2 solution.²⁰⁷ The salt has been characterized by microanalysis and by infrared, ^1H and ^{19}F n.m.r. spectra. The infrared spectrum of the solid salt indicated a strong band at 1620 cm^{-1} assigned to the C=N stretching mode. The ^1H n.m.r. spectrum of the salt, $[(\text{Me}_2\text{N})_2\text{CS-SC}(\text{NMe}_2)_2][\text{CF}_3\text{SO}_3]_2$, in CD_3CN consisted of a singlet at 3.4 ppm. By analogy with the above described data, the species formed from the oxidation of tmtu in the redox reaction of $[\text{Cu}(\text{NCMe})_5][\text{PF}_6]_2$ and tmtu in MeCN solution, was formulated as $[(\text{Me}_2\text{N})_2\text{CS-SC}(\text{NMe}_2)_2][\text{PF}_6]_2$.

The electronic spectrum of the pink intermediate, presumably a Cu(II) tmtu complex was recorded at 243 K by conventional electronic spectroscopy using concentrations $[\text{Cu}^{\text{II}}] = 0.5 \times 10^{-2}\text{ mol dm}^{-3}$ and $[\text{tmtu}] = 2.5 \times 10^{-2}\text{ mol dm}^{-3}$. Two bands were observed at $\bar{\nu}_{\text{max}}$ 19600 cm^{-1} and 25000 cm^{-1} and were in good agreement with the spectrum of a similar species reported in the literature.²⁰⁵ In the reaction of Cu(II), with tmtu, in MeCN solution, the red intermediate has been characterized as a $\text{Cu}^{\text{II}}\text{-S}$ bonded species by an e.p.r study.

4:3 Discussion.

The reaction of $[\text{Cu}(\text{NCMe})_4]^+$ with Me_2S or Me_3N in acetonitrile solution does not result in the coordination of the ligand. This is presumably due to the high stability of the solvated cation. For an incoming ligand to react, it must have the potential to produce a more stable cation. The potential to stabilize a cation is a function of the relative σ -donor and π -acceptor ability of the ligand, the steric requirement and the relative hardness or softness of the

ligand. The ligand Me_3N is harder than MeCN and lacks π -acceptor ability hence is not ligated to Cu(I) which is a soft acid, although there are many examples of hard ligands bound to soft acids and vice versa. Dimethyl sulphide, on the other hand, is a soft base and forms 1:1 complexes with copper(I) halides in the absence of a solvent.²⁰⁸ Thus the reaction of Me_2S with $[\text{Cu}(\text{NCMe})_4]^+$ should be feasible but it evidently does not occur. It is, therefore, suggested that Me_2S and Me_3N are not able to compete with MeCN ligands towards Cu^{I} .

The cation, $[\text{Cu}(\text{NCMe})_4]^+$, in MeCN solution can undergo substitution reaction when reacted with PMe_3 or tmtu . Both these ligands possess a relatively better σ -donor and π -acceptor ability and are softer bases than MeCN . Thus they can compete easily with MeCN ligands and are coordinated to Cu^{I} . Complexes of tmtu with Cu^{I} have been reported in the literature and have been prepared by reacting $\text{Cu}(\text{BF}_4)_2$ and $\text{Cu}(\text{ClO}_4)_2$ with tmtu in water²⁰⁴ and in MeCN ²⁰⁵. In the former case the formulation $[\text{Cu}(\text{tmtu})_3][\text{BF}_4]$ has been made on the basis of x-ray study whereas in the latter case the composition, $[\text{Cu}(\text{tmtu})_4][\text{ClO}_4]$ has been proposed. Although the composition of the Cu^{I} - tmtu complex has not been determined in the present study, it is more likely to propose the formulation, $[\text{Cu}(\text{tmtu})_4]^+$, by analogy with the Cu^{I} complexes, $[\text{Cu}(\text{tmtu})_4]^+$,²⁰⁵ $[\text{Cu}\{\text{P}(\text{OMe})_3\}_4]^+$ ¹⁹⁹ and $[\text{Cu}(\text{PMe}_3)_4]^+$, identified in MeCN solution. It has been reported in the literature that PMe_3 forms tetrameric, $[\text{Me}_3\text{PCuCl}]_4$, dimeric, $[(\text{Me}_3\text{P})_2\text{CuCl}]_2$, and monomeric, $[(\text{Me}_3\text{P})_3\text{CuCl}]$, complexes with $\text{Cu}^{\text{I}}\text{Cl}$ in benzene.²⁰⁹ The formation of the polymeric complexes in benzene may be due to the poor solvating ability of the medium. Acetonitrile is a good coordinating solvent and thus favours the formation of monomeric complexes such as $[\text{Cu}(\text{PMe}_3)_4][\text{PF}_6]$. It has been shown

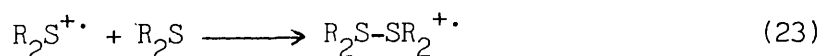
that PF_3 , which is an excellent π -acceptor and a poor σ -donor, is not able to coordinate to Cu^{I} in MeCN.²⁰¹ However, in liquid SO_2 , a much poorer solvent for Cu^{I} , PF_3 does react with Cu^{I} forming a 1:1 adduct, $[\text{CuPF}_3]^+$, which can be isolated as the AsF_6^- salt.²¹⁰ Trimethyl amine has been shown to form a complex with Cu^{II} in MeOH presumably in this solvent Cu^{II} is more stable than Cu^{I} .¹⁵⁷ This is in contrast to the redox reaction observed in the present study between Me_3N and Cu^{II} in MeCN solution. These reactions emphasize the importance of the medium in determining the identity of the species formed.

Thallium(I) hexafluorouranate in MeCN solution reacts with Me_3N or Me_3P forming insoluble salts. The low solubility of the Tl(I) salts in many solvents including water has been widely reported.⁶⁸ The infrared spectra of the insoluble Tl^{I} salts indicate the presence of coordinated ligands (Me_3N or Me_3P). The salts are assumed to have the composition, $[\text{Tl}^{\text{I}}\text{L}_2][\text{UF}_6]$, ($\text{L} = \text{Me}_3\text{N}$ or Me_3P) on the basis of the analysis of C, H and N. This formulation is consistent with the composition of the known Tl^{I} salts.^{122,211} Dimethyl sulphide, on the other hand, does not coordinate to Tl^{I} , whereas complexation should have been expected as Tl^{I} and Me_2S are respectively a soft acid and a soft base. The interactions between Tl^{I} and the organic ligands have been reported to be very weak.²¹² This is confirmed in the present study when the Tl^{I} salts, $[\text{Tl}^{\text{I}}\text{L}_2][\text{UF}_6]$, are found to lose the ligands on pumping under vacuum.

The species, $[\text{Cu}(\text{NCMe})_6]^{2+}$ and $[\text{Tl}(\text{NCMe})_6]^{3+}$, in MeCN solution undergo redox reactions when reacted with Me_3N , Me_2S , Me_3P and tmtu. This is consistent with the known oxidising abilities of the solvated Cu^{2+} or solvated Tl^{3+} cations in MeCN.^{46,84} The redox reactions involving solvated Cu^{2+} or solvated Tl^{3+} cations and the above mentioned ligands are apparently similar, the only significant difference being in the

nature of the cation derived from the oxidation of the ligand. In the redox reactions, solvated Cu^{2+} and solvated Tl^{3+} cations are reduced to the +1 oxidation state whereas the ligands are oxidised to the corresponding monomeric radical cations. The monomeric radical cations formed in the redox reactions involving Me_2S or Me_3N , presumably combine with a free ligand molecule forming the dimeric radical cation. In the redox reactions involving PMe_3 or tmtu, the monomeric radical cations formed are assumed to combine with another radical cation forming a dimeric dication.

Dimeric radical cations derived from simple aliphatic sulphides have been widely reported and characterized by e.p.r. spectroscopy. These radical cations have been generated by various methods, for example pulse radiolysis of air saturated aqueous alkyl sulphide solutions,²¹³ electron irradiation of the aqueous aliphatic sulphide solutions,²¹⁴ γ -irradiation of the alkyl sulphides at 77 K²¹⁵ and the electrochemical oxidation of the alkyl sulphides.²¹⁶ The dimeric radical cations are formed via the monomeric radical cations, $\text{R}_2\text{S}^{+\cdot}$ as represented in equations 22 and 23.



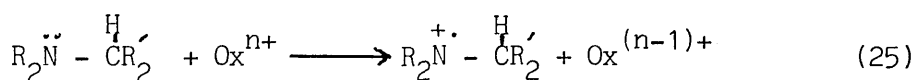
The transient optical absorption of the dimeric radical cation, $\text{Me}_2\text{S-SMe}_2^{+\cdot}$ in t.butyl alcohol has been measured, $\bar{\nu}_{\text{max}}$ 21500 cm^{-1} , over the concentration range 10^{-4} to 3×10^{-3} mol dm^{-3} . The resonance Raman spectrum of the transient dimeric radical cation, $\text{Me}_2\text{S-SMe}_2^{+\cdot}$, has been recorded by optical channel detection.²¹⁴ Vibrational bands at 276 and 139 cm^{-1} have been assigned to the S-S stretching mode and to the CSS deformation mode respectively. By analogy with the resonance Raman spectrum of the species, $\text{Me}_2\text{S-SMe}_2^{+\cdot}$, it seems reasonable to assign the

band observed in the infrared spectrum of the species, $[\text{Me}_2\text{S-SMe}][\text{X}]$, ($\text{X} = \text{BF}_4, \text{PF}_6$ and UF_6), at $\bar{\nu}_{\text{max}}$ 280-290 cm^{-1} to the S-S stretching mode. There is no evidence in the literature for the reaction (equation 24) presumably the studies have been carried out in aqueous



solution in which the breakdown of the radical cation, $\text{Me}_2\text{S-SMe}_2^{+\bullet}$ is thought to be much more complicated.

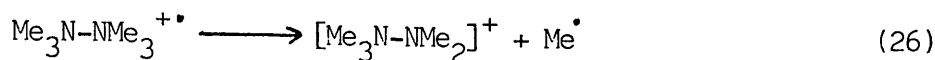
Non-aromatic aminium radicals, $\text{R}_3\text{N}^{+\bullet}$ have been observed as transient intermediates in a number of redox reactions.²¹⁸ The oxidants such as alkaline ferricyanide, iron(III) complexed with substituted phenanthroline, octacyanomolybdate and chlorine dioxide, have been shown to generate aminium radicals by oxidising the corresponding amines. The general pathway proposed for the amine oxidation is represented in equation 25.



The aminium radicals then undergo proton abstraction by one of the species involved in the reaction forming the cation, $\text{R}_2\overset{+}{\text{N}}=\text{CR}'_2$. This species gives rise to a strong absorption at $\bar{\nu}_{\text{max}}$ 1690 cm^{-1} due to the C=N stretching mode. Because of the absence of proton abstracting species in the present systems, no such cations are formed in the redox reactions involving Cu^{2+} or Tl^{3+} and Me_3N in MeCN solution. Instead it is assumed that the monomeric radical cation formed in the redox reaction combines with free Me_3N producing the dimeric radical cation, $\text{Me}_3\text{N-NMe}_3^{+\bullet}$.

The breakdown of the dimeric radical cations, $\text{Me}_2\text{S-SMe}_2^{+\bullet}$ and $\text{Me}_3\text{N-NMe}_3^{+\bullet}$, is speculative but may be of the form (equation 24 and

equation 26).



The methyl radicals dimerize forming ethane which has been identified by gas chromatography.



The cations, $[\text{Me}_2\text{S-SMe}]^+$ and $[\text{Me}_3\text{N-NMe}_2]^+$, have been identified by infrared, ^1H and ^{13}C n.m.r. spectroscopy. The ^1H chemical shifts of the various species are listed in Table 3 and where comparisons can be made the values are in good agreement with the values reported in the literature.

The reaction between $[\text{Cu}(\text{NCMe})_6]^{2+}$ and Me_2S or Me_3N , in MeCN solution, involves the formation of a green intermediate presumably a mixture of cations, $[\text{CuL}_x(\text{NCMe})_{6-x}]^{2+}$ ($\text{L} = \text{Me}_2\text{S}$ or Me_3N) related by appropriate equilibrium constants. The decay of the intermediate can be followed by conventional electronic spectroscopy using $[\text{Cu}^{\text{II}}]:[\text{L}] < 1:5$. The electronic spectra consist of two bands which are listed in Table 4. The electronic spectra of the Cu^{2+} species, under normal conditions, contain only one d-d band (Table 4). In aqueous solution, the successive formation constants for Cu(II) ion with NH_3 as a ligand are $K_1 = 12000$, $K_2 = 3000$, $K_3 = 800$, $K_4 = 120$, $K_5 = 0.3$ and $K_6 = 0.0 \text{ dm}^3 \text{ mol}^{-1}$.²¹⁹ There is an increase in the $\bar{\nu}_{\text{max}}$ from 11000 cm^{-1} , ($[\text{Cu}(\text{H}_2\text{O})_6]^{2+}$) to 16800 cm^{-1} , ($[\text{Cu}(\text{NH}_3)_4(\text{H}_2\text{O})_2]^{2+}$) as the concentration of NH_3 is increased. Similar results have been obtained while recording the electronic spectra of the $[\text{Cu}(\text{NCMe})_6]^{2+}$ and pyridine mixtures in MeCN solution.²²⁰ Therefore, the two bands observed in the redox reactions of the

Table 3.

^1H Chemical Shifts of the Species Derived from the Oxidation of Me_2S and Me_3N with Solvated Cu^{2+} or Solvated Tl^{3+} Cations in MeCN.

Species.	Chemical Shifts(ppm)		Relative Intensities	Reference
	Signal 1	Signal 2		
$[\text{Me}_2\text{S-SMe}][\text{BF}_4]$	3.20	2.80	2:1	197
$[\text{Me}_2\text{S-SMe}][\text{PF}_6]$	2.95	2.35	2:1	this work
$[\text{Me}_2\text{S-SMe}][\text{UF}_6]$	3.10	2.80	1:2	" "
$[\text{Me}_3\text{N-NMe}_2][\text{PF}_6]$	2.45	1.90	3:2	" "
$[\text{Me}_3\text{N-NMe}_2][\text{UF}_6]$	2.25	1.95	2:3	" "
$[\text{Me}_2\text{S-SMe}][\text{BF}_4]$ + Me_2S	2.80	2.65	1:4	197
$[\text{Me}_2\text{S-SMe}][\text{UF}_6]$ + Me_2S	2.70	2.40	1:4	this work

Table 4.

Electronic Spectra of the Cu^{II} Species in MeCN Solution.

Cation	ν_{\max} (cm ⁻¹)	Reference
[Cu(NCMe) ₆] ²⁺	13500 (28) <u>a</u>	220
[Cu(NH ₃) _x (NCMe) _{6-x}] ²⁺ <u>b</u>	17000 (65)	220
[Cu(Py) _x (NCMe) _{6-x}] ²⁺ <u>c</u>	17200 (75)	220
[Cu(Me ₃ N) _x (MeOH) _{6-x}] ²⁺ <u>d</u>	13900	157
[Cu(Me ₂ S) _x (NCMe) _{6-x}] ²⁺	14300 and 24300	this work
[Cu(Me ₃ N) _x (NCMe) _{6-x}] ²⁺	14400 and 24400	this work
[Cu(tmtu) _x (NCMe) _{6-x}] ²⁺	19600 and 25000	this work
[Cu{P(OMe) ₃ } _x (NCMe) _{6-x}] ²⁺	<u>e</u> and 29000	84

a) Molar extinction coefficients (dm³mol⁻¹cm⁻¹)

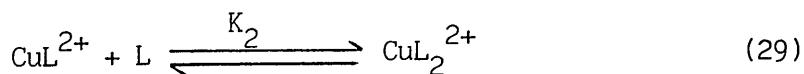
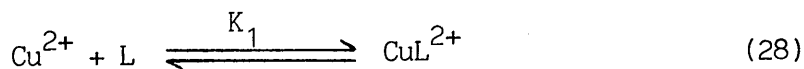
b) [Cu^{II}]:[NH₃] = 1:4

c) [Cu^{II}]:[Py] = 1:4

d) in MeOH, [Cu^{II}]:[Me₃N] = 1:2

e) The expected region has not been studied.

$[\text{Cu}(\text{NCMe})_6]^{2+}$ cation with Me_2S or Me_3N in MeCN solution, are either the d-d bands or one of them is a d-d band and the other is due to the intermediate dimeric radical cation. The latter possibility is ruled out for two reasons. Firstly the absorption region of the dimeric radical cation, $[\text{Me}_2\text{S-SMe}_2]^{+\bullet}$, $\bar{\nu}_{\text{max}}$ 21500 cm^{-1} ,²¹⁷ is significantly different from either of the two absorption regions observed in the present systems. Secondly no such absorptions have been observed in the redox reactions involving Tl^{III} and Me_2S or Me_3N . It is, therefore, assumed that the two bands observed in the above described systems are d-d bands. The low energy band presumably arises from mixtures of Cu^{II} species, $[\text{CuL}_x(\text{NCMe})_{6-x}]^{2+}$ ($x = 0$ to 2) in which MeCN is the predominant ligand and the high energy band from the more highly substituted species, $[\text{CuL}_x(\text{NCMe})_{6-x}]^{2+}$ for example with $x = 3$ to 5 . These highly substituted species are assumed to be redox active. The above hypothesis is derived from the following considerations. Complex formation between Cu^{II} and Me_3N has been studied spectrophotometrically in methanol.¹⁵⁷ The successive formation constants for the mono and disubstituted species are $K_1 = 750$ and $K_2 = 100 \text{ dm}^3 \text{ mol}^{-1}$. The formation of mono and disubstituted species in the reaction of $[\text{Cu}(\text{NCMe})_6]^{2+}$, (Cu^{2+}), and Me_3N or Me_2S , (L), in MeCN solution is represented by the equilibria (equations 28 and 29)



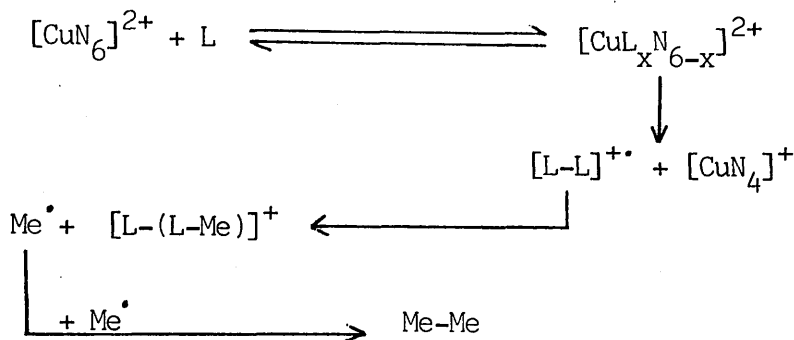
The stepwise formation constants, K_1 and K_2 are given by the expressions,

$$K_1 = \frac{[\text{CuL}]}{[\text{Cu}][\text{L}]} \quad \text{and} \quad K_2 = \frac{[\text{CuL}_2]}{[\text{CuL}][\text{L}]}$$

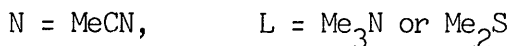
By assuming that the values of K_1 and K_2 are the same as have been determined for the Cu^{II} and Me_3N system in MeOH , the concentrations of the various species present in the equilibria solution (equations 28 and 29) can be calculated. As an example, for the initial concentrations of Cu^{II} and L equal to 5×10^{-4} and $20 \times 10^{-4} \text{ mol dm}^{-3}$ respectively and a concentration ratio, $[\text{Cu}^{\text{II}}]:[\text{L}] = 1:4$, the calculated concentrations of $[\text{CuL}_2]$, $[\text{CuL}]$, $[\text{L}]$ and $[\text{Cu}]$ in solution are $[\text{CuL}_2] = 3.9 \times 10^{-5}$, $[\text{CuL}] = 28 \times 10^{-5}$, $[\text{Cu}] = 1.8 \times 10^{-4}$ and $[\text{L}] = 14 \times 10^{-4}$. These calculated concentration values indicate that in these equilibria, a significant amount of unreacted Cu^{II} is present and that the amount of CuL_2^{2+} formed is only one tenth of the CuL^{2+} species. The extinction coefficient, ϵ , value for the species, CuL^{2+} is assumed to be similar as that for $[\text{Cu}(\text{NCMe})_6]^{2+}$ by analogy with the Cu^{II} -pyridine system in MeCN .²²⁰ It is, therefore, likely that the low energy band in the electronic spectra of the $[\text{Cu}(\text{NCMe})_6]^{2+}$ and Me_3N system arises mainly from the species, $[\text{CuL}_x(\text{NCMe})_{6-x}]^{2+}$, $x = 0-1$. The high energy band is assigned to the species, $[\text{CuL}_x(\text{NCMe})_{6-x}]^{2+}$, $x = 3-5$. These species will be present only in small amounts and the electronic transitions are observed because of intensity borrowing from the charge transfer transition of the complexes. The low energy band decays much more rapidly than the high energy band presumably due to the faster rate of substitution at Cu^{II} as compared with the decay of the redox active species responsible for the observation of the high energy band.

The electron transfer reaction in the $[\text{Cu}(\text{NCMe})_6]^{2+}$ and Me_2S or Me_3N redox systems does not involve the coordination of the ligands to Cu^{I} formed. This increases the chances of the

availability of free ligands to react with the monomeric radical cations forming the dimeric radical cations, $[L-L]^{\bullet+}$. The redox reactions involving $[\text{Cu}(\text{NCMe})_6]^{2+}$ and Me_3N or Me_2S , (L), in MeCN solution may be represented by the generalized Scheme 1.

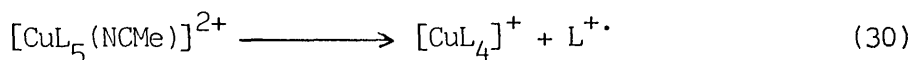


(Scheme 1.)



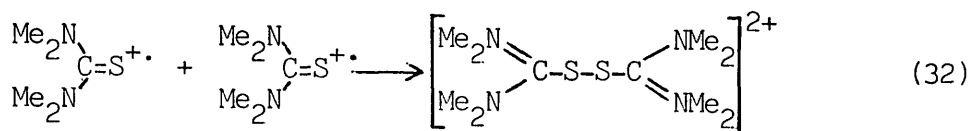
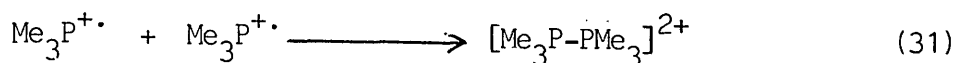
The redox reaction between $[\text{Tl}(\text{NCMe})_6]^{3+}$ and Me_2S , in MeCN solution, presumably involves the formation of the Tl^{2+} intermediate as is observed by a change in colour from green to yellow. The $\text{Tl}(\text{II})$ intermediate would be expected to decay rapidly forming $\text{Tl}(\text{I})$. The Tl^{I} formed does not have coordinated Me_2S , whereas in the redox reactions involving $[\text{Tl}(\text{NCMe})_6]^{3+}$ and Me_3N or Me_3P , the Tl^{I} formed contains coordinated ligands. Thallium(III) has been found to oxidise a number of organic ligands in acidic solutions, for example in aqueous HClO_4 solution, Tl^{III} reacts with glycolic or glyoxylic acid (ga) forming the Tl^{I} complex, $[\text{Tl}(\text{ga})_2]^+$.²²¹ The products of oxidation depend on the initial concentration ratio of the reactants, for example in a 1:1 mole ratio reaction, the products are HCHO and CO_2 .

The reactions between $[\text{Cu}(\text{NCMe})_6]^{2+}$ and PMe_3 or tmtu (L) in MeCN solution, involve the formation of a pink intermediate, presumably the mixed ligand cations, $[\text{CuL}_x(\text{NCMe})_{6-x}]^{2+}$. The electronic spectrum of the intermediate, $[\text{Cu}(\text{tmtu})_x(\text{NCMe})_{6-x}]^{2+}$, is recorded at 253 K by conventional electronic spectroscopy and consists of two bands listed in Table 3. An attempt to record the electronic spectrum of the species, $[\text{Cu}(\text{PMe}_3)_x(\text{NCMe})_{6-x}]^{2+}$ by conventional electronic spectroscopy, even at 253 K, was unsuccessful. By analogy with the $\text{Cu}^{\text{II}}-\text{NMe}_3$ redox system, the low energy band is assigned to the species, $[\text{CuL}_x(\text{NCMe})_{6-x}]^{2+}$, ($x = 0-1$) whereas the high energy band is due to the redox active species, $[\text{CuL}_x(\text{NCMe})_{6-x}]^{2+}$ ($x = 3-5$). By analogy with the $\text{Cu}^{\text{II}}-\text{P}(\text{OMe})_3$ system,⁸⁴ the substitution occurs rapidly until all the Cu^{II} is present as $[\text{CuL}_4(\text{NCMe})_2]^{2+}$. At this stage the substitution of another ligand molecule at the copper centre to form $[\text{CuL}_5(\text{NCMe})]^{2+}$, makes the Cu^{II} ion a strong oxidising agent. It oxidises one of the coordinated ligands to the radical cation, $\text{L}^{+\cdot}$, and itself is reduced to Cu^{I} .



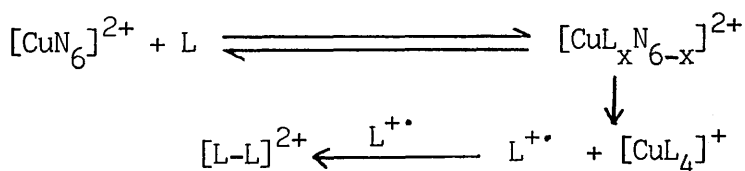
The monomeric radical cation of PMe_3 is known and has been generated by the γ -irradiation of dilute solution of PMe_3 in CFCl_3 at 77 K.²²² There is no evidence in the literature for the formation of the dimeric dication, $[\text{Me}_3\text{P}-\text{PMe}_3]^{2+}$ from the monomeric radical cation, $\text{PMe}_3^{+\cdot}$. The monomeric radical cation formed in the $\text{Cu}^{\text{II}}-\text{PMe}_3$ or tmtu redox reactions, may combine with another radical cation forming the dication or with the free ligand producing dimeric radical cation. The electron transfer reactions (equation 30) involve the coordination of the ligands, thus reducing the chances of the availability of free ligands to combine with the radical cation, $\text{L}^{+\cdot}$.

It is, therefore, assumed that the radical cation combines with another radical cation forming the dimeric dication.



Both these cations are known in the form of stable salts and have been characterized by microanalysis and spectral analysis.^{203,207} The spectral data obtained for these cations in the present work, are in good agreement with those reported previously.

The characterization of the cation, $[\text{Me}_3\text{P-PMe}_3]^{2+}$, in the present work and in that reported by Y.P. Makovetaki and co-workers,²⁰³ contradicts the suggestion made by D. Schomburg *et al.*,²²³ that the quaternization of the two directly bonded phosphorus atoms can not be achieved until the two phosphorus atoms are bridged by bulky groups. The redox reactions involving $[\text{Cu}(\text{NCMe})_6]^{2+}$ and PMe_3 or tmtu (L) in MeCN solution may be represented by scheme 2.



(Scheme 2)

N = MeCN; L = Me_3P or tmtu

4:4 Conclusions.

Solvated Cu(II) and solvated Tl(III) cations are very good

oxidising agents in MeCN as is indicated by the redox reactions of these cations with ligands such as Me_2S , Me_3N , Me_3P and tmtu. The redox reactions involving $[\text{Cu}(\text{NCMe})_6]^{2+}$ or $[\text{Tl}(\text{NCMe})_6]^{3+}$ and the ligands, Me_2S , Me_3N , Me_3P and tmtu are apparently similar. The only difference is in the nature of the cation derived from the oxidised form of the ligand. The products formed in these redox reactions are the metal cations in the +1 oxidation state and the monomeric radical cations of the ligands. In case of $\text{Cu}^{\text{II}}-\text{Me}_3\text{N}$ or Me_2S redox systems, the monomeric radical cations prefer to combine with a free ligand molecule whereas the reaction of the monomeric radical cations with the radical cations is preferred in the $\text{Cu}^{\text{II}}-\text{PMe}_3$ or tmtu systems. The reaction of $[\text{Cu}(\text{NCMe})_6]^{2+}$ with Me_2S or Me_3N , in MeCN solution involves the formation of a green intermediate whereas a pink intermediate is formed when $[\text{Cu}(\text{NCMe})_6]^{2+}$ is reacted with PMe_3 or tmtu. The redox reactions involving $[\text{Cu}(\text{NCMe})_6]^{2+}$ and Me_2S or Me_3N are slow as compared with the $\text{Cu}^{\text{II}}-\text{PMe}_3$ or tmtu systems. If the electron transfer reaction is the rate determining step the energy barrier for reduction of Cu^{II} to Cu^{I} is lower for $\text{Cu}^{\text{II}}-\text{PMe}_3$ or tmtu intermediates than it is for $\text{Cu}^{\text{II}}-\text{Me}_2\text{S}$ or Me_3N intermediates. The majority of these Cu^{II} species are strongly oxidising in MeCN, presumably due to the high stability of the corresponding tetrahedral $[\text{Cu}(\text{NCMe})_4]^+$, $[\text{Cu}(\text{PMe}_3)_4]^+$ and $[\text{Cu}(\text{tmtu})_4]^+$ complexes.

4:5 Experimental.

4:5:1 Preparation of Solvated Copper(II) and Copper(I) Hexafluorophosphates.¹⁸³

A mixture of CuF_2 (2.4mmol) and PF_5 (1.5mmol) in MeCN (5ml) was shaken mechanically for a period of about 6 hours at room temperature. The clear blue solution was decanted into the empty limb of the

reaction vessel from which a blue solid, pentakis(acetonitrile) copper(II) hexafluorophosphate, was isolated after removal of the volatile material. The infrared spectrum of the blue solid indicated the presence of coordinated MeCN $\bar{\nu}_{\max}$ 2330 (CN comb), 2350 (C≡N str.), 1033 (CH₃ rock), 950 cm⁻¹ (C-C str) and the PF₆⁻ anion $\bar{\nu}_{\max}$ 850, 810 (ν₃) and 560 cm⁻¹ (ν₄).

A solution of [Cu(NCMe)₅][PF₆]₂ in acetonitrile solution was reacted with Cu metal, and the mixture was shaken for about 4 hours. A white solid, tetrakis(acetonitrile) copper(I) hexafluorophosphate, was isolated from the resulting colourless solution after removal of the volatile material. The infrared spectrum of the white solid indicated the presence of coordinated MeCN, $\bar{\nu}_{\max}$ 2290 (CN comb), 2265 (C≡N str) and 1030 cm⁻¹ (CH₃ rock), and the PF₆⁻ anion, $\bar{\nu}_{\max}$ 835 (ν₃) and 556 cm⁻¹ (ν₄).

The electronic spectrum of Cu(II) hexafluorophosphate, in MeCN solution, consisted of a broad band at $\bar{\nu}_{\max}$ 13400 cm⁻¹ (ε = 24 dm³ mol⁻¹ cm⁻¹) with a pronounced shoulder at 10600 cm⁻¹ characteristic of the Cu(II) ion in a distorted octahedral environment.

4:5:2 Reactions of Solvated Copper(I) in MeCN Solution

(i) with dimethylsulphide or trimethylamine.

[Cu(NCMe)₄][PF₆], (0.5mmol) Me₂S or Me₃N (3mmol) and MeCN (5ml) were shaken for a period of about 12 hours at room temperature. There was no visible evidence for the reaction. A white solid was isolated from the resulting solution when the volatile material was removed. The infrared spectrum of the white solid suggested the product to be [Cu(NCMe)₄][PF₆], with bands at $\bar{\nu}_{\max}$ 2286 (CN comb), 2265 (C≡N str), 1033 (CH₃ rock), 840 (ν₃PF₆⁻) and 560 cm⁻¹ (ν₄PF₆⁻). There was no evidence for the presence of coordinated Me₂S or Me₃N.

(ii) with trimethylphosphine.

The salt, $[\text{Cu}(\text{NCMe})_4][\text{PF}_6]$ (0.5mmol) was dissolved in MeCN (5ml) and PMe_3 (2.5mmol) was distilled at 77 K. On warming to room temperature, a colourless solution was formed. An off-white solid was isolated from this solution after removal of the volatile material. This solid was identified by spectroscopy and microanalysis as tetrakis(trimethylphosphine)copper(I)hexafluorophosphate. Found: C, 28.1; H, 6.9; Cu, 12.6; F, 22.1 and P, 30.0%. $\text{C}_{12}\text{H}_{36}\text{CuF}_6\text{P}_5$ requires: C, 28.1; H, 7.0; Cu, 12.5; F, 22.2 and P, 30.2%. The solid state infrared spectrum is listed in Table 2. The $^{31}\text{P}\{-^1\text{H}\}$ n.m.r. spectrum of the solid in CD_3CN solution is illustrated in Figure 3. The ^{31}P chemical shifts observed were -41.5 and -144.9 ppm with coupling constants of $J_{^{63}\text{Cu-P}} = 795$, $J_{^{65}\text{Cu-P}} = 851$ and $J_{\text{P-F}} = 707$ Hz.

(iii) with tetramethylthiourea.

The solution of tmtu (2.0mmol) in MeCN (5ml) was mixed with the salt, $[\text{Cu}(\text{NCMe})_4][\text{PF}_6]$ (0.5mmol). The resulting solution was shaken for about 15 minutes and an off-white solid was obtained after removing the volatile material. The infrared spectrum of the solid product consisted of bands due to coordinated tmtu¹⁷⁵ and the PF_6^- anion, and listed in Table 5. Bands due to coordinated MeCN were absent. The ^1H n.m.r. spectrum of the solid in CD_3CN consisted of a sharp singlet at 3.2 ppm. By analogy with the known Cu(I) complexes with tmtu, $\text{P}(\text{OMe})_3$ and PMe_3 formed in MeCN, the solid was suggested to be tetrakis (tetramethylthiourea) copper(I) hexafluorophosphate. Microanalysis of the complex was not attempted because of the difficulty in obtaining the complex free from the unreacted ligand.

4:5:3 Preparation of Dimethylthiomethylsulphonium tetrafluoroborate.¹⁹⁷

Trimethyloxonium tetrafluoroborate (0.2mmol) was loaded in a

Table 5.

Infrared Spectrum of the Complex $[\text{Cu}(\text{tmtu})_4][\text{PF}_6^-]$

Wavenumber (cm^{-1})	Assignment	Corresponding band of free ligand(cm^{-1}) 175
2930	CH asym str.	2924
1545	NCN antisym str	1495
1468	CH_3 asym.bend	1450
1390	CH_3 sym.bend	1360
1310	$\text{H}_3\text{C-N}$ sym.str	1275
1268	NCN sym.str	1250
1155	CS str	1140
1115	CH_3 rock	1105
1095	CH_3 rock	1060
880	CN torsion	885
840	PF_6^-	ν_3
660	CS str.	637
560	PF_6^-	ν_4
480	CH_3NC asym.def.	445

reaction vessel and dissolved in MeCN(5ml) added by vacuum distillation. Methyl disulphide(0.6mmol) was distilled in at 77 K. The reaction mixture was warmed to room temperature and shaken for about 15 minutes. An off-white solid was isolated from the solution after the removal of volatile material. The infrared spectrum of the solid is listed in Table 1. The ^1H n.m.r. spectrum of the solid in CD_3CN contained two sharp singlets at 3.2 and 2.86 ppm with a relative intensity of 2:1 (Figure 1). The ^1H n.m.r. spectrum of a 1:1 mixture of the solid and Me_2S in CD_3CN consisted of two singlets at 2.8 and 2.60 ppm with a relative intensity of 1:4. The spectra were in good agreement with the reported data. Therefore, the compound was identified as dimethylthiomethylsulphonium tetrafluoroborate, $[\text{Me}_2\text{S-SMe}][\text{BF}_4]$.

4:5:4 Preparation of Hexamethyl diphosphonium hexafluorophosphate.

A solution of iodine(0.2mmol) in MeCN(5ml) was prepared in vacuo and PMe_3 (0.6mmol) was added to the frozen solution. On warming the mixture to room temperature, a white precipitate was formed, which was isolated by decanting the liquid phase into the empty limb and drying the precipitate under vacuum. The infrared spectrum of the solid product consisted of bands at $\bar{\nu}_{\text{max}}$ 1308 (CH bend), 975 and 945 (CH_3 rock), 775 and 650 (P-C str), and a band at 325 cm^{-1} possibly due to P-P bending mode. The compound was characterized by micro-analysis and infrared spectroscopy as hexamethyl diphosphonium bis iodide. Found: C, 17.4; H, 4.5; I, 62.9 and P, 15.3%.

$\text{C}_6\text{H}_{18}\text{I}_2\text{P}_2$ requires: C, 17.6; H, 4.4; I, 62.6 and P, 15.4%

The reaction of a solution of NOPF_6 (0.2mmol) in MeCN with the salt, $[\text{Me}_3\text{P-PMe}_3][\text{I}]_2$, resulted in the formation of a brown solution and the evolution of a colourless gas. An off-white solid was

isolated from the brown solution after removal of the volatile material. The infrared spectrum of the solid product contained bands at $\bar{\nu}_{\max}$ 1310 (CH bend), 975 and 945 (CH_3 rock), 775 and 650 (P-C str) and 325 cm^{-1} (P-P bend) and the PF_6^- bands at $\bar{\nu}_{\max}$ 840 and 560 cm^{-1} . The $^{31}\text{P}\{-^1\text{H}\}$ n.m.r.

spectrum of the solid in CD_3CN consisted of a sharp singlet at 27.8 ppm. Thus the compound was characterized as hexamethyl diphosphonium hexafluorophosphate from its microanalysis, infrared and $^{31}\text{P}\{-^1\text{H}\}$ n.m.r. spectra. Found: C, 16.1; H, 4.3 and P, 27.9%. $\text{C}_6\text{H}_{18}\text{F}_{12}\text{P}_4$ requires C, 16.3; H, 4.1; and P, 28.0%.

4:5:5 Reactions of Solvated Copper(II) in Acetonitrile Solution.

(i) with dimethyl sulphide or trimethyl amine.

The compound, $[\text{Cu}(\text{NCMe})_5][\text{PF}_6]_2$ (0.3mmol) was dissolved in MeCN and Me_2S or Me_3N (3.0mmol) was distilled in at 77 K. On warming a deep green colour developed as the Me_2S or Me_3N melted and flowed onto the frozen solution. The colour decayed slowly and disappeared on shaking. The final solution was colourless. The volatile product distilled from the reaction mixture at 183 K was identified as ethane by using the technique of gas chromatography. The removal of the volatile material from the reaction mixture left a white solid. This was shown to be a mixture of $[\text{Cu}(\text{NCMe})_4][\text{PF}_6]$ and $[\text{Me}_2\text{S-SMe}][\text{PF}_6]$ or $[\text{Me}_3\text{N-NMe}_2][\text{PF}_6]$, as indicated by the infrared and ^1H n.m.r. spectra.

Conventional electronic spectroscopic studies. The reaction between $[\text{Cu}(\text{NCMe})_5][\text{PF}_6]$ and Me_2S or Me_3N in MeCN solution was studied by conventional electronic spectroscopy. The concentration of Cu(II) was maintained at $5.0 \times 10^{-4} \text{ mol dm}^{-3}$ and the concentrations of the ligand (Me_2S or Me_3N) were varied between 5.0×10^{-4} and $5.0 \times 10^{-3} \text{ mol dm}^{-3}$. The solutions of Cu(II) were

loaded in reaction vessels containing Spectrosil cells along with the frangible ampoule in which the appropriate concentration of the ligand was sealed. The electronic spectra of these solutions were recorded in the range, 12500 to 33350 cm^{-1} , at 298 K. The vessel was kept in a thermostatted holder at 298 K while recording the spectra.

(ii) with trimethyl phosphine.

The copper(II) salt, $[\text{Cu}(\text{NCMe})_5][\text{PF}_6]_2$ (0.3mmol) was dissolved in MeCN(5ml) and PMe_3 (3.0mmol) was added by vacuum distillation. On warming to room temperature, it was observed that a pink colour developed as the PMe_3 melted and mixed with the solution. The colour decayed rapidly even at temperatures below 230 K, forming a colourless solution. An off-white solid was isolated from this solution after removal of the volatile material. The solid was shown to be predominantly $[\text{Cu}(\text{PMe}_3)_4][\text{PF}_6]$, by comparison of the infra-red and the n.m.r. spectra of the solid with those of a sample of the compound characterized from the reaction of $[\text{Cu}(\text{NCMe})_4][\text{PF}_6]$ with trimethyl phosphine. The hexamethyl diphosphonium cation, $[\text{Me}_3\text{P}-\text{PMe}_3]^{2+}$, was also identified among the solid products, by $^{31}\text{P}-\{^1\text{H}\}$ n.m.r. spectroscopy.

(iii) with tetramethyl thiourea

The compound, $[\text{Cu}(\text{NCMe})_5][\text{PF}_6]_2$ (0.3mmol) was loaded in one limb of a reaction vessel and tmtu(1.5mmol) into the other. Acetonitrile (5ml) was distilled onto tmtu and the resulting solution was mixed with $[\text{Cu}(\text{NCMe})_5][\text{PF}_6]_2$ at 233 K, when a pink colour solution was formed. The colour of the solution decayed rapidly as the temperature was raised. The final solution was colourless from which an off-white solid was isolated after removing the volatile material. The solid was identified as a mixture of the Cu(I) salt, $[\text{Cu}(\text{tmtu})_4][\text{PF}_6]$ and the dication disulphide salt, $[(\text{Me}_2\text{N})_2\text{CS}-\text{SC}(\text{NMe}_2)_2][\text{PF}_6]_2$

by infrared and ^1H n.m.r. spectroscopy.

The electronic spectrum of the Cu(II)-tmtu intermediate was recorded at 243 K using concentrations, $\text{Cu}^{\text{II}} = 0.5 \times 10^{-2} \text{ mol dm}^{-3}$ and $\text{tmtu} = 2.5 \times 10^{-2} \text{ mol dm}^{-3}$. The Cu(II) solution was loaded in a Spectrosil cell fitted with a septum cap. The tmtu solution was injected through the septum cap by keeping the solution at 233 K. To record the spectrum at 243 K, the cell was placed in a cell holder designed to allow the circulation of nitrogen gas previously cooled by passing through a slush coolant (Acetone + Dry ice). The temperature was kept constant by controlling the flow of N_2 gas. The cell compartment was flushed with dry nitrogen before recording the spectrum to prevent moisture condensation on the cell surfaces.

4:5:6 Preparation of Thallium(I) and Thallium(III)hexafluorouranate.

The salts, $\text{Tl}^{\text{I}}\text{UF}_6$ and $[\text{Tl}^{\text{III}}(\text{NCMe})_5][\text{UF}_6]_3$, were prepared as described in chapter 2.

4:5:7 Reactions of Thallium(I) hexafluorouranate in MeCN Solution

(i) with dimethyl sulphide.

The salt, $\text{Tl}^{\text{I}}\text{UF}_6$ (0.5mmol) was dissolved in MeCN(5ml) and Me_2S (5.0mmol) was distilled in at 77 K. The resulting solution was shaken for about one hour. A light green solid was isolated from the solution after removal of the volatile material. The infrared spectrum of the solid showed the product to be $\text{Tl}^{\text{I}}\text{UF}_6$. There was no evidence for the coordinated Me_2S .

(ii) with trimethyl amine

The solution of $\text{Tl}^{\text{I}}\text{UF}_6$ (0.5mmol) in MeCN(5ml) was mixed with Me_3N (5.0mmol) in a reaction vessel, when a green precipitate was formed. The infrared spectrum of the green precipitate indicated the

presence of coordinated Me_3N , $\bar{\nu}_{\text{max}}$ 3220 (CH str), 1475 (CH_3 rock), 1055 cm^{-1} (CN str) and the UF_6^- anion, $\bar{\nu}_{\text{max}}$ 520 cm^{-1} . Bands due to coordinated MeCN were absent. The precipitate was identified by infrared spectrum and by the analysis of C,H and N as bis(trimethylamine) thallium(I) hexafluorouranate(V). Found: C=10.3; N = 2.4 and N = 3.8% $\text{C}_6\text{N}_{18}\text{F}_6\text{N}_2\text{TlU}$ requires: C = 10.6; H = 2.6 and N = 4.1% The salt was found to lose Me_3N on pumping under vacuum.

(iii) with trimethyl phosphine.

The salt, $\text{Tl}^{\text{I}}\text{UF}_6$ (0.5mmol) was dissolved in MeCN(5ml) and the resulting solution was mixed with Me_3P (5.0mmol). A blue green precipitate was formed which was isolated by removing the liquid phase and dried under vacuum. The infrared spectrum of the solid indicated bands due to coordinated PMe_3 , $\bar{\nu}_{\text{max}}$ 1305 (CH bend), 950 (CH_3 rock), 726 (PC asym.str) and 665 cm^{-1} (PC sym.str) and the UF_6^- anion, $\bar{\nu}_{\text{max}}$ 520 cm^{-1} . Bands due to coordinated MeCN were absent. By analogy with the $\text{Tl}(\text{I})\text{-Me}_3\text{N}$ salt, the solid was suggested to be bis(trimethylphosphine) thallium(I) hexafluorouranate(V).

4:5:8 Reactions of Solvated Thallium(III) in MeCN Solution

(i) with dimethyl sulphide.

The compound, $[\text{Tl}^{\text{III}}(\text{NCMe})_5][\text{UF}_6]_3$ (0.5mmol) was dissolved in MeCN(5ml) and Me_2S (5.0mmol) was added by vacuum distillation. On warming to room temperature, a lemon yellow intermediate was formed which decayed rapidly. The final solution was light green in colour from which a pale green solid was isolated after removing the volatile material. The volatile product distilled at 183 K was identified as ethane by gas chromatography. The solid product was shown to be a mixture of $\text{Tl}^{\text{I}}\text{UF}_6$ and $[\text{Me}_2\text{S-SMe}][\text{UF}_6]$ from its infrared electronic, ^1H , ^{13}C and ^{205}Tl n.m.r. spectra.

(ii) with trimethylamine.

The salt, $[\text{Tl}^{\text{III}}(\text{NCMe})_5][\text{UF}_6]_3$, (0.5mmol) was dissolved in MeCN (5ml) and the resulting solution was mixed with Me_3N (5.0mmol). A green precipitate and a light green solution were formed. From the solution, a pale green solid was isolated after the removal of the volatile material. The precipitate was shown to be $[\text{Tl}(\text{Me}_3\text{N})_2][\text{UF}_6]$ from its infrared spectrum. The pale green solid was suggested to be $[\text{Me}_3\text{N-NMe}_2][\text{UF}_6]$ from its infrared, electronic and ^1H n.m.r. spectra. The volatile material distilled at 183 K was identified as ethane by gas chromatography.

(iii) with trimethyl phosphine

The compound $[\text{Tl}^{\text{III}}(\text{NCMe})_5][\text{UF}_6]_3$ (0.5mmol) was dissolved in MeCN (5ml) and the solution was mixed with Me_3P (5.0mmol). A blue green precipitate and a light green solution were formed. From the solution a pale green solid was isolated after the removal of the volatile material. The precipitate was shown to be $[\text{Tl}(\text{Me}_3\text{P})_2][\text{UF}_6]$ from its infrared spectrum. The pale green solid was suggested to be $[\text{Me}_3\text{P-PMe}_3][\text{UF}_6]_2$ from its infrared, electronic and $^{31}\text{P}\{-^1\text{H}\}$ n.m.r. spectra.

CHAPTER FIVE

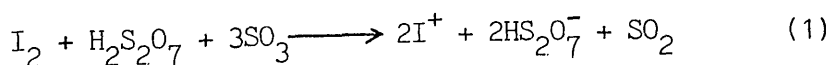
Redox and Substitution Reactions
of the Solvated Iodine(+1) Cation
in Acetonitrile

5:1 Introduction.

The existence of monovalent non-metal cations especially halogens has occasionally been reported in the literature. Such cations are mostly postulated in solution and only a few have been isolated in the solid state. The search for the existence of positive cations of iodine has been stimulated as a result of the general trend of the periodic table that the electropositive character of the elements increases with an increase in atomic number in a particular group. Iodine is the second most electropositive element of group VII, it should have a tendency to form the iodonium cation(I⁺). The monovalent cations of halogens are electron deficient with respect to the element itself and thus are highly electrophilic. They are accordingly stable in solvents which can solvate them effectively without undergoing any disproportionation reactions. Acetonitrile, for example, is a moderately weak base and has a good solvating ability whereas water is a sufficiently strong base to react with these cations. It is, therefore, not surprising that the discovery of non-metal cations especially those of the halogens owes much to recent developments in the chemistry of non-aqueous solvents.

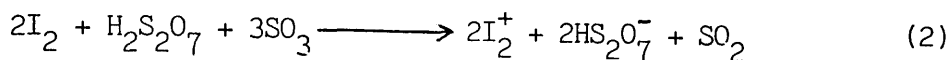
5:1:1 Historical Background.

It has been known for many years that iodine dissolves in strongly oxidising solvents such as oleum to form deep blue paramagnetic solutions. It was suggested by M.C.R. Symons and co-workers²²⁴ that the blue colour resulting from the dissolution of I₂ in oleum, was due to a species containing iodine in the +1 oxidation state.

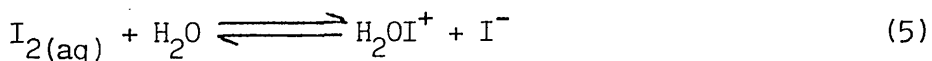
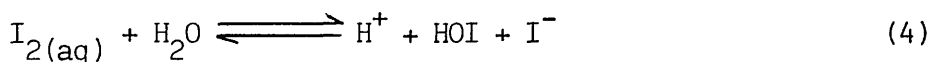
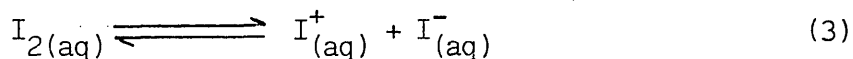


The reinvestigation of the blue solution of iodine in oleum by

conductometric, spectrophotometric and cryoscopic methods has contradicted the above suggestion,⁵⁶ and is in accord with the presence of I_2^+ instead of the I^+ cation.



The cation of iodine (I^+) has been identified in the gas phase by emission and mass spectroscopy. The spark spectrum of iodine shows lines attributable to the electronically excited iodine cation.²²⁵ The short lived existence of iodine cations in aqueous medium has been proposed by Bell and Gells.²²⁶ The following equilibria have been postulated on the basis of the free energy data computed by means of thermodynamic cycles.



The free energy data have been derived from only partly justifiable extrapolations and hence may be considerably in error. The discovery that iodine and iodine mono-chloride formed conducting solutions in ethanol and that iodine itself conducted in the vapour phase and in the molten state, led to the conclusion that the iodine cation was present in these systems.²²⁷

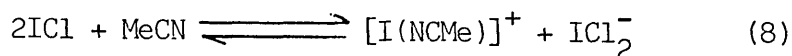


In the presence of excess iodine, I^+ cation would have a tendency to be converted to the I_3^+ cation hence a better description of the self-

ionization of iodine is given in equation (7).



The electrical conductance of iodine monochloride in MeCN solution has been interpreted due to the equilibrium, (equation 8)²²⁸



The existence of the I^+ cation solvated by MeCN has recently been postulated as one component of an electrical energy storage cycle.²²⁹

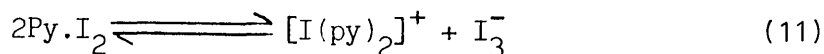
A solution of I_2 and LiBF_4 in MeCN when electrolysed in the anodic chamber of a divided cell, equipped with a platinum anode and a lithium cathode, undergoes the following reactions.



5:1:2 Charge Transfer Complexes of Iodine.

Iodine readily dissolves in a number of organic solvents and the colour of the solution depends on the nature of the solvent.²³⁰ The solutions of iodine in aliphatic hydrocarbons or CCl_4 are bright violet (λ_{max} 520-540 nm), those in aromatic hydrocarbons are pink or reddish brown and those in stronger donor solvents such as alcohols, ethers or amines are deep brown (λ_{max} 460-480 nm). This variation in colour may be explained in terms of a weak donor-acceptor interaction leading to complex formation between the solvent (donor) and iodine (acceptor) which alters the optical transition energy. The most direct evidence for the formation of a complex, $\text{L} \rightarrow \text{I}_2$, in solution comes from the appearance of an intense charge-transfer band

in the near ultraviolet spectrum. Such a band occurs in the region 230-330 nm with a molar extinction coefficient, ϵ , of the order of 10^3 - 10^4 dm³ mol⁻¹ cm⁻¹. The dissolution of I₂ in polar solvents such as pyridine may result in further interaction leading to ionic dissociation which renders the solution electrically conducting.

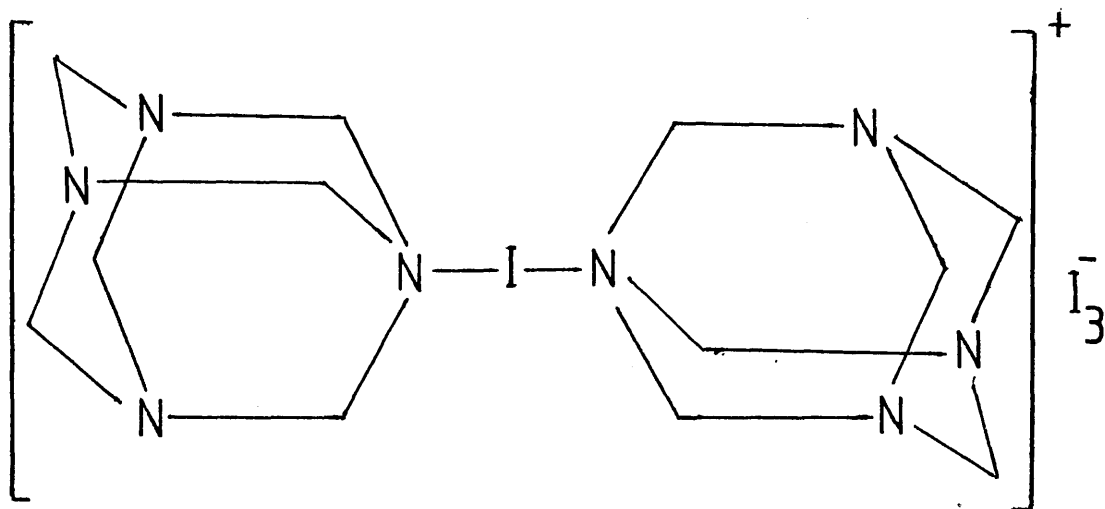


A number of solid complexes have been crystallized from brown solutions of iodine in organic solvents. The x-ray structural data of a number of 1:1 addition compounds, formed by dissolving iodine in amines, show the compounds to be true charge-transfer complexes in which one iodine atom is linked to the donor atom and the second one points away from the donor atom.

5:1:3 Solid Complexes of the I⁺ Cation.

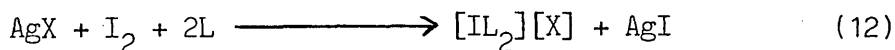
The first known example of an I⁺ complex in the solid state, is the salt, [I(py)₂][I₃] which has been prepared by reacting an alcoholic solution of I₂ with pyridine.²³¹ The x-ray analysis of the compound indicates that the crystals are built up of centrosymmetric [I(py)₂]⁺ and I₃⁻ ions. The cation, [I(py)₂]⁺, has been shown to have a linear N-I-N linkage. The second known complex of the I⁺ cation is the solid compound, [I(tu)₂][I], (tu = thiourea) which has been prepared by the reaction of thiourea with iodine dissolved in CH₂Cl₂.²³² The crystal structure of the complex has been determined by x-ray studies and consists of separate [I(tu)₂]⁺ and I⁻ ions. The cation, [I(tu)₂]⁺ like the [I(py)₂]⁺ species has been shown to have a linear S-I-S linkage. Another example is the complex, bis(hexamethylene-tetramine) iodonium triiodide.²³³ This complex has been prepared by the addition of a solution of I₂ in ethanol to a solution of hexa-

methylenetetramine(hmta) in CHCl_3 . The structure of the complex, $[\text{I}(\text{hmta})_2][\text{I}_3^-]$, has been determined by x-ray crystallography,²³⁴ and consists of centrosymmetric cations, $[\text{I}(\text{hmta})_2]^+$, and asymmetric anions, I_3^- .



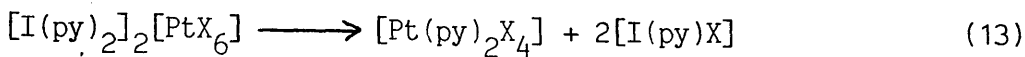
The N-I distances within the cation, $[\text{I}(\text{hmta})_2]^+$, (2.35Å) are significantly longer than in the $[\text{I}(\text{py})_2]^+$ cation (2.21Å).

The complexes, $[\text{IL}_2][\text{X}]$, (L = pyridine or 2,4,6-trimethyl pyridine, and X = NO_3^- , ClO_4^- , BF_4^- or PF_6^-) have been prepared by the addition of the corresponding silver salt to a mixture of the ligand and iodine in CHCl_3 ²³⁵ or in CH_2Cl_2 .^{236,237}



The compounds, $[\text{I}(\text{py})_2][\text{X}]$. X = NO_3^- or ClO_4^- , have been studied by ^{129}I -iodine²³⁸ and ^{127}I -iodine²³⁹ Mössbauer spectroscopy. The isomer shifts in these compounds indicate a high s-electron density on the iodine nucleus and that the I-N bonding is largely of p-character. The compounds, $[\text{I}(\text{py})_2]_2[\text{PtX}_n]$ (X = Cl or Br and n = 6 or 4), have been obtained by the addition of solid $\text{K}_2[\text{PtX}_n]$ salts to a solution of

$[\text{I}(\text{py})_2][\text{NO}_3]$ in dimethylformamide and precipitating the complexes by the addition of water.²⁴⁰ The thermal decomposition of the complex, $[\text{I}(\text{py})_2]_2[\text{PtX}_6]$, is said to involve ligand replacement-redistribution reactions as represented in equation 13.



The reaction indicates that both the octahedral configuration of the coordination sphere of platinum(IV) and the linear configuration of the coordination sphere of iodine(I) are preserved.

The complexes, $[\text{I}(\text{NCMe})_2][\text{MF}_6]$, (M = Mo or U) have been prepared in this Department by the oxidation of molecular iodine dissolved in MeCN using molybdenum or uranium hexafluoride as the oxidising agents.^{48,241} Addition of MoF_6 or UF_6 to a frozen solution of iodine in MeCN ($\text{MF}_6:\text{I}_2$ mole ratio $\gg 1:1$) results in a rapid colour change red - yellow green as the mixture is allowed to warm at ambient temperature. In marked contrast, iodine is oxidised by UF_6 in iodine pentafluoride to form the I_2^+ cation which undergoes further oxidation whereas I_2 and MoF_6 do not react.⁴¹ This emphasises the importance of the solvent in redox reactions. Polynuclear cations, for example I_3^+ , which are characteristically formed when iodine is oxidised in strongly acidic solvents,⁵⁸ are apparently not formed in the basic solvent, MeCN.⁴⁸

5:1:4 Reactions of the I^+ Complexes.

The $[\text{I}(\text{py})_2]^+$ cation has been used as an electrophilic reagent for example its addition to double bonds is suggested to proceed via iodonium intermediates to give the trans adducts.^{242,243}

Table 1.

Infrared Spectra of the Complexes $[I(SMe_2)_2][MF_6]$, M = Mo or U.

Wavenumber (cm ⁻¹)		Assignment ²⁴⁵
$[I(SMe_2)_2][MoF_6]$ ^a	$[I(SMe_2)_2][UF_6]$ ^b	
3000 (w) } 2920 (w) }	3010 (w) } 2925 (w) }	CH str.
1325 (m)	1320 (m)	CH ₃ sym.def.
1040 (s) } 980 (s) }	1035 (s) } 975 (s) }	CH ₃ rock.
725 (m) } 675 (m) }	730 (m) } 680 (m) }	C-S str.
630 (v.s)	-	MoF ₆ ⁻ (ν ₃)
-	520 (v.s)	UF ₆ ⁻ (ν ₃)
245 (s)	-	MoF ₆ ⁻ (ν ₄)
230 (m)	230 (m)	S-I-S str.

w = weak; m = medium; s = strong; v.s. = very strong

^a yellow in colour.^b green in colour.

solvated I^+ cation. The cation, $[I(NCMe)_2]^+$ in acetonitrile solution oxidises Cu^I to Cu^{II} , NO to NO^+ and Tl metal to a mixture of Tl^I and Tl^{III} .

The aim of the work described in this chapter is to develop the coordination chemistry of the cation, $[I(NCMe)_2]^+$, in MeCN using simple nitrogen, phosphorus and sulphur donor and macrocyclic nitrogen donor ligands. The aim was also to compare the substitution reactions of the solvated I^+ cation with those of the solvated metal cations described earlier in this thesis. For comparison, the reactions of $[Fe(NCMe)_6]^{2+}$ with macrocyclic ligands have been included in this chapter. The final part of the chapter describes the electrochemistry of the I^+ complexes, obtained from the substitution reactions, using the technique of cyclic voltammetry.

5:2 Results.

5:2:1 Reactions of the solvated I^+ cation.

The complex bis(acetonitrile) iodine(I) hexafluorouranate(V) in MeCN solution reacts with dimethyl sulphide forming a green solution. A green solid was isolated from this solution after removal of the volatile material. The infrared spectrum of the solid indicated the presence of coordinated Me_2S^{245} and the UF_6^- anion, and is listed in Table 1. The bands due to coordinated MeCN were absent. The complex was identified from its infrared spectrum and microanalysis as bis(dimethylsulphide) iodine(I) hexafluorouranate(V). The electronic spectrum of the complex $[I(Me_2S)_2][UF_6^-]$, in MeCN solution, consisted of bands due to the UF_6^- anion, $\bar{\nu}_{max}$ 7300, 7430, 7580 and 7940 cm^{-1} in the visible and near-infrared regions,⁴⁵ and a strong charge transfer band with a cut off at about 18000 cm^{-1} . The reaction of the salt, $[I(NCMe)_2][MoF_6^-]$, in MeCN solution, with

Me₂S resulted in the formation of a yellow solution from which a yellow solid was obtained. The infrared spectrum of the solid indicated the presence of coordinated Me₂S and the bands at $\bar{\nu}_{\max}$ 630 and 245 cm⁻¹ due to the MoF₆⁻ anion. By analogy with the complex, [I(Me₂S)₂][UF₆], the yellow solid was characterized as bis(dimethylsulphide) iodine(I) hexafluoromolybdate(V). The electronic spectrum of the solid, [I(Me₂S)₂][MoF₆], in MeCN solution indicated a strong charge transfer absorption with a cut off at 17500 cm⁻¹. The ¹H and ¹³C n.m.r. spectra of the complex [I(Me₂S)₂][MoF₆], in CD₃CN, each consisted of sharp singlets at 2.90 and 51.0 ppm respectively.

The reaction of [I(NCMe)₂][MoF₆] with tetramethylthiourea (tmtu), mole ratio 1:2, in MeCN solution resulted in the formation of an orange solution. An orange sticky solid was isolated from this solution which became crystalline when cooled to 263 K. The infrared spectrum of the solid contained bands due to coordinated tmtu and the MoF₆⁻ anion and is listed in Table 2. By analogy with the I⁺ complexes, [I(tu)₂]⁺ 232 and [I(SMe₂)₂]⁺, the solid salt was formulated as [I(tmtu)₂][MoF₆]. The ¹H and ¹³C n.m.r. spectra of the solid, [I(tmtu)₂][MoF₆], in CD₃CN, each consisted of singlets at 2.5 and 49.5 ppm. The ¹H and ¹³C chemical shifts of pure tmtu in CD₃CN were 2.1 and 47.5 ppm respectively. The electronic spectrum of the complex, [I(tmtu)₂][MoF₆], in MeCN consisted of a strong charge transfer band with cut off at about 17500 cm⁻¹.

The complex, [I(NCMe)₂][MoF₆], in MeCN solution underwent a substitution reaction when allowed to react with 2,2-bipyridyl(bipy). The solid salt isolated from the reaction mixture with [I⁺]:[bipy], 1:1, indicated weak bands due to coordinated MeCN in its infrared spectrum whereas no such bands were present in the i.r. spectrum of the solid obtained from [I⁺]:[bipy] mole ratio 1:2. Bands due to

the free ligand ²⁴⁶ were absent in both the cases. By analogy with the complex, $[\text{I}(\text{hmta})_2]^+$, ²³³ (hmta = hexamethylenetetramine), the solid salt isolated from $[\text{I}^+]:[\text{bipy}]$ mole ratio 1:2, was formulated as $[\text{I}(\text{bipy})_2][\text{MoF}_6]$. The infrared spectrum of the complex, $[\text{I}(\text{bipy})_2]-[\text{MoF}_6]$ is listed in Table 3. The electronic spectrum of the solid, $[\text{I}(\text{bipy})_2][\text{MoF}_6]$, in MeCN solution consisted of a band at $\bar{\nu}_{\text{max}} 21800 \text{ cm}^{-1}$.

The reaction of macrocyclic ligands, 1,4,8,11-tetraazacyclotetradecane, ($[\text{14}]\text{-aneN}_4$) and 1,4,8,12-tetraazacyclopentadecane, ($[\text{15}]\text{-aneN}_4$), with $[\text{I}(\text{NCMe})_2][\text{MoF}_6]$ in MeCN solution resulted in the substitution of the coordinated MeCN by the ligand. A dark purple solid was isolated from the $[\text{14}]\text{-aneN}_4$ reaction whereas the solid obtained from the $[\text{15}]\text{-aneN}_4$ reaction, was mustard coloured. The solids were identified from the infrared spectra and by the analysis of C, H, I and N, as $[\text{I}([\text{14}]\text{-aneN}_4)][\text{MoF}_6]$ and $[\text{I}([\text{15}]\text{-aneN}_4)][\text{MoF}_6]$. The solid state infrared spectra of the complexes are listed in Table 4. The band at $\bar{\nu}_{\text{max}} 540 \text{ cm}^{-1}$ was assumed to be due to the I-N₄ stretching mode by analogy with the Ru-N stretching modes observed at $\bar{\nu}_{\text{max}} 470\text{-}510 \text{ cm}^{-1}$ in the infrared spectra of the complexes, $[\text{Ru}([\text{14}]\text{-aneN}_4)_2]^+$. ²⁴⁷ The electronic spectra of the complexes, $[\text{I}([\text{14}]\text{-aneN}_4)][\text{MoF}_6]$ and $[\text{I}([\text{15}]\text{-aneN}_4)][\text{MoF}_6]$, in MeCN solution consisted of a band at $\bar{\nu}_{\text{max}} 18500 \text{ cm}^{-1}$ ($\epsilon = 500 \text{ dm}^3 \text{ mol}^{-1} \text{ cm}^{-1}$) and at 18200 cm^{-1} (shoulder) respectively. The ¹H n.m.r spectrum of the complex $[\text{I}([\text{14}]\text{-aneN}_4)][\text{MoF}_6]$, in CD₃CN consisted of a multiplet having five sharp signals with chemical shifts in the range 0.89 to 0.82 ppm. The ¹H n.m.r. spectrum of $[\text{14}]\text{-aneN}_4$ in CDCl₃ consisted of a multiplet with chemical shifts in the range 2.8-2.6 ppm and a weak singlet at 2.2 ppm.

The reaction of $[\text{I}(\text{NCMe})_2][\text{MoF}_6]$ with P(OMe)₃ in MeCN solution resulted in the formation of an oily mass. The infrared spectrum

Table 2.

Infrared Spectrum of the Complex $[\text{I}(\text{tmtu})_2][\text{MoF}_6]$

Wavenumber (cm^{-1})	Assignment ¹⁷⁵
1620 (s)	NCN asym.str.
1565 (s)	NCN sym.str.
1260 (s)	$\text{H}_3\text{C-N}$ asym.str.
1160 (s)	C=S asym.str.
1100 (s)	C=S sym.str.
1060 (s)	CH_3 rock.
945 (m)	$\text{H}_3\text{C-N}$ sym.str.
875 (s)	CN torsion
630 (v.s)	$\text{MoF}_6^- (\nu_3)$
245 (s)	$\text{MoF}_6^- (\nu_4)$
230 (m)	S-I-S str.

m = medium;

s = strong;

v.s = very strong

Table 3.

Infrared Spectrum of the Complex $[I(bipy)_2][MoF_6]$

Wavenumber (cm^{-1})	Corresponding band of ²⁴⁶ free ligand (cm^{-1})
1605 (m)	1580 (m)
1570 (m)	1558 (m)
1318 (s)	-
1285 (m)	-
1245 (m)	1255 (s)
1170 (m)	1140 (s)
1075 (s)	1090 (s)
1050 (m)	1040 (s)
1012 (s)	995 (s)
968 (m)	975 (m)
778 (s)	755 (s)
725 (m)	740 (m)
630 (s) ^a	-
250 (m) ^a	-

s = strong; m = medium

^a MoF_6^- bands

Table 4.

Infrared Spectra of the Complexes, $[\text{IL}][\text{MoF}_6]_L$, $L = [14]\text{-aneN}_4$ or $[15]\text{-aneN}_4$.

Wavenumber (cm^{-1})		Assignment ²⁴⁷
$[\text{I}([14]\text{-aneN}_4)][\text{MoF}_6] \text{ } \underline{\text{a}}$	$[\text{I}([15]\text{-aneN}_4)][\text{MoF}_6] \text{ } \underline{\text{b}}$	
3200 (m)	3200 (m)	NH str.
1620 (m)	1625 (m)	NH def.
1105 (w)]	1100 (w)]	CN str.
1065 (m)]	1060 (m)]	
1040 (m)]	1035 (m)]	C-C str.
975 (m)]	975 (m)]	
868 (m)]	865 (m)]	CH_2 rock.
820 (m)]	825 (m)]	
630 (v.s)	625 (v.s)	$\text{MoF}_6^- (\nu_3)$
545 (s)	540 (s)	I-N str.
240 (m)	245 (m)	$\text{MoF}_6^- (\nu_4)$

w = weak; m = medium; s = strong; v.s = very strong

a dark purple in colour

b mustard in colour

of this mass consisted of bands due to coordinated $\text{P}(\text{OMe})_3$, $\bar{\nu}_{\text{max}}^{176}$ 990 and 930 cm^{-1} ($\text{P}(\text{OC})_3\text{str}$), 800 and 755 cm^{-1} ($\text{P}(\text{O})_3\text{str}$), and the MoF_6^- anion, $\bar{\nu}_{\text{max}}$ 620 (ν_3) and 245 cm^{-1} (ν_4). Bands due to coordinated MeCN were absent. A detailed study of the complex was not attempted because of its oily nature. Trimethyl phosphine reacted with $[\text{I}(\text{NMe})_2][\text{MoF}_6^-]$ in MeCN solution forming a mustard coloured solution. A mustard solid was isolated from this solution after removal of the volatile material. The solid was shown to be a mixture of species from its microanalysis and $^{31}\text{P}-\{^1\text{H}\}$ n.m.r. spectrum which contained a number of singlets and multiplets. The infrared spectrum of the solid consisted of bands due to a Me-P moiety and the MoF_6^- anion with the addition of a band at $\bar{\nu}_{\text{max}}$ 325 cm^{-1} possibly due to a P-P bending mode. The electronic spectrum of the solid in MeCN solution consisted of a band at $\bar{\nu}_{\text{max}}$ 17200 cm^{-1} .

The electronic spectra of the I^+ complexes (Table 5) consist of strong charge transfer bands in the region $17000\text{-}22000 \text{ cm}^{-1}$ assigned to the ligand $\rightarrow \text{I}^+$ charge transfer transitions. The electronic spectrum of 2,2-bipyridyl in a number of solvents consists of two bands at $\bar{\nu}_{\text{max}}$ 35700 and 42550 cm^{-1} , ²⁴⁸ hence the band at $\bar{\nu}_{\text{max}}$ 21800 cm^{-1} in the electronic spectrum of the complex, $[\text{I}(\text{bipy})_2]^+$, can not be assigned to the internal transitions of the ligand.

An electrochemical study of the I^+ complexes with ligated Me_2S , tmtu, bipy, [14]-ane N_4 and [15]-ane N_4 , was carried out by cyclic voltammetry. The procedure of this technique is described in Chapter 6. The results of this study are listed in Table 6. All the results are internally referenced with respect to the couple, $\text{MoF}_6/\text{MoF}_6^-$. A representative cyclic voltammogram of the complex, $[\text{I}([14]\text{-aneN}_4)][\text{MoF}_6^-]$, is represented in Figure 1. The cyclic voltammograms in each case, are consisted of three quasi-reversible

Table 5.

Electronic Spectra of the I⁺ and Fe²⁺ Complexes in MeCN Solution.

Complex	Absorption Maxima (cm ⁻¹)
[I(bipy) ₂][MoF ₆]	21800
[I([14]-aneN ₄)] [MoF ₆]	18500
[I([15]-aneN ₄)] [MoF ₆]	18200
[Fe([14]-aneN ₄)(NCMe) ₂][PF ₆] ₂	18500 (50) ^a , 27000 (95)

^a Molar extinction coefficient (dm³ mol⁻¹ cm⁻¹)

Table 6.

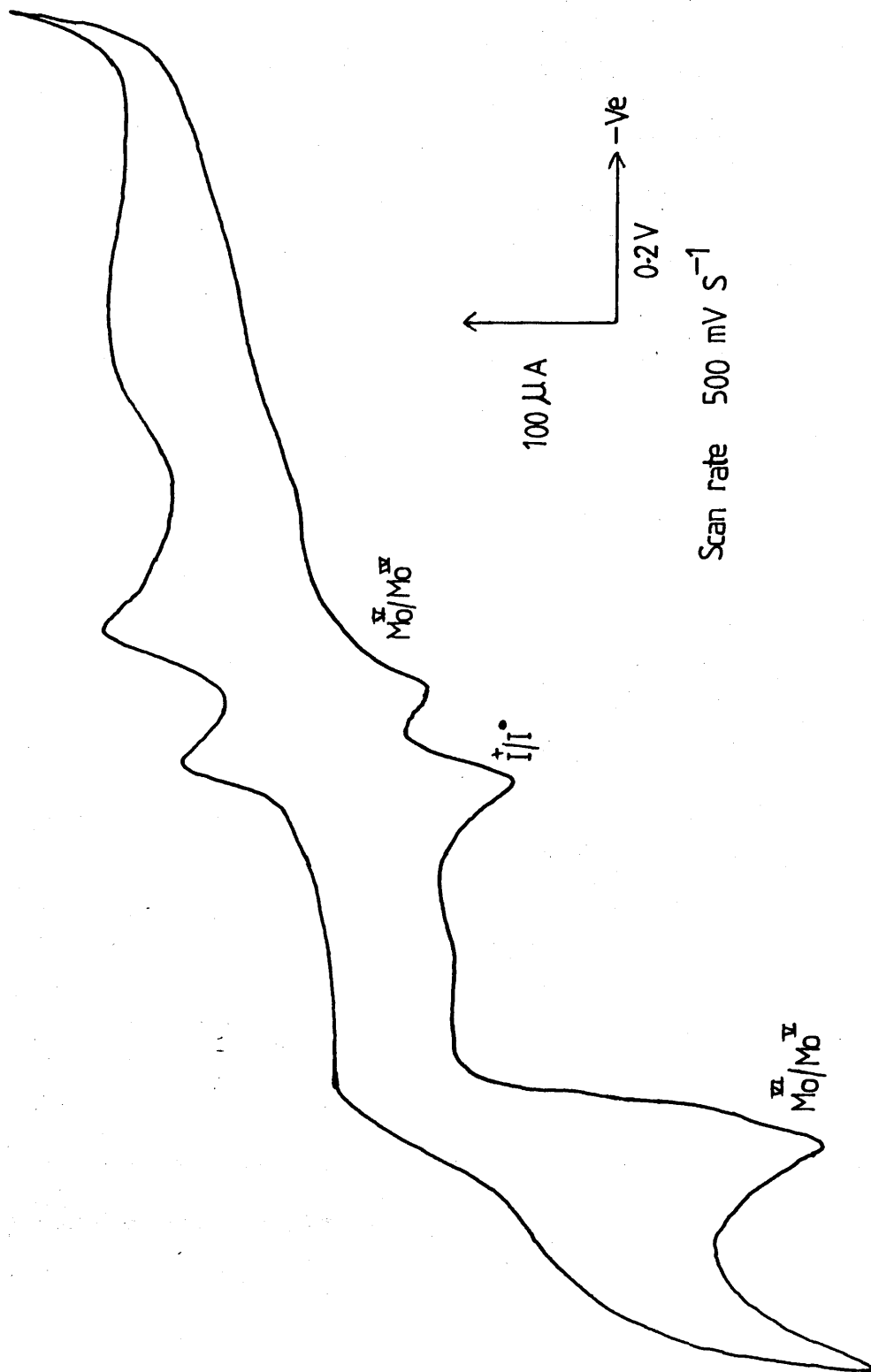
Results of Cyclic Voltammetry Studies of I⁺ Complexes in MeCN Solution.

Complex	Half-wave Potential, E _{1/2} (V)		MoF ₆ ⁻ /Mo ^{IV}
	MoF ₆ /MoF ₆ ⁻	I ⁺ /I [•] ^a	
[I(Me ₂ S) ₂][MoF ₆]	+ 1.60	+ 0.32 (100) ^b	-0.41
[I(tmtu) ₂][MoF ₆]	+ 1.60	+ 0.28 (95)	-0.39
[I(bipy) ₂][MoF ₆]	+ 1.60	+ 0.25 (80)	-0.41
[I([14]-aneN ₄)][MoF ₆]	+ 1.60	+ 0.12 (90)	-0.38
[I([15]-aneN ₄)][MoF ₆]	+ 1.60	+ 0.12 (85)	-0.39

^a Relative to Ag⁺/Ag using MoF₆/MoF₆⁻ as an internal reference.

^b Peak-to-peak separation (mV) in parentheses.

Figure 1. Cyclic Voltammogram of $[I([14]\text{-aneN}_4)][\text{MoF}_6]$



waves, two of these are assigned to the couples, $\text{MoF}_6^-/\text{MoF}_6^-$ and $\text{MoF}_6^-/\text{Mo}^{(\text{IV})}$, by comparison with previous studies of the silver and copper salts.⁴⁶ The third wave in these voltammograms was presumed to arise from the couple $\text{I}^+/\text{I}^\cdot$.

5:2:2 Reactions of Solvated Fe^{2+} Cation with [14]-ane N_4 and [15]-ane N_4 .

The salt, $[\text{Fe}(\text{NCMe})_6][\text{PF}_6]_2$, reacts with [14]-ane N_4 in MeCN solution forming a purple solution. A purple solid was isolated after removal of the volatile material. The infrared spectrum of the solid indicated the presence of coordinated [14]-ane N_4 , $\bar{\nu}_{\text{max}}$ 3290 (NH str), 1105 (CN str), 930 cm^{-1} (C-C str), coordinated MeCN, $\bar{\nu}_{\text{max}}$ 2300 (CN comb), 2275 (C \equiv N str), 980 cm^{-1} (C-C str) and the PF_6^- anion, $\bar{\nu}_{\text{max}}$ 840 (ν_3) and 560 cm^{-1} (ν_4) and is listed in Table 7. By analogy with the known iron(II)-[14]-ane N_4 complex,¹²⁵ the solid complex was identified as $[\text{Fe}([\text{14}\text{-aneN}_4)(\text{NCMe})_2][\text{PF}_6]_2$. The electronic spectrum of the complex in MeCN solution consisted of two bands at $\bar{\nu}_{\text{max}}$ 18500 ($\epsilon = 50 \text{ dm}^3 \text{ mol}^{-1} \text{ cm}^{-1}$) and 27000 cm^{-1} ($\epsilon = 95 \text{ dm}^3 \text{ mol}^{-1} \text{ cm}^{-1}$) assigned to the ${}^1\text{A}_{1g} \rightarrow {}^1\text{A}_{2g}$ and ${}^1\text{A}_{1g} \rightarrow {}^1\text{E}_g$ d-d transitions of a low spin d^6 iron(II) in D_{4h} symmetry. The results are in good agreement with the data reported in the literature.

The complex, $[\text{Fe}([\text{14}\text{-aneN}_4)(\text{NCMe})_2][\text{PF}_6]$, in MeCN solution underwent a redox reaction when reacted with NOPF_6 . The purple solution of the complex turned yellow and a yellow solid was isolated from this solution after removal of the volatile material. There was no evidence for the evolution of NO gas. The infrared spectrum of the solid consisted of bands due to coordinated [14]-ane N_4 , $\bar{\nu}_{\text{max}}$ 3280 and 1100 cm^{-1} , MeCN, $\bar{\nu}_{\text{max}}$ 2320, 2290 and 1040 cm^{-1} and the PF_6^- anion, $\bar{\nu}_{\text{max}}$ 840 and 560 cm^{-1} . A strong band at $\bar{\nu}_{\text{max}}$ 1940 cm^{-1} was presumed to be due to the NO stretching mode. The electronic

Table 7.

Infrared Spectra of the Complexes, $[\text{FeL}(\text{NCMe})_2][\text{PF}_6]_2$, $\text{L} = [14]\text{-aneN}_4$ or $[15]\text{-aneN}_4$

Wavenumber (cm^{-1})		Assignment	125
$[\text{Fe}([14]\text{-aneN}_4)(\text{NCMe})_2][\text{PF}_6]_2$ <u>a</u>	$[\text{Fe}([15]\text{-aneN}_4)(\text{NCMe})_2][\text{PF}_6]_2$ <u>b</u>		
3290 (m)	3285 (m)	NH str.	
2300 (w)	2300 (w)	CN comb.	
2275 (m)	2280 (m)	$\text{C}\equiv\text{N}$ str.	
1105 (m)	1100 (m)	C-N str.	
1060 (m)	1055 (m)	CH_3 rock	
1025 (m)	1020 (m)		
980 (m)	980 (m)	C-C str.	
930 (m)	925 (m)		
840 (s)	840 (s)	PF_6^- (ν_3)	
560 (s)	560 (s)	PF_6^- (ν_4)	

w = weak; m = medium; s = strong

a purple in colourb lemon yellow in colour

spectrum of the solid in MeCN solution consisted of two shoulders at $\bar{\nu}_{\max}$ 24100 and 27000 cm^{-1} .

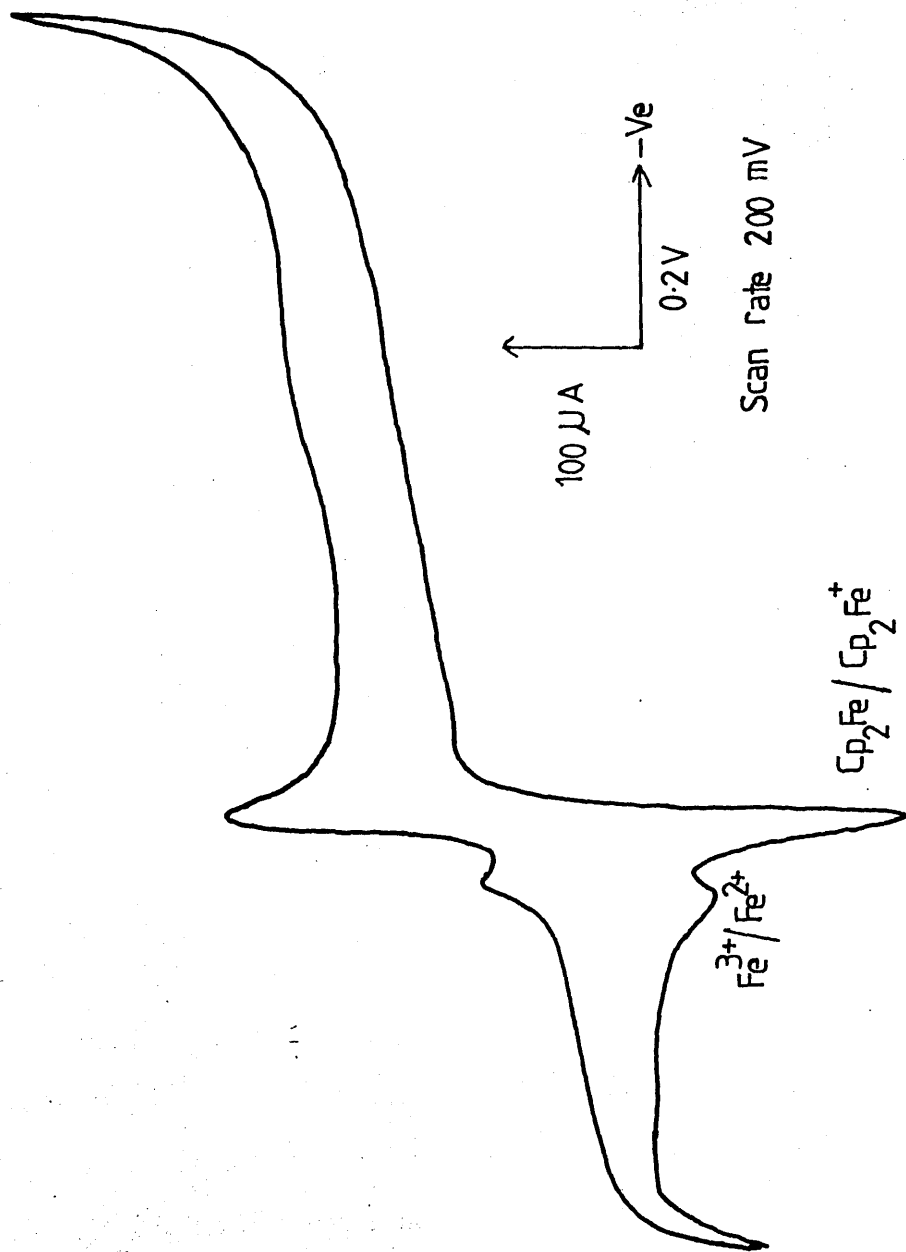
The reaction of $[\text{Fe}(\text{NCMe})_6][\text{PF}_6]_2$ with [15]-ane N_4 in MeCN solution resulted in the formation of a lemon yellow solution from which a pale yellow solid was isolated. The infrared spectrum of the solid consisted of bands due to coordinated [15]-ane N_4 , $\bar{\nu}_{\max}$ 3285, 1100 and 925 cm^{-1} , MeCN, $\bar{\nu}_{\max}$ 2300, 2280 and 980 cm^{-1} , and the PF_6^- anion, $\bar{\nu}_{\max}$ 840 and 560 cm^{-1} and is listed in Table 7. By analogy with the known Fe^{II} -[15]-ane N_4 complex,¹²⁵ the pale yellow solid was identified as $[\text{Fe}([\text{15}]\text{-aneN}_4)(\text{NCMe})_2][\text{PF}_6]_2$. The electronic

spectrum of the complex in MeCN solution consisted of a broad asymmetric band at $\bar{\nu}_{\max}$ 13900 cm^{-1} ($\epsilon = 4 \text{ dm}^3 \text{ mol}^{-1} \text{ cm}^{-1}$) and was in good agreement with the spectrum reported in the literature. The band was assigned to the ${}^5\text{T}_{2g} \rightarrow {}^5\text{E}_g$ d-d transition of a high spin d^6 iron(II). The reaction of the complex, $[\text{Fe}([\text{15}]\text{-aneN}_4)(\text{NCMe})_2][\text{PF}_6]_2$, with NOPF_6 in MeCN solution resulted in a colour change of the solution from pale yellow to orange. An orange solid was isolated from the final solution after removal of the volatile material.

There was no evidence for the evolution of NO gas. The infrared spectrum of the solid indicated bands due to coordinated [15]-ane N_4 , $\bar{\nu}_{\max}$ 3280 and 1095 cm^{-1} , MeCN, 2320 and 2290 cm^{-1} and the PF_6^- anion, $\bar{\nu}_{\max}$ 840 and 560 cm^{-1} . A strong band at $\bar{\nu}_{\max}$ 1945 cm^{-1} was assumed to be due to the NO stretching mode. The electronic spectrum of the complex in MeCN solution consisted of a strong charge transfer band which obscured the d-d bands.

The complexes, $[\text{FeL}(\text{NCMe})_2][\text{PF}_6]_2$, (L = [14]-ane N_4 or [15]-ane N_4) were studied by cyclic voltammetry. The cyclic voltammograms were recorded using ferrocene as an external reference. A quasi-reversible wave was observed in each of the two cases (Figure 2) with $E_{1/2}$

Figure 2. Cyclic Voltammogram of $[\text{Fe}([\text{14}]\text{-aneN}_4)(\text{NCMe})_2][\text{PF}_6]_2$



$(\text{Fe}^{3+}/\text{Fe}^{2+}) = + 0.325\text{V}$ vs Ag^+/Ag . This corresponded to a value of $+ 0.415\text{V}$ vs S.C.E. The average peak to peak distances, ΔP , were about 85 mV.

5:3 Discussion

The chemistry of iodine(+1) in MeCN seems to be analogous to the coordination chemistry found for many monopositive metal cations, for example Ag^+ , in the same solvent. This is evident for a number of reasons. The EXAFS study of the complexes, $[\text{IL}_2][\text{MoF}_6]$, $\text{L} = \text{MeCN}$ or py , indicates that $[\text{IL}_2]^+$ exist as discrete cations in MeCN solution, a situation similar to that found for metal cations.¹¹¹ This study also confirms that the coordination number of iodine(+1) in MeCN is two, a situation similar to that of the Ag^+ cation.²²⁰ The analogies observed between iodine(+1) and the metal cation coordination chemistry in MeCN in the present study are the facile substitution of the coordinated MeCN by ligands such as Me_2S , tmtu, 2,2-bipyridyl, [14]-ane N_4 and [15]-ane N_4 . However, some interesting differences are observed between the chemistry of iodine (+1) and those of the metal cations in MeCN. The reaction of Me_2S with $[\text{I}(\text{NCMe})_2]^+$ in MeCN results in the substitution of the coordinated MeCN molecules by Me_2S whereas a reaction between $[\text{Cu}(\text{NCMe})_6]^{2+}$ and Me_2S results in the reduction of Cu^{II} to Cu^{I} as described in chapter 4. The cation, $[\text{I}(\text{NCMe})_2]^+$, in MeCN solution is capable of oxidising solvated Cu^{I} to solvated Cu^{II} .⁴⁸ It is, therefore, suggested that Me_2S has stabilized the iodine (+1) and due to this reason the cation, $[\text{I}(\text{SMe}_2)_2]^+$, is not redox active. On the other hand the Cu^{II} species, $[\text{Cu}(\text{SMe}_2)_x(\text{NCMe})_{6-x}]^{2+}$, is a stronger oxidising agent as compared with $[\text{Cu}(\text{NCMe})_6]^{2+}$, hence is capable of oxidising the coordinated Me_2S as described in chapter 4.

The reaction of PMe_3 with $[\text{I}(\text{NCMe})_2]^+$, in MeCN should have resulted in the formation of the cation, $[\text{I}(\text{PMe}_3)_2]^+$ but instead a complicated reaction is observed. It is suggested from the experimental data that the substitution of the coordinated MeCN molecules by PMe_3 occurs initially forming the cation $[\text{I}(\text{PMe}_3)_2]^+$. This cation is unstable with respect to internal redox reaction hence coordinated PMe_3 is oxidised to the radical cation, $\text{PMe}_3^{+\cdot}$, and iodine (+1) is reduced to I_2 . The free PMe_3 then reacts with I_2 forming the cation, $[\text{Me}_3\text{P}-\text{PMe}_3]^{2+}$, which may also be formed from the combination of two monomeric radical cations as described in chapter 4. The complex nature of the reaction is evident from the $^{31}\text{P}-\{^1\text{H}\}$ n.m.r. spectrum of the product isolated from the $[\text{I}(\text{NCMe})_2]^+$ and PMe_3 reaction. The spectrum contains a number of resonances (singlets and multiplets) from which only the singlet at 32.0 ppm can be tentatively assigned to the cation, $[\text{Me}_3\text{P}-\text{PMe}_3]^{2+}$ by analogy with the species, $[\text{Me}_3\text{P}-\text{PMe}_3]^{2+}$, described in chapter 4.

The reaction of $[\text{I}(\text{NCMe})_2]^+$ with macrocyclic ligands, [14]-ane N_4 and [15]-ane N_4 (L) in MeCN solution, results in the formation of stable complexes. An attempt to obtain the single crystals of the complex, $[\text{I}(\text{[14]-aneN}_4)][\text{MoF}_6]$, has not yet been successful. Thus the structures of the complexes are not known but they would be of great interest. Macrocyclic nitrogen donor ligands such as [14]-ane N_4 possess remarkable complexing properties towards metal ions.²⁴⁹ The coordinative properties of the ligands have been shown to be determined by a number of effects. The most important is the metal-nitrogen donor bond length in relation to the hole size of the macrocycle. It has been found from a number of structural studies of the metal ion-[14]-ane N_4 complexes that square planar coordination of the ligand requires an optimum M-N distance of 2.07Å.²⁵⁰

Such a distance corresponds to a metal ion with an ionic radius of about $0.65 - 0.7 \text{ \AA}$. Small deviations in radius on either side of this optimum value may be accommodated because of the flexibility of the macrocyclic ring. The structures of the macrocyclic ligands, [14]-aneN₄ and [15]-aneN₄, are shown in Figure 3.

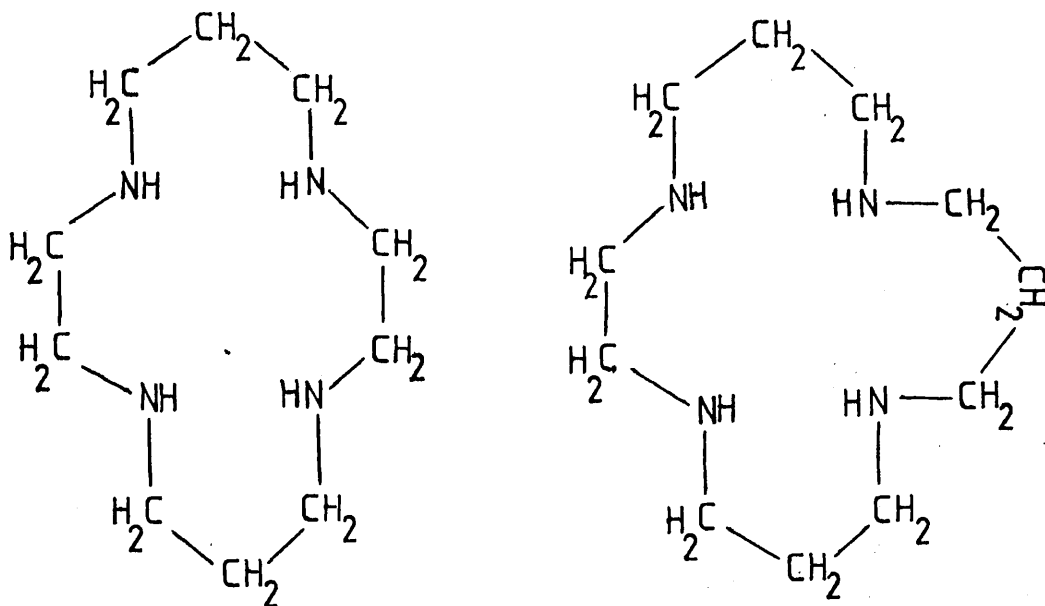


Figure 3. [14]-aneN₄

[15]-aneN₄

The I-N distances determined for the cations, $[\text{I}(\text{py})_2]^+$, (2.21 \AA)¹¹¹ and $[\text{I}(\text{hmta})_2]^+$, (2.35 \AA)²³⁴ are greater than the optimum M-N distance of 2.07 \AA , although the different coordination numbers of the cations, might effect this comparison to some extent. The ionic radius of the I⁺ cation has been determined by the Sanderson method²⁵¹ and shown to have the values 0.62 or 0.83 \AA , the first value corresponds to the cation in the gas phase and the second to the coordinated ion with a coordination number 2.²⁵² Polydentate ligands such as cryptand [2.2.2] with a cavity diameter equal to 2.8 \AA have been shown to form complexes with the I⁺ cation, the complexes being prepared by the induced I⁺...I⁻ dissociation of the iodine

molecule.²⁵² The covalent radius of iodine is $1.33 \overset{\circ}{\text{A}}^{10}$ and it is expected that the ionic radius of I^+ cation should be smaller than $1.33 \overset{\circ}{\text{A}}$. However, it is unlikely that it would be as small as $0.83 \overset{\circ}{\text{A}}$.²⁵² It is, therefore, suggested that the ionic radius of I^+ cation is too large to be accommodated within the cavity of the ligands, [14]-ane N_4 or [15]-ane N_4 , in a regular square planar geometry. The ligands are thus considered to be distorted and the most likely geometry of the ligands in the complexes, [IL][MoF $_6$], (L = [14]-ane N_4 or [15]-ane N_4), is assumed to be the folded conformation.

The folded conformation of the macrocyclic ligands is known in the metal complexes such as $[\text{Hg}([\text{14}]\text{-aneN}_4)\text{Cl}]_2[\text{HgCl}_4]$ and $[\text{Pb}([\text{14}]\text{-aneN}_4)][\text{NO}_3]_2$.²⁵³ The ionic radii of the cations, Hg^{2+} ($1.1 \overset{\circ}{\text{A}}$) and Pb^{2+} ($1.2 \overset{\circ}{\text{A}}$), are large enough to force the ligand to adopt a folded conformation as shown in Figure 4.²⁵³

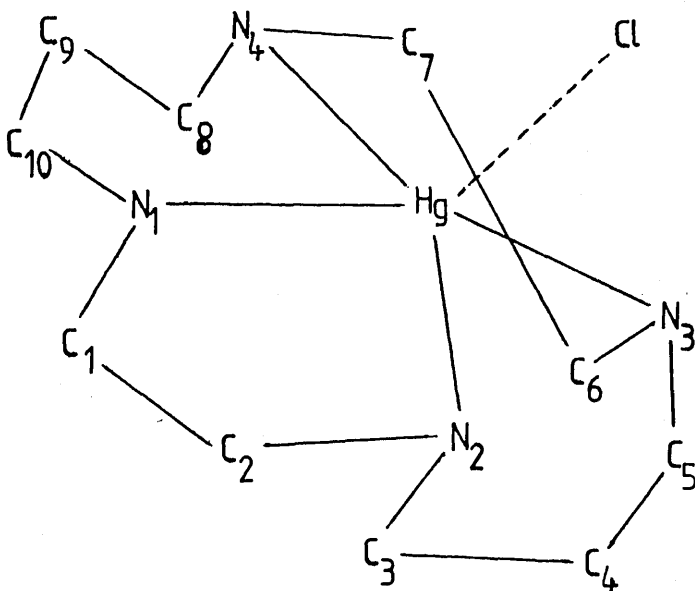


Figure 4: Molecular Structure of the Cation, $[\text{Hg}([\text{14}]\text{-aneN}_4)\text{Cl}]^+$

The Hg-N bond distances in the complex, $[\text{Hg}([\text{14}]\text{-aneN}_4)\text{Cl}]^+$ are $\text{Hg-N}_1 = 2.42$, $\text{Hg-N}_2 = 2.28$, $\text{Hg-N}_3 = 2.38$ and $\text{Hg-N}_4 = 2.38 \overset{\circ}{\text{A}}$. These distances are much larger than the M-N distances in complexes having

a square planar geometry of the nitrogen atoms of a macrocyclic ligand.

The definitive resolution of the structure of the complex, $[\text{I}([\text{14}]\text{-aneN}_4)][\text{MoF}_6]$ must await an x-ray study, however, the following suggestions can be made. Iodine in the complex, $[\text{I}([\text{14}]\text{-aneN}_4)]^+$, is pseudo-seven coordinate with three lone pairs, hence there are three possible geometrical arrangements: the pentagonal bipyramid (Figure 5a) of symmetry D_{5h} ; the capped octahedron (Figure 5b), symmetry C_{3v} and the capped trigonal prism (Figure 5c) of symmetry C_{2v} . These geometries are readily interconvertible hence seven coordinate complexes, in general, are stereochemically non-rigid.²⁵⁴

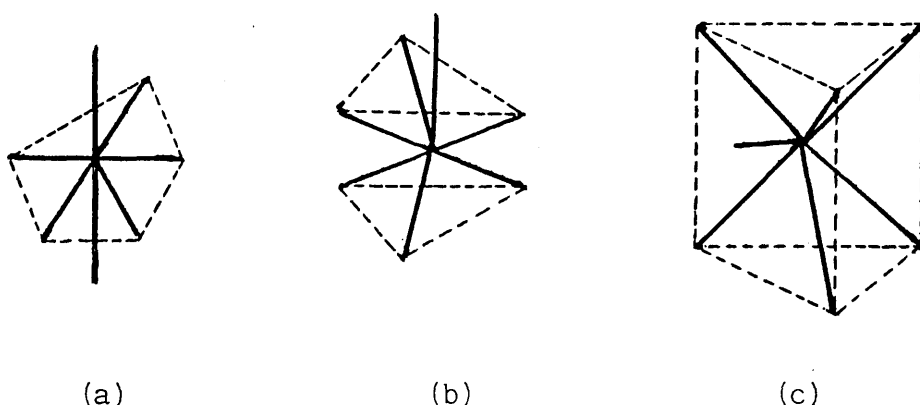


Figure 5: Geometric arrangements of seven-vertex polyhedra.

Therefore the macrocyclic ligand has to adopt a conformation that is compatible with one of these geometries. A pentagonal-pyramidal coordination of tellurium in a macrocyclic tetradentate complex, $[(\text{cyclenH}_3)_2\text{Te}_2\text{O}_2]^{2+}$, based on an underlying tellurium(IV) pentagonal-bipyramid with a lone pair in axial position, has more recently been reported.²⁵⁵

The position of the N-H stretching mode of the macrocyclic ligands in the infrared spectra of the complexes may be used as an evidence for the folded conformation of the ligand although it is not definitive. From the reported infrared spectra of the metal-[14]-aneN₄ complexes, the N-H stretching mode occurs in the region

3260-3300 cm^{-1} in complexes having a square planar geometry of the ligand.¹²⁵ The position of the N-H stretching mode is shifted towards lower energy if the ligand has a folded conformation, for example, in the complexes, $[\text{M}([\text{14}]\text{-aneN}_4)]^{2+}$, ($\text{M} = \text{Cd}^{2+}$, Hg^{2+} and Pb^{2+}), it is observed at 3210 cm^{-1} .²⁵³ Also the N-H bending mode is too weak to be observed in the normal square planar geometry of the ligand whereas in a folded conformation, it becomes strong enough to be observed in the infrared spectrum. The infrared spectra of the complexes, $[\text{IL}][\text{MoF}_6]$, ($\text{L} = [\text{14}]\text{-aneN}_4$ or $[\text{15}]\text{-aneN}_4$), indicate the N-H stretching and bending modes respectively at $\bar{\nu}_{\text{max}}$ 3200 and 1620 cm^{-1} .

The reactions of $[\text{Fe}(\text{NCMe})_6]^{2+}$ with macrocyclic ligands, $[\text{14}]\text{-aneN}_4$ or $[\text{15}]\text{-aneN}_4$, result in the formation of the complexes, $[\text{FeL}(\text{NCMe})_2]^{2+}$. The infrared spectra of the complexes indicate that the N-H stretching mode is at $\bar{\nu}_{\text{max}}$ 3290 cm^{-1} whereas the N-H bending mode is not observed. Cyclic voltammetry of the complexes indicates that the half-wave potential ($E_{1/2}$) for the couple $\text{FeL}^{3+}/\text{FeL}^{2+}$ is 0.325V vs Ag^+/Ag^0 . This value of the half-wave potential differs from the $E_{1/2}$ value of the couple, $\text{FeL}^{3+}/\text{FeL}^{2+}$, (0.54V vs Ag^+/Ag^0) previously determined for the salt, $[\text{Fe}([\text{14}]\text{-aneN}_4)(\text{NCMe})_2][\text{ClO}_4]_2$, in MeCN.²⁵⁶ The cyclic voltammogram of the complex, $[\text{Fe}([\text{14}]\text{-aneN}_4)(\text{NCMe})_2][\text{PF}_6]_2$, in MeCN solution (Figure 2) consists of a quasi-reversible wave, an indication of the oxidation $\text{Fe}^{\text{II}} \rightleftharpoons \text{Fe}^{\text{III}}$, possible only due to the stabilization of the Fe^{III} state by the ligand. In comparison the cyclic voltammogram of the complex, $[\text{Fe}(\text{NH}_3)_6]^{2+}$, described in chapter 3, consists of only the irreversible oxidation wave due to the inability of NH_3 to stabilize the Fe^{III} state under the conditions used.

The ligand, $[\text{14}]\text{-aneN}_4$, is well-known for its ability to

stabilize high oxidation states of several metals. A number of Ni^{II} 257 and Ag^{II} 258 complexes having coordinated macrocyclic ligands, ([14]-aneN₄) have been oxidised to the corresponding M^{III} cations using NO⁺ as an oxidising agent, which itself is reduced to NO. Iron(II), in the complexes, [FeL(NCMe)₂][PF₆]₂, (L = [14]-aneN₄ or [15]-aneN₄), is oxidised to Fe^{III} when reacted with NO⁺. The coordination of NO, formed as a result of the redox reaction, to the Fe^{III} centre is indicated by a strong band at $\bar{\nu}_{\max}$ 1945 cm⁻¹, in the infrared spectra of the Fe^{III} complexes. The band at $\bar{\nu}_{\max}$ 1945 cm⁻¹ indicates that NO is ligated as the neutral ligand (3e⁻ donor).²⁵⁹ Therefore, the products formed as a result of the oxidation of the Fe^{II} complexes, [FeL(NCMe)₂][PF₆]₂ using NOPF₆ as an oxidising agent, are formulated as [Fe^{III}L(NO)(NCMe)][PF₆]₃. By analogy with the oxidation of Fe^{II} to Fe^{III} observed in the presence of ligated [14]-aneN₄, it is possible that [I[14]-aneN₄]⁺ may be oxidised to a higher oxidation state of iodine using an appropriate oxidising agent. This experiment would be the starting point for future work.

5:4 Conclusions

The chemistry of iodine (+1) in MeCN, can be placed on a firm basis as a result of the present work. It is apparent that analogies exist between iodine (+1) and metal cation coordination chemistry in MeCN. The ligands, Me₂S, tmtu, 2,2-bipyridyl, [14]-aneN₄ and [15]-aneN₄ are strong enough to displace coordinated MeCN in the cation, [I(NCMe)₂]⁺ and thus are effective in stabilizing iodine (+1). The ligands, [14]-aneN₄ and [15]-aneN₄ (L) are well known for their ability to stabilize high oxidation states of several metals. It is, therefore, possible that iodine (+1) in the complex [IL][MoF₆], may be oxidised to a higher oxidation state by using an appropriate

oxidising agent. Iodine (+1) in the complexes, $[\text{IL}][\text{MoF}_6]$, is pseudo-seven coordinate with three lone pairs of electrons, hence the structure of these complexes might be a fertile source of unusual coordination polyhedra.

5:5 Experimental

5:5:1 Preparation of Bis(acetonitrile)iodine(I) Hexafluorometalates(V).⁴⁸

(a) Bis(acetonitrile)iodine(I)hexafluoromolybdate(V).

A solution of iodine (0.2mmol) in MeCN (5ml) was prepared in a double limbed reaction vessel and MoF_6 (6mmol) was added to the frozen solution. On warming the mixture to room temperature, a rapid colour change, brown to green to yellow was observed. The final solution was pale yellow in colour from which a white solid was isolated after removing the volatile material. The infrared spectrum of the solid consisted of bands due to coordinated MeCN, $\bar{\nu}_{\text{max}}$ 2310, 2295, 2280 1030 and 940 cm^{-1} and the MoF_6^- anion, $\bar{\nu}_{\text{max}}$ 630 and 245 cm^{-1} .

(b) Bis(acetonitrile)iodine(I) hexafluorouranate(V).

Uranium hexafluoride (6mmol) was added to a frozen solution of iodine (0.2mmol) in MeCN (5ml). The colour of the solution changed from brown to green as the UF_6 melted onto frozen solution of iodine in MeCN. The final solution was pale green from which a pale green solid was isolated after removal of the volatile material. The infrared spectrum of the solid indicated the presence of coordinated MeCN, $\bar{\nu}_{\text{max}}$, 2305, 2295, 2280, 1030 and 940 cm^{-1} and the UF_6^- anion, $\bar{\nu}_{\text{max}}$ 520 cm^{-1} .

5:5:2 Reactions of $[\text{I}(\text{NCMe})_2][\text{MF}_6]$, (M = Mo or U), with Me_2S in MeCN.

A mixture of $[\text{I}(\text{NCMe})_2][\text{UF}_6]$ (0.5mmol), dimethyl sulphide (5mmol) and MeCN (5ml) was allowed to warm to room temperature when a green

solution was formed. A green solid was isolated from this solution and was identified as bis(dimethyl sulphide)iodine(I) hexafluorouranate(V).

Found: C, 7.9; H, 1.9; F, 18.7; I, 20.9; S, 10.4; U, 39.6.

$C_4H_{12}F_6IS_2U$ requires C, 7.9; H, 1.9; F, 18.9; I, 21.0; S, 10.5;

U, 39.5%. The infrared spectrum of the solid is listed in Table 1.

The electronic spectrum of the complex, $[I(Me_2S)_2][UF_6]$, in MeCN solution showed the characteristic f-f transitions of the UF_6^- anion.

The reaction of dimethylsulphide (5mmol) with $[I(NCMe)_2][MoF_6]$ (0.5mmol) in MeCN (5ml) solution resulted in the formation of a yellow solution. A yellow solid was obtained from this solution after removal of the volatile material. By analogy with the complex, $[I(Me_2S)_2][UF_6]$, the solid was identified as bis(dimethylsulphide) iodine(I) hexafluoromolybdate(V). The infrared spectrum of the complex, $[I(Me_2S)_2][MoF_6]$, is listed in Table 1.

5:5:3 Reactions of $[I(NCMe)_2][MoF_6]$ in MeCN.

(a) with tetramethylthiourea.

The salt, $[I(NCMe)_2][MoF_6]$, (0.5mmol) was loaded in one limb of a reaction vessel and tmtu (1.0mmol) into the other. MeCN (5ml) was distilled onto tmtu and the resulting solution was mixed with the salt, $[I(NCMe)_2][MoF_6]$. From the orange solution so obtained, an orange sticky solid was isolated after removal of the volatile material. By analogy with the complex, $[I(Me_2S)_2][MoF_6]$, the solid was identified as bis(tetramethylthiourea) iodine(I) hexafluoromolybdate(V). The infrared spectrum of the solid, $[I(tmtu)_2][MoF_6]$, is listed in Table 2.

(b) with 2,2-bipyridyl

The complex, $[I(NCMe)_2][MoF_6]$, (0.5mmol) and bipyridyl (1.0mmol) (mole ratio 1:2) were loaded into each of the two limbs of a reaction

vessel. MeCN (5ml) was distilled onto bipyridyl and the solution so obtained was mixed with $[I(NCMe)_2][MoF_6]$. A light brown solid was isolated from the resulting solution. The infrared spectrum of the solid indicated bands due to coordinated bipyridyl and the MoF_6^- anion and is listed in Table 3. By analogy with the complex, $[I(hmta)_2][I_3]$, (hmta = hexamethylenetetramine), the solid was identified as bis(bipyridyl) iodine(I) hexafluoromolybdate(V).

The solid isolated from a mixture of $[I(NCMe)_2][MoF_6]$, (0.5mmol), bipyridyl, (0.5mmol) (mole ratio 1:1) and MeCN (5ml), indicated the presence of both coordinated MeCN and bipyridyl in its infrared spectrum.

(c) with 1,4,8,11-tetraazacyclotetradecane.

A solution of $[I(NCMe)_2][MoF_6]$ (0.5 mmol) in MeCN (5ml) was mixed with [14]-ane N_4 (0.5mmol) at room temperature. The clear solution was decanted into the empty limb and a dark purple solid was isolated from this solution. The solid was identified as mono-(1,4,8,11-tetraazacyclotetradecane) iodine(I) hexafluoromolybdate(V).

Found: C, 22.0; H, 4.4; I, 23.2; N, 10.0. $C_{10}N_{24}F_6IMoN_4$ requires C, 22.2; H, 4.5; I, 23.5; N, 10.3%. The infrared spectrum of the solid $[I[14]-aneN_4][MoF_6]$ is listed in Table 4. The samples for electronic and n.m.r. spectroscopy were prepared as described in chapter 6.

(d) with 1,4,8,12-tetraazacyclopentadecane.

A mixture of $[I(NCMe)_2][MoF_6]$ (0.5mmol), [15]-ane N_4 (0.6mmol) and MeCN (5ml) was shaken for a few minutes at room temperature. The clear solution was decanted into the empty limb from which a mustard coloured solid was isolated after removal of the volatile material. The solid was identified as mono(1,4,8,12-tetraazacyclopentadecane) iodine(I) hexafluoromolybdate(V). Found: C, 23.5; H, 4.5; I, 22.6;

N, 9.9. $C_{11}H_{26}F_6IMoN_4$ requires C, 23.8; H, 4.7; I, 22.9; N, 10.1%. The infrared spectrum of the solid $[I[15]-aneN_4][MoF_6]$ is listed in Table 4.

(e) with trimethyl phosphine

A solution of $[I(NCMe)_2][MoF_6]$ (0.5mmol) in MeCN (5ml) was mixed with trimethylphosphine (3.0mmol) at room temperature. A dark brown solid was isolated from the resulting solution after removal of volatile material. The infrared spectrum of the solid consisted of bands at $\bar{\nu}_{max}$ 1300, 1280 (CH sym.bend) 950, 875 (CH_3 rock), 745, 725 (P-C asym.str), 660 (P-C sym.str), 620 ($\nu_3 MoF_6$), 325 (P-P bend) and 245 cm^{-1} ($\nu_4 MoF_6^-$). The $^{31}P\{-^1H\}$ n.m.r spectrum of the solid in CD_3CN consisted of resonances at 32.0, 7.4, 3.3, 1.3, -10.6, -14.5 and -27.7 ppm. Some of these resonances were singlets and some were multiplets. The electronic spectrum of the solid in MeCN contained a strong band at $\bar{\nu}_{max}$ 17200 cm^{-1} . The solid was thus assumed to be a mixture of species.

(f) with trimethylphosphite.

A mixture of $[I(NCMe)_2][MoF_6]$ (0.5mmol.), $P(OMe)_3$ (3.0mmol) and MeCN (5ml) was allowed to warm to room temperature. The solution was shaken for a few minutes and an oily mass was obtained from the solution after removal of the volatile material. The infrared spectrum of the mass consisted of bands at $\bar{\nu}_{max}$ 1320 (CH_3 rock), 990, 930 ($P(OC)_3$ str), 800, 755 ($P(O)_3$ str), 620 ($\nu_3 MoF_6^-$), 510 ($P(OC)_3$ bend) and 245 cm^{-1} ($\nu_4 MoF_6^-$). A detailed study of the complex was not attempted because of its oily nature.

5:5:4 Reactions of $[\text{Fe}(\text{NCMe})_6][\text{PF}_6]_2$ in MeCN(a) with 1,4,8,11-tetraazacyclotetradecane

A solution of $[\text{Fe}(\text{NCMe})_6][\text{PF}_6]_2$ (0.2mmol) in MeCN (5ml) was mixed with [14]-aneN₄ (0.3mmol) in a reaction vessel, at room temperature. The purple coloured liquid phase was decanted into the empty limb and a purple solid was obtained from the solution. The infrared spectrum of the solid consisted of bands due to coordinated [14]-aneN₄, MeCN, and the PF_6^- anion. The infrared spectrum of the solid is listed in Table 7. By analogy with the known $\text{Fe}^{\text{II}}\text{-[14]-aneN}_4$ complex, the solid was identified as $[\text{Fe}(\text{[14]-aneN}_4)(\text{NCMe})_2][\text{PF}_6]_2$.

(b) with 1,4,8,12-tetraazacyclopentadecane.

A mixture of $[\text{Fe}(\text{NCMe})_6][\text{PF}_6]_2$ (0.2mmol), [15]-aneN₄ (0.3mmol) and MeCN (5ml) was shaken for a few minutes at room temperature. The resulting lemon coloured liquid phase was decanted into the empty limb of the reaction vessel. A lemon yellow solid was obtained from the solution after removing the volatile material. The infrared spectrum of the solid contained bands due to coordinated [15]-aneN₄, MeCN and the PF_6^- anion. The infrared spectrum is listed in Table 7. By analogy with the known $\text{Fe}^{\text{II}}\text{-[15]-aneN}_4$ complex, the solid was formulated as $[\text{Fe}(\text{[15]-aneN}_4)(\text{NCMe})_2][\text{PF}_6]_2$.

5:5:5 Reactions of NOPF_6 in MeCN.(a) with $[\text{Fe}(\text{[14]-aneN}_4)(\text{NCMe})_2][\text{PF}_6]_2$.

The solution of NOPF_6 (0.2mmol) in MeCN (5ml) was mixed with $[\text{Fe}(\text{[14]-aneN}_4)(\text{NCMe})_2][\text{PF}_6]_2$ (0.2mmol) when a yellow coloured solution was formed. A yellow solid was isolated from this solution after removal of the volatile material. The infrared spectrum of

the solid indicated bands due to coordinated [14]-aneN₄, MeCN and the PF₆⁻ anion with the addition of a strong band at $\bar{\nu}_{\max}$ 1945 cm⁻¹. This band at $\bar{\nu}_{\max}$ 1945 cm⁻¹ was assigned to the NO stretching mode. The electronic spectrum of the solid in MeCN solution consisted of two bands (shoulders) at $\bar{\nu}_{\max}$ 24100 and 27000 cm⁻¹. The solid was formulated as [Fe([14]-aneN₄)(NO)(NCMe)][PF₆]₃ on the basis of its infrared spectrum.

(b) with [Fe([15]-aneN₄)(NCMe)₂][PF₆]₂.

A mixture of NOPF₆ (0.2mmol), MeCN (5ml) and [Fe([15]-aneN₄)(NCMe)₂][PF₆]₂ (0.2mmol) was shaken for a few minutes at room temperature. An orange solid was isolated from the resulting solution after removing the volatile material. The infrared spectrum of the solid consisted of bands due to coordinated [15]-aneN₄, MeCN and the PF₆⁻ anion. A strong band at $\bar{\nu}_{\max}$ 1945 cm⁻¹ was assigned to the NO stretching mode. The electronic spectrum of the solid in MeCN solution consisted of a strong charge transfer band, the d-d bands were thus obscured and not observed. The solid was formulated as [Fe([15]-aneN₄)(NO)(NCMe)][PF₆]₃ on the basis of its infrared spectrum.

5:5:6 Cyclic Voltammetry of Iodine(I) and Iron(II) Complexes in MeCN Solution.

Cyclic voltammetry studies were carried out using the experimental procedure described in chapter 6. The complexes studied were [IL₂][MoF₆], (L = Me₂S, tmtu or bipy), [IL][MoF₆], (L = [14]-aneN₄ or [15]-aneN₄), [FeL(NCMe)₂][PF₆]₂, L = [14]-aneN₄ or [15]-aneN₄. In the case of iodine(I) complexes, MoF₆⁻ was used as an internal reference whereas for Fe^{II} complexes, ferrocene was used as an external reference. The half-wave potential of the couple Cp₂Fe/Cp₂Fe⁺ equal to 0.07V vs

Ag^+/Ag^0 ⁴⁶ and 0.16V vs S.C.E. ²⁶⁰ was taken as a reference value.

The cyclic voltammetry of the I^+ complexes and the iron(II) complexes, $[\text{FeL}(\text{NCMe})_2][\text{PF}_6]_2$, (L = 14-ane N_4 and 15-ane N_4), was studied in a low temperature cell shown in Figure 9 of Chapter 6. The salt, $[\text{Fe}(\text{NH}_3)_6][\text{PF}_6]_2$, was studied in a room temperature cyclic voltammetric cell shown in Figure 8 of Chapter 6.

CHAPTER SIX

Experimental Techniques

A number of techniques were used during the course of this project to synthesize and characterize the complex compounds both in solution and solid state. Some general outlines concerning the theory and the experimental aspects of these techniques are described here.

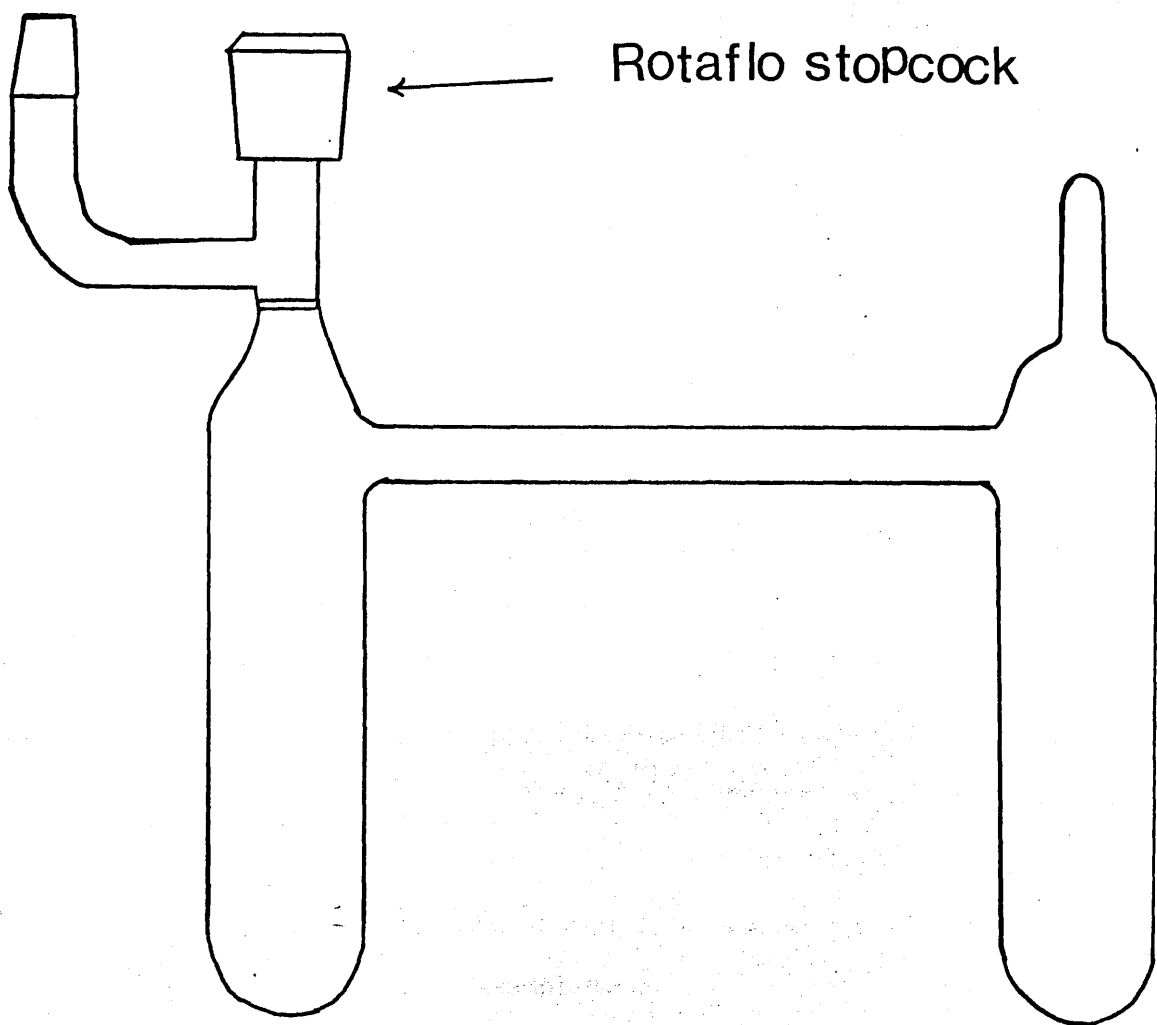
6:1 Vacuum Line and Dry Box Techniques.

All manipulations were carried out in a conventional Pyrex glass vacuum line. A rotary oil pump (Edwards high vacuum) and a mercury diffusion pump (Jencons) arranged in series were capable of providing a vacuum of 10^{-4} Torr. Standard glass joints were sealed with Apiezon black and greased with high vacuum grease Apiezon N or Voltalef Kel-F. The polytetrafluoroethylene (P.T.F.E.) Pyrex stop-cocks (J.Young or Rotaflo) were used when required. All the glass-ware was flamed out before use. Reactions were carried out in Pyrex double limb vessels (Figure 1) fitted with J.Young or Rotaflo stop-cocks. Similar vessels with one limb replaced by an n.m.r. tube, Pyrex capillary for Raman or a Spectrosil cell for U.V., were used to prepare samples for spectroscopic analysis. Non-volatile compounds were loaded in the vessels in a N_2 -atmosphere glove box (Lintott, $H_2O < 5\text{ppm}$). The box was provided with an evacuable air-lock on one end to be used as a transfer port. Molecular sieves and manganese oxide were used for the removal of moisture and oxygen respectively from the box.

6:2 Vibrational Spectroscopy.^{261, 262}

Infrared and Raman spectroscopy were used to identify the coordinated ligands and the fluoroanions in the complexes synthesized during the course of the present study. Vibrational modes of a molecule are

Figure 1. Double-Limbed Reaction Vessel.



excited by the absorption of quanta whose energy lies in the infrared region of the spectrum from about 4000 cm^{-1} downwards. The vibrational transitions are also detected in Raman scattering. The selection rules for infrared absorption differ from those governing Raman scattering. A molecular vibration is infrared active if there is an overall change of the electric dipole moment during a normal mode of vibration. Raman scattering is produced if the molecule vibrates in a way that its polarizability is changed during the vibration. The mutual exclusion rule for a polyatomic molecule having a centre of symmetry states that the vibrations symmetric with respect to the centre of symmetry are Raman active but infrared inactive and the vibrations antisymmetric with respect to the centre of symmetry are infrared active but Raman inactive.

The information obtained from vibrational spectroscopy depends on the size and symmetry of a molecule. A vibrational frequency is directly related to a force constant which in turn is related to the bond length. For example in the MeCN molecule upon coordination to a cation via nitrogen, the force constant of the C≡N bond is significantly increased as compared to that of the free molecule. This increase in the force constant causes the C≡N stretching frequency to be shifted to higher wave-number.^{18,19} The number of bands expected in the spectrum of a molecule is predictable from the symmetry of the molecule by the method of group theory as illustrated in the following examples.

Acetonitrile molecule belongs to the point group C_{3v} and has eighteen degrees of freedom. The eighteen cartesian displacement vectors generate the following reducible representation.

C_{3v}	E	$2C_3$	$3\sigma_v$
Γ	18	0	4

This can be reduced giving

$$\Gamma = 5A_1 + A_2 + 6E$$

Eliminating the irreducible representations corresponding to translations and rotations, the genuine normal modes are

$$4A_1 + 4E$$

The inspection of the group C_{3v} character table shows that the A_1 and E modes of vibration are both infrared and Raman active.

The complex fluoroanions, MF_6^- , ($M = P, Mo, W$ or U) belong to the point group O_h . The twenty one cartesian displacement vectors form a basis for the following representation:

O_h	E	$8C_3$	$6C_2$	$6C_4$	$3C_2(=C_4^2)$	i	$6S_4$	$8S_6$	$3\sigma_h$	$6\sigma_d$
Γ	21	0	-1	3	-3	-3	-1	0	5	3

The representation, Γ , reduces as follows:

$$\Gamma = A_{1g} + E_g + T_{1g} + 3T_{1u} + T_{2g} + T_{2u}$$

The O_h group character table shows that the translations account for T_{1u} , the rotations for T_{1g} , leaving the genuine internal vibrations

$2T_{1u}$	infrared active
A_{1g}, E_g, T_{2g}	Raman active
T_{2u}	inactive

The Raman spectroscopic technique, in the present work, did not prove to be successful as the samples either burned or decomposed in the laser beam.

Infrared Sampling Procedure.

For solid samples, a mull or paste was made by grinding a few milligrams (2-5mg) of the solid in an agate mortar with a drop of liquid paraffin oil e.g. Nujol or a fluorinated liquid polymer e.g. Fluorolube. The paste was formed into a thin film by compressing it between silver chloride or silicon plates which were then mounted in a suitable sample holder. The spectrum was recorded over the region $4000-400\text{ cm}^{-1}$ (AgCl plates) or $400-200\text{ cm}^{-1}$ (Silicon plates). Gaseous samples were studied by permitting the volatile material or the gas to expand into an evacuated 5 cm path length cell at a measured pressure. The cell was made of Pyrex glass with AgCl windows joined to the glass with silicon sealant (RS Components Ltd).

6:3 Electronic Spectroscopy. ^{263,264}

Electronic spectroscopy is associated with electronic transitions which usually occur in the visible and ultraviolet region of the spectrum, that is $10,000 - 50,000\text{ cm}^{-1}$. Such transitions mostly involve non-bonding and pi electrons and may occur through electric dipole, magnetic dipole or electric quadrupole mechanisms.²⁶⁵ Light of these wave numbers may be absorbed by a complex for a variety of reasons. These possible interactions are classified as follows:

(1) Ligand spectra. Ligands such as water and organic molecules possess characteristic absorption bands that are normally in the ultraviolet.

(2) Charge transfer spectra. These spectra arise from transitions between orbitals centered mainly on the ligand to one centred on the metal atom or vice versa. Thus an electron is transferred either from the metal to the ligand or from the ligand to the metal. The charge transfer transitions are mostly allowed hence the charge

transfer bands are always strong. The main charge transfer band is usually located in the ultraviolet region frequently trailing in the visible, hence most of the charge transfer complexes are red or yellow. Because of their intensity the charge transfer bands mostly obscure the ligand field spectra if the two types of transitions are close to each other. For example in the Fe^{III} complexes, obtained from the oxidation of Fe^{II} in the present study (Chapter 5), the d-d bands were observed as weak shoulders on the charge transfer absorptions. The complexes derived from $[\text{I}(\text{NCMe})_2]^+$ and the ligands such as Me_2S , tmtu, [14]-ane N_4 and [15]-ane N_4 (Chapter 5) owe their colour to the charge transfer spectra.

(3) Ligand field spectra. The transitions responsible for these spectra arise from the splitting of the d-orbitals of a transition metal in a ligand field. The electric dipole transitions are mostly responsible for the observation of the transition metal (d-block) spectra. Transitions from one energy level to a higher energy level occur by absorption of radiations, bands shifting towards the u.v. region of the spectrum with increasing ligand field strength. These transitions are mainly of two types and a number of limitations called selection rules determine the nature of the transitions.

The first selection rule states that any transitions in which there is a change in the number of unpaired electrons, are forbidden. Thus an allowed transition is the one in which the spin state of the complex does not change. For example in a low spin Fe^{2+} complex (t_{2g}^6) having an octahedral environment, the transitions ${}^1\text{A}_{1g} \longrightarrow {}^1\text{T}_{1g}$ and ${}^1\text{A}_{1g} \longrightarrow {}^1\text{T}_{2g}$ are spin allowed whereas ${}^1\text{A}_{1g} \longrightarrow {}^3\text{T}_{1g}$ and ${}^1\text{A}_{1g} \longrightarrow {}^3\text{T}_{2g}$ transitions are spin forbidden.

The second rule, called the Laporte rule, states that in the complexes with a centre of symmetry, the allowed transitions are those

with a change of parity that is gerade to ungerade, $g \rightarrow u$, and ungerade to gerade, $u \rightarrow g$, transitions are allowed but $g \rightarrow g$ and $u \rightarrow u$ transitions are forbidden. Since all the d-orbitals have gerade symmetry hence all the d-d transitions in centrosymmetric molecules are forbidden. The Laporte rule forbidding the d-d transitions is relaxed to some extent in molecules which do not have a centre of symmetry as mixing of p- and d-orbitals can take place to some extent in such molecules. Thus the transitions can occur between d-orbitals containing different amounts of p-character. Also if the metal to ligand bonding in the complex is largely covalent, then the transitions will not be pure d-d as the p-orbitals of the ligand and the d-orbitals of the metal cause mixing.

The parity selection rule can be relaxed in a centrosymmetric molecule if the centre of symmetry is removed temporarily by an odd vibration. On mixing the vibrational and electronic parts of the wave function (so called vibronic coupling), the ground term may become mixed with a g-type vibration and the excited term with a u-type vibration. The transition thus becomes partly $g \rightarrow u$ instead of $g \rightarrow g$ and is allowed.

The position of an absorption band in the electronic spectrum corresponds to the energy of the transition and its intensity depends on the nature and quantity of the absorbing material. The relationship between the absorbance, A , the path length, l and the concentration, C , is represented by the Beer-Lambert law

$$A = KCl \quad (1)$$

where K is a constant characteristic of the material. For a path length of 1cm and the concentration expressed in moles per unit volume, the constant K becomes ϵ , the molar extinction coefficient.

Allowed transitions generally have molar extinction coefficients in the range, 10^3 to $10^5 \text{ dm}^3 \text{ mol}^{-1} \text{ cm}^{-1}$ whereas the d-d transitions are much weaker with ϵ ranging from 10^{-1} to $10 \text{ dm}^3 \text{ mol}^{-1} \text{ cm}^{-1}$.

The intensity stealing phenomenon is observed if a ligand field transition has the same energy as that of the charge transfer band. This is due to the mixing of the electronic wave function of the forbidden excited term with the allowed level resulting in electronic transitions to the excited term becoming more allowed. For example in the spectrophotometric titration of $[\text{Cu}(\text{NMe})_6]^{2+}$ with Me_2S in MeCN, the d-d band due to the intermediate species, $[\text{Cu}(\text{Me}_2\text{S})_x(\text{NMe})_{6-x}]^{2+}$ ($x = 3-5$) is too intense to be observed in the early stages of the reaction.

Sample Preparation. Sample solutions for recording the electronic spectra, were prepared in a one-limb reaction vessel provided with a 10mm Spectrosil cell. The vessels are specially designed for handling of the air and moisture sensitive compounds (Figure 2). The reactions were carried out in the vessel, the clear solution decanted into the cell and the spectrum recorded on a Beckman U.V.5270 or Perkin-Elmer Lambda 9, over the range 1600-200 nm.

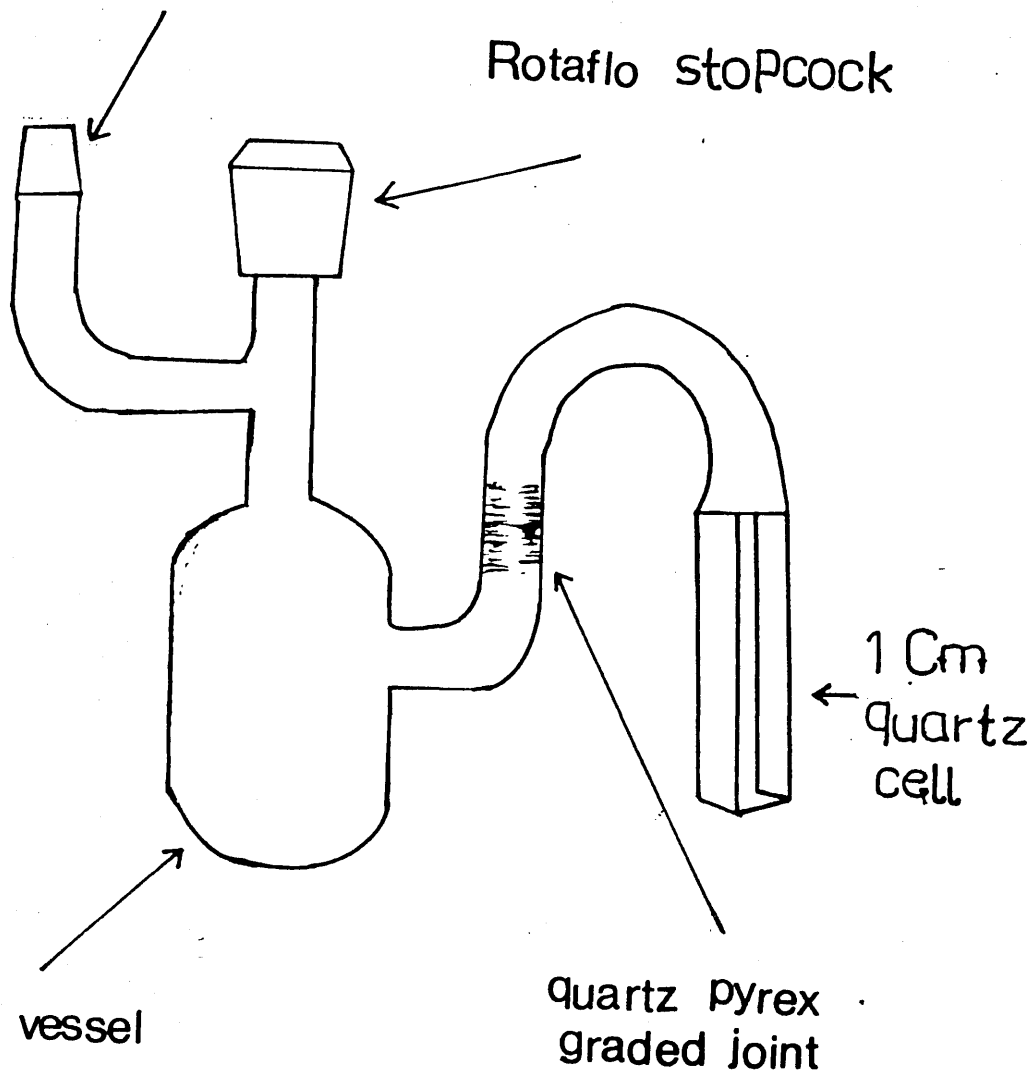
6:4 Stopped-Flow Spectroscopy.

A large number of chemical reactions involve the formation of an intermediate which has such a transitory existence that it cannot be observed by the use of conventional instrumentation. The common methods for observing such intermediates, are those involving flow or rapid mixing where the time taken to mix the reactants is greatly reduced. The reaction is then followed by recording the change in a physical property, such as absorbance, of the mixture with time.

Roughton²⁶⁶ was the first to use the stopped-flow method for

Figure 2. Evacuatable Cell for Electronic Spectroscopy.

B14 Ground glass cone



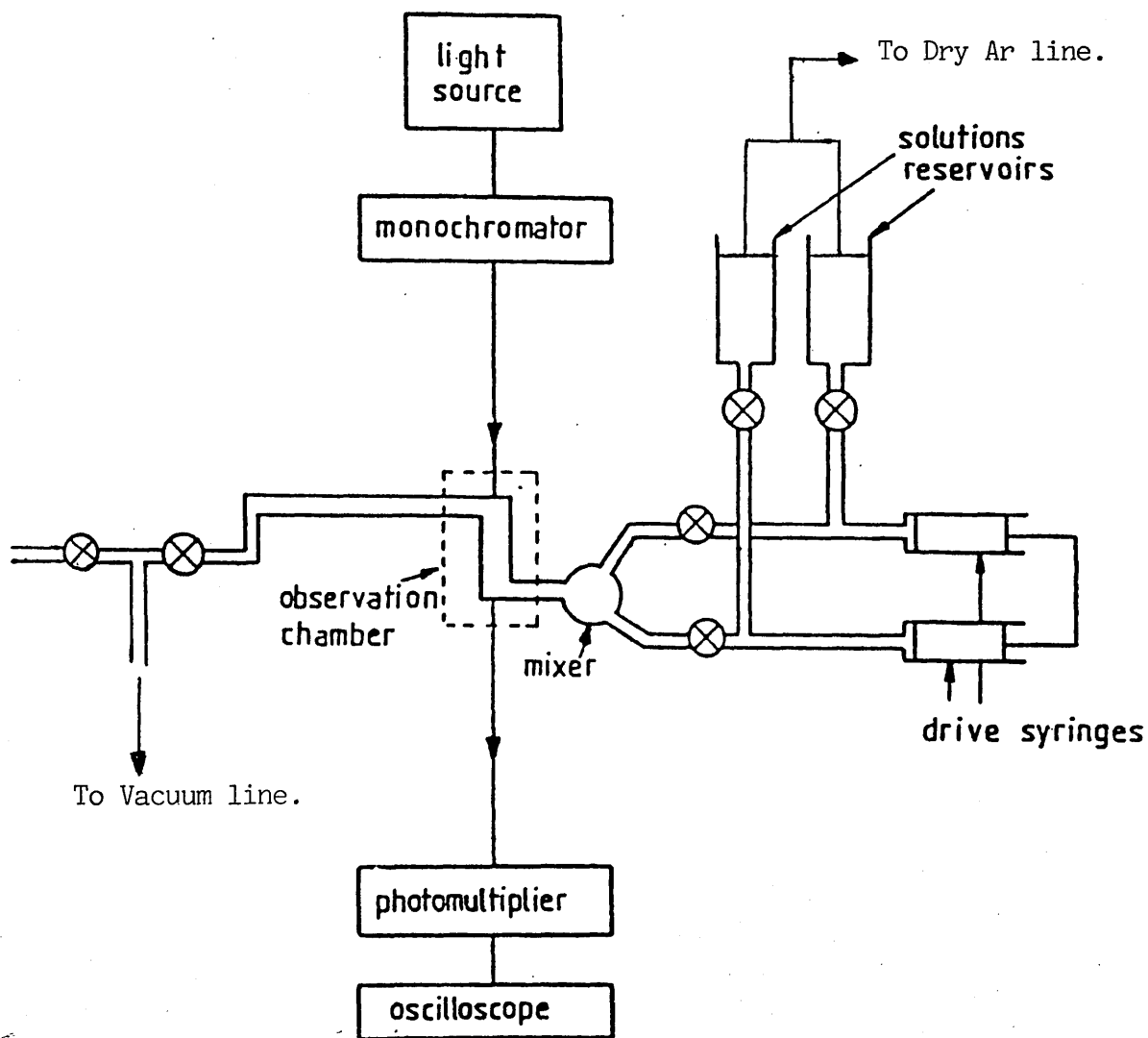
reaction times of about 10 seconds. Later, Chance²⁶⁷ improved the method to enable the study of the processes with reaction times of a few milliseconds.

Stopped-flow apparatus. A diagrammatic representation of a stopped-flow system is given in Figure 3. Stock solutions of the reagents are stored in the reservoirs from which they are fed into the drive syringes. These syringes are driven with constant pressure provided by a cylinder of nitrogen, forcing the solutions to mix rapidly in the cell. Light from a monochromatic source is passed through the cell. The transmitted light is detected by a photomultiplier connected to an oscilloscope. The oscilloscope is triggered through a pulse transmitted by a stopping plate which stops the flow of the solutions and a trace of the reaction is recorded on the oscilloscope screen. This trace is a direct measure of the changes in light intensity due to the absorbance changes occurring during the reaction. The trace is photographed from which absorbance is measured. By carrying out the experiment point by point at 10nm intervals over a range of wavelengths throughout the region of interest, it is possible to build up the spectrum of the intermediate under investigation. This is accomplished by plotting the total change in absorbance during the reaction as a function of wavelength. An example of this is shown in Figure 1 of chapter 3 for the reaction of $[\text{Fe}(\text{py})_6]^{2+}$ and $\text{P}(\text{OMe})_3$ in MeCN solution.

The stopped-flow instrument, (Hi-Tech SF-3L System with SFL-36 evacuable flow module and dry Argon line) was evacuated and flushed with argon gas prior to a run. The system was additionally flushed with anhydrous MeCN to ensure the conditions as moisture free as possible.

Figure 3.

Schematic Diagram of Stopped-flow Instrument.



Measurement of absorbance. In order to analyse the photograph of the trace recorded on the oscilloscope screen, the voltage as a function of time is converted to the equivalent absorbance. The optical density (O.D) or the absorbance is given by the expression (equation 2)

$$\text{O.D.} = \log \frac{I_o}{I_t} \quad (2)$$

where I_o is the intensity of light initially and I_t is the intensity of the transmitted light. The voltage from the photomultiplier is directly proportional to the intensity of light transmitted from the cell, so equation (2) can be expressed as

$$\text{O.D.} = \log \frac{V_o}{V_t} \quad (3)$$

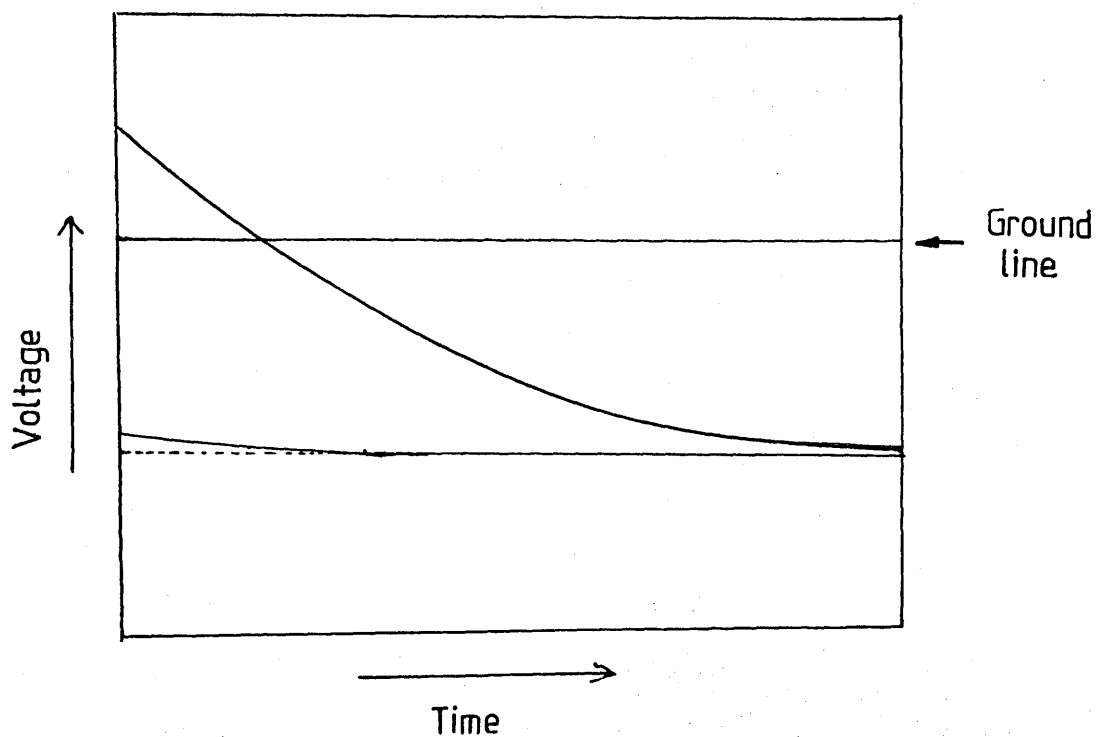
where V_o is the initial voltage and V_t is the voltage of the transmitted light. When V_o is the voltage at time 0 and V_t is the voltage at time t, then equation (3) gives the change in optical density from time 0 to time t.

For the understanding of different parameters involved in the procedure for calculation of the optical density from equation (3), a hypothetical trace is shown in Figure 4. The trace measures the voltage derived from the transmitted light thus a decrease on the trace indicates an increase in absorbance of the solution and vice versa. In Figure 4, the absorbance is increasing hence it shows the formation of a species. In the trace shown in Figure 4, the ground line represents the voltage obtained in the absence of any applied signal. This is the reference back-off abbreviated as R.B.O. From the value of the 'back-off' and a calibration factor for the

Figure 4. Trace of the Reaction, $[\text{Fe}(\text{py})_6]^{2+}$ and $\text{P}(\text{OMe})_3$ recorded at wavelength 430 nm.

Concentration of $[\text{Fe}(\text{py})_6]^{2+} = 4.5 \times 10^{-3} \text{ mol dm}^{-3}$

Concentration of $\text{P}(\text{OMe})_3 = 0.45\text{M}$



instrument, in the present case 0.005535, the absolute voltage of the ground line ($V_{B,0}$) can be calculated. To evaluate the voltage V_t , of a point on the trace at a particular time, its distance from the ground line is determined and is multiplied by the gain of the oscilloscope to get $V_t - B.O.$ This value is then added to $V_{B,0}$ to get V_t . The same trend can be applied to get V_∞ , the voltage at infinite time. Thus the optical density at intervals from t_0 to t_∞ can be measured with the help of equation (3). A representative set of data for the reaction of $[\text{Fe}(\text{py})_6]^{2+}$ and $\text{P}(\text{OMe})_3$ is given in Table 1. A plot of $-\log (O.D._\infty - O.D._t)$ versus time, t , is linear with the slope equal to $K/2.303$ and is illustrated in Figure 5.

6:5 Cyclic Voltammetry.

Cyclic voltammetry is the technique in which the current that flows in a system is recorded as a function of the applied potential, however, the potential axis is also a time axis. The theory and technique of voltammetry have been extensively discussed.²⁶⁸ A brief outline is described here.

A voltammogram, that is the variation of current with applied potential is shown in Figure 6. This applies to a one electron reduction but the same argument can be true for an oxidation step. As the applied potential becomes increasingly negative, the current rises slowly from A to B. This residual potential is due to a condenser current, a consequence of charging of a double layer at the electrode surface, and a diffusion current due to traces of oxidisable and reducible material in the solution. At point B, near the formal electrode potential of the redox active species, the current rises sharply as reduction of the species begins. This current rises to C, where the approach of the species to the electrode and the subsequent

Table 1. The Values of O.D. and $-\log(O.D._\infty - O.D._t)$ at Particular Times for the Reaction of $[Fe(py)_6]^{2+}$ with $P(OMe)_3$ in MeCN.

Concentration of $[Fe(py)_6]^{2+} = 4.5 \times 10^{-3} \text{ mol dm}^{-3}$,

Concentration of $P(OMe)_3 = 0.45 \text{ mol dm}^{-3}$

Wavelength $\lambda = 430 \text{ nm}$.

Time (S)	$O.D._t = \log \frac{V_o}{V_t}$	$-\log(O.D._\infty - O.D._t)$
0	0	0.886
0.2	0.019	0.957
0.4	0.036	1.030
0.6	0.050	1.091
0.8	0.058	1.142
1.0	0.069	1.202
1.2	0.076	1.273
1.4	0.084	1.314
1.6	0.087	1.371
1.8	0.093	1.440
2.0	0.096	1.471
∞	0.123	-

Figure 5. Plot of $-\log(O.D._\infty - O.D._t)$ vs Time for the Reaction of $[Fe(py)_6]^{2+}$ and $P(OMe)_3$

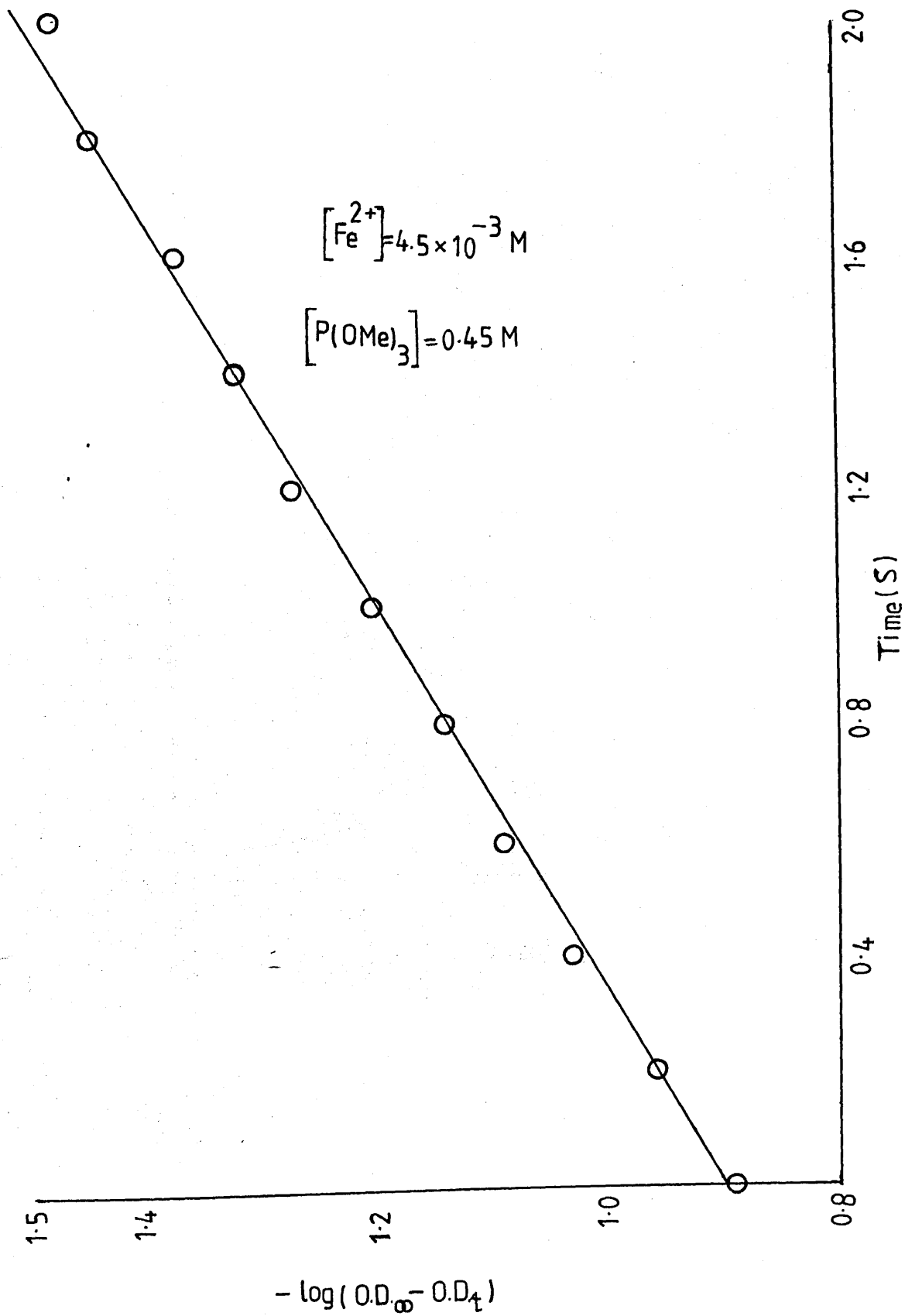
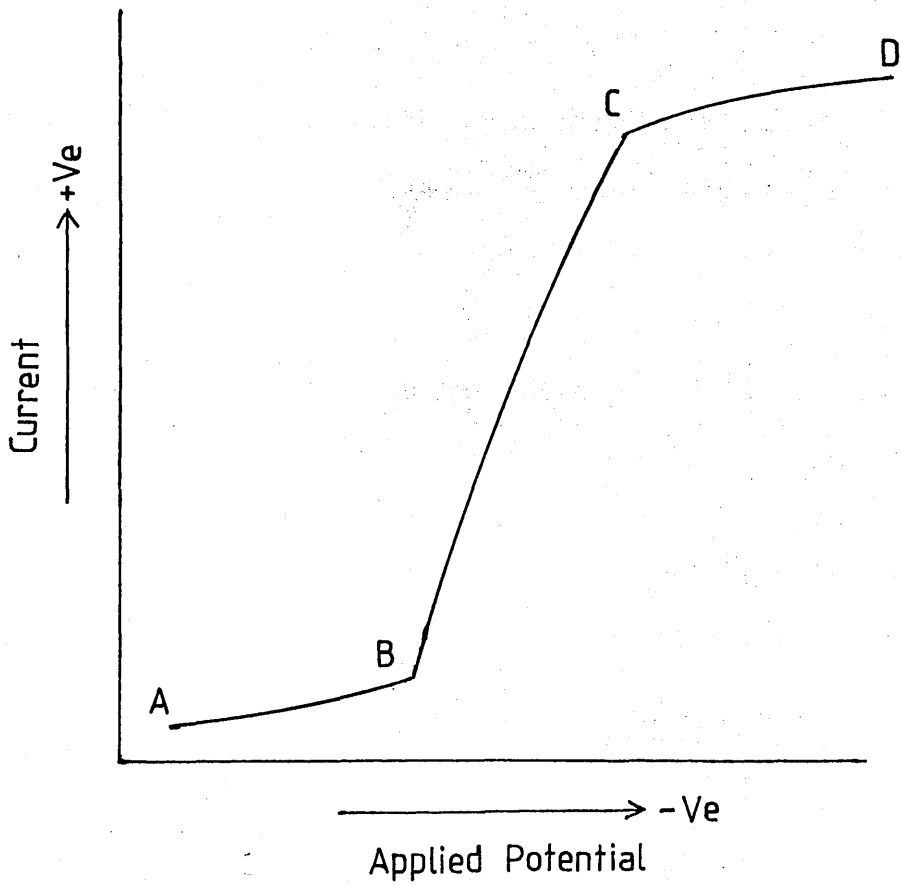
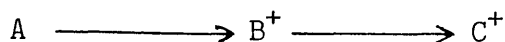


Figure 6. Current vs Applied Potential.



reduction are at a maximum as determined by diffusion. At higher negative potentials, the current rises slowly due to the residual current. As a result the current vs voltage plots assume the form of a wave. For a reversible wave, $E_{\frac{1}{2}} \approx E^{\circ}$, where $E_{\frac{1}{2}}$ is the half-wave potential and E° is the formal electrode potential. For a non-reversible wave, $E_{\frac{1}{2}}$ is not equal to E° , so the system must be tested for reversibility before equating $E_{\frac{1}{2}}$ with E° . Some waves are not reversible because one of the species in the couple is involved in a chemical reaction.

In the process



the species A is oxidised electrochemically to produce B^{+} which being chemically reactive produces C^{+} . The reduction potentials of the species, B^{+} and C^{+} , will be different hence the wave is not reversible.

In cyclic voltammetry the potential of the working electrode is changed at a constant rate, backwards and forwards, between the two limits. These limits are adjusted to lie within the voltammetric range of the solution. A typical cyclic voltammogram for a reversible one electron process, for example the $C_{p_2}Fe^{+}/C_{p_2}Fe$ couple in MeCN, is shown in Figure 7. For a reversible system ²⁶⁹

$$E_{\text{Red}} = E_{\frac{1}{2}} - \frac{0.0285}{n} \text{ V} \quad (4)$$

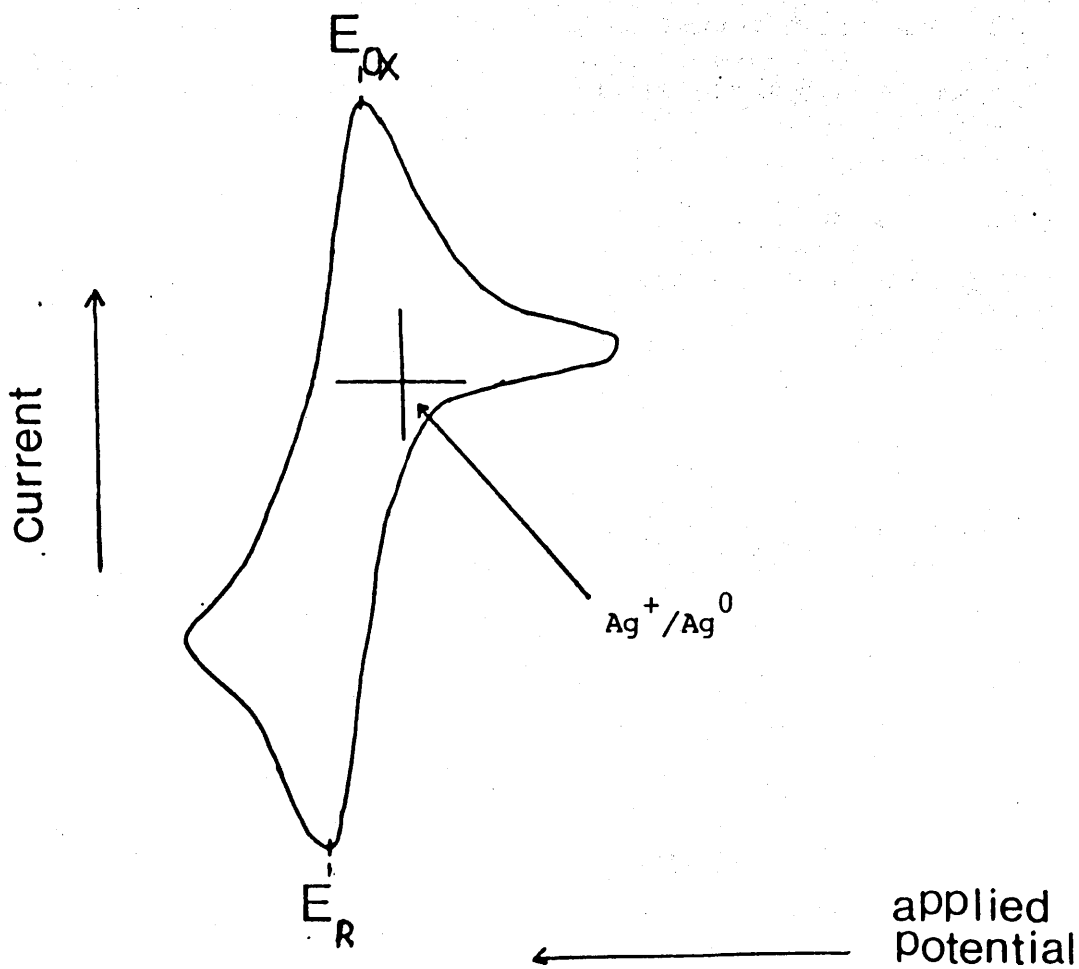
$$E_{\text{Oxid}} = E_{\frac{1}{2}} + \frac{0.0285}{n} \text{ V} \quad (5)$$

where E_{Red} and E_{Oxid} are respectively the reduction and oxidation potentials, $E_{\frac{1}{2}}$ is the half-wave potential and n , the number of electrons transferred. The separation of the peak potentials for a reversible one electron process is thus given by equation 6.

$$E_{\text{Oxid}} - E_{\text{Red}} = 57 \text{ mv} \quad (6)$$

Figure 7.

Cyclic Voltammogram of $(\eta^5\text{-C}_5\text{H}_5)_2\text{Fe}$



$$\frac{E_{ox} + E_R}{2} = E_{1/2}$$

The reversible waves obtained for rapid electron transfer process followed by a slow chemical reaction are sometimes called quasireversible waves.²⁷⁰ This situation can easily be observed in a voltammogram because if it is present, the height of the anodic peak is less than that of the cathodic peak when the starting material is the oxidised form of the couple, and vice versa for the reduced form.²⁷¹ This is exemplified by the behaviour of $[I([14]-aneN_4)] [MoF_6]$ in MeCN, where the couple, MoF_6/MoF_6^- , is quasi-reversible as described in chapter 5 (Figure 1). If one half of a redox couple is involved in a chemical reaction, for example the oxidised form, then the reduction peak will be absent altogether. This situation arises when all of the oxidised form is used in the reaction and is not reduced on the return sweep. Such a system is called an irreversible system.

Experimental Cells.

Two types of cyclic voltammetric cells have been used in the present study. The cell for studying the cyclic voltammetry of complexes at room temperature is shown in Figure 8. It contains three electrodes, a reference, a working and an auxiliary electrode. The reference electrode is Ag^+/Ag^0 (0.1 mol dm^{-3} in MeCN) and both the working and auxiliary electrodes are platinum wires (1.0 mm diameter). The platinum wires including the reference wire are vacuum sealed through the glass by spot welding to tungsten wires and sheathing the assembly in uranium glass. The cell contains three sections made from 24 and 10-15mm diameter tubing and joined by B14 and B19 greaseless O ring joints. Connections to vacuum and to storage ampoules for reference, bridging and working electrodes and for addition of solvent are by P.T.F.E. Pyrex stop-cocks. The reference, bridging and working compartments are connected using vycor-tips joined to glass by heat shrunk P.T.F.E. tubing.

Figure 8. Evacuatable Cell for Room Temperature Cyclic Voltammetry.

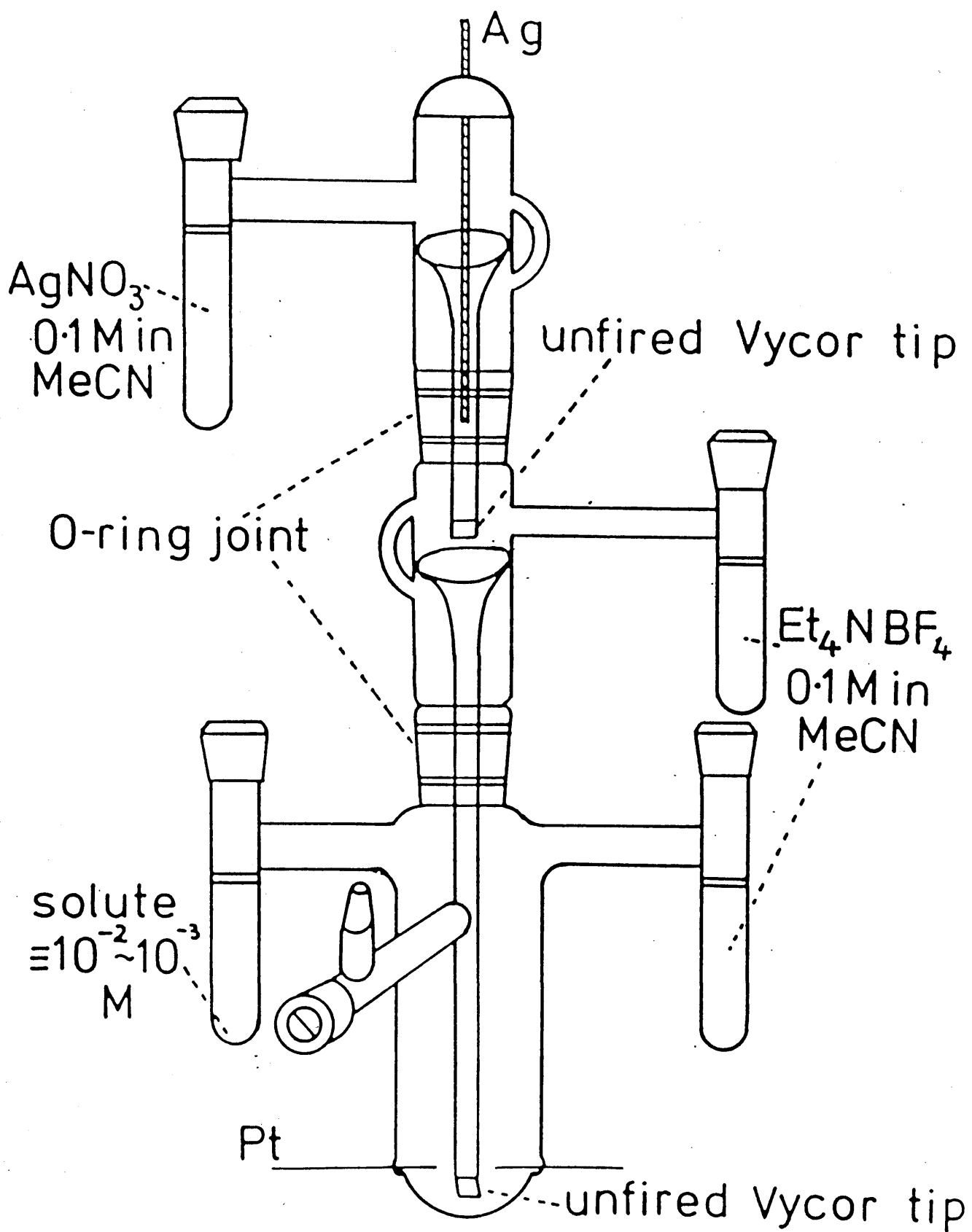
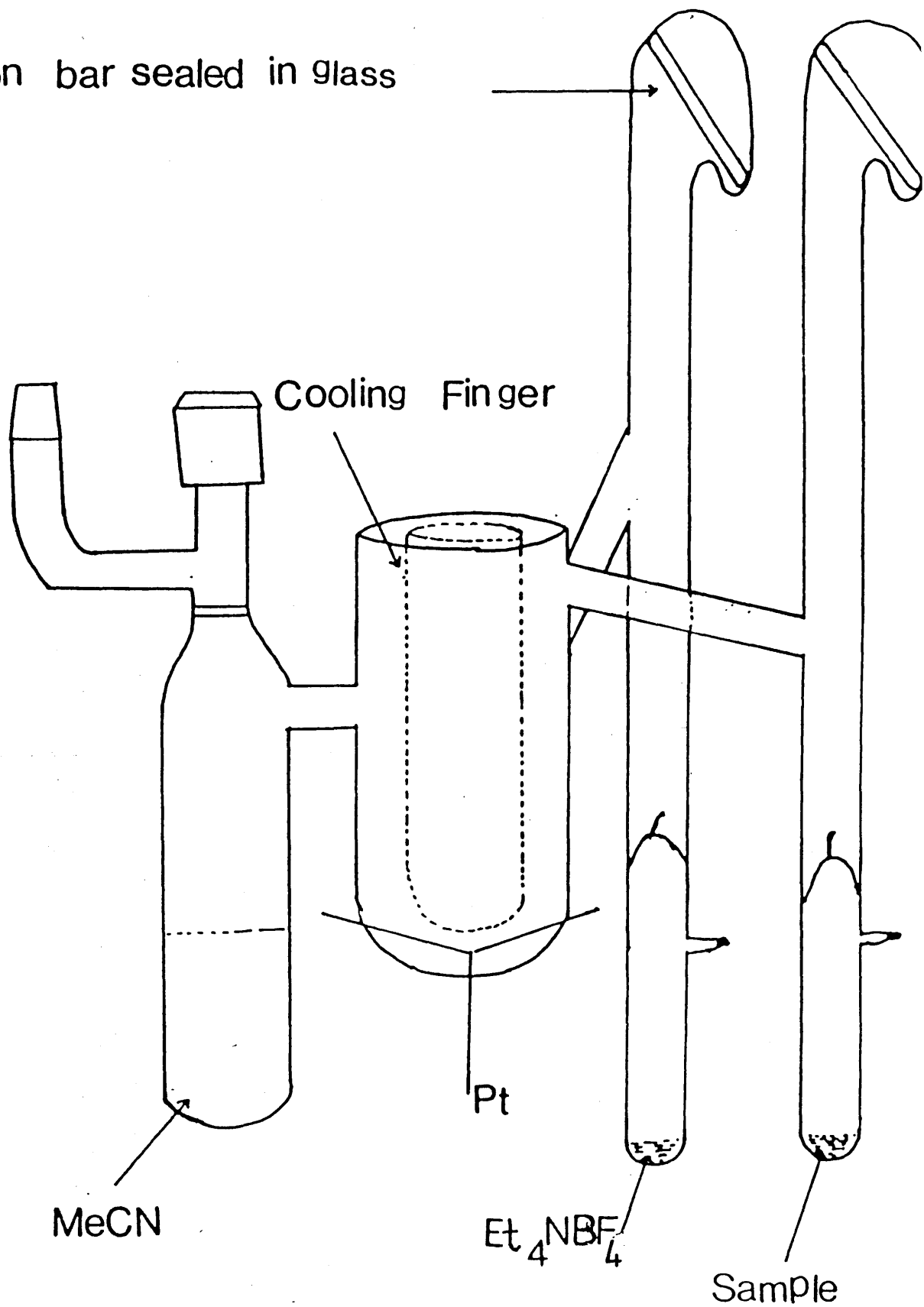


Figure 9. Evacuatable Cell for Low Temperature Cyclic Voltammetry.

Iron bar sealed in glass



The cell used to study the cyclic voltammetry of complex compounds at low temperature is shown in Figure 9. It is an all-glass cell and incorporates a cold finger which requires a slush bath to cool the solution up to a temperature of 243 K. The cell contains only the working and the auxiliary electrodes in the working compartment which on one side is provided with a vessel and on the other with two side arms. An internal or external reference has to be used in this cell. For example ferrocene and the couple, $\text{MoF}_6/\text{MoF}_6^-$, were used respectively as the external and the internal references in the present study.

Supporting electrolyte. A supporting electrolyte is required in cyclic voltammetry because of the following reasons. It decreases the electrical resistance of the solution by acting as a current carrier and thus ensures the movement of the electroactive species by diffusion and not by electrical migration in the voltage field across the cell. Tetraethylammonium tetrafluoroborate (Et_4NBF_4) was used as the supporting electrolyte in the present work and was prepared²⁷² by neutralizing fluoroboric acid with Et_4NOH using a pH meter. The product obtained was recrystallised from ethanol. It was dissolved in MeCN and the solvent removed by rotary evaporation at 313-318 K. The white compound obtained was pumped under vacuum overnight and stored in the dry box.

Experimental method. The solutions for room temperature cyclic voltammetry study, were prepared as follows. The complex was sealed in a frangible ampoule under vacuum and the C.V. cell evacuated and flamed out on the vacuum line. The cell was transferred to the dry box where the reference ampoule was loaded with the silver nitrate solution (2ml, 0.1mol dm^{-3} in MeCN). The solution of the electrolyte

(2ml and 8ml, 0.1 mol. dm^{-3} in MeCN respectively for bridging and working compartments) and the frangible ampoule containing the complex, were loaded into their respective vessels. The cell was re-attached to the line, solutions degassed and tipped into the respective compartments. The cell was then linked to a potentiostat (CV-1A, Bioanalytical Systems Inc.) and XY recorder. After determining the working potential range of the electrolyte solution, the frangible ampoule was broken, the complex dissolved in solution and the voltammogram recorded. The scan rate, current amplification factor and the voltage scale factor were varied depending upon the species under investigation.

The low temperature cell was loaded as follows. Two previously evacuated and flamed out break seal tubes were transferred to the dry box, one loaded with the complex (0.005 mmol) and the other with the electrolyte (1 mmol). The tubes were degassed, sealed and then glass blown to the side arms of the cell as shown in Figure 9. Acetonitrile (12 ml) was distilled into the vessel of the cell, the glass seal of the tube containing electrolyte was broken by a glass sheathed iron bar, the electrolyte dissolved in MeCN and the solution was tipped into the working compartment. After determining the working potential range of the electrolyte solution, the seal of the tube containing the complex was broken, the complex dissolved and its voltammogram recorded. If ferrocene was used as a reference, then the frangible ampoule containing ferrocene was broken after recording the voltammogram of the complex. After dissolving ferrocene, the voltammogram was recorded again. Cyclic voltammograms were recorded using a P.A.R. Model 175 Universal programmer and model 173 potentiostat-galvanostat.

6:6 Purification of Acetonitrile.

Acetonitrile was used as a solvent in the present work because of the reasons described in chapter 1. The solvent for the synthetic and electrochemical work should be free from all the oxidisable and reducible impurities. A number of methods have been used by different workers for the purification of MeCN. The method developed in this Department ¹⁶ is an extension of the method of Walter and Ramelay. ²⁷³ It consists of a series of refluxes of HPLC Grade S MeCN (Rathburn Chemicals Ltd) in a Pyrex still equipped with 0.75m silvered vacuum jacketed separating column. The following sequence of reagents was used; the quantities and times are given in parentheses:

- (i) anhydrous AlCl_3 (15g dm^{-3} , 1h)
- (ii) KMnO_4 + Li_2CO_3 (10g dm^{-3} each, 15 min)
- (iii) KHSO_4 (15g dm^{-3} , 1h)
- (iv) CaH_2 (20g dm^{-3} , 1h)
- (v) and (vi) P_2O_5 (1g dm^{-3} , 30 min)

After each reflux, MeCN is rapidly distilled topping and tailing by approximately 3%. During refluxing and distillation, MeCN was protected from atmospheric moisture by silica gel drying tubes. The distilled MeCN is collected in vessels containing activated alumina (neutral 60 mesh), degassed twice in vacuo and distilled in storage vessels over activated 3A molecular sieves. The purified MeCN had an absorbance of less than 0.1 (H_2O reference) at 200 nm and an apparent U.V. cut-off point ca. 175 nm.

6:7 Nuclear Magnetic Resonance Spectroscopy. ²⁷⁴

The study of the absorption of radiofrequency radiations by nuclei is called nuclear magnetic resonance spectroscopy. Absorption of radiation in the radiofrequency region of the electromagnetic

spectrum can be observed for those nuclei which have a nuclear spin(I) of $\frac{1}{2}$ or higher although the spectra are more complicated in the latter cases. The atoms which have a nuclear spin of zero, give no resonance signals and include ^{12}C and ^{16}O . Modern techniques, which involve observation by pulse irradiation followed by Fourier transformation, have now extended the n.m.r. methods to a large number of magnetic isotopes in the periodic table. The great importance of n.m.r. is that the magnetic field actually experienced by a particular nucleus is the sum of the applied field and the fields induced in the electrons around the magnetic nucleus. The atoms of the same element which are in different chemical environments resonate at slightly different values of the external field and these differences in chemical shifts may be detected and yield the structural information. Further information can be obtained from the fine structure of the n.m.r. signals which arises from the effects of spin-spin coupling. If an atom with a nuclear spin is bonded to an atom also having a nuclear spin then the local magnetic field will be affected by the orientation of the spin of the second nucleus.

In the present work ^1H , ^{13}C , ^{31}P and ^{205}Tl n.m.r. spectroscopy were employed to identify the products obtained in various redox and substitution reactions. ^{31}P n.m.r. spectroscopy was also used to study the step-wise substitution in the reaction, $[\text{Fe}(\text{NMe}_3)(\text{NCMe})_5]^{2+}$ and $\text{P}(\text{OMe})_3$ whereas ^{205}Tl n.m.r. spectroscopy was used to investigate the effects of complex fluoroanions on Tl^{I} and Tl^{III} chemical shifts.

Sample Preparation. Samples for n.m.r. spectroscopy were prepared in a 5mm precision n.m.r. tube which were sealed off in vacuo before recording the spectra. $[\text{}^2\text{H}]$ -Hydrogen labelled acetonitrile was used as a solvent. For ^{13}C and ^1H spectra, tetramethyl silane (TMS) was used as an external reference whereas for ^{31}P n.m.r. spectra,

CD₃CN was used as a 'lock' and phosphoric acid (H₃PO₄) was used as an external reference. The spectra were recorded on a Bruker-200 at 200 MHz (¹H), and Varian XL-100 at 100 MHz (¹H), 40.5 MHz (³¹P) and 25 MHz (¹³C).

6:8 Magnetic Susceptibility.

The magnetic susceptibility of the iron(II) complexes with different nitrogen donor ligands, have been determined by Gouy method. A brief outline of the method is described here.

The sample contained in a cylindrical tube is suspended between the poles of the magnet. Paramagnetic substances are attracted by the magnetic field which increases the weight of the sample; whereas diamagnetic substances are repelled causing a decrease in weight. The force(F) on the sample in the magnetic field is given by

$$F = g\Delta W = \frac{1}{2} (K - K_{\text{air}}) H^2 A \quad (7)$$

where 'g' is a constant (981 dyne sec⁻²), ΔW change in weight, K and K_{air} (c.g.s.units) are the volume susceptibilities of the sample and air respectively, H is the magnetic field strength and A, the cross sectional area of the sample. H²A is calculated by using a substance of known volume susceptibility (K). Thus by knowing H²A, the volume susceptibility of the sample can be calculated. The gram magnetic susceptibility, X, of the complex is given by the expression

$$X = \frac{K}{\rho}$$

ρ, being the density of the sample. The gram susceptibility, X, is converted to molar susceptibility X_m, by multiplying with the formula weight of the sample. To obtain the magnetic moment of the metal ion alone, a diamagnetic correction should be made.

$$\therefore X_m^{\text{corr.}} = X_m - (-\text{diamagnetic correction}) \quad (8)$$

The effective magnetic moment, $\mu_{\text{eff.}}$, of the metal ion is given by the equation

$$\mu_{\text{eff}} = 2.84 \sqrt{X_m^{\text{corr}} \cdot T} \quad (9)$$

Experimental method. A cylindrical glass tube of known volume, fitted with a quickfit stopper, was filled with the sample in the dry box. All measurements were made using a Cahn TA 450 micro-balance and a Newport $1\frac{1}{2}$ " electromagnet type C. A standard, $\text{HgCo}(\text{NCS})_4$, (mercury tetrathiocyanato cobalt(II) ; $X = 16.44 \times 10^{-6}$ c.g.s. at 293 K) was used to calculate H^2A and the value obtained was used in equation (1) to determine 'K' of the compound. A standard compound of known magnetic moment, $\text{Mn}(\text{acac})_3$ (Manganese(III)tris-(acetylacetonate)) was used to check the correct operation of the equipment. The magnetic moment of $\text{Mn}(\text{acac})_3$ was found to be 4.97 BM (literature value 4.95 BM).²⁷⁵

Acetonitrile has proved to be an ideal solvent for studying the non-aqueous chemistry of the metal and non-metal cations especially in the vacuum system. Solvated metal and non-metal cations are easily obtained in this solvent, either by the oxidation of the element with an appropriate oxidising agent or by Lewis acid - Lewis base reactions. The oxidation states of metals and non-metals which are unstable with respect to disproportionation or hydrolysis in aqueous solution, are easily accessible in this solvent. Acetonitrile is a weak ligand and is readily replaced by stronger bases such as NH_3 or PMe_3 . The solvating ability of MeCN is evident from the formation of the mononuclear cation, $[\text{I}(\text{NCMe})_2]^+$, whereas in acidic solvents such as liquid SO_2 , polynuclear cations, I_2^+ , are formed. The reaction of Cu^{I} with PMe_3 in MeCN results in the formation of the mononuclear complex, $[\text{Cu}(\text{PMe}_3)_4]^+$, whereas in benzene, Cu^{I} reacts with PMe_3 forming polynuclear complexes, $[(\text{PMe}_3)\text{CuCl}]_4$ and $[(\text{PMe}_3)_2\text{CuCl}]_2$.

The nature of cation-anion interactions in solution, is normally obtained indirectly for example by infrared, Raman, electronic and n.m.r. spectroscopy. The exceptional sensitivity of the ^{205}Tl n.m.r. chemical shift to the environment of the ^{205}Tl nucleus coupled with the accessibility of Tl^{I} and Tl^{III} fluorometalate salts in MeCN make ^{205}Tl n.m.r. spectroscopy an excellent direct probe for cation-anion interactions. The ^{205}Tl chemical shift data obtained for a number of thallium(I) complex fluoroanion salts indicate that some degree of ion-pairing is present in the MeCN solution of these salts, and that Tl^{3+} is effectively more solvated by MeCN as compared with Tl^+ hence direct ion-pairing is less important.

The simple N-donor ligands such as pyridine (py), NH_3 and NMe_3 are found to substitute the coordinated solvent molecules in the

cation, $[\text{Fe}(\text{NCMe})_6]^{2+}$, to give $[\text{FeL}_6]^{2+}$, ($\text{L} = \text{py}$ or NH_3) or $[\text{Fe}(\text{NMe}_3)(\text{NCMe})_5]^{2+}$. The cation, $[\text{Fe}(\text{NH}_3)_6]^{2+}$, exists as a discrete entity in MeCN whereas $[\text{Fe}(\text{py})_6]^{2+}$ loses pyridine to give $[\text{Fe}(\text{py})_{6-x}(\text{NCMe})_x]^{2+}$. The reaction of these high spin Fe^{II} cations with $\text{P}(\text{OMe})_3$ or PMe_3 in MeCN at room temperature are apparently similar, however, three different types of behaviour can be distinguished. The stereochemistry of the intermediate cations formed with $\text{P}(\text{OMe})_3$ depends on the identity of the N-donor ligands present. The reaction between $[\text{Fe}(\text{py})_6]^{2+}$ and $\text{P}(\text{OMe})_3$ involves the rearrangement $\text{fac} \rightarrow \text{mer}-[\text{Fe}\{\text{P}(\text{OMe})_3\}_3\text{py}_3]^{2+}$ and there is a marked preference for $\text{cis}-[\text{Fe}\{\text{P}(\text{OMe})_3\}_4\text{py}_2]^{2+}$ over the trans isomer. The reaction between $[\text{Fe}(\text{NH}_3)_6]^{2+}$ and $\text{P}(\text{OMe})_3$ appears to be similar as the only cation positively identified by $^{31}\text{P}-\{^1\text{H}\}$ n.m.r. spectroscopy is $\text{cis}-[\text{Fe}\{\text{P}(\text{OMe})_3\}_4(\text{NH}_3)_2]^{2+}$.

The reaction between $[\text{Fe}(\text{NMe}_3)(\text{NCMe})_5]^{2+}$ and $\text{P}(\text{OMe})_3$ proceeds by a different pathway. In the initial stages both cis and trans- $[\text{Fe}\{\text{P}(\text{OMe})_3\}_2(\text{NMe}_3)(\text{NCMe})_3]^{2+}$ species are observed in the $^{31}\text{P}-\{^1\text{H}\}$ n.m.r. spectra whereas in the latter stages the route involving the cation, $\text{trans}-[\text{Fe}\{\text{P}(\text{OMe})_3\}_4(\text{NMe}_3)(\text{NCMe})]^{2+}$, is dominant. This different behaviour may be rationalized in terms of the steric properties of the N-donor ligands.

The outcome of the reactions, $[\text{FeL}_6]^{2+}$, ($\text{L} = \text{NCMe}$, py or NH_3) or $[\text{Fe}(\text{NMe}_3)(\text{NCMe})_5]^{2+}$ and PMe_3 is determined solely by PMe_3 because of its being a better sigma donor to Fe^{II} than $\text{P}(\text{OMe})_3$. The identity of the N-donor ligands in these reactions is important only in the exchange reactions involving the solvent and the ligand molecules. The reactions of high spin Fe^{II} -nitrogen donor cations with $\text{P}(\text{OMe})_3$ or PMe_3 in MeCN at room temperature result in the ligation of up to five $\text{P}(\text{OMe})_3$ or three PMe_3 molecules thus emphasizing the importance of

both steric and electronic properties of the P-donor ligands in determining the outcome of the reactions.

The oxidising abilities of solvated Cu^{2+} and solvated Tl^{3+} cations in MeCN are established from the redox reactions of these cations with simple N,P and S- donor ligands such as NMe_3 , PMe_3 , Me_2S and tmtu. These redox reactions are apparently similar and result in the reduction of the metal cation to the +1 oxidation state with concomitant oxidation of the ligand. It is assumed that the ligands are oxidised to the monomeric radical cations which then combine either with the free ligand molecules or with the radical cations forming respectively the dimeric radical cations and the dimeric dications. The former situation is observed in the redox reactions involving Me_3N and Me_2S whereas the redox reactions involving PMe_3 and tmtu come under the latter category.

The chemistry of iodine(+1) in MeCN is analogous to the coordination chemistry of metal cations especially the monovalent cations such as Ag^+ . The simple ligands such as Me_2S , 2,2-bipyridyl and tmtu are able to stabilize the iodine (+1) in MeCN. The macrocyclic N-donor ligands such as 1,4,8,11-tetraazacyclotetradecane, ([14]-ane N_4) and 1,4,8,12-tetraazacyclopentadecane, ([15]-ane N_4) also form stable complexes with iodine (+1) cations. Iodine (+1) in the complexes, $[\text{IL}][\text{MoF}_6]$, (L = [14]-ane N_4 or [15]-ane N_4), is pseudo-seven coordinate with three lone pair of electrons. The possible geometric arrangements are the pentagonal bipyramid (D_{5h}), the capped octahedron (C_{3v}) and the trigonal prism (C_{2v}), hence the structure of these complexes will be a fertile source of unusual coordination polyhedra.

The ligands, [14]-ane N_4 and [15]-ane N_4 , are well known for their ability to stabilize the higher oxidation states of metals and non-metals hence it is possible that oxidation of iodine (+1) in the

complexes, $[\text{IL}][\text{MoF}_6]$, may be achieved by using an appropriate oxidising agent. This experiment would be the starting point for the future work.

REFERENCES

1. F.A.Cotton and G.Wilkinson, 'Advanced Inorganic Chemistry' 4th Edition, Wiley Interscience London, 1980, p.754.
2. N.N.Greenwood and A.Earnshaw, 'Chemistry of the elements' Pergamon Press New York, 1984, p.1265.
3. T.I.Morrison, A.H.Reis, G.S.Knapp and E.Klippert, J.Am.Chem.Soc., 1978, 100, 3262.
4. J.M.Knudsen, E.Lorsen, J.E.Moreira and O.F.Nielsen, Acta.Chem.Scand. 1975, 29A, 833.
5. N.N.Greenwood and A.Earnshaw, 'Chemistry of the elements', Pergamon Press New York, 1984, p.1387.
6. L.H.Jones, J.Chem.Phys., 1958, 29, 463.
7. C.R.Davis and K.L.Stevenson, Inorg.Chem., 1982, 21, 2514.
8. T.F.Braish, R.E.Duncan, J.J.Harber, R.L.Steffen and K.L.Stevenson, Inorg.Chem., 1984, 23, 4072.
9. C.Kappenstein and R.P.Hugel, Inorg.Chem., 1978, 17, 1945.
10. F.A.Cotton and G.Wilkinson, 'Advanced Inorganic Chemistry' 4th Edition, Wiley Interscience London, 1980, p.334 and 542.
11. K.M.Mackay and R.A.Mackay, 'Introduction to modern Inorganic Chemistry' 3rd Edition, International textbook Company, London, 1981, p.97.
12. B.G.Cox, G.R.Hedwig, A.J.Parker and D.W.Watt, Aust.J.Chem., 1974, 27, 477.
13. A.J.Parker, Chem.Rev., 1969, 69, 1.
14. J.Burgess, 'Metal ions in solution', Ellis Horwood Limited, England, 1978, p.139.
15. J.E.Huheey, 'Inorganic Chemistry', 3rd Edition, Harper International S.I. edition London, 1983, p.337.
16. J.M.Winfield, J.Fluorine Chemistry, 1984, 25, 91.
17. R.A.Walton, Quart.Rev.Chem.Soc., 1965, 19, 126; B.N.Storhoff and H.C.Lewis, Coord.Chem.Rev., 1977, 23, 1.
18. J.Zarabowitch and R.Maleki, Spectrochim.Acta. 1983, 39A, 43.
19. M.Kulioto and D.L.Johnson, J.Inorg.Nucl.Chem., 1967, 29, 769.

20. B.J.Hathaway and A.E.Underhill, J.Chem.Soc., 1961, 3091.
21. B.J.Hathaway, D.G.Holah and A.E.Underhill, J.Chem.Soc., 1962, 2444.
22. N.Bartlett, Angew.Chem.Int.Ed., 1968, 7, 433.
23. J.H.Levy, J.C.Taylor and A.B.Waugh, J.Fluorine Chem., 1983, 23, 29.
24. J.L.Beauchamp, J.Chem.Phys., 1976, 64, 929.
25. P.M.George and J.L.Beauchamp, Chem.Phys., 1979, 36, 345.
26. B.K.Annis and S.Datz, J.Chem.Phys., 1977, 66, 4468.
27. R.N.Compton, P.W.Reinherd and C.D.Cooper, J.Chem.Phys., 1978, 68, 2023.
28. J.Burgess, I.Haigh, R.D.Peacock and P.Taylor, J.Chem.Soc. Dalton Trans., 1974, 1064.
29. J.Burgess and R.D.Peacock, J.Fluorine Chem., 1977, 10, 479.
30. L.N.Sidorov, A.Y.Borshcheusky, E.B.Rudny and V.D.Butsky, Chem. Phys., 1982, 71, 145.
31. A.T.Pyatanko, A.V.Guisarov and L.N.Gorokhov, Russ.J.Phys.Chem., 1982, 56, 1164.
32. A.T.Pyantanko, A.V.Guisarov and L.N.Gorokhov, Russ.J.Phys.Chem., 1984, 58, 1.
33. T.E.Mallouch, G.L.Rosenthal, G.Miller, R.Brusasco and N.Bartlett, Inorg.Chem., 1984, 23, 3167.
34. P.R.Hammond and W.S.McEwan, J.Chem.Soc., 1971, A, 3812.
35. P.R.McLean, D.W.A.Sharp and J.M.Winfield, J.Chem.Soc.Dalton Trans., 1972, 676.
36. J.D.Webb and E.R.Bernstein, J.Am.Chem.Soc., 1978, 100, 483.
37. J.R.Geichman, E.A.Smith, S.S.Trond and R.R.Ogle, Inorg.Chem., 1962, 1, 661.
38. T.A.O'Donnell and D.F.Stewart, Inorg.Chem., 1966, 5, 1434 & 1438.
39. J.Shamir and J.G.Malm, J.Inorg.Nucl.Chem., 1976, Suppl., 107.
40. A.M.Bond, I.Irvine and T.A.O'Donnell, Inorg.Chem., 1975, 14, 2408; ibid. 1977, 16, 841.

41. J.A.Berry, A.Prescott, D.W.A.Sharp and J.M.Winfield, J.Fluorine Chem., 1977, 10, 247.
42. N.S.Nikolaev, A.T.Sadikova and V.F.Sukhoverkhov, Russ.J.Inorg. Chem., 1973, 18, 751.
43. G.B.Hargreaves and R.D.Peacock, J.Chem.Soc., 1957, 4212; ibid. 1958, 3776.
44. A.Prescott, D.W.A.Sharp and J.M.Winfield, J.Chem.Soc.Dalton Trans., 1975, 936.
45. J.A.Berry, R.T.Poole, A.Prescott, D.W.A.Sharp and J.M.Winfield, J.Chem.Soc.Dalton Trans. 1976, 272.
46. G.M.Anderson, J.Iqbal, D.W.A.Sharp and J.M.Winfield, J.Fluorine Chem., 1984, 24, 303.
47. C.J.Barbour, J.H.Cameron and J.M.Winfield, J.Chem.Soc.Dalton Trans., 1980, 2001.
48. G.M.Anderson and J.M.Winfield, J.Chem.Soc.Dalton Trans, 1986, 337.
49. A.C.Baxter, J.H.Cameron, A.McAuley, F.M.McLaren and J.M.Winfield, J.Fluorine Chem., 1977, 10, 289.
50. P.A.W.Dean, C.D.Desjardins and J.Passmore, J.Fluorine Chem., 1975, 6, 379.
51. R.D.W.Kemmitt, M.Murray, V.M.McRae, R.D.Peacock, M.C.R.Symons and T.A.O'Donnell, J.Chem.Soc., 1968, A, 862.
52. C.G.Davies, R.J.Gillespie, P.R.Ireland and J.M.Sowa, Can.J.Chem. 1974, 52, 2048.
53. J.Passmore, G.Sutherland and P.S.White, Inorg.Chem., 1981, 20, 2169.
54. J.Passmore, P.Taylor, T.Whidden and P.S.White, Can.J.Chem., 1979, 57, 968
55. A.J.Edwards, G.R.Jones and R.J.C.Sills, J.Chem.Soc. Chem.Commun., 1968, 1527.
56. R.J.Gillespie and J.Passmore, 'Adv. in Inorg.Chem and Radiochem' 1975, 17, 49.
57. R.J.Gillespie and J.Passmore, Chem.Brit., 1972, 8, 475.
58. T.A.O'Donnell, Chem.Soc.Rev., 1987, 16, 1.
59. A.P.Zuur and W.L.Groeneveld, Rec.Trev.Chim., 1967, 86, 1089.

60. P.P.K.Claire, G.R.Willey and M.G.B.Dew, J.Chem.Soc.Chem.Commun., 1987, 1100.
61. W.L.Groeneveld and J.Reedijk, Rec.Trev.Chim., 1967, 86, 1103.
62. A.Prescott, D.W.A.Sharp and J.M.Winfield, J.Chem.Soc.Dalton Trans., 1975, 934.
63. D.K.Sanyal, D.W.A.Sharp and J.M.Winfield, J.Fluorine Chem., 1981/82, 19, 55.
64. J.P.Manners, K.G.Morallee and R.J.P.Williams, J.Chem.Soc.Chem. Commun., 1970, 965.
65. J.Reuben and F.J.Kayne, J.Biol.Chem., 1971, 246, 6227.
66. F.J.Kayne, Arch.Biochem.Biophys., 1971, 143, 232.
67. S.Krasne and G.Elsenman, 'Membranes - A series of Advances', Vol. II, Mercel Dekker New York, 1973.
68. J.F.Hinton, K.R.Metz and R.W.Briggs, 'Annual Reports on NMR Spectroscopy', 1982, 13, 211.
69. J.F.Hinton and K.R.Metz, J.Solution Chem., 1980, 9, 197.
70. G.S.Laurence and K.J.Ellis, J.Chem.Soc.Dalton, 1972, 1667.
71. M.L.Tobe, 'Inorganic Reaction Mechanisms', Nelson, 1972, p.132.
72. K.F.Purcell and J.C.Kotz, 'Inorganic Chemistry', W.B.Saunders Co. London, 1977, p.661.
73. H.Taube and H.Mayers, J.Am.Chem.Soc., 1954, 76, 2103.
74. M.Simic and J.Lilie, J.Am.Chem.Soc., 1974, 96, 291.
75. A.G.Sharpe, 'Inorganic Chemistry' Longman Group Limited, London 1981, p.507.
76. H.Taube, Chem.Rev., 1952, 50, 69.
77. R.G.Wilkins, 'The Study of Kinetics and Mechanism of Reactions of Transition Metal Complexes', Allyn and Bacon Inc. Boston, 1974, p.182.
78. J.Burgess, 'Metal ions in solution', Ellis Horwood Limited, England, 1978, p.320.
79. A.Hioki, S.Funahashi, M.Ishii and M.Tanaka, Inorg.Chem., 1986, 25, 1360.
80. R.T.Myers, Inorg.Chem., 1978, 17, 952.

81. A.Anichini, L.Fabbrizzi and P.Paoletti, J.Chem.Soc.,Dalton Trans., 1978, 577.
82. F.A.Cotton and G.Wilkinson, 'Advanced Inorganic Chemistry', 4th Edition, Wiley Interscience London, 1980, p.755 and 801.
83. D.A.Zatko and B.Kratochvil, Anal.Chem., 1968, 40, 2120.
84. G.M.Anderson, J.H.Cameron, A.G.Lappin and J.M.Winfield, Polyhedron, 1982, 1, 467.
85. F.A.Cotton and G.Wilkinson, 'Advanced Inorganic Chemistry', 4th Edition, Wiley Interscience London, 1980, p.333.
86. H.A.Bent, Chem.Rev., 1968, 68, 587.
87. M.K. Kuya and O.A. Serra, J. Coord. Chem., 1980, 10, 13.
88. A.E.Elia, B.D. Santarsiero, E.C. Lingafeltar and V.Shomaker, Acta cryst., 1982, B38, 3020.
89. R.M. Morrison, R.C.Thompson and J. Trotter, Can.J.Chem., 1983, 61, 1651.
90. S.A. Preston and D.J. Cole-Hamilton, J.Chem.Soc.Dalton, 1986, 1055.
91. E. Horn, M.R. Snow and E.R.T.Tiekink, Aust.J.Chem., 1987, 40, 761.
92. R.M. Morrison, R.C. Thompson and J. Trotter, Can.J.Chem., 1980, 58, 238.
93. Y. Yamemoto, A. Aoki and H. Yamazaki, Inorg.Chem.Acta, 1982, 68, 75.
94. M. Oltmanns and R. Mews, Z. Naturforsch, 1980, 35B, 1324.
95. K. Rasli, B. Olgemollar, K. Schloter and W. Beck, J. Organometallic Chem, 1981, 214, 81.
96. H. Nakei, Bull.Chem.Soc.Japan, 1983, 56, 1637.
97. A.A.G. Tomlinson, M. Bonamico, G. Dessy, V. Fares and L. Scaramuzza, J.Chem.Soc.Dalton, 1972, 1671.
98. A.P. Gaughen, Z. Dori and J.A. Ibers, Inorg.Chem. 1974, 13, 1657.
99. B.L. Kindberg, E.H. Griffith and E.L. Amma, J. Chem.Soc.Chem. Comm., 1977, 461.
100. E.N. Becker and G.E. Norris, J.Chem.Soc.Dalton, 1977, 877.
101. I.R. Beattie and K.R. Millington, J.Chem.Soc.Dalton, 1987, 1521.
102. S.A.Bell, J.C.Lancaster and W.R. McWhinnic, Inorg.Nucl.Chem. Lett., 1971, 7, 405.

103. R.M. Morrison and R.C. Thompson, Can.J.Chem, 1982, 60, 1048.
104. R.M. Morrison and R.C. Thompson, Inorg.Nucl.Chem.Lett., 1976 12, 937.
105. R.M. Morrison, R.C. Thompson and J. Trotter, Can.J.Chem., 1979, 57, 135.
106. B.J. Hathaway, J.Chem.Soc.Dalton., 1972, 1196.
107. R. Okawara, B.J. Hathaway and D.E. Webster, Proc.Chem.Soc., 1963, 13.
108. C.M. Mikulski, L.S. Gelfand, E.S.C.Schwartz, L.L. Pytewski and N.M. Karayannis, Inorg. Chim. Acta, 1980, 39, 143.
109. E. Horn and M.R. Snow, Aust.J. Chem., 1984, 37, 1375.
110. J. Iqbal, D.W.A.Sharp and J.M.Winfield, J.Chem.Soc.Dalton., in press.
111. C.D. Garner, L. McGhee, A.Steel and J.M.Winfield, unpublished results.
112. A.J.Edwards and R.D.Peacock, J.Chem.Soc., 1961, 4253.
113. V. Gutmann, Coord.Chem.Rev., 1976, 18, 225.
114. R.W.Briggs, K.R.Metz and J.F. Hinton, J.Solution Chem., 1979, 8, 479.
115. R.W.Briggs and J.F. Hinton, J.Solution Chem., 1977, 6, 827.
116. J.O.M. Bockris and A.K.Reddy, 'Modern Electrochemistry', Vol.1 Plenum Press, New York, 1970.
117. R.G.Kidd, 'The Multinuclear Approach to NMR Spectroscopy', eds. J.B. Lambert and F.G. Riddell, N.A.T.O. AS1 Series, D. Reidel, Dordrecht, Boston, Lancaster 1983, p-329.
118. J. Gleser and U. Henrikson, J.Am.Chem.Soc., 1981, 103, 6642.
119. S. Hefner and N.H.Nachlutriab, J.Chem.Phys. 1964, 40, 2891.
120. Gutowsky and McGarvey, Physics Rev., 1953, 91, 81.
121. B.N. Figgis, Trans. Faraday Soc., 1959, 55, 1075.
122. M.D. Noirot, O.P. Anderson and S.H. Strauss., Inorg.Chem., 1987, 26, 2216.
123. I.C. McLeod, D.M. Muir, A.J. Parker and P. Singh, Aust.J.Chem., 1977, 30, 1423.
124. J.R. Geichman, E.A. Smith, S.S. Trond and R.R. Ogle, Inorg.Chem., 1962, 1, 661.
125. D.D. Watkins, D.P. Riley, J.A. Stone and D.H. Busch, Inorg. Chem., 1976, 15, 387.
126. L. Asch, G.K. Shenoy, L.M. Friedt, J.P. Adloff and R. Kleinberger, J.Chem.Phys., 1975, 62, 2335.

127. B. Brunst, Chem.Phys.Lett., 1975, 32, 187.
128. L. Asch, G.K. Shenoy, L.M. Friedt and J.P. Adloff, J.Chem.Soc., Dalton Trans., 1975, 1235.
129. K.H. Schmidt and A. Muller, Inorg. Chem., 1975, 14, 2183.
130. M. Badri and J.W.S. Jamieson, Can.J.Chem., 1977, 55, 3530.
131. J.R. Allan, D.H. Brown, R.H. Nuttall and D.W.A. Sharp, J.Chem.Soc., 1966, A2, 1031.
132. R.J. Deedens and L.F. Dahl, J.Am.Chem.Soc., 1966, 88, 4847.
133. B.D. Pandey and D.C. Rupainwar, Trans.Met.Chem., 1981, 6, 249.
134. M.L.H. Green, D.O. Hare and L.L. Wong, J.Chem.Soc., Dalton Trans. 1987, 2031.
135. S.M. Pankowski, B. Demerseman and G. Bouquet, J.Organomett.Chem., 1972, 35, 155.
136. J.W. Rathke and E.L. Muettertides, J.Am.Chem.Soc., 1975, 97, 3272.
137. P.F. Meier, A.E. Merbach, M. Dartiquenave and Y. Dartiquenave, Inorg.Chem., 1979, 18, 610.
138. H.F. Klein and H.H. Karsch, Chem.Ber., 1975, 944.
139. H.F.Klein and H.H. Karsch, Inorg. Chem., 1975, 14, 473.
140. B. Capelle, A.L. Beauchamp, M. Dartiquenave, Y. Dartiquenave and H.F. Klein, J.Am.Chem.Soc., 1982, 104, 3891.
141. B. Beagley, C.A. McAuliffe, K. Minton and R.G. Pritchard, J.Chem.Soc., Dalton Trans., 1987, 1999.
142. C.A. Tolman, J.Am.Chem.Soc., 1970, 92, 2953.
143. E.L. Muettertides and J.W. Rathke, J.Chem.Soc.Chem.Commun., 1974, 850.
144. S.D. Ittel, A.D. English, C.A. Tolman and J.P. Jesson, Inorg.Chim.Acta., 1979, 33, 101.
145. A.D. English, S.D. Ittel, C.A.Tolman, P. Meakin and J.P. Jesson, J.Am.Chem.Soc., 1977, 99, 117.
146. G.M. Bancroft and E.T. Libby, J.Chem.Soc., Dalton Trans., 1974, 87.
147. S.D. Ittel, F.A.V. Catledge and J.P. Jesson, J.Am.Chem.Soc., 1979, 101, 3874.
148. A. Drummond, J.F. Kay, J.H. Morris and D. Reed, J.Chem.Soc., Dalton Trans., 1980, 284.
149. G. Albertin, S. Antoniutti, M. Lanfranchi and E. Bordignon, Inorg.Chem., 1986, 25, 950.
150. A.G. Lappin, J.H. Cameron, J.M. Winfield and A. McAuley, J.Chem.Soc., Dalton Trans., 1981, 2172.
151. Lawrence McGhee, L.R.S.C. Dissertation, Chemistry Dept., Glasgow University, Scotland, 1983.

152. K.W. Dixon, B.Sc. Thesis, Chemistry Dept, Glasgow University, Scotland, 1982.
153. J.P.Fackler, T. Moyer, J.A. Costamagna, R. Latorre and J. Granifo, Inorg.Chem., 1987, 26, 836.
154. H.E. Toma, A.A. Batista and H.B Gray, J.Am.Chem.Soc., 1982, 104, 7509.
155. J.W.Emsley, T. Feeney and L.H. Sutcliffe, 'High Resolution N.M.R. Spectroscopy', Pergamon Press, London, 1965.
156. V.M. Linhard, H. Siebert, B.Britenstein and G. Trammel, Z.Anorg. Allg.Chem.,1972, 389, 22.
157. A.P. Sakhorov, J.Gen.Chem.U.S.S.R.,1971, 41, 2145.
158. D.B. Rorabacher and C.A. Melendez-Cepeda, J.Am.Chem.Soc., 1971, 93, 6071.
159. S.F. Lincoln, A.M. Howinslow and A.N. Boffa, Inorg.Chem.,1986, 25, 1038.
160. Y.Ducamun, K.E. Newman and A.E. Merbach, Inorg.Chem., 1980, 19, 3696.
161. F.K. Meyer, K.E. Newman and A.E. Merbach, J.Am.Chem.Soc., 1979, 101, 5588.
162. A.E. Merbach, Pure.Appl.Chem., 1982, 54, 1479.
163. M.J. Sisley, Y. Yano and T.W. Swaddle, Inrog.Chem., 1982, 21, 1141.
164. D.H. Macartney and A. McAuley, Inorg.Chem.,1979, 18, 2891.
165. T.R. Sullivan, D.R. Stranks, J. Burgess and R.I. Haines, J.Chem.Soc.Dalton Trans, 1977, 1460.
166. J. Curtis, G.A. Lawrence, P.A.Lay and A.M. Sargeson, Inorg. Chem., 1986, 25, 484.
167. D.L. Dubois and A. Miedarer, Inorg.Chem., 1986, 25, 4642.
168. C.A. Tolman, Chem.Rev., 1977, 77, 313.
169. C.A. Tolman, J.Am.Chem.Soc., 1970, 92, 2956.
170. N.S. Gill, R.H. Nuttall, D.E. Scaife and D.W.A. Sharp, J.Inorg. Nucl. Chem., 1961, 18, 79.
171. G.M. Begun and A.C. Ruthenberg, Inorg.Chem., 1967, 6, 2212.
172. L. Sacconi, A. Sebatini and P. Gano, Inorg. Chem.,1964, 1772.
173. J.N. Gayles, Spectrachim Acta.Part.A., 1967, 23, 1521.
174. J. Reedijk, A.P. Zuur and W.L. Groeneveld, Rec. Trav. Chim., 1967, 86, 1127.

175. U. Anthoni, P.H. Nielsen, G. Borch, J. Gustaisen and P. Klaboe, Spectrochim Acta, 1977, 33A, 403.
176. R.A. Noyquist, Spectrochim Acta, Part A, 1966, 22, 1315.
177. M. Halmann, Spectrochim. Acta, 1960, 16, 407.
178. P. Singh, I.D. Macleod and A.J. Parker, Aust.J.Chem., 1983, 36, 1675.
179. J. Gazo, I.B. Bersuker, J. Garay, M. Kabesoua, J. Kohout, H. Langefelderova, M. Melnik, M. Serator and F. Valach, Coord. Chem.Rev., 1976, 19, 253.
180. B.J. Hathaway and A. Murphy, Acta Cryst, 1980, 36B, 295.
181. L.P. Battaglia, A.B. Corradi, G. Marcatrigiano and G.C. Pellacani, Inorg.Chem., 1979, 18, 148.
182. I. Csoregh, P. Kierkegaard and R. Norrestam, Acta.Cryst., 1975, 31B, 314.
183. A.C. Baxter, J.H. Cameron, A.McAuley, F.M.McLaren and J.M. Winfield, J. Fluorine Chem., 1977, 10, 289.
184. P.M. Colman, H.C. Freeman, J.M. Guss, M. Murata, V.A. Norris, J.A.M. Ramshaw and M.P. Venkatappa, Nature, (London), 1978, 272, 319.
185. E.T. Adman, R.E. Stenkamp, L.C. Sieker and L.H. Jonsen, J.Mol.Biol., 1978, 123, 35.
186. N. Aishi, Y. Nishida, K. Ida and S. Kida, Bull.Chem.Soc.Jpn., 1980, 53, 2847.
187. J.V. McArdle, C.L. Coyle, H.B. Gray, G.S. Yaneda and R.A. Holwerda, J.Am.Chem.Soc., 1979, 101, 2297.
188. M. Ostern, J. Pelezar, H. Kozlowski and B.J. Trzebiatowska, Inorg. Nucl.Chem.Lett., 1980, 16, 251.
189. J.M. Winfield, Personal communication.
190. K.L. Baker, D.A. Edwards, G.W.A. Fowles and R.G. Williams, J. Inorg. Nucl. Chem., 1967, 29, 1881.
191. R. Kiesel and E.P. Schram, Inorg. Chem., 1973, 12, 1090.
192. G. Annibale, L. Canavese, L. Cattalini and G. Natila, J.Chem. Soc., Dalton Trans., 1980, 1017.
193. A.G. Skyes, Adv. Inorg. Chem.Radiochem., 1967, 10, 153.
194. B. Falcinella, P.D. Felgate and G.S. Lawrence, J.Chem.Soc. Dalton Trans, 1975, 1.
195. J.L. Kice and N.A. Favstritsky, J.Am.Chem.Soc., 1969, 91, 1751.
196. R.A. Goodrich and P.M. Treichel, J.Am.Chem.Soc., 1966, 88, 3509.
197. S.H. Smallcombe and M.C. Caseria, J.Am.Chem.Soc., 1971, 93, 5826.

198. J.L. Ryan, J.Inorg.Nucl.Chem., 1971, 33, 153; M.J. Reisfield and G.A. Grosby, Inorg.Chem., 1965, 4, 65.
199. A. Nieuwpoort and J. Reedijk, Inorg.Chim.Acta, 1973, 7, 323; R. Savoie and M. Guay, Can.J.Chem., 1975, 53, 1387.
200. T.A. Lane and J.T. Yoke, Inorg.Chem., 1976, 15, 484.
201. J.H. Cameron, Ph.D. Thesis, Chemistry Dept., Glasgow University, Scotland, 1980.
202. Y.P. Mokovetskii, N.G. Feshchenko, V.V. Malovik, V.Y. Semenii, I.E. Boldeskul, V.A. Bonder and N.P. Chernukho, J.Gen.Chem. U.S.S.R., 1980, 50, 1967.
203. P. Mokovetskii, V.E. Lidkovskii, I.E. Boldeskul, N.G. Feshchenko and N.N. Kalibabchuk, J.Gen.Chem.U.S.S.R., 1982, 52, 1989.
204. M.S. Weininger, G.W. Hunt and E.L. Amma, J.Chem.Soc.Chem.Comm., 1972, 1140.
205. D.A. Zatko and B. Kratochvil, Anal.Chem., 1968, 40, 2120.
206. E.A.H. Griffith, W.A. Spofford and E.L. Amma, Inorg.Chem., 1978, 17, 1913.
207. G. Maas and P.J. Strang, J.Org.Chem., 1981, 46, 1606.
208. J.S. Filippo, L.E. Zyontz and J. Potenza, Inorg.Chem., 1975, 14, 1667.
209. H. Schmidbaur, J. Akofer and K. Schiurten, Chem.Ber., 1972, 105, 3382.
210. C.D. Desjardins, D.B. Edwards and J. Passmore, Can.J.Chem., 1979, 57, 2714.
211. W. Bublak, H. Schmidbaur, J. Riede and G. Muller, Angew.Chem., Int.Ed.Engl., 1985, 24, 414.
212. H. Schmidbaur, Angew.Chem.,Int.Ed.Engl., 1985, 24, 893.
213. M.J. Davies, B.C. Gilbert and R.O.C. Norman, J.Chem.Soc.Perkin. Trans.II, 1984, 503.
214. R. Wilbrandt, N.H. Jensen, A.H. Sillesen and K.B. Hansen, J. Raman Spect., 1981, 11, 24.
215. R.L. Petersen, D.J. Nelson and M.C.R. Symons, J.Chem.Soc.Perkin Trans.II, 1978, 225.
216. W.B. Gara, J.R.M. Giles and B.P. Roberts, J.Chem.Soc.Perkin Trans. II, 1979, 1444.
217. J. Monig, M. Gobl and K.D. Asanus, J.Chem.Soc.Perkin Trans. II, 1985, 647.
218. Y.L. Chow, W.C. Danen, S.F. Nelsen, and D.H. Rosenblatt, Chem.Rev., 1978, 78, 243.

219. B.J. Hathaway and A.G. Tomlinson, Coord.Chem.Rev., 1970, 5, 1.
220. J. Iqbal, Ph.D. Thesis, Chemistry Dept., Glasgow University, Scotland, 1985.
221. P. Gupta, P.D. Sharma and Y.K. Gupta, J.Chem.Soc.Dalton Trans., 1984, 1867.
222. M.C.R. Symons and G.D.G. McConnachie, J.Chem.Soc.Faraday Trans.I, 1984, 1005.
223. D. Schomburg, G. Bettermann, L. Ernst and R. Schmutzler, Angew. Chem.Int.Ed.Engl., 1985, 24, 975.
224. J. Arotzky and M.C.R. Symons, Quart.Rev.Chem.Soc., 1962, 12, 282.
225. Murokawa, Z. Physik, 1948, 5C, 84.
226. R.P. Bell and E. Gells, J.Chem.Soc., 1951, 2734.
227. G.N. Lewis, J.Am.Chem.Soc., 1916, 38, 762.
228. W.B. Person, R.E. Humphrey, W.A. Deskin and A.I. Popov, J.Am.Chem.Soc., 1958, 80, 2049.
229. T. Shono, M. Sawamura and S. Kashimura, J.Chem.Soc.Chem.Commun., 1984, 1204.
230. N.N. Greenwood and A. Earnshaw, 'Chemistry of the Elements', Pergamon Press, New York, 1984, p. 940.
231. O. Hassel and H. Hope, Acta.Chem.Scand. 1961, 15, 407.
232. H. Hope and G.H. Lin, J.Chem.Soc.Chem.Commun, 1970, 169.
233. G.A. Bowmaker and S.F. Hannan, Aust.J.Chem., 1971, 24, 2237.
234. H. Pritzkow, Acta.Cryst., 1975, B31, 1505.
235. J.W. Lown and A.V. Joshua, J.Chem.Soc.Perkin Trans.I, 1973, 2680.
236. J. Barluenga, J.M. Gonzalez, P.J. Campos and G. Asensio, Angew. Chem. Int.Ed.Engl., 1985, 24, 319.
237. R.D. Evans and J.H. Schauble, Synthesis, 1987, 6, 551.
238. C.H.W. Jones, J.Chem.Phys., 1975, 62, 4343.
239. T. Birchall and R.D. Myers, Adv.Chem.Ser., 1981, 194, 375.
240. Y.N. Kukushkin and V.N. Damidor, Zh. Neorg.Khim, 1982, 27, 2590 and 2839.
241. G.M.Anderson, I.F. Fraser and J.M. Winfield, J.Fluorine Chem., 1983, 23, 403.
242. J.W. Lown and A.V. Joshua, Can.J.Chem., 1977, 55, 122 and 508.
243. F. Effenberger, Angew.Chem.Int.Ed.Engl. 1980, 19, 151.
244. R.D. Evans and J.H. Schauble, Synthesis, 1986, 727.
245. Y. Shiro, M. Ohsaku, M. Haysshi and H. Murata, Bull.Chem.Soc.Jpn, 1970, 43, 609.
246. R.G.Inskeep, J. Inorg. Nucl.Chem., 1962, 24, 763.
247. E.J. Bounsall and S.R.Koprach, Can.J.Chem, 1970, 48, 1481.

248. W.R. McWhinnie and J.D. Muller, Adv.Inorg.Chem.Radio.Chem., 1969, 12, 135.
249. M. Nonoyama, T. Yamaguchi and H. Kimijiri, Polyhedron, 1986, 5, 1885; R.I. Haines and A. McAuley, Coord.Chem.Rev., 1981, 39, 77.
250. E.K. Barefield, A. Bianchi, P.J. Connolly and D.G.V. Derveer, Inorg.Chem., 1986, 25, 4197; C.M. Che, S.S. Kwong, C.K. Poon, T.F. Lai and T.C.W. Mak, Inorg.Chem, 1985, 24, 1359; M.Yamashita, K. Toriumi and T. Its, Acta.Cryst., 1985, C41, 1607; V.J. Thom, C.C. Fox, J.C.A. Boeyens and R.D. Hancock, J.Am.Chem.Soc, 1984, 106, 5947.
251. R.T. Sanderson, 'Chemical Bond and Bond Energy'. Academic Press, 1976.
252. R.L. Goaller, H. Handel, P. Labbe and J.L. Pierre, J.Am.Chem.Soc, 1984, 106, 1694.
253. N.A. Alcock, E.H. Curson, N. Herron and P. Moore, J.Chem.Soc. Dalton Trans, 1979, 1486 and 1987.
254. F.A. Cotton and G. Wilkinson, 'Advanced Inorganic Chemistry', 4th Edition, wiley Interscience London, 1980, p-53.
255. R.B. King, S.A. Sangokoya and E.M. Holt, Inorg.Chem, 1987, 26, 4307.
256. M.P. Suh, S.G. Kang and K.W. Woo, J.Korean.Chem.Soc., 1984, 28, 384.
257. E.K. Barefield and D.H. Busch, J.Chem.Soc.Chem.Commun, 1970, 522.
258. E.K. Barefield and M.T. Mocella, Inorg.Chem, 1973, 12, 2829.
259. K.G. Caulton, Coord.Chem.Rev, 1975, 14, 317.
260. K. Moock, L. Turewsky and K. Seppelt, J. Fluorine Chem, 1987, 37, ~~253~~.
261. D.A. Skoog, D.M. West, 'Principles of Instrumental Analysis', 2nd Edition, Saunders College Publishing Ltd, London 1980.
262. F.A. Cotton, 'Chemical Applications of Group Theory', 2nd Edition, Wiley Interscience, London 1970.
263. D. Nicholls, 'Complexes and First Row Transition Elements', The Macmillan Press Ltd, London, 1974.
264. A.B.P. Lever, 'Inorganic Electronic Spectroscopy', Elsevier, Oxford, 1984.
265. J.H. Van Vleck, J.Phys.Chem., 1937, 41, 67.
266. F.J.W. Roughton, Proc.Roy.Soc., 1934, A158, 473.
267. B. Chance, Rev. Sci. Instr. 1951, 22, 619.
268. D.T. Sawyer and J.L. Roberts, 'Experimental Electrochemistry for Chemists', Wiley Interscience, London, 1974.

269. J.B. Headridge, 'Electrochemical Technique for Inorganic Chemistry', Academic Press, London, 1969.
270. L. Meites, 'Polarographic Techniques', 2nd Edition, Interscience, New York, 1965.
271. R.S. Nicholson and I. Shain, Analyt. Chem, 1964, 36, 706.
272. G.A. Heath, G.T. Hefter, C.D. Desjardins and D.W.A. Sharp, J. Fluorine Chem, 1978, 11, 399.
273. M. Walter and L. Ramalay, Analyt. Chem, 1973, 45, 165.
274. R.K. Harris, 'Nuclear Magnetic Resonance Spectroscopy', Pitman, London, 1983.
275. L.C. Jackson, Proc. Roy. Soc, 1933, A140, 695.